National Aeronautics and Space Administration

Space Shuttle Entry Digital Autopilot

February 2010

SP -2010-3408

NASA STI PROGRAM ... IN PROFILE

Since its founding, NASA has been dedicated to the advancement of aeronautics and space science. The NASA Scientific and Technical Information (STI) Program Office plays a key part in helping NASA maintain this important role.

The NASA STI Program Office is operated by Langley Research Center, the lead center for NASA's scientific and technical information. The NASA STI Program Office provides access to the NASA STI Database, the largest collection of aeronautical and space science STI in the world. The Program Office is also NASA's institutional mechanism for disseminating the results of its research and development activities. These results are published by NASA in the NASA STI Report Series, which includes the following report types:

- TECHNICAL PUBLICATION. Reports of completed research or a major significant phase of research that present the results of NASA programs and include extensive data or theoretical analysis. Includes compilations of significant scientific and technical data and information deemed to be of continuing reference value. NASA's counterpart of peer-reviewed formal professional papers but has less stringent limitations on manuscript length and extent of graphic presentations.

- TECHNICAL MEMORANDUM. Scientific and technical findings that are preliminary or of specialized interest, e.g., quick release reports, working papers, and bibliographies that contain minimal annotation. Does not contain extensive analysis.

- CONTRACTOR REPORT. Scientific and technical findings by NASA-sponsored contractors and grantees.

- CONFERENCE PUBLICATION. Collected papers from scientific and technical conferences, symposia, seminars, or other meetings sponsored or cosponsored by NASA.

- SPECIAL PUBLICATION. Scientific, technical, or historical information from NASA programs, projects, and mission, often concerned with subjects having substantial public interest.

- TECHNICAL TRANSLATION. English-language translations of foreign scientific and technical material pertinent to NASA's mission.

Specialized services that complement the STI Program Office's diverse offerings include creating custom thesauri, building customized databases, organizing and publishing research results . . . even providing videos.

For more information about the NASA STI Program Office, see the following:

- Access the NASA STI Program Home Page at http://www.sti.nasa.gov

- E-mail your question via the internet to help@sti.nasa.gov

- Fax your question to the NASA Access Help Desk at (301) 621-0134

- Telephone the NASA Access Help Desk at (301) 621-0390

- Write to:
  NASA Access Help Desk
  NASA Center for AeroSpace Information
  7121 Standard
  Hanover, MD 21076-1320

NASA/SP–2010–3408

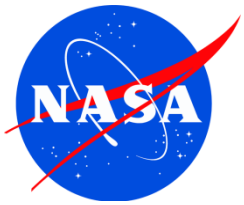

Space Shuttle Entry Digital Autopilot

Larry B. McWhorter
NASA Johnson Space Center, Houston, Texas

Milt Reed
(Primary Author, 2009 Update)
Honeywell (retired)/Barrios Technology

Contributing Authors, 2009 Update:

Gordon C. Kafer
Honeywell (retired)/BATECH

Mark Hammerschmidt
NASA Johnson Space Center, Houston, Texas

Wes Dafler, Dr. Daigoro Ito, Dan Nelson
Boeing

Brian Bihari
Jacobs Engineering

National Aeronautics and
Space Administration

Lyndon B. Johnson Space Center
Houston, Texas 77058

February 2010

Available from:

NASA Center for AeroSpace Information
7115 Standard Drive
Hanover, MD 21076-1320
301-621-0390

National Technical Information Service
5285 Port Royal Road
Springfield, VA 22161
703-605-6000

This report is also available in electronic form at http://ston.jsc.nasa.gov/collections/TRS/

Preface

The Space Transportation System program was formally launched on January 5, 1972, when President Nixon announced that the National Aeronautics and Space Administration (NASA) would proceed with the development of a reusable Space Shuttle system, with North American Aviation (later Rockwell International, now Boeing) selected to be the prime contractor. This followed early "Phase A" studies beginning in October 1968 and "Phase B" studies in 1970, during which various concepts and designs were evaluated. In 1977, during the Approach and Landing Test (ALT) phase of the program, five free flights of the Orbiter *Enterprise* landed under astronaut control and verified the flight characteristics of the Orbiter design with several aerodynamic and weight configurations. From the first flight of *Columbia* in April 1981, through the landing of *Discovery* in September 2009, there were 128 Orbiter launches and 126 landings. (*Challenger* was lost during launch on January 28, 1986, and *Columbia* during entry on February 1, 2003.)

This document provides a historical summary of the design, development, verification, and flight test of the entry flight control system (FCS), including its integration with the guidance and navigation systems. (Note that the entry FCS is also known as the entry digital autopilot [DAP]; these two terms are used interchangeably throughout this document.) Emphasis is placed on design drivers, including performance requirements and database impacts, together with the thinking and logic that went into design decisions and solutions. The FCS was certified and considered operational for the first flight, and no significant performance anomalies have been encountered since STS-1. However, the FCS has continued to evolve over the years, with modifications made both to resolve minor anomalies and to enhance performance capability. The overall success of the entry FCS program can be attributed to the cooperative effort of countless individuals, working for various corporate and government entities, with the common goal of ensuring safe entry and landing of the Space Shuttle Orbiter.

A comprehensive draft of this document was written and released by Larry McWhorter NASA-Johnson Space Center (JSC) in June 1992, but was not formally published at that time. A major update completed in 2009 captures the various studies and FCS upgrades that have occurred during the intervening years. An attempt was made to retain the original material untouched (Sections 1 through 5, 9, and 10), except for some typographical corrections and formatting changes necessary for publication, but some additions and updates were incorporated; most of these are indicated by footnotes or *italicized* in-line text.

The 2009 update was compiled primarily by Milt Reed (contracting to Barrios), with significant contributions coming from various members of the entry guidance, navigation, and control [GN&C] community. In particular, Mark Hammerschmidt (NASA-JSC) documented the wraparound DAP flight test program, Brian Bihari (Jacobs Engineering) provided valuable inputs to the reaction control system [RCS] redlines discussion, and Gordon Kafer (contracting to BATECH) contributed the ALT program summary contained in Appendix C. Other contributors are listed on the title page. Much of the material presented in Section 6 was obtained from Honeywell and Rockwell heavyweight certification and forward center-of-gravity [CG] expansion reports, and the discussions of flight-specific and generic FCS certification in Section 7 rely heavily on the certification reports authored by Dr. Steve Everett (Boeing). It is with sincere appreciation that we acknowledge the help of Sue McDonald in editing this document for publication.

FCS details presented in this document are considered correct as of November 2009. Appendix D contains block diagrams illustrating the entry DAP control laws at that time. However, the FCS is still subject to change, so if the reader wants accurate up-to-date information, the latest versions of Flight Subsystem Software Requirements [FSSR] and I-load data books should be consulted.

Contents

Figures

Tables

Acronyms and Abbreviations

AA	accelerometer assembly
ABLT	asymmetric boundary layer transition
ADB	Aerodynamic Data Book
ADTA	air data transducer assembly
ADI	attitude direction indicator
A/E	ascent/entry
AFT	aft
A/L	approach and landing
ALT	Approach and Landing Test
AOA	abort once around
APU	auxiliary power unit
ASE	airborne support equipment
ASI	aerodynamic stick inputs
ATP	Authority to Proceed
b	span reference length
BF	bodyflap
BFS	backup flight system
BNA	Boeing North America
CA	axial force coefficient
CD	drag force coefficient
CDR	Orbiter Commander
CFT	common facility tests
CG	center-of-gravity
CHR	Cooper-Harper rating
CL	lift force coefficient
Cl	rolling moment coefficient
CIR	cargo integration review
CLBA	rolling moment due to bent airframe
Cm	pitching moment coefficient
CN	normal force coefficient
Cn	yawing moment coefficient
CNBA	yawing moment due to bent airframe
CPES	Crew Procedures Evaluation Simulator
CPDS	Computer Program Development Specification
CPU	computer processing unit
CR	change request
CRT	cathode ray tube
CSS	control stick steering
CSTAR (C*)	type of pitch axis control law
CTF	commit to flight
CY	side force coefficient
Da	delta aileron
DA	design assessment
DAP	digital autopilot
dB	decibel
DCSP	entry flight control signal (roll axis)
DDT&E	Design, Development, Test, and Evaluation
DE	elevator
DFRC	Dryden Flight Research Center
DIGIKON	Honeywell Linear Stability Program
DPS	data processing system
DR	discrepancy report
DRB	Data Review Board
DRRCL	entry flight control signal (yaw axis)

DST	dynamic stability test(s)
DTO	detailed test objective
EDO	Extended Duration Orbiter
EDST	entry dynamic stability test
EDW	Edwards Air Force Base
EI	entry interface
EOM	end of mission
ET	external tank
ET-SEP	external tank separation
FAD	flight assessment deltas
FCAN	flight control anomaly notice
FCHL	Flight Control Hydraulic Laboratory
FCS	flight control system
FDIR	fault detection, isolation, and reconfiguration
FDO	Flight Dynamics Officer
FF	free flight
FSL	Flight Simulation Laboratory
FSSR	Flight Subsystem Software Requirements
ft	feet
FWD	forward
g	gravity
GALR	entry flight control gain (roll axis)
GDA	entry flight control gain (roll axis)
GDR	entry flight control gain (yaw axis)
GJET	entry flight control gain (pitch axis)
GN&C	guidance, navigation, & control
GPAY	entry flight control gain (yaw axis)
GPC	general purpose computer
GPS	Global Positioning System
GPX	entry flight control gain (pitch axis)
GQAL	entry flight control gain (pitch axis)
GRAM	Global Reference Atmosphere Model
GRAY	entry flight control gain (yaw axis)
GRO	Gamma Ray Observatory
GRTLS	glide return to launch site
GTRA	entry flight control gain (roll axis)
GTRR	entry flight control gain (yaw axis)
GTS	GN&C Test Station
GUIDCOMP	guidance computation
HAC	TAEM heading alignment cone
HFGM	high-frequency gain margin
HFPM	high-frequency phase margin
HFT	horizontal flight test
HI	Honeywell International
HUD	heads-up display
Hz	cycles per second
IAS	indicated airspeed
I/B	inboard
IC	initial condition
ICD	Interface Control Document
IEE	integrated entry environment
IGN&C	Integrated guidance, navigation, & control
I-load	initialization load
IMU	inertial measurement unit
IPHASE	phase counter in TAEM and GRTLS guidances
ISS	International Space Station
ITEM	special keyboard key
IUS	Inertial Upper Stage

Ixx	inertia about the X axis
Iyy	inertia about the Y axis
Izz	inertia about the Z axis
JAEL	JSC Avionics Engineering Laboratory
JSC	Johnson Space Center
JSL	jet selection logic
KALPHA	GRTLS unique flight control gain (roll axis)
KEAS	knots of equivalent airspeed
K-load	constant load
KSC	Kennedy Space Center
L/D	lift-to-drag ratio
LCDP	lateral control departure parameter
LDCP	lateral directional control parameter
LFGM	low-frequency gain margin
LH_2	liquid hydrogen
LO_2	liquid oxygen
LON	launch on need
LOS	loss of signal
LRU	line replaceable unit
LVAR	lateral aerodynamic uncertainties
M/C	mated coast
MATCRAM	Boeing linear stability program
MDM	multiplexer-demultiplexer
MECO	main engine cutoff
MEDS	multifunction electronic display system
MIL	man-in-the-loop
min	minutes
MMLE	Modified Maximum Likelihood Estimator (computer program)
MSBLS	Microwave Scanning Beam Landing System
MM	major mode
MOD	Mission Operations Directorate
MOV	main oxidizer valve
MPS	main propulsion system
NASA	National Aeronautics and Space Administration
NAVDAD	navigation-derived air data
NEOM	nominal end of mission
NOR	Northrop (White Sands) landing site
NSTS	National Space Transportation System
NWS	nosewheel steering
Ny	lateral acceleration
Nz	normal acceleration
O/B	outboard
OADB	Operational Aero Database
OCCB	Orbiter Configuration Control Board
OFT	Orbital Flight Test
OMS	Orbiter maneuvering system
OPS	Orbiter program segment
OV	Orbiter vehicle
OVEI	Orbiter vehicle end item
p	body roll rate (about X axis)
PASS	primary avionics software system
PBI	pushbutton indicator
Pc or PC	roll rate command
PFS	primary flight system
PIO	pilot-induced oscillation
PLT	Orbiter Pilot
PM	phase margin
p-p	peak-to-peak

PRCB	Program Requirements Change Board
PRL	priority rate limiting
PRO	software keyboard command to proceed
psf	pounds per square foot
PTI	programmed test input
PVAR	pitch aerodynamic uncertainties
$\bar{q}$	dynamic pressure
Qbar	dynamic pressure
q	body pitch rate (about Y axis)
r	body yaw rate (about Z axis)
RA	radar altimeter
RCS	reaction control system
RECON	reconfiguration module in FCS
RGA	rate gyro assembly
RHC	rotation hand controller
RI	Rockwell International
rps	radians per second
RPTA	rudder pedal transducer assembly
RTHL	entry flight control gain (yaw axis)
RTLS	return to launch site
RSOC	Rockwell Space Operations Company
SAIL	Shuttle Avionics Integration Laboratory
SB	speedbrake
SBTC	speedbrake/thrust controller
SCB	Software Control Board
SCOTS	Shuttle Commercial Orbital Transfer Stage
SCR	software change request
sec	second
SDAP	Shuttle Descent Analysis Program
SDSS	Shuttle Dynamics Simulation System
SDM	Systems Definition Manual
SES	Shuttle Engineering Simulator
SIMEX	Honeywell Digital Simulation
SMS	Shuttle Mission Simulator
SMTAS	Shuttle Modal Test and Analysis System
SOP	Subsystem Operating Program
SPEC	special keyboard key
SPS	Shuttle Procedures Simulator
sps	samples per second
SSFS	Space Shuttle Functional Simulator
SSME	Space Shuttle Main Engine
SRB-SEP	solid rocket booster separation
STA	Shuttle Training Aircraft
STAMPS	Spacecraft Trajectory Analysis and Mission Planning Simulation
STRIM	Boeing trim and aerodynamic coefficient program
STS	Space Transportation System
SVDS	Shuttle Vehicle Dynamics Simulator
TACAN	tactical air navigation
TAEM	terminal area energy management
TAL	transatlantic abort landing
TDRS	Tracking Data Relay Satellite
TIFS	CALSPAN Total In-Flight Simulator
TIM	technical interchange meeting
TRD	test requirements document
TRIM	Honeywell trim and aerodynamic coefficient program
Unc	uncertainty
UPP	user parameter propagator
USA	United Space Alliance

VMS	Ames Vehicle Motion Simulator
V-N	airspeed versus load factor (Nz) envelope
Vrel	relative velocity
WON	weight on nose gear
WOW	weight on wheels
WOWLON	weight on wheels discrete in entry FCS
α	angle of attack
ß	sideslip angle
δA	aileron
δR	rudder
δy	Y-axis center-of-gravity offset

1.0 Introduction

The Orbiter entry digital autopilot (DAP) is an all-digital, fly-by-wire system that provides vehicle stability, control, and handling qualities necessary to fly within the narrow entry corridor. This entry control system comprises sensors to measure the current Orbiter states, a computation system to convert the automatic and/or manual commands to a set of effector commands for the unpowered Orbiter, and a set of effectors (i.e., aerodynamic surfaces, control jets, and nosewheel steering). This control system, with minor modifications, is also used during the gliding segment of a return-to-launch-site (RTLS) abort.

The Orbiter flight control system (FCS) had to succeed over its entire, unprecedented flight envelope (Mach 25 to 0) on its first flight. Because it was not possible to conduct the normal progression of flight tests for the Orbiter program, the entry control system was subjected to one of the most—if not the most—extensive certifications (by analysis and simulation programs) in the history of aviation. The control system development was also supported by the most extensive wind tunnel program in the history of the aerospace industry.

Three basic approaches were used for analysis: 1) classical linear stability analysis with describing functions to represent key nonlinear elements, 2) nonlinear time-domain analysis, and 3) man-in-the-loop (MIL) simulations to obtain handling qualities ratings (Cooper-Harper) and general comments by the crew. The time-domain simulations varied in complexity from simple point-response tools, such as SIMEX (a Honeywell digital simulation), to fully functional MIL guidance, navigation, and control (GN&C) simulations. The latter included the fixed-base Shuttle Procedures Simulator (SPS) Phase I and the Shuttle Engineering Simulator (SES) at Johnson Space Center (JSC), the Flight Simulation Laboratory (FSL) in Downey, California, and the non-real-time Spacecraft Trajectory Analysis and Mission Planning Simulation (STAMPS) at United Space Alliance (USA). Landing and rollout studies, in which motion cues were extremely important, utilized the moving base Flight Simulator for Advanced Aircraft (FSAA) and Vehicle Motion Simulator (VMS) at Ames Research Center in California, along with the Orbiter Avionics Simulator (OAS) at JSC. Extensive avionics integration and design verification testing were also performed. Accuracy and fidelity of the analysis programs were maintained by correlating analyses predictions with test results.

This report summarizes the evolution of the entry DAP from the mid-1970s into 2009. Emphasis is on the key events and decisions, database content, and programmatic requirements that forged the entry control system of today. Section 2 gives overview descriptions of the GN&C system elements and processes. A history of program requirements and FCS evolution through the post-STS-51L upgrades is presented in Section 3. A summary of flight and ground test programs in Section 4 is included to provide insight into the high degree of interaction between the test programs and the DAP evolution. Key FCS issues remaining in 1992 are reviewed in Section 5. The 2009 update in Sections 6 and 7 summarizes the major FCS studies and DAP modifications since 1992, as well as the entry FCS recertification conducted after the STS-107 *Columbia* tragedy. Section 8 discusses the November 2009 status of the entry FCS program. A number of lessons learned during this program are presented in Section 9. Section 10 is a concluding summary. Appendix A provides brief details of all orbital flights from STS-1 (April 1981) through STS-128 (September 2009). Appendix B lists many of the key individuals involved in the entry FCS and GN&C program. Appendix C describes the Approach and Landing Test (ALT) phase and lists ALT flights. Appendix D provides a set of simplified DAP block diagrams that the reader of this document may find a helpful reference.

2.0 Entry Flight Control Systems Overview

The Orbiter data processing system (DPS) that contains the autopilot and sensor/effector interface software is comprised of a primary flight system (PFS), four AP101B general purpose computers (GPCs) that function as a redundant set, and a backup flight system (BFS) set of software that resides in a fifth computer. (Upgraded IBM AP-101S flight computers made their maiden flight aboard *Atlantis* in April 1991. By the middle of that year, AP-101S computers had completely replaced the AP-101Bs.) IBM developed the primary software and Rockwell programmed the backup software. A second programming contractor was used for the BFS to minimize the chance of a generic programming error that might result in loss of all command and control capability. The DPS system configuration is shown in figure 2-1.

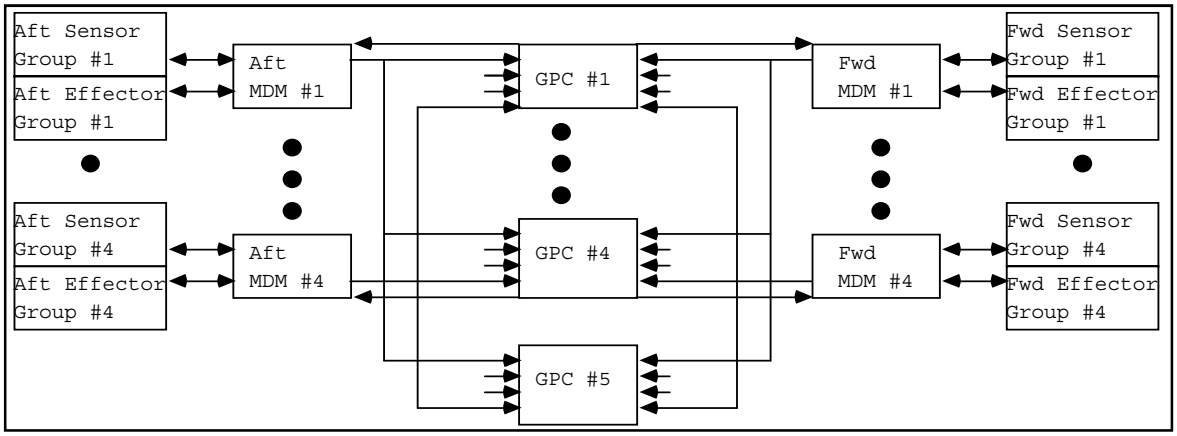

Figure 2-1. Orbiter Data Processing System Data Flow

For entry, the BFS DAP is very similar to the PFS DAP, with two major exceptions: the BFS does not have an automatic pitch or lateral control mode, and the various surface trim integrators are grounded until the pilot activates the BFS system. (Only the pilot can command the backup system to take over control of the Orbiter.) A special set of first-pass logic is executed at BFS activation.

The BFS software has not been engaged during an actual flight, and no plans are in existence to flight-test the system. The need to retain the backup set of software has been discussed a number of times, with the decision always being to retain it.

The following sections give an overview of the Orbiter entry control system elements (software, sensors, effectors, and crew interface) and the basic flight profile parameters within which the system must function.

2.1 GPC GN&C Software

The flow of data through the various elements of the GN&C software functions in the Orbiter's GPCs is diagrammed in figure 2-2. In general, the sensor data flows to the navigation and flight control functions. The navigation function computes the inertially-derived parameters required to support guidance, flight control, and crew displays. The guidance function computes the attitudes required to reach the landing site, and the flight control function maneuvers the vehicle to the required attitudes using the aerodynamic surfaces and reaction control system (RCS) primary jets. In parallel with these activities, the crew can interact with the automatic and manual systems by using switches, controllers—e.g., rotational hand controller (RHC), rudder pedal transducer assembly (RPTA) and speedbrake/thrust controller (SBTC)—and cathode ray tube (CRT) displays. *STS-101*/Atlantis *in May 2000 was the first flight to use the multifunction electronic display system (MEDS) cockpit upgrade, in which electro-mechanical and cathode-ray displays were replaced with liquid-crystal flat panel displays. This "glass cockpit" improved crew/Orbiter interaction with easy-to-read, graphic portrayals of key flight indicators and brought the Space Shuttle cockpit displays up to date with technology that is now common in many commercial airliners.*

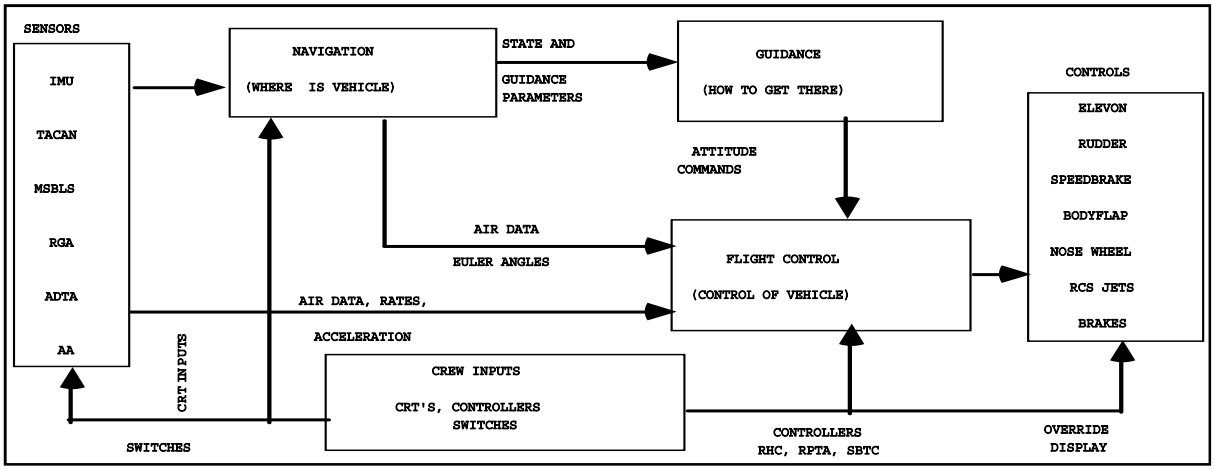

Figure 2-2. Guidance, Navigation, and Control Data Flow

2.1.1 Navigation System

The Orbiter entry navigation system (see figure 2-3) has four parts: 1) state (position and velocity) propagation software, 2) attitude estimation, 3) state updating using external sensor measurements, and 4) computation of parameters for guidance (GUIDCOMP) and flight control (navigation-derived air data, or NAVDAD). The state propagation software, referred to as the outer-loop navigation, is executed at either 0.25 Hz or 0.5 Hz. The higher rate is used after the microwave scanning beam landing system (MSBLS) is acquired (at approximately 14,000 ft) to support the autoland guidance. When the outer-loop navigation is being executed at 0.25 Hz, the software maintains separate states based on the number (one to three) of active inertial measurement units (IMUs). Separate states are maintained to prevent corrupting all the states with bad data from one IMU. After transition to the faster outer loop processing, a single state based on selected IMU data is maintained.

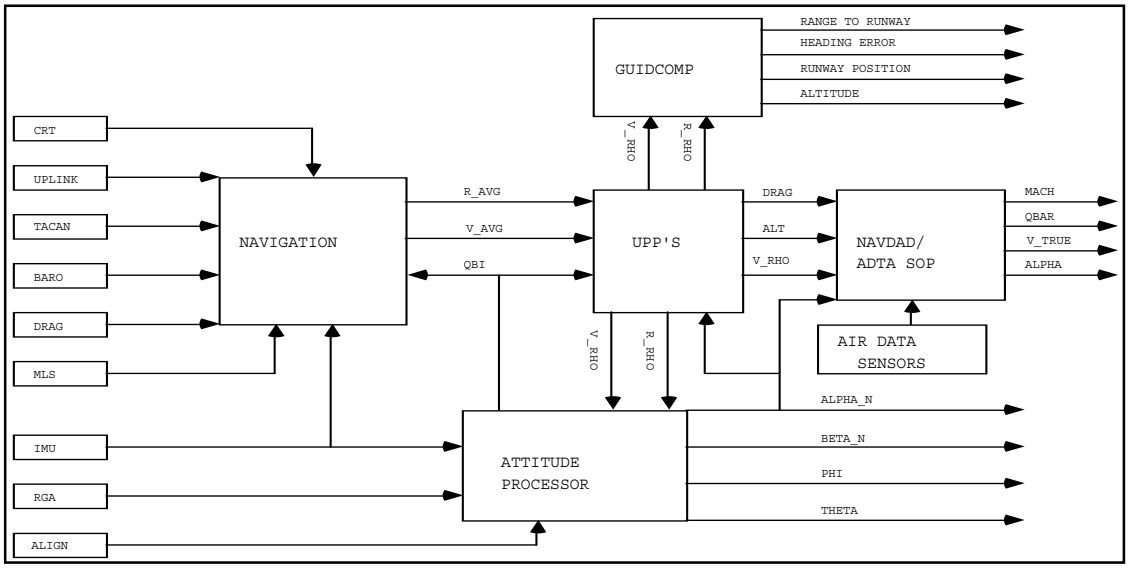

Figure 2-3. Navigation Block Diagram

The attitude estimate is attained by reading IMU gimbal angles every 0.96 sec and using rate gyro data to estimate the attitude at points between the IMU readings. The rate gyro data is passed through two first-order lag filters at 25 Hz and 12.5 Hz to smooth the signal before being used in the integration logic in the attitude processor. The integration is done at 6.25 Hz. For comparison, the same logic is used during ascent, with the exception that only one first-order lag is used (25 Hz), and the integration is done at 12.5 Hz. This approach minimizes the computer processing unit (CPU) computation time requirements. The software maintains its attitude estimate in the form of an inertial-to-body quaternion.

The navigation software uses a combination of tactical air navigation system (TACAN) (for range and bearing), air data transducer assembly (ADTA) (for barometric altitude), MSBLS (in the PFS only, for range, azimuth, and elevation), and drag altitude to update the outer loop states. Drag altitude refers to the derivation of an estimate of the current Orbiter altitude from the measured drag, assumed Orbiter drag coefficient as a function of alpha and Mach, and a standard altitude-density profile (62-standard, hot, or cold). This technique is used between the point that the drag acceleration reaches 11 ft/sec^2 until the altitude is less than 85,000 ft. TACAN data is used between approximately 150,000 ft (Mach 7) and start of MSBLS processing. The TACAN data has produced extremely good results during actual flights. The barometric altitude is used between Mach 2.5 and start of MSBLS processing with the exception of the Mach jump region (1.4>Mach>.9). Finally, MSBLS is used below an altitude of approximately 14,000 ft to the ground. When a landing site is not equipped with MSBLS, TACAN and barometric data are used at the lower altitudes.

Beginning with STS-118, the first 3-string Global Positioning System (GPS) flight (OV-105 with no TACANs installed), GPS data has been used from approximately 150,000 ft altitude to the start of MSBLS processing. This is also applicable to vehicles with 3 TACAN transceivers and 1 GPS receiver installed (OV-103 & OV-104). During the GPS data processing period, the GPS state vector is used to replace the onboard navigation state vector as a whole-state-replacement at an interval of approximately every 42 sec. Between GPS update cycles, the TACAN range and bearing data (when applicable), along with barometric altitude data, are heavily down-weighted due to the much smaller covariance matrix which reflects the accuracy of the GPS solution. Although GPS accuracy is comparable to MSBLS, MSBLS processing is still the prime navigation sensor from approximately 16,500 ft altitude to the ground.

It should be noted that the crew controls the updating of the state vector through a set of AUTO-FORCE-INHIBIT commands on horizontal display (SPEC 50), a CRT display used for control of navigation sensors and other functions for all external sensors except the MSBLS. AUTO indicates that a set of automatic logic should be used to determine if the sensor data should be used, INHIBIT indicates that the data should not be used, and FORCE indicates that the automatic logic should be overridden and the data should be used provided no failure has been detected by the fault detection, isolation, and reconfiguration (FDIR) logic.

Because the guidance and flight control need parameters that must be derived from navigation data at higher rates than those at which the outer loop is executed, a separate state (called the user parameter propagator [UPP] state) is maintained at 6.25 Hz. From this state, parameters such as range to the landing site, angle of attack, altitude, and altitude rate are estimated.

2.1.2 Guidance Techniques

During atmospheric flight, four guidance techniques are used: 1) entry, 2) terminal area energy management (TAEM), 3) approach and landing, or autoland, and 4) glide return to launch site (GRTLS). As part of the OI-8C primary software release, an automatic normal acceleration (Nz) control logic was added to the GRTLS guidance to support contingency abort operations. The first three techniques are used for nominal end of mission (NEOM) and the last two are used for RTLS abort mode. Plots of altitude, range, angle of attack, and roll angle as a function of relative velocity (reproduced from the operational flight profiles of STS-41D) are given in figure 2-4.

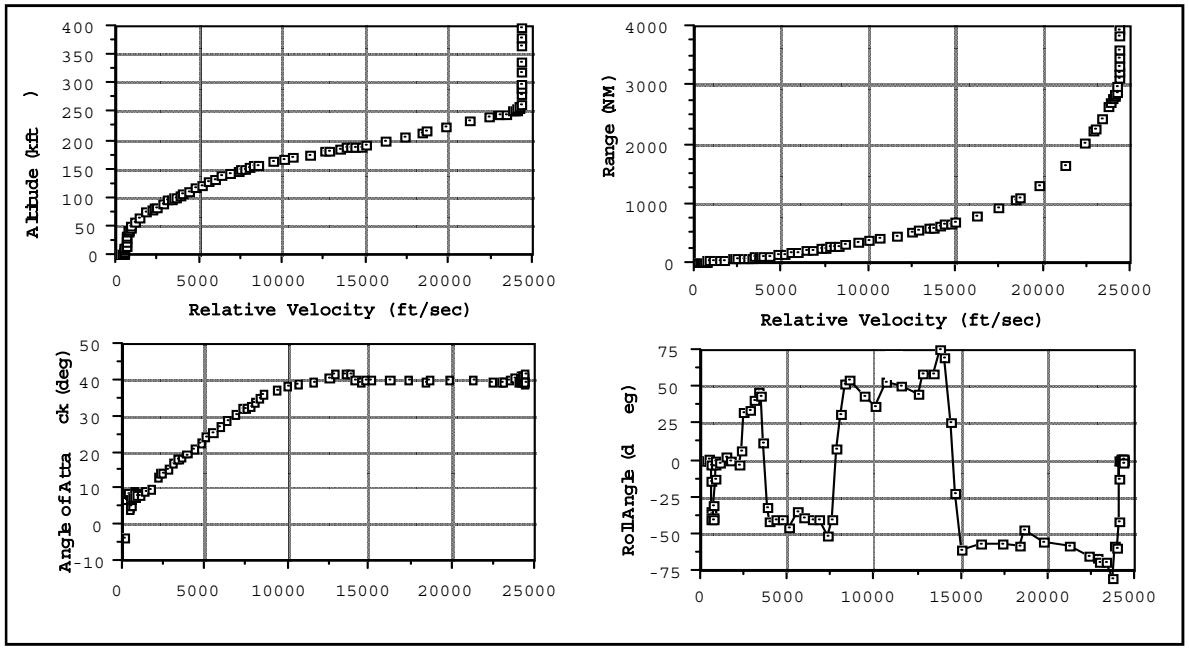

Figure 2-4. Nominal End of Mission Trajectory Parameters

The **Entry guidance** guides the Orbiter during software major mode (MM) 304 (entry interface to a relative velocity of 2,500 ft/sec). This guidance attempts to follow a desired drag-velocity profile using the following second order control law:

$$L/D_{des} = L/D_{ref} + C1*(Drag - Drag_{ref}) + C2*(Hdot - Hdot_{ref})$$
$$Roll_{cmd} = \cos^{-1}(L/D_{des} / L/D_{measured}) + K_{alpha}*(Alpha - Alpha_{ref})$$

A typical roll profile is charted in figure 2-4. Roll reversals are required to keep the Orbiter's relative velocity vector pointing toward the landing site. The number of reversals is determined by the initial cross range and velocity at entry interface. The alpha-related term in the $Roll_{cmd}$ computation is required to maintain the reference alpha profile. The actual alpha command is computed using the following equation.

$$Alpha_{cmd} = Alpha_{ref} + C3 * (Drag - Drag_{ref})$$

The C3 coefficient is set to zero during the very early part of entry to allow the system to settle onto the desired angle of attack. The alpha modulation logic is activated when the velocity is below a given value or the drag is above the reference value. If the delay until the reference value were not included, the system would immediately pitch up to the maximum allowed angle of attack.

An approximation of the nominal drag-velocity profile is given in figure 2-5. The drag level is selected to ensure that the trajectory parameters remain within the capability of the Orbiter's thermal, structural, propulsion, venting, and control systems. The software will iterate on the drag level until the predicted range potential of the trajectory matches the range to landing site computed by GUIDCOMP.

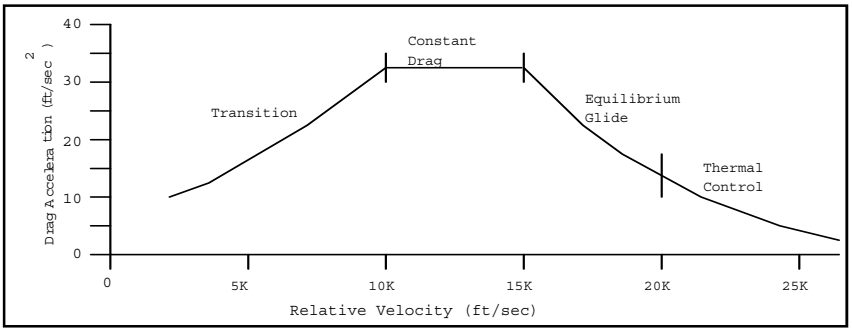

Figure 2-5. Typical Drag-Velocity Profile

There are two ways to initiate a roll reversal. The first is for the magnitude of the heading error to exceed the limits within the guidance (see figure 2-6). The second is for the pilot to manually roll the Orbiter to the opposite bank. When the guidance notes that the sign of the actual roll angle is different from the commanded roll angle and the heading error is within the programmed limits, the guidance assumes that the pilot has requested a reversal and changes the sign of the desired roll angle. This capability was added late in the STS-1 development cycle to allow the pilot to avoid reversals in selected flight regimes, or to keep the heading error small in low-energy cases.

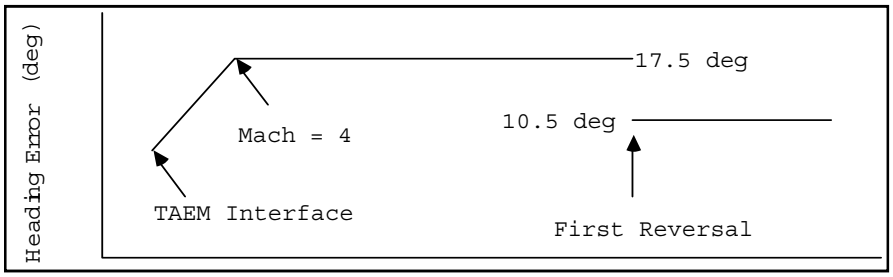

Figure 2-6. Heading Error Limits

The angle-of-attack command is derived primarily from an angle-of-attack versus relative-velocity profile with small deviations allowed to maintain the desired drag-velocity profile. A close look at the alpha profile in figure 2-4 shows transient increases after each roll reversal. The trajectory lofting that accompanies a roll through wings level causes a small reduction in dynamic pressure. The increase in alpha is required to increase the drag coefficient in proportion to the reduction in dynamic pressure. The profile is primarily derived to minimize heating during entry and, with the exception of a minor change starting with STS-6, the same profile has been used for all flights. As part of the contingency abort software upgrade after STS-51L, the capability to fly a longer range (lower angle-of attack profile) was added to support low-energy transatlantic abort landings (TALs). Figure 2-7 is an approximation of the reference nominal alpha profiles.

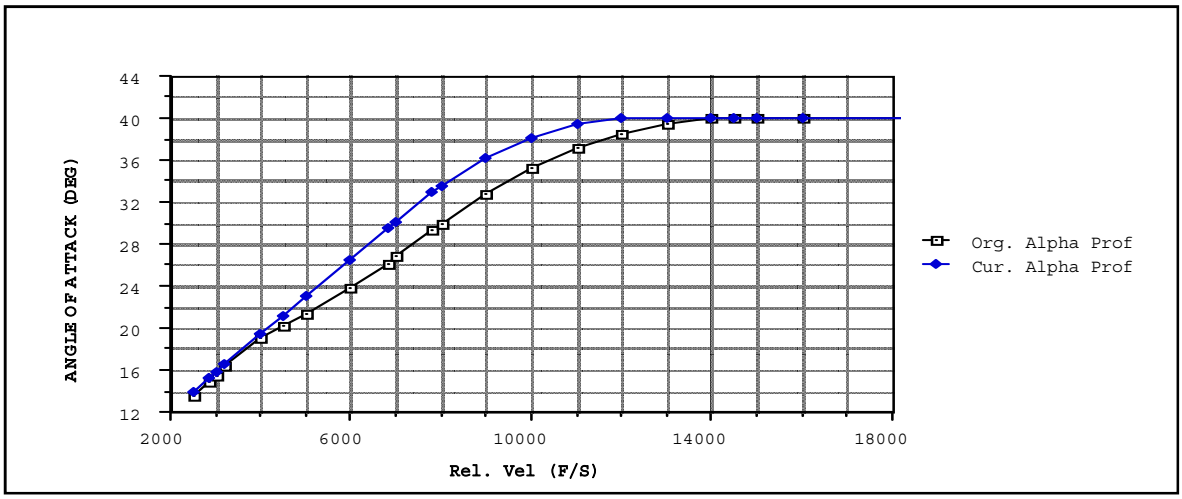

Figure 2-7. Reference Angle-of-Attack Profile

The **TAEM guidance** is used from the start of MM 305 until the transition to approach guidance between 10,000 ft and 5,000 ft. This guidance attempts to follow an altitude versus range to the runway profile in the vertical channel and a fixed ground track profile. It uses the roll angle to control the ground track and the normal acceleration (Nz) level to control the vertical channel profile. When the Orbiter is low in altitude, the Nz will be increased to reduce the energy loss rate (which assumes the vehicle is operating on the front side of the L/D curve). Similarly, the Nz level will be reduced to increase the energy loss rate when the Orbiter is high on altitude. The guidance will also constrain the Orbiter to stay within the Nz and Qbar limits. The Orbiter will fly a ground track similar to the profile shown in figure 2-8. The heading alignment cones (HACs) are normally positioned approximately 36,000 ft from the end of the runway.

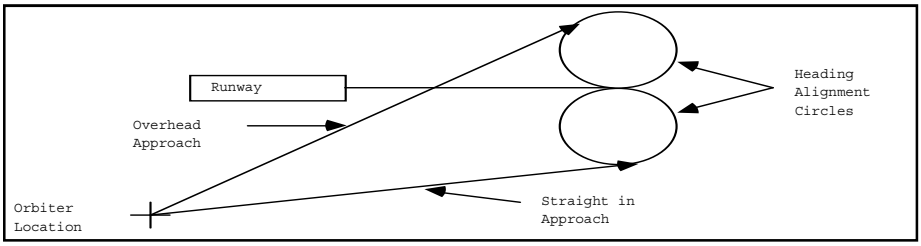

Figure 2-8. Typical TAEM Ground Track

The speedbrake is used to control airspeed directly once the Orbiter has gone subsonic. A modification to this logic to make the speedbrake an energy rate controller was implemented in OI-22, which resolved some wind-related concerns. In cases where the energy is extremely high, the guidance will increase the distance to be flown by banking the Orbiter to turn the velocity vector away from the HAC. This maneuver is referred to as an S-turn. For extremely low energy cases, the crew can direct the computer to move the HAC to 30,000 ft from the end of the runway to reduce the distance to be flown. In addition, the TAEM guidance will reduce the radius of the HAC from 15,000 ft to 5,000 ft to reduce the distance to be flown.

The **approach and landing guidance** controls the final part of the Orbiter flight profile. This guidance attempts to fly a fixed glide slope (17 or 19 deg) until the preflare maneuver at 2,000 ft, where the Orbiter transitions to a 1.5-deg inner glide slope. The 17-deg glide slope is used for weights greater than 220,000 lb; the 19-deg glide slope is used for lighter-weight landings. *(As part of a suite of approach and landing guidance updates made in 1993 to increase touchdown energy, the heavyweight and lightweight glide slopes were raised to 18 and 20 deg, respectively.)* At approximately 100 ft, the Orbiter executes a final flare maneuver. The speedbrake is used to control the Orbiter airspeed. A typical approach profile is shown in figure 2-9. Roll angle is used to align the Orbiter with the runway. Although Sperry (designers of the approach and landing guidance) completed all the analyses required to commit the Orbiter to an autoland for midrange weights, autoland demonstration tests have never been accomplished. However, the automatic landing system has been used to as low as 100 ft. The BFS does not include approach and landing guidance or MSBLS navigation.

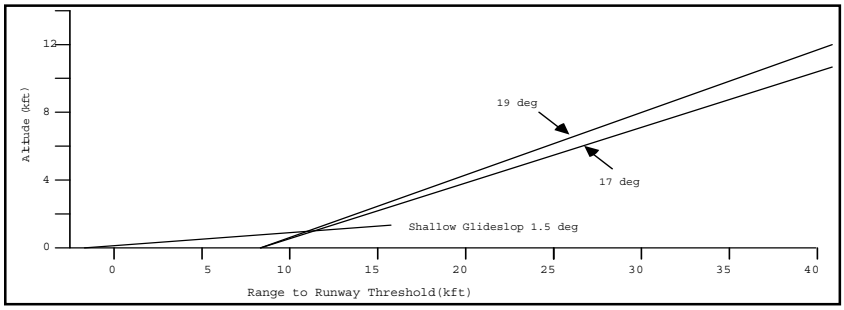

Figure 2-9. Autoland Range/Altitude Profiles

Upon sensing weight on main wheels (WOWLON) and the airspeed decreasing to a desired value (180 KEAS), a slapdown maneuver is executed by the pitch control system, the speedbrake is opened to provide aerobraking, and the lateral guidance is transferred to the yaw control logic. After nosegear touchdown, the elevons are commanded to provide load relief/load balancing, and lateral control to the runway centerline is accomplished by a combination of nosewheel steering and rudder control. The pilot may use the brakes to supplement the primary lateral control effectors.

The **GRTLS guidance** is sometimes referred to as the extended TAEM guidance because below 3,200 ft/sec (MM 603), the GRTLS guidance is almost exactly the same as the NEOM TAEM guidance. Figure 2-10 presents typical angle-of-attack and normal acceleration profiles during the GRTLS unique trajectory segment. To handle the flight phase (MM 602) between external tank separation (ET-SEP) and start of MM 603, three open-loop phases (alpha hold, Nz hold, and alpha transition) were added. These guidance phases attempt to control the plunge into the atmosphere caused by the low ratio of the Orbiter's inertial velocity to circular velocity at main engine cutoff (MECO). During the alpha hold phase (IPHASE 6), a constant angle of attack of 50 deg is held and the roll command is set to zero. During the Nz-hold phase (IPHASE 5), a constant normal acceleration level (2 g) is commanded and the roll

command is maintained at zero. The final open-loop phase, alpha transition (IPHASE 4), follows a fixed alpha relative velocity profile, and the roll angle is proportional to the angle between the relative velocity vector and the tangent to the desired HAC. The only energy control is the option to execute an S-turn in the alpha transition phase.

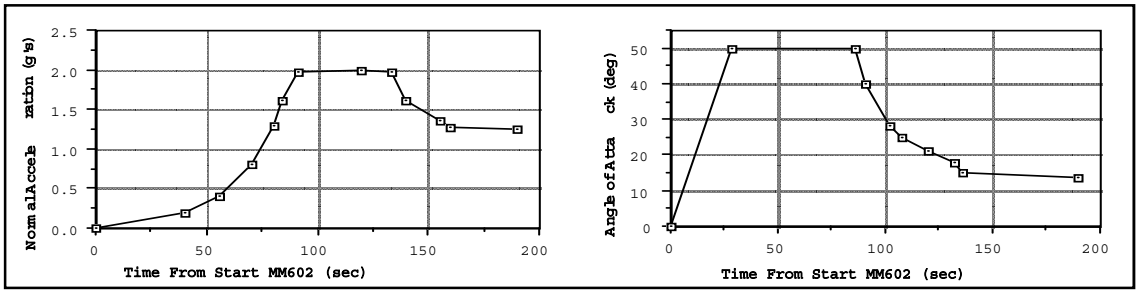

Figure 2-10. GRTLS Profile Parameters

2.2 Entry DAP Configuration

The DAP has both manual (with stability augmentation) and automatic modes that are selectable by axis (pitch, roll/yaw, or nosewheel steering) or by secondary effector (bodyflap or speedbrake). The pilot is free to mix and match modes for any combination. One of many possible combinations is auto-pitch, CSS-lateral, manual-speedbrake, and auto-bodyflap. Early in the program, a direct mode—which had elevator, aileron, and rudder commands directly proportional to the RHC and/or RPTA displacement (no feedback)—was evaluated and found not to be a flyable mode. The current manual mode, which is often referred to as the CSS (control stick steering) mode, is a rate-command system with almost the same rate damping stability loop that the automatic system uses. The automatic system replaces the RHC-generated rate commands with commanded rates computed from the errors in the body roll angle in the lateral axis, and either the angle of attack error or the Nz error in the pitch axis, depending on the flight phase. The RHC is used as a two-axis controller (no yaw input) to generate the desired pitch rate and the desired stability axis roll rate. Roll maneuvers are done while maintaining the desired angle of attack with minimum sideslip. This is accomplished by the addition of automatic turn coordination logic based on the set of desired stability axis rates. Normally, the desired stability axis yaw rate (- $ß_{dot}$) is zero. The equations used to convert body rates to stability axis rates follow:

$$P_{stability} = P_{body} \cos(alpha) + R_{body} \sin(alpha)$$

$$ß_{dot} = - R_{stability} = P_{body} \sin(alpha) - R_{body} \cos(alpha)$$

Simplified block diagrams of the pitch, roll, and yaw axes of the entry/GRTLS DAP are shown in figures 2-11, 2-12, and 2-13. These diagrams are based on the OI-8B software release. (Diagrams based on the OI-25 and OI-27 software releases are shown in Appendix D.) As shown in these simplified diagrams, each axis can be divided into five basic elements: 1) rate command computation logic, 2) shaping gains and filters, 3) trim logic, 4) bending suppression, and 5) command limiting. Typically, the inner stability loops (rate damping) and RHC operations are done at 25 Hz by the computer, while the guidance interface blocks are done at 6.25 Hz. The RCS jet computations are done at 12.5 Hz to provide a minimum ON time of 80 msec.

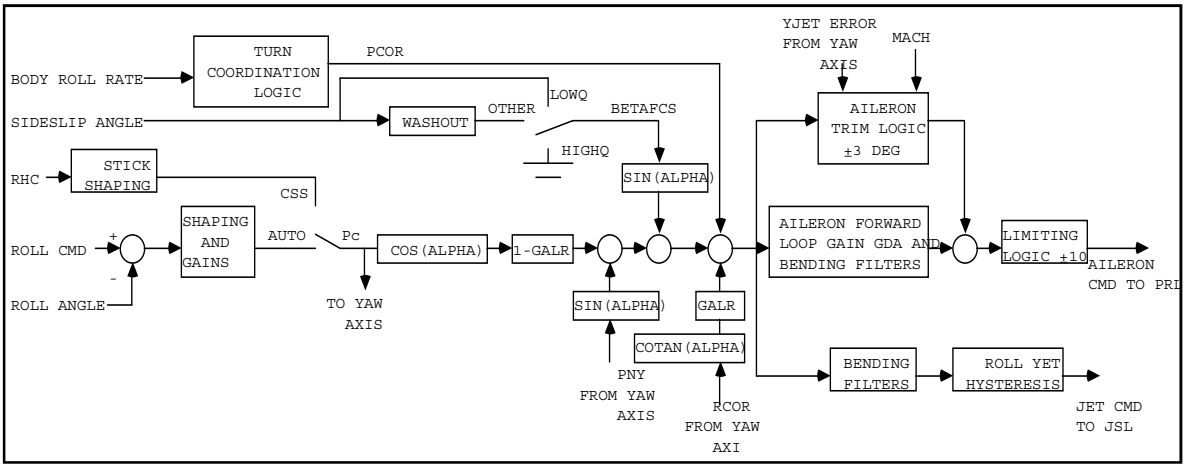

Figure 2-11. Simplified Roll Axis Block Diagram

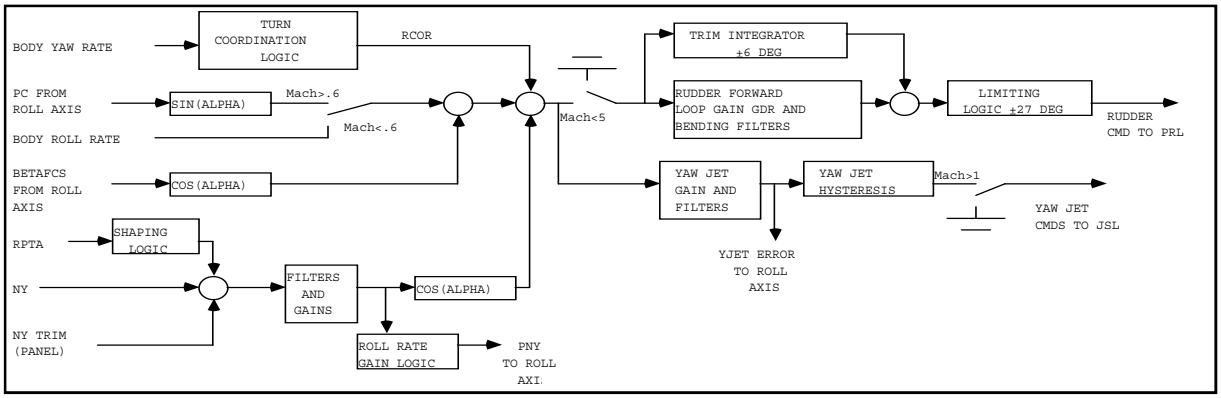

Figure 2-12. Simplified Yaw Axis Block Diagram

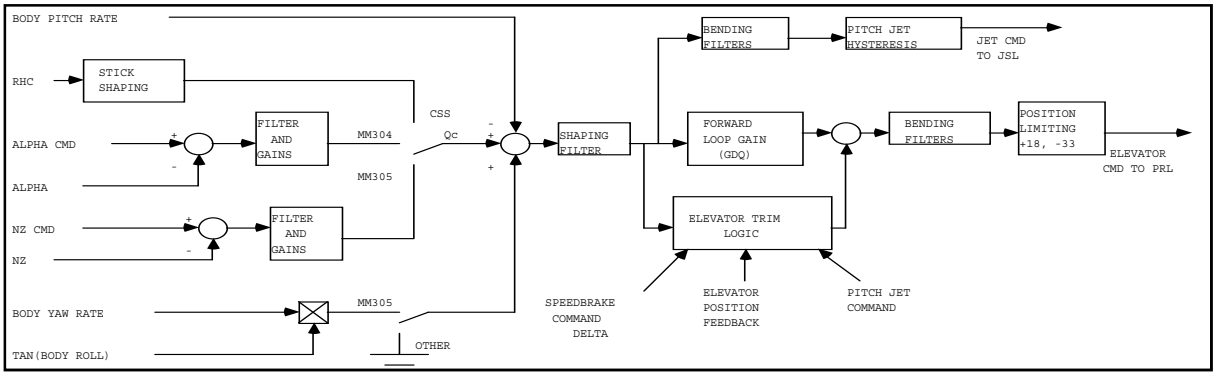

Figure 2-13. Simplified Pitch Axis Block Diagram

The high degree of interaction between the roll and yaw axis control logic has resulted in the combination referred to as the lateral axis, and all stability and response analysis is conducted for a combination of the two axes.

The elevator trim logic consists of two distinct sets. During the initial phase of entry, a forward-loop integrator using the shaped pitch rate error and pitch jet command as input is used to compute the trim position for the elevator. After the high-Qbar flag (Qbar > I-load) has been set true, the output of a lag filter (for which the input is the current sensed elevator position), is used for trim. It should be noted that during GRTLS only the lagged elevator position logic is used.

The pilot can lower the surface (elevator, aileron, and rudder) forward loop gains by selecting the "low gain" position on the entry roll mode switch. By using the same switch, the pilot can select the "no-yaw-jet" mode. When this mode is selected, the lateral axis will be immediately changed to the CSS mode. These two options are the remains of the extensive entry "downmoding" capability that existed for the first five flights. None of the original or current downmoding logic has been used in flight.

The pilot also has the option, using the "beep" trim on the RHC, to input a steady-state pitch or stability roll rate command. Currently, this capability has never been used in flight, nor is its use planned. There is no way to monitor the exact value of the integrators that compute the beep rate command. Therefore, once a rate has been trimmed into the system, there is no way to be sure the command has been removed without going from CSS to automatic and back to CSS. (This action will cause the integrators to be reinitialized to zero.) A more useful capability, which has not been used in flight, is that to manually aid the trimming process. This is done using momentary panel switches that are gained and summed with the normal signals that make up the inputs in the aileron and elevator trim integrators. The outputs of aileron and rudder trim integrators are displayed to the flight crews on the entry trajectory displays.

Although the pilot does not have a direct input into the rudder integrator, he or she can bias the lateral acceleration (Ny) that the DAP is trying to maintain. This could be extremely useful in nulling the effects of a large bias in the lateral accelerometer output. The values of the Ny bias and the measured Ny are displayed to the pilot on the trajectory displays. The pilot has the capability to actively command a lateral acceleration by deflecting the rudder pedals. This command is executed by using the rudder and yaw jets (Mach > 1) in all flight phases below Mach 5 and by using the rudder and nosewheel during rollout.

2.3 Trajectories and Events[1]

Key events in the NEOM profile are listed in table 2-1. The locations of some NEOM events relative to basic trajectory parameters are shown in figure 2-14. An abort-once-around (AOA) has the same events as NEOM, whereas TAL mode has the additional events listed in table 2-2.

[1] *The following figures and tables may indicate bodyflap activation at Qbar=0.5 and other events at Qbar=20. Bodyflap activation has been updated to Qbar=2.0, and all DAP RECON HIGHQ events to Qbar=40, as discussed in Section 6.1.*

Table 2-1. Key Events in NEOM Profile[1]

Event	Action
1. PRO to MM 304	Start Entry Software
	Maneuver to Alpha = 40 and Roll = 0
2. Dynamic Pressure = .5 psf	Activate Bodyflap
3. Dynamic Pressure = 2 psf	Activate Elevator And Aileron
	Activate Beta Washout Logic
4. Dynamic Pressure = 8 psf	Activate Entry Guidance
5. Dynamic Pressure = 10 psf	Deactivate Roll Jets
6. Dynamic Pressure = 20 psf	Deactivate Beta Logic
	Activate Ny Logic
	Allow 4 Yaw Jets To Fire
7. Dynamic Pressure = 40 psf	Deactivate Pitch Jets
	Use Elevator Feedback for Pitch Trim
8. Mach = 12	Start Ramp to Front Side of L/D Curve
9. Mach = 10	Start Opening of Speedbrake
10. Mach = 5	Activate Rudder
	Deploy Air Data Probes
11. Mach = 4	Start Transition to Normal Aileron Control (GALR)
12. Altitude = 125,000 ft	Increase RCS Jet Minimum ON Time to 320 msec
13. Mach = 2.5	Start MM 305
	Activate TAEM Guidance
	Incorporate Measured Air Data Information
14. Mach = 1	Deactivate Yaw Jets
	Activate Lower Order Bending Filters
15. Mach = .95	Start Using Speedbrake for Energy Control
16. Mach = .6	Start Using Body Roll Rate in Yaw Channel
17. Altitude = 14,000 ft	Acquire MSBLS to Update Navigation State
18. Altitude = 10,000 ft	Transition to Approach Landing Guidance
	Move Bodyflap to Trail
19. Altitude = 3,500-500 ft	Terminate Active Speedbrake Energy Control
20. Altitude = 200 ft	Deploy Landing Gear
21. Main Gear Touchdown	Transition to Slapdown Logic (WOWLON)
22. Nose Gear Touchdown	Transition to Rollout Logic
	Activate Nosewheel Steering
	Activate Load Relief
23. 140 KEAS	Start Manual Braking

[1] *Post 1992 updates to approach and landing events:*

19a. Altitude = 3000 ft Retract Speedbrake
19b. Altitude = 500 ft Adjust Speedbrake
20. Altitude = 300 ft Deploy Landing Gear

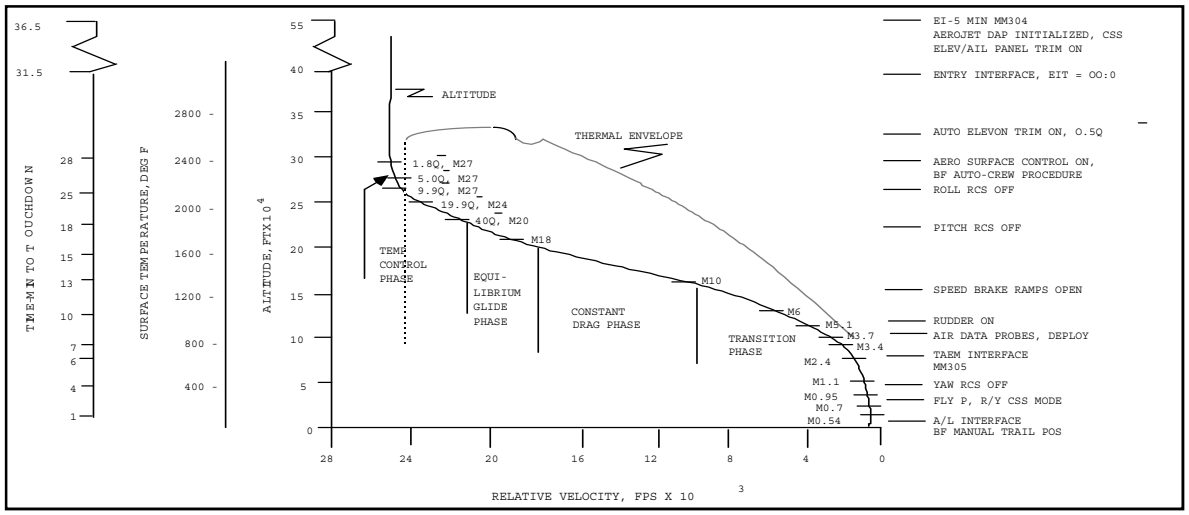

Figure 2-14. Nominal End-of-Mission Events

Table 2-2. Additional Key Events in TAL Profile

	Event	Action
1.	Enter MM 304,	Start Main Oxidizer Valve (MOV) and RTLS 1½ in LH_2 Dump Open 8 inch LH_2 Fill and Drain Valve Activate TAL Unique FCS Logic
2.	MM 304 + approx. 20 sec,	Start Nominal 100 ft/sec OMS Burn
3.	Dynamic Pressure = 2 psf,	Activate Bodyflap
4.	Mach = 20,	Open 8 inch LO_2 Fill and Drain Valve Deactivate TAL Unique FCS Logic
5.	Mach = 8,	Start +X RCS Dump

The surface temperature data shown in figure 2-14 is for the stagnation point on a reference sphere. Various points on the Orbiter may be at higher or lower temperatures, depending on the local flow field. Early in the program, a simplified heating model was developed for use in the GN&C design and evaluation and trajectory simulations. This model has been very useful as a trend indicator in evaluating various change proposals and in the design of the nominal descent profiles. Figure 2-14 shows the various entry guidance phases and MM 304 and 305 interface. Care should be taken in using the time-to-touchdown scale because of the nonlinearity in the points used to make the plot.

The locations of some GRTLS events relative to basic trajectory parameters are shown in figure 2-15. The large difference in the altitude-versus-relative-velocity profiles for GRTLS and NEOM is evident. Key events in the GRTLS profile are listed in table 2-3.

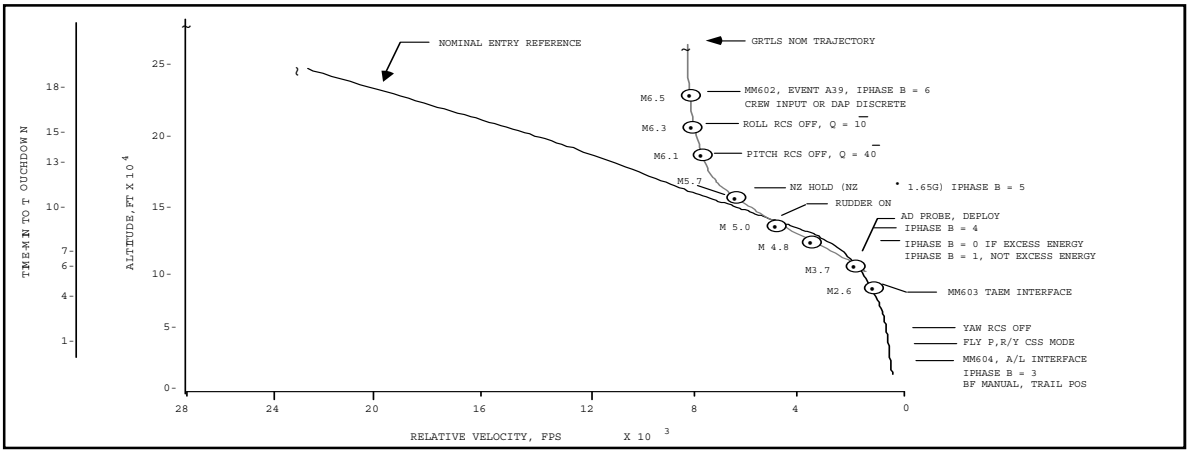

Figure 2-15. GRTLS Events

Table 2-3. Key Events in GRTLS Profile[1]

	Event	Action
1.	ET-SEP + 10 sec and	Start GRTLS Software (MM 602)
	alpha > 10 deg	Activate Bodyflap
		Activate Elevator and Aileron
		Activate Beta Washout Logic
		Start Alpha Recovery Phase (IPHASE = 6)
		Start MOV and RTLS 1½ in LH_2 Dump
		Use Elevator Feedback for Pitch Trim
2	MM 602 + 20 sec	Start +X RCS Dump
		Alpha = 50 deg.
		Start Opening Speedbrake
3.	Dynamic Pressure = 10 psf	Deactivate Roll Jets
4.	Dynamic Pressure = 20 psf	Activate Ny Logic
		Allow 4 Yaw Jets to Fire
		Open LH_2 and LO_2 8 inch Fill-and-Drain Valves
5.	Dynamic Pressure = 40 psf	Deactivate Pitch Jets
6.	Nz = 2g	Start Nz Hold Phase (IPHASE = 5)
7.	Hdot > -250 ft/sec	Start Alpha Transition Phase (IPHASE = 4)
8.	Mach = 5	Activate Rudder
		Deploy Air Data Probes
9.	Mach = 4	Transition to Normal Aileron Control (GALR)
10.	Altitude = 125,000 ft	Increase RCS Jet Minimum ON Time to 320 msec
11.	Mach = 3.2	Start MM 603
		Activate TAEM Guidance
12.	Mach = 2.5	Incorporate Measured Air Data Information
13.	Mach = 1	Deactivate Yaw Jets
		Activate Reduced Order Bending Filters
14.	Mach = .95	Start Using Speedbrake for Energy Control
15.	Mach = .6	Start Using Body Roll Rate in Yaw Channel
16.	Altitude = 14,000 ft	Acquire MSBLS to Update Navigation State
17.	Altitude = 10,000 ft	Transition to Approach Landing Guidance
		Move Bodyflap to Trail
18.	Altitude = 3500-500 ft	Terminate Active Speedbrake Energy Control
19.	Altitude = 200 ft	Deploy Landing Gear
20.	Main Gear Touchdown	Transition to Slapdown Logic
21.	Nosegear Touchdown	Transition to Rollout Logic
		Activate Nosewheel Steering
		Activate Load Relief
22.	140 KEAS	Start Manual Braking

[1] *Post 1992 updates to approach and landing events:*

19a. Altitude 3000 ft — Retract Speedbrake
19b. Altitude 500 ft — Adjust Speedbrake
20. Altitude 300 ft — Deploy Landing Gear

2.4 Sensors and Effectors

As can be seen in nominal and intact abort trajectory profiles, the entry and GTRLS DAPs have to function over a variety of flight regimes (between Mach 25 and wheels stop, angles of attack of -4 deg (rollout) to 50 deg (GRTLS abort), and dynamic pressures from 0 to 375 psf) with changing effectors and sensors. Because the sequencing logic between flight regimes is extremely critical, considerable design effort was required to smooth these transitions. Even though they are not normally considered to be control effectors, the brakes were used as the primary lateral control effector during rollout on all flights before STS-61A.

Early in the program, other effectors such as canards, tip fins, and ventral fins were evaluated, but were not incorporated into the final design for various reasons (such as complexity, weight, and cost).

2.4.1 Effectors

During entry, the Orbiter FCS uses a combination of aerodynamic surfaces and aft-mounted reaction control jets. Before entering the sensible atmosphere, the DAP is configured for all-RCS operation and

then sequences to a hybrid RCS-plus-surface system. Finally, at Mach 1, the system terminates use of the yaw jets and becomes a surface-only system. Figure 2-16 presents a graphical layout of effector utilization criteria. The regions shown are based on the STS-26 return-to-flight configuration. The effectors and the regions in which they are used are shown in table 2-4 (surface) and table 2-5 (RCS).

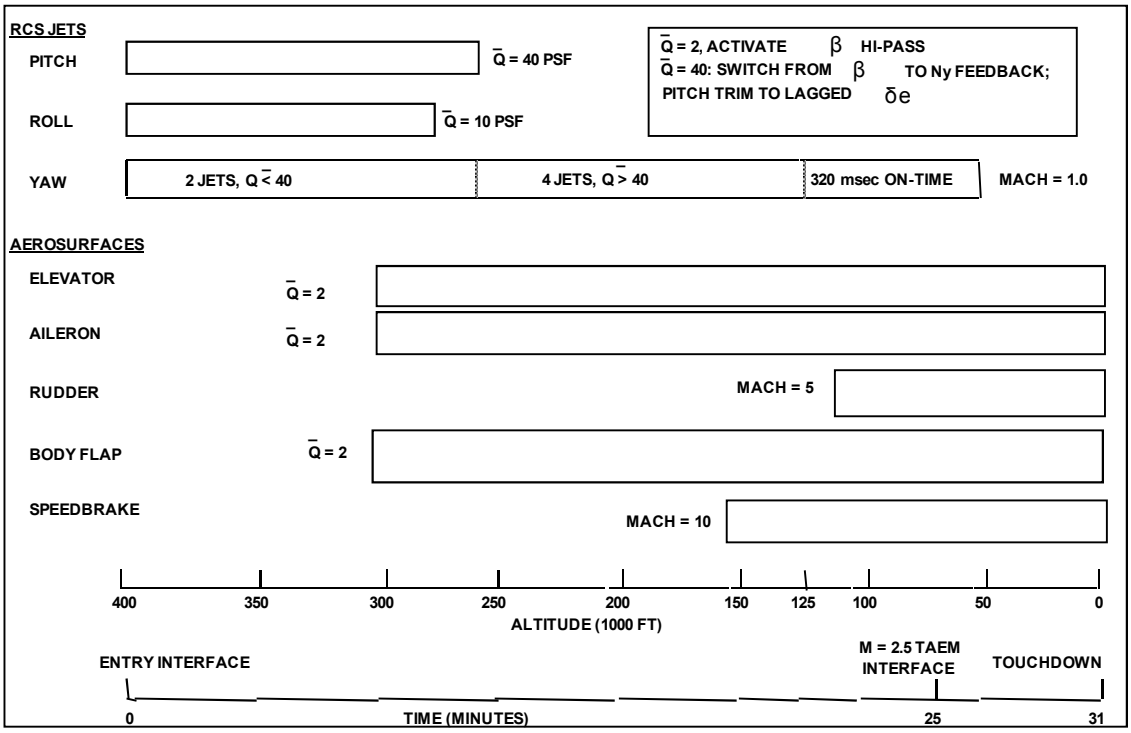

Figure 2-16. Entry Effector Utilization

Table 2-4. Actuator-Driven Effectors

EFFECTOR	REGION	USAGE
ELEVATOR	QBAR > 2	PITCH ATTITUDE/RATE CONTROL PITCH TRIM LOAD RELIEF DURING ROLLOUT
AILERON	QBAR > 2	ROLL ATTITUDE/RATE CONTROL YAW TRIM – MACH > 3.5 ROLL TRIM – MACH < 3.5
RUDDER	MACH < 5	YAW ATTITUDE/RATE/ACCEL CONTROL YAW TRIM – MACH < 5
BODY FLAP	QBAR > 0.5 *(OI-26 UPDATE: QBAR > 2)*	MAINTAIN ELEVATOR ON SCHEDULE
SPEEDBRAKE	MACH < 10	MAINTAIN ELEVATOR IN DESIRED LOCATION ENERGY CONTROL (MACH < 0.95) PROVIDE NOSE-UP MOMENT DURING SLAPDOWN ADDITIONAL DRAG DURING ROLLOUT
NOSEWHEEL	ROLLOUT	MAINTAIN LATERAL CONTROL ON RUNWAY
BRAKES	ROLLOUT	MAINTAIN LATERAL CONTROL ON RUNWAY STOP VEHICLE

Table 2-5. RCS Effectors

UNIT	REGION	USAGE
ROLL JETS (2, 4)	QBAR < 10	ROLL ATTITUDE/RATE CONTROL
PITCH JETS (2, 4)	QBAR < 40	PITCH ATTITUDE/RATE CONTROL
YAW JETS (2, 3, 4)	MACH > 1 (H > 80K)	YAW ATTITUDE/RATE/ACCEL CONTROL
AFT JETS (4)	MACH < 8 QBAR > 20	DUMP FOR CG/WEIGHT CONTROL ON ABORTS
FWD YAW JETS (2, 4)	MACH < 15 QBAR > 20	DUMP FOR CG-WEIGHT CONTROL ON ABORTS (NOT TO BE USED UNTIL PTI PROGRAM COMPLETED

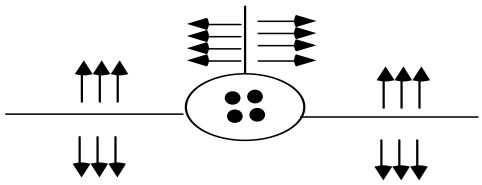

It should be pointed out that the aileron and elevator commands are implemented using the same surfaces. The Orbiter has four elevons (two on each side) that are moved symmetrically for elevator and antisymmetrically for aileron control. Similarly, rudder and speedbrake are obtained using common physical surfaces. The panels are moved symmetrically for speedbrake and antisymmetrically for rudder. Unlike the elevons, the rudder and the speedbrake have different drive units. The equations for computing aileron, elevator, speedbrake, and rudder from the physical surface deflections are given in table 2-6.

Table 2-6. Aerodynamic Surface Position Computations

Elevator	=	$(\text{Elevon}_{left} + \text{Elevon}_{right}) / 2$
Aileron	=	$(\text{Elevon}_{left} - \text{Elevon}_{right}) / 2$
Speedbrake	=	$\text{Panel}_{left} - \text{Panel}_{right}$
Rudder	=	$(\text{Panel}_{left} + \text{Panel}_{right}) / 2$

Each of the primary actuator systems receives four independent commands (which will be equal if the computer system is working correctly) from the data processing system. Built into each actuator is a hydraulic fault detection and isolation system which has the authority to bypass one of the channels when a failure has been detected and isolated. The pilot has the ability to override the automatic FDIR logic and either bypass a channel or prevent the system from bypassing a system it perceives to have failed.

The aerodynamic surfaces are driven by a set of three independent hydraulic systems that are powered by three auxiliary power units (APUs). The FCS uses a software rate and authority limiting function—priority rate limiting (PRL)—to maintain the commanded surface rates within the capability of the hydraulic system. Figure 2-17 shows how the load is distributed between the hydraulic systems during nominal operation. In this figure, the following notations are used: the symbols "A," "S1," and "S2" indicate which hydraulic system is the active system, primary standby, and the secondary standby, respectively, for each of the primary control effectors. If any of the systems fail, switching valves automatically start using one of the other systems for the effectors that had been using the failed system. Currently, only system 1 can supply flow to support the nosewheel steering system.

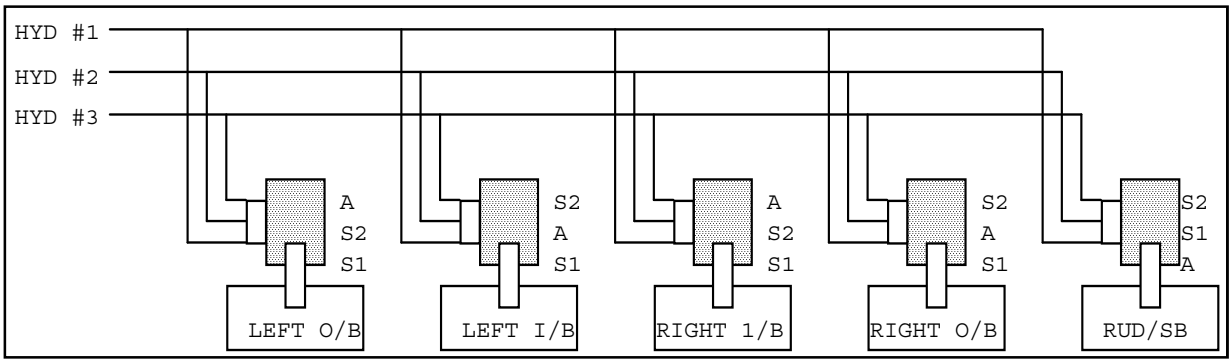

Figure 2-17. Surface/Hydraulic System Configuration

The system was designed to supply the required power with one failure and only a small reduction in rudder rate capability, and no reduction in elevon rate capability. Table 2-7 lists the maximum surface rates as a function of the number of working hydraulic systems. When two failures have occurred, the system will continue to operate, but at significantly reduced surface rates. (The FCS system has not been certified for operating with only one APU, but simulations have shown that the system is acceptable except for some large crosswind cases at landing. The probability of a pilot-induced oscillation (PIO) is greater under single-APU operation.)

Table 2-7. Surface Rate Limits[1]

SURFACE	3 SYSTEMS	2 SYSTEMS	1 SYSTEM
Elevator	20 deg/sec	20 deg/sec	13.9 deg/sec
Aileron	20 deg/sec	20 deg/sec	13.9 deg/sec
Rudder	14 deg/sec	12 deg/sec	7 deg/sec
Speedbrake	10.86 deg/sec	10.86 deg/sec	3.8 deg/sec

Early in the program, it was recognized that the surface forward-loop gains had to be a function of Mach, angle of attack, and dynamic pressure to account for the changing surface effectiveness. This was accomplished by directly scheduling the gains with Mach number and dividing them by either the dynamic pressure (on aileron and rudder) or the square root of the dynamic pressure (on elevator) to remove the dynamic pressure effects. The square root formulation was used in the pitch channel to reduce the effects of errors in the estimation of dynamic pressure. Direct scheduling with angle of attack was found

[1] Table 6-10 contains 2009 updated values of the surface rate limits.

to be necessary (a by-product of flying fixed alpha Mach profiles) only in the aileron channel during a small segment of a GRTLS trajectory (discussed in detail in Section 3.2.7 as one of the STS-6 updates). In all cases, gain limits, after the division by dynamic pressure, were included in the formulation to prevent excessive rate requirements. These limits were necessary to prevent excessive surface motion that could reduce the FCS structural attenuations or saturate control authority.

The entry DAP uses only the aft side and up/down firing jets for control, but contains the logic to dump excess propellants through the forward yaw jets or the +X aft jets. The jets all have the same thrust level (approximately 870 lb force). Average rolling and pitching moments from one up-down jet are approximately 15,000 ft-lb and 30,000 ft-lb, respectively. (Canting of the down-jets results in slightly lower moments than from up-jets.) A single side jet produces a yawing moment of approximately 30,000 ft-lb. Unlike the on-orbit DAP, neither the entry nor the GRTLS DAPs take into account the translation accelerations from control firings, because the effect of the resultant translation accelerations is small compared to the aerodynamic effects. Included in table 2-5 is a depiction of the number of jets available in each direction (at a forward viewpoint from behind the Orbiter).

Two sets of tanks are capable of feeding the aft jets (one on the left and one on the right). Normally, the right tanks feed the right jets and left tanks the left jets, but the pilot has the capability to cross-feed the jets. In a left-to-right cross-feed, all the jets are being fed by the left tanks, and in a right-to-left cross-feed, all the jets are being fed by the right tanks. When a cross-feed is in operation, the DAP limits the number of jets being fired for control purposes to a maximum of four, otherwise the limit is four jets per pod. *CR 93086A, implemented in OI-33, changes these limits to seven for GRTLS (see the FCAN 1 paragraph in Section 7.5).* The jet selection logic (JSL) in the software gives priority to up/down jet commands over yaw jet commands when all commands cannot be satisfied. Jets being used for dumping are not included in the limit. (This was an oversight in the original design and has been addressed during the return-to-flight activities.)

The numbers under each jet type in table 2-5 indicate the levels of command the flight control system is allowed to send to the JSL. The JSL is a set of software that takes the roll, pitch, and yaw jet commands and selects the optimum jet combination to satisfy the commands. The tank constraints (maximum number of jets from a single tank) are protected by this software module.

2.4.2 Sensors

The Orbiter sensors for entry can be divided into two groups—navigation and flight control—based on their primary usage. The rate gyro assemblies (RGAs), accelerometers (AAs), and ADTAs are considered the primary FCS sensors, but without accurate navigation data, the control system would not function: loss of state vector data or attitude data would result in loss of the Orbiter. The primary navigation sensors are the IMU, TACANs, and MSBLS. A pair of radar altimeters is used for display only during the final phase of landing. A summary of primary FCS sensor usage is given in table 2-8.

Table 2-8. FCS Sensors

SENSOR	PARAMETER	USAGE
RATE GYROS (4 SETS)	INERTIAL ANGULAR RATES (P, Q, R)	INNER LOOP RATE DAMPING ATTITUDE RATE FILL LOGIC DISPLAY
LINEAR ACCELEROMETERS (4 SETS)	LINEAR ACCELERATIONS (NY AND NZ)	LATERAL CONTROL GUIDANCE COMMANDS DISPLAY
AIR DATA (2 UNITS)	MEASURED AIR DATA PARAMETERS – MACH < 2.5 (MACH, QBAR, ALPHA, TAS, EAS)	GAIN SCHEDULING TURN COORDINATION ATTITUDE LIMITING DISPLAY
IMU (3 UNITS)	ATTITUDE AND ACCELERATION (POSITION, VELOCITY, ATTITUDE AND AIR DATA)	GAIN SCHEDULING ATTITUDE LIMITING TURN COORDINATION DISPLAY

Selection and placement of flight-control-related sensors were key design decisions. Placement is important because of the need to obtain rigid body rates and acceleration data for the control system. The RGAs were moved to the payload bay aft 1307 bulkhead on the main spar because of problems with local structural modes found during the hot fire vehicle before STS-1. (Section 4 contains a description of the ground tests and a summary of the results.) The accelerometers and IMUs are located in the front of the vehicle, *where the vibration and temperature environments are favorable*, on a hard mount to reduce the effects of local structural modes. For most analyses, the RGAs are modeled as first-order linear systems with a break frequency of 50 radians per second (rps). The AAs are modeled as second-order linear systems with a damping of .5 and a natural frequency of 15 rps cascaded with a 90 rps first-order lag. (Rigid-body-only simulations normally use only the second-order filter because of their low computation rates.)

Sampling frequencies for the sensors are 1) RGA and AA—25 Hz, 2) IMU accelerations—6.25 Hz, 3) IMU, gimbals and ADTA—1.04 Hz, 4) MSBLS—.5 Hz, and 5) TACAN—.25 Hz. These rates correspond to use by the on-board GN&C system, not to the frequencies at which the data are read by the avionics system. The transport delay from sensor read to force-effector write (multiplexer-demultiplexer [MDM] read to MDM write) is specified in the Level B Computer Program Development Specification (CPDS) as a function of such elements as MM or GN&C path. This is normally approximated for analysis purposes as half of the sampling interval.

Two air data probes are deployed at Mach 5 from each side of the vehicle through doors located just below and in front of the crew module. Each probe has two air data system computers to provide the required redundancy. The probes have been calibrated in wind tunnels only below Mach 2.5, and the software has been defined to limit use of measured air data to below Mach 2.5. These specifications are consistent with the ADTA calibration data. To remove the limit on the use of measured air data, the crew must execute an “item enter” on special keyboard key (SPEC) 50.

Early analyses and SPS simulations of the integrated GN&C system demonstrated the inability of the inertial navigation system to calculate acceptable dynamic pressure using the estimated altitude and velocity. An algorithm using the measured drag and a curve fit of the Orbiter drag coefficient was developed for use above 1,400 ft/sec. Below this point, a set of default values is used if the measured data is not available. The default values were determined by looking at the variation of dynamic pressure and angle of attack from sets of Monte Carlo runs, stability margins, performance tests, and MIL simulations. Default values were not included in the BFS because of core restrictions, a typical example of protection for multiple failures not being incorporated into the BFS software. The BFS requirements require single failure tolerance only.

2.4.3 Redundancy Management

Redundancy management is applied to the flight control sensors, manual controls, switches, actuator positions, steering damping system, RCS, and GPCs to ensure adequate FCS performance even if system failures occur.

For each type of sensor, logic was provided in both the PFS and BFS to select the best estimate of the actual value of a measured parameter. The PFS includes failure detection logic to identify failed units. The FDIR is normally executed at a low (1 to .5 Hz) rate, whereas the selection logic is executed at a high (6.25 to 25 Hz) rate.

The FDIR is based on the assumption that for a number of FDIR cycles, a failed unit will provide data significantly different from that of the remaining good units. The number of cycles and the magnitude of data difference before failure is declared depend on the type of sensor being processed. This assumption may not work if failure is near null (zero) or if a second unit fails before identification of the first failure. For example, it is almost impossible to identify a failed pitch RGA during entry because of the low values of pitch rate.

Three basic types of selection filters are used to compute the best estimate: 1) quad midvalue (four units), 2) midvalue (three units), and 3) averaging (two units). The averaging method simply takes the arithmetic average of the two units. The midvalue method selects the value in the middle of the three units, and the quad midvalue normally selects the unit in the middle with the larger magnitude of output. The quad midvalue logic, designed to handle dual null failure, was added after STS-4, when the Orbital Flight Test (OFT) program was completed. Because the BFS is required to be only one-fault tolerant, it uses only

the averaging and the midvalue filters; even when four units are available, the BFS uses only the first three. The one-fault-tolerant requirement may change when additional memory becomes available. The difference in BFS and PFS memory has caused extra crew training, analyses, and verification testing.

In orbital program segment (OPS) 3, the crew was given the capability to override the automatic FDIR logic via keyboard entries. Because of memory limitations, the same capability was not provided to the crew in OPS-1 through OPS-6 until upgraded computers (AP101S machines) and OI-20 became available in 1991.

2.5 Formal Verification Process

The planned formal verification process for the Orbiter entry/GRTLS FCS consisted of traditional stability analysis, time domain simulations, ground vehicle tests, and laboratory tests combining the flight system with models of the environment, sensors, and effectors in a real-time MIL simulation. Figure 2-18 diagrams the elements and flow of the process with the data requirements.

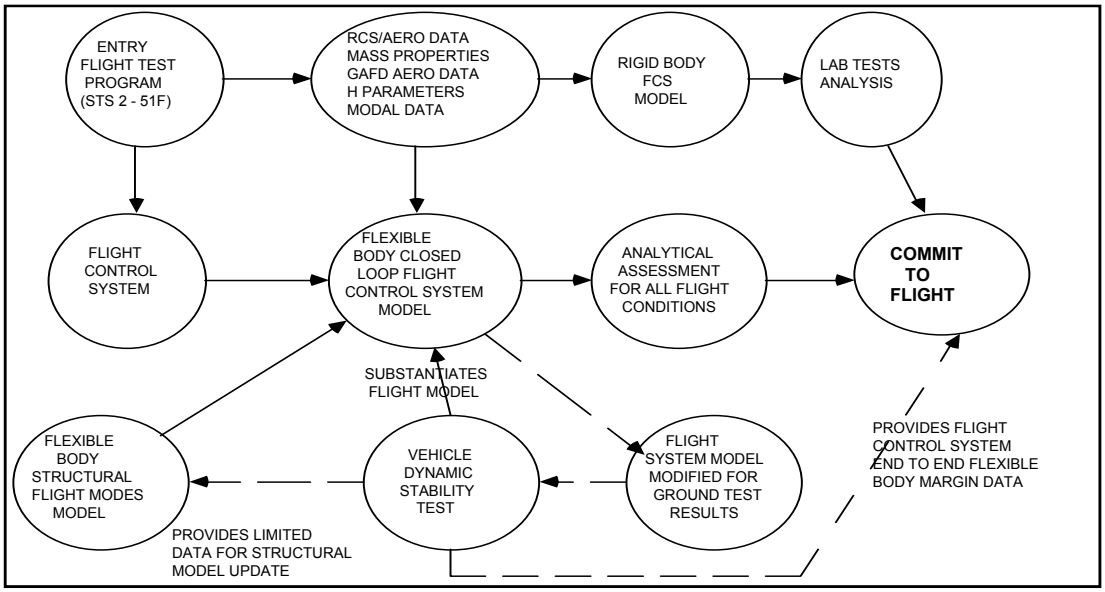

Figure 2-18. FCS Verification Elements

This diagram shows the flow of data into the analysis and tests for both the rigid- and flexible-body processes. Even though two paths are shown, the interplay between the paths is very important. The three key events leading to the commit-to-flight signoff were planned to be the vehicle ground test, FSL testing, and Honeywell analytical verification. The role of the aerodynamic flight test program in updating and validating the wind-tunnel-derived aerodynamic and RCS force and moment data is also included. This process led to changes in the database and in the FCS itself.

The same process (possibly reduced, depending on characteristics of the change) was followed in validating each change before it was incorporated into the FCS.

2.6 Acknowledgement of Key Individuals

The Space Shuttle entry DAP in use today is based on many years of work following authority to proceed in 1969. This effort has involved a large number and a wide variety of people. Participants are from Rockwell (prime contractor); Honeywell (subcontractor for FCS); Sperry (subcontractor for autoland); JSC civil servants and McDonnell Douglas and Lockheed support contractors; and other NASA centers with their subcontractors and consultants (Langley, Ames, DRFC, Draper Labs, STI) and support programs (such as the Calspan Total In-Flight Simulator [TIFS] and the Shuttle Training Aircraft [STA]). Although it is not possible to list everyone who had a significant impact on the design of the DAP, many key individuals are listed in Appendix B. Nor it is possible, for purposes of this document, to list all the individuals contributing to the design of the DAP in their roles as technical sponsors of principal avionics elements (such as FCS line replaceable units [LRUs], displays & controls, air-data, and G&N) or as test pilots and

astronaut crew. Other NASA and contractor counterpart groups deserving recognition for their significant role in the FCS/DAP design, development, test, and evaluation (DDT&E) include AERO, Structures, Mission Ops and Natural Environments.

Some individuals with corporate memory are still available today, but most of the senior people have transferred to other assignments or retired, and many have died. Corporate memory is available in engineering documentation, and technical journal articles and conference papers, because the STS program was managed to be open and serve the public.

3.0 History

A complete written history of the evolution of the entry DAP would require hundreds of pages and the work of many individuals (some of whom have left the program). This summary can present only the basic programmatic requirements and an overview of the evolutionary process since the start of the Space Shuttle Program.

3.1 Requirements

It should be pointed out that although an Orbiter Flying Qualities Specification, JSC-07151 [JSC internal document], was authorized for distribution, NASA did not impose these or a classical set of design requirements (i.e., step response and phase and gain margins) on the prime contractor. The definition of the margins is shown on a typical phase-gain plot in figure 3-1.

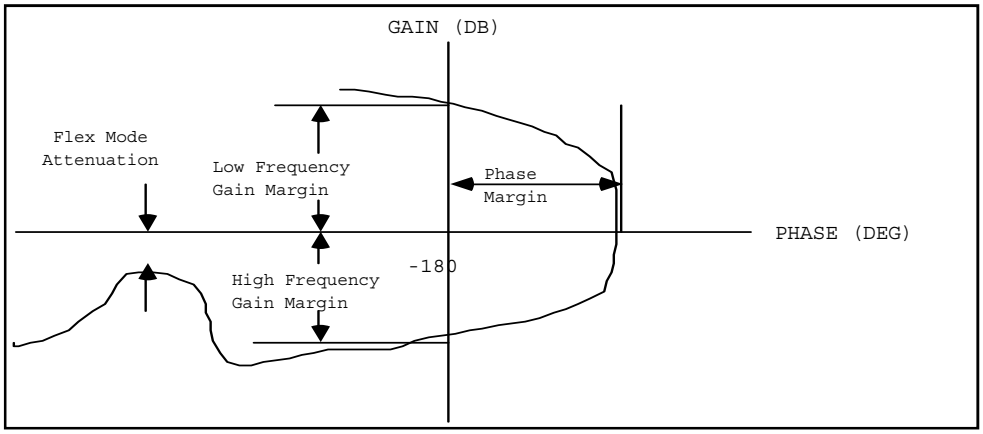

Figure 3-1. Control Stability Margins Definitions

The Level II and III requirements documents, NSTS 07700, Vol. X, and Orbiter vehicle end item (OVEI) specifications [JSC internal documents], simply state that the Orbiter shall have both automatic and manual modes during entry and landing, and shall not require piloting abilities greater than that of a high-performance land-based aircraft. One requirement given in Vol. X was a center-of-gravity (CG) envelope of 65 to 67.5%. Based on this requirement, Rockwell, with the concurrence of the JSC flight control community, placed the detailed stability and response requirements in the specification given to Honeywell in the Systems Definition Manual (SDM). Although the response envelope has been modified on several occasions as Orbiter characteristics evolved, the stability requirements listed in table 3-1 have remained largely unchanged.

Table 3-1. Stability Requirements

Rigid Body				
Axis	**Condition**	**Low Frequency Gain**	**Phase**	**High Frequency Gain**
Pitch	Nominal	6 dB	30 deg	6 dB
	Off-nominal*	4 dB	20 deg	4 dB
Lateral	Nominal	6 dB	30 deg	6 dB
	Off-nominal*	4 dB	20 deg	4 dB
* When worst-on-worst pre-STS-1 aero variations were included, the only requirement was that the pilot could maintain control.				

Flex Body		
	Condition	**Requirement**
Frequencies < 6 Hz*	Nominal system	6 dB gain and 30 deg phase margins
	Off-nominal system**	4 dB gain and 20 deg phase margins
Frequencies > 6 Hz	Nominal system	6 dB of gain attenuation
	Off-nominal system**	4 dB of gain attenuation
* Although the requirements allow phase stabilization, the original intent was to have attenuation for all flexible body modes. When the IUS upgrade was developed, phase stabilization was not accepted for the 3-Hz modes. ** 3-sigma on any parameter or 3-sigma composite (1.5-sigma on each parameter in worst combination).		

In cases where the linear flexible attenuation requirements were not met, Honeywell used SIMFLEX, a version of SIMEX that includes the effect of the Orbiter and payload structural characteristics to obtain nonlinear time domain data on the control system margins. The concern in these cases was the magnitude of the limit cycle, APU fuel usage, RCS consumables, and pilot loads. Cases with nominal flight control gains, as well as increased gains to verify the linear margins, were included in the typical run matrix. In some of the flexible body test cases, instead of changing the DAP gains, the test matrix included the effect of uncertainties in local structural deflections as well as other structural characteristics.

Based on various structural tests, the damping for each mode is specified separately. Early in the program it was assumed that all the modes had a damping of 1%, but this was ultimately found to be excessively conservative. Normally, 2% damping is used on the first Z-bending mode; 1.5% is used on wing-symmetric, wing-antisymmetric, and several other Orbiter modes; and 1% is used on the remaining modes. All payload modes are assumed to have 1% damping unless the payload supplier provides other data. The c*urrent (2009) Shuttle FCS Flex Engineering Analysis Standard Operating Procedure (Reference 3-1) assumes 1% damping on all Orbiter modes as well. Damping specifications for Orbiter structural modes are relaxed to the known damping ratios when the minimum modal attenuations are not met and damping relief is required.*

The response envelope contains restrictions on response delay, rise time, overshoot, settling time, and residual errors. These restrictions change as a function of the test point and the axis being evaluated. A typical response envelope for a unit input is shown in figure 3-2. The commands used in the response testing were angle of attack, normal acceleration, roll angle, pitch rate, yaw rate, and stability roll rate.

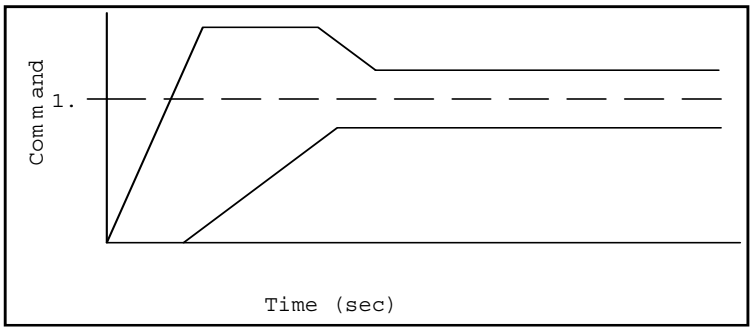

Figure 3-2. Typical Response Envelope

The basic guideline that designers and analysts used during design and verification was to maintain acceptable nominal stability, response, and handling quality characteristics while providing maximum coverage for off-nominal aerodynamics, environment conditions (atmosphere, mass properties, trajectory dispersions), systems, and structural characteristics. A summary of the analysis cases and simulation runs would show that a large majority of the cases included off-nominal items such as aerodynamics (lateral and longitudinal), navigation errors (alpha, beta, dynamic pressure, Mach), sensor and effector

characteristics (response, biases, failures), and structural characteristics (modal frequency, mode shape, damping). Concern for the possibility of encountering extreme off-nominal conditions led to the development of the extensive downmoding capability that existed during the orbital flight test program (STS-1 through STS-4) and the first operational flight (STS-5).

Computation bandwidth requirements were based on the requirement to actively stabilize the rigid body frequencies (less than 10 rps). This required a computation frequency of 25 samples per second (sps) (40 msec), which does not allow active stabilization of the structural modes of the Orbiter. In addition, a maximum transport delay on the inner stability loop of less than 20 msec was written in the Level A CPDS.

3.2 Evolution

The history of entry control system development can be divided into nine phases.

1) Entry 1 DAP (1975): the period before the first integrated DAP
2) The development of Entry 5 DAP (1978)
3) The aborted attempt to certify Entry 5 DAP for flight
4) Tiger team redesign/verification effort (1979-80)
5) Resolution of STS-1 anomalies
6) Addition of TAL for STS-3
7) STS-6 upgrade
8) Landing rollout upgrades (STS-9 and STS-61A)
9) Post-STS-51L upgrades

The three phases before STS-1 are sequential in time, but the six phases between STS-1 and STS-51L had some parallel activities. For example, the work to develop the Inertial Upper Stage (IUS) modifications paralleled the tiger team effort and resolution of STS-1 anomalies. Also, a number of major studies have been completed that provide a better understanding of the capabilities of the as-built entry FCS.

3.2.1 Development of Entry 1 DAP (1975)

From the start of Orbiter development until the first integrated entry DAP (a single DAP capable of flying from entry interface through rollout), the entry control work was divided into two groups: 1) the terminal area (TAEM and approach/landing) phase, with emphasis on the subsonic flight phase, and 2) the entry area, which worked basically in the high Mach region. The division point between these two areas was not well defined, and the method of lateral axis transition from an entry-type control system to a normal subsonic system was one of the major design issues. The early integrated DAPs had a discrete transition point based on a combination of Mach and angle of attack. Typical of this logic was a criterion such as Mach less than 3.5 and alpha less than 25 deg.

In the early days of the program, there were two approaches to rolling the Orbiter at high Mach and high alpha. The first was to use the “reverse aileron” (System 11) technique. This technique commanded the aileron to roll the Orbiter away from the desired direction in order to build a sideslip that would cause the Orbiter to roll in the direction desired. The strong adverse yaw ($-C_n$) aileron combined with the large roll due to sideslip were the physical reasons this approach worked. The second technique used the aft yaw jets (System 10) to induce the sideslip angle required to roll the Orbiter in the desired direction.

Because the Orbiter is not statically stable in yaw during supersonic flight, the parameter C_{n_β} Dynamic (C_{n_β}*) is used as a measure of the static restoring moment in the combined roll and yaw axis. The Orbiter design requirements specified (in NSTS 07700) that the unaugmented value of C_{n_β}* should remain positive (stable) throughout entry. The equation for C_{n_β}* is:

$$C_{n_\beta}{}^{*} = C_{n_\beta}\cos(\alpha) - \left(\frac{I_{ZZ}}{I_{XX}}\right)C_{l_\beta}\sin(\alpha)$$

The first integrated DAP (Entry 1) used the yaw jet (System 10) approach for two reasons: 1) pilots did not like the initial roll in the wrong direction and the increase in roll rate required to stop the maneuver, and 2) System 11 was more sensitive to uncertainties in the Orbiter aerodynamic characteristics. The

no-yaw-jet downmoding technique that was incorporated as a backup system before STS-1, and which has been upgraded as part of the post-STS-51L activities, is a derivative of System 11.

The low-speed part of the Entry 1 DAP was designed to roll the vehicle in the normal aircraft approach. Roll was controlled with the aileron and yaw with the rudder. This technique required at least a small negative yaw from the aileron or a positive yaw moment from the aileron and a good strong rudder.

The first block diagrams for the Entry 1 DAP were sketched by Guy Bayle and Earl Woosley just before their transfer to the ALT project. These diagrams were first implemented on the Crew Procedures Evaluation Simulator (CPES) in JSC building 5 for a short study. In parallel, the DAP was implemented by Ray DeVall on the SPS in JSC building 35. Between this time and the final definition of the Entry 5 system in 1978, the SPS would evolve into the primary design tool for the development of the entry autopilot. (In 1981, the SPS program was moved to a new computer in JSC building 16 and integrated with a new cockpit to form the current entry SES simulation.) Other simulations that would be used during this period were Howard Stone's entry simulation at Langley Research Center and the Shuttle Dynamics Simulation System (SDSS) in building 4 at Downey.

The pitch axis was a straightforward rate damping proportional plus integral system, with an outer loop that changed from an angle-of-attack controller to an Nz controller at TAEM interface. The automatic bodyflap channel was implemented as a trim channel to maintain the elevator on the desired schedule (function of Mach number), with capability for the pilot to manually position the bodyflap as desired.

The speedbrake channel provided automatic control either to a preflight-selected schedule as a function of Mach number (to position the elevator and bodyflap at the desired position), or to follow the TAEM or autoland speedbrake commands for energy control. It was found that energy control using the speedbrake could not be allowed above Mach 1 because its position had to be restricted to a small envelope to maintain proper elevator positioning for lateral control. Capability to manually position the speedbrake was also provided.

3.2.2 Development of Entry 5 DAP

During the 3 years between the first integrated DAP and the baselining of Entry 5 DAP, which was supposed to be the DAP for STS-1, a number of events forced the multiple redesigns. There are no clear records that provide definitions of each of the DAPs before formal documentation of the Entry 5 DAP. A number of configurations are documented in notes from meetings of the Entry FCS Mode Team. During this time, the aerodynamic and structural databases were updated. Effects of navigation errors, winds, aerodynamic uncertainties, RCS uncertainties, flexible body attenuation requirements, computer limitations (core and CPU), and systems constraints became part of the design database. Primary differences between the Entry 1 and Entry 5 DAPs and the issues that caused the changes are discussed in the following paragraphs.

Aerodynamic Uncertainties: One of the key items in the design process was Joe Gamble's identification of aerodynamic uncertainty combinations, each including a scale factor for each of the primary stability and control derivatives. These combinations were meant to identify the worst combination of derivatives for factors such as lateral trim, damping, minimum surface effectiveness, and maximum surface effectiveness. Joe Gamble published an internal JSC memorandum listing approximately 30 combinations. Over the years, the flight control community has come to refer to specific combinations by the number assigned to each set in the appendix to his memorandum. During an SPS simulation that lasted several months, it was found that the list could be reduced to approximately seven significant lateral directional variation sets. Figure 3-3 presents a graph of how the variation sets looked, and table 3-2 lists the scale factors associated with the major lateral directional variation sets.

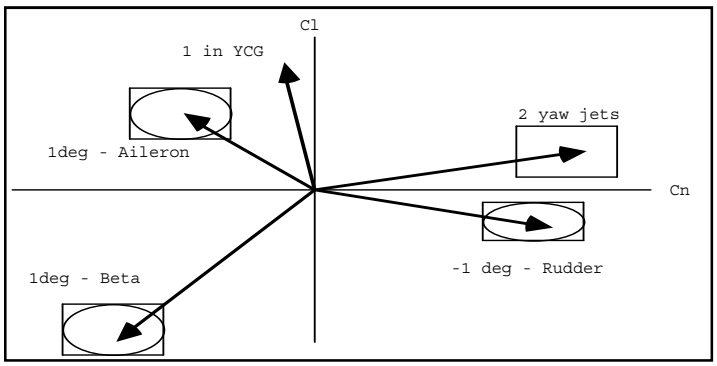

Figure 3-3. Example C_l and C_n Diagram

Table 3-2. Lateral Aerodynamic Variations Scale Factors

Var. No.	Sideslip		Aileron		Rudder		Yaw RCS		Pitch Mom
	C_l	C_n	C_l	C_n	C_l	C_n	C_l	C_n	C_m
2	-1	-1	+1	-1	-1	+1	+1	-1	+1
9	+1	-1	-1	-1	-1	+1	-1	-1	+1
11	-1	-1	-1	-1	-1	+1	-1	-1	+1
12	-1	+1	+1	+1	+1	-1	-1	+1	+1
19	-1	+1	-1	+1	-1	+1	+1	-1	-1
20	+1	-1	-1	+1	-1	+1	+1	-1	-1
23	+1	+1	-1	-1	-1	+1	-1	-1	+1

Before STS-1, the Williams Committees, a group of blue ribbon technical committees, were formed to review the Space Shuttle design, certification, and verification process. Dr. Duane McRuer was selected to head the Entry GN&C Committee. At the first meeting between Dr. McRuer and Milton Contella, the entry GN&C manager, the committee's first question was how the design and verification process was addressing uncertainties, especially those in aerodynamics. This question shows the importance the technical community put on the inclusion of off-nominal conditions in the design process.

Normally, a set of "bent airframe" biases was added to the total C_l and C_n to account for any asymmetries in the Orbiter airframe and the resultant flow around the vehicle. Numbers up to .0005 were used. Finally, a value of .00025 was baselined for design and verification studies when other uncertainties were included. The larger number, .0005, should be used without the uncertainties for design purposes. These parameters are very important in determining the lateral CG capability of the Orbiter. Flight data have shown that the full bent airframe does not exist over the entire profile, but a significant asymmetry can be seen as the flow over the bottom of the Orbiter transitions from laminar to turbulent. The pattern of changes, which varies from flight to flight, does not occur at the same Mach number for all flights. A transient can be seen in the aileron trim and the yaw RCS commands when the transition is in process.

The method of combining the variations was discussed in great detail. Two approaches were taken. Most of the design trade studies and analyses used the worst-on-worst rectangular variations, but it was ultimately decided that formal verification would use the worst-on-worst elliptical variations. The difference in the two approaches, illustrated in figure 3-3, is as follows: 1) the rectangular variations allowed the combined rolling and yawing moment uncertainty to be anywhere in a rectangle defined by the full yawing moment and rolling moment uncertainties; 2) the elliptical approach required the combined uncertainties to be within an ellipse defined by the magnitude of the rolling moment uncertainty, the yawing moment uncertainty, and the expected correlation between the uncertainties.

The vector diagram format in figure 3-3 was used extensively throughout the FCS community to visualize the various combinations of uncertainties. It should be noted that mapping from rectangular to elliptical is not a clean process: for example, elliptical 12 and rectangular 12 are not the same; elliptical 10 is the best match for rectangular 12. The best approach to understanding the relationship between rectangular and elliptical variations is the C_l vs. C_n plot shown in figure 3-3.

No acceptable technique has been devised to evaluate the effects of pitch axis stability derivative uncertainties in a time-domain simulation, although various techniques have been tried. The most

successful approach was to multiply the uncertainties by the output of washout filters on the elevator position and the current angle of attack. The primary challenge of this technique was to find a time-constant that was long enough to avoid adding a new dynamic element to the simulation and short enough to handle the transients induced by pilot inputs. Most of the work to evaluate the pitch aerodynamic stability derivative uncertainties (PVARs) has been done in the frequency domain, although some work has been done on the SPS, the SES, and the FSL.

Other longitudinal aerodynamic uncertainties used extensively in FCS and GN&C testing were those in lift force coefficient (CL) and drag force coefficient (CD). These parameters were prime drivers in causing variations from expected values of dynamic pressure during an entry or GRTLS profile. The aerodynamic community also included the maximum allowed variation in the CL-to-CD ratio. Figure 3-4 shows how CL and CD uncertainties were combined to stay within the allowed variation in the CL-to-CD ratio.

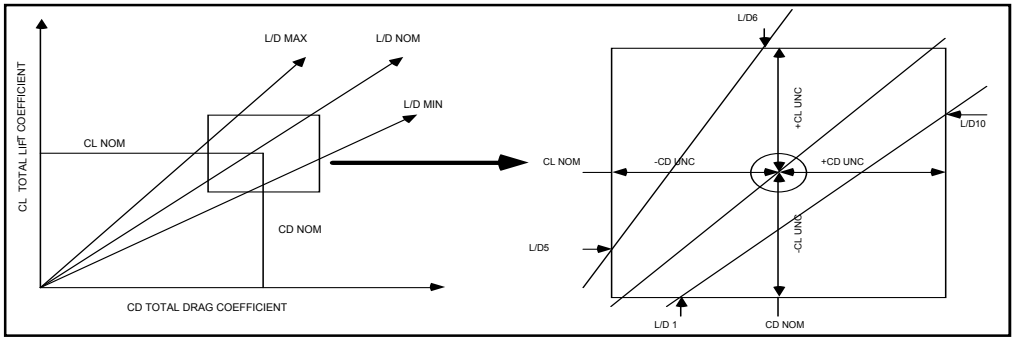

Figure 3-4. Combinations of Lift and Drag Uncertainties

The uncertainty in the lift-to-drag ratio (L/D) was reduced very quickly by analysis of flight data, because this ratio can be computed directly from IMU data, although the individual coefficients cannot be computed without knowledge of the environmental dynamic pressure. Thus reducing the individual coefficient uncertainties took longer.

Throughout the Orbiter development and verification program, it has been assumed that the lateral and longitudinal uncertainties were uncorrelated, and that the pitching moment uncertainty was not correlated with either.

A complete evaluation of all possible combinations of aerodynamic variations was not feasible with the tools that existed during this time period, and so has never been completed. (The new "mu" test system may make this type of evaluation possible for future programs.)

Alpha Error Effects: During the later part of the first SPS simulation, Howard Stone, from Langley, identified a case that resulted in loss of control in his lateral axis simulation. The case called for the following setup: lateral aerodynamic uncertainties (LVAR) set number 19, two yaw jets failed, and 4-deg error in alpha. The flight condition should be near Mach 7 on a nominal entry profile. The same case, when run on the SPS, resulted in a lateral divergence and loss of control. Additional runs made to further investigate the case revealed that control was lost with nominal aerodynamics and no jet failures when a roll reversal was attempted with a 4-deg alpha error. A detailed review of the data showed that the reason for the loss of control was that the alpha error caused the DAP to induce a steady increase in the sideslip angle during a roll maneuver (error in computation of desired body roll rate to match the commanded body yaw rate). The equation for the rate error is given below. This error would be integrated during the reversal to induce an increasing sideslip angle until the yawing moment from the induced sideslip became greater than the torque from the available yaw jets. At this point, control would be lost.

$$p_{error} = r * GALR * [\text{cotan}(\text{alpha}_{actual}) - \text{cotan}(\text{alpha}_{estimated})]$$

It was at this point in the evolution of the DAP that the lateral accelerometer feedback was added, with a gain that was a function of the body roll rate. This gain, referred to as the "boosted" Ny, was sent to both the roll and the yaw channels. The Ny signal was designed to limit the peak sideslip angle during a reversal to the level two yaw jets can control. The concern for angle-of-attack errors was not dropped from the flight rules until the aerodynamic variations were reduced using the data from the flight test program. Early flights had a flight rule telling the crew to execute a bank reversal manually around Mach 10 if they had lost two yaw jets. This rule was designed to prevent a reversal in the Mach 7 region where winds can

cause a large angle-of-attack error. *(Note: The navigation system computes the angle of attack using its estimate of the ground relative velocity vector before incorporation of the air data system at Mach 2.5. No attempt is made in the navigation to estimate the winds or to correct for known winds.)*

There is a simple method, in theory, to correct the angle of attack for wind effects using the navigation-derived sideslip and roll angles and the measured lateral acceleration. Given a measurement of the current lateral acceleration and $C_{n_{ß}}$, the actual sideslip angle can be estimated from the yawing moment equation. This technique was incorporated into the flight software, but it was later I-loaded out because the possible errors due to the Space Shuttle's sensors were on the same order as the errors due to winds. (Code was deleted as part of the OI-8C build.) The equation used is as follows:

$$alpha_{error} = (ß_{estimate} - ß_{nav}) \tan(\text{roll angle})$$

RCS Uncertainties: The first edition of the uncertainties in the RCS jet effectiveness when used in the atmosphere was baselined in 1977. Although there was little uncertainty in the vacuum effectiveness of the jets, there was a large question about the effect of interaction between the flow from the jets and the normal air flow around the Orbiter. This condition, especially at the hypersonic Mach numbers, could not be simulated in wind tunnels. Joe Gamble again took the lead in defining combinations of the earlier aerodynamic variations and the new RCS uncertainties. In general, the technique was to combine effective jets with high gain aerodynamic conditions and low effective jets with low effective aerodynamics surfaces. The defined database added the entire flow field interaction effects to the vacuum forces and moments when the first jet was fired. (Flight test data has shown the interaction effects to be a function of the number of jets firing.) Because of the large effect the interaction terms had on the forces and moments from a single yaw jet, it was found that an unstable low-frequency (approximately 60-sec period) oscillation existed with LVAR 20. This instability would not cause a loss of control directly, but would result in over 3,000 lb of RCS being used when the projected budget for entry was 2,200 lb. The solution was to fire a minimum of two yaw jets. (The operational aerodynamic database may show that the DAP can be reconfigured to the original one, two, three, four firing order.)

Jet Loops: In the same time interval, the RCS subsystem manager requested that the minimum firing time be increased from 40 to 80 msec to prevent possible damage to the jets by incomplete combustion. As a result of this request and a CPU scrub, the computation frequency of the jet loops was reduced from 25 to 12.5 sps. Based on SPS studies, the minimum ON time below 125,000 ft was increased to 320 msec, but the computation of commands was kept at the 12.5-sps rate. The higher computation rate was maintained to allow the jets to be commanded 'off' in 80-msec intervals after the minimum time requirement was met. This configuration has resulted in firing opposing jets (left and right) at same time during some of the programmed test input (PTI) maneuvers below 125,000 ft. A reduction in the minimum ON time would improve the performance of the DAP for some off-nominal aerodynamic cases, but would require the concurrence of the RCS subsystem manager and a possible redesign of the yaw RCS bending filters.

The jet select logic uses a first-on-first-off logic to minimize extra firing time below 125,000 ft. No attempt is made to balance the jet duty cycle during entry. A jet select logic with this capability was in the early Flight Subsystem Software Requirements (FSSR) documents, but it was never implemented by IBM. The current jet select logic uses a strict priority system to determine which jet should be fired.

Another compromise during this time period was in the criteria to stop using the RCS. The OVEI specification stated that the jets were not to be used below 70,000 ft (Mach approximately 2.0); but to handle the pre-STS-1 aerodynamic uncertainties, the jets were required to Mach 1. At one time Rockwell proposed a software change to turn the jets off above Mach 1 to meet the Orbiter vehicle end Item (OVEI) specifications. (Finally, post STS-1, the OVEI specification was changed to allow the jets to fire down to an altitude of 45,000 ft. The software still deactivates the yaw jets at Mach 1.) The jets were maintained until Mach 1 to handle the lateral directional uncertainties.

During this time, the jet thresholds (level-of-error signals at which a jet will be commanded to fire) were increased to the current values (0.25 in pitch and 0.35 in roll and yaw) to reduce RCS toggling caused by noise on the RGA/AA signal and to prevent the jets from firing too long and pushing the error signal past the zero point, which created a jet limit cycle. This was especially important with the increased minimum ON time and reduced computation frequency.

The decision on when to stop using the up/down jets was based on two factors: 1) the largest dynamic pressure at which the aerodynamic/RCS database (including worst-case uncertainties) predicted a significant moment in the desired direction (which defined the longest time the jets could be kept on); and

2) the smallest dynamic pressure at which the aerodynamic surfaces could control the vehicle (which defined the shortest time the jets could be kept on). The final selections of 10 psf for roll and 20 psf for pitch were compromises and assumed a limited X-axis CG (XCG) range for STS-1. An interconnect between the pitch RCS jet commands and the elevator trim loop was added to provide good surface trim capability with the worst-case RCS and Cm_o pitching moment uncertainties. (STS-1 showed that the high-Mach pitching moment was one of the very few parameters that differed significantly from nominal values in the preflight database.) This automatic feature was shown to be superior (based on SPS simulation results) to the manual trim (panel trim switch) technique that was the alternative.

Lateral Trim: One unique feature of the initial versions of the high-Mach early DAP was the mechanization of the aileron trim logic. Early versions incremented the aileron trim by a fixed amount (normally .05 deg) each time the yaw jet command went from a zero to a nonzero value. Later it was changed to increase incrementally each time the number of jets commanded was increased to handle extreme lateral trim cases. In the final version of the Entry 5 DAP, this discrete formulation was replaced by the traditional trim integrator with a Mach-scheduled gain and Mach-dependent inputs. The input to the aileron trim integrator in the hypersonic regime was the yaw jet error signal. Below this point, the aileron error signal was used as input to the aileron trim integrator. The basic approach in both implementations was to trim the yaw moment to zero and allow the aileron to damp the resulting roll motion. The problem with the discrete formulation was the inability to incrementally increase aileron trim during steady jet firings in LVAR 19 and LVAR 20 cases before activation of the rudder.

Prior to rudder activation, lateral trim is obtained by a combination of induced sideslip and aileron to counter the moments caused by a Y-axis CG (YCG) and asymmetric characteristics. The amount of aileron and sideslip (beta) required to trim a YCG before activation of the rudder can be computed using the equations in table 3-3. The denominator of these equations is referred to as the lateral directional control parameter (LDCP). This parameter must remain positive until the rudder becomes active for the aileron trim loop to work correctly.

Table 3-3. Early Entry Lateral Trim Equations

$$\text{Aileron}_{\text{Trim}} = \frac{\Delta y(C_N C_{n\beta} + C_A C_{l\beta})}{b(C_{l\beta} C_{n\delta a} - C_{n\beta} C_{l\delta a})}$$

$$\text{Beta}_{\text{Trim}} = \frac{-\Delta y(C_A C_{n\delta a} + C_N C_{l\delta a})}{b(C_{l\beta} C_{n\delta a} - C_{n\beta} C_{l\delta a})}$$

If the ratios C_l/C_n for the aileron and sideslip are equal, no trim solution will exist; the denominator of the above equations is equal to zero. In this case, the aileron will integrate to its limit (3 deg) and the yaw RCS will have to be used to maintain lateral trim. The effects of uncertainties will cause the amount of trim for a specific YCG to vary considerably. When the ratios are nearly the same, the DAP will have problems maintaining good trim characteristics using the aileron only. The yaw jets will be used to complete the trim requirements at the cost of excessive fuel use. The point in a trajectory at which a trim problem will occur is a function of Mach and alpha. The general tendency is for problems to occur at lower Mach and lower angles of attack. However, when flight assessment deltas (FADs) based on flight tests through STS-51F (FAD 26) were incorporated into the analysis process, a trim problem was observed in the Mach 10 region with the most forward XCG and LVAR 19. The other contributor is the elevon position: up-elevon causes poor lateral trim characteristics due to reduced aileron effectiveness. LVARs 19 and 20 were the worst trim cases.

After rudder activation, the rudder can be used to null yawing moments, and the aileron to null rolling moments caused by YCG effects and the large roll caused by rudder deflections (rudder is located well above the CG). It was possible, using worst-on-worst rectangular variations, to align the aileron and rudder control vectors. LVAR 9 has this tendency. A few FSL and SPS runs encountered a “force fight” problem, which happens when the aileron and rudder vectors align and both are trying to trim the vehicle. Variations have since been reduced; thus a force fight should not occur in a nominal entry or GRTLS trajectory. However, the problem has been observed on some recent contingency abort profiles.

During Entry 5 DAP development, two approaches were evaluated for transition from using the yaw error signal to using the roll error signal as input to the aileron trim integrator. Both approaches reinitialized the

value of the aileron trim to zero at Mach between 2 and 3.5 (rudder activation) and summed this with the output of a fader. Initial fader value was the value of the aileron trim integrator at the transition point. The differences in the approaches were selected Mach number for transition and time constant associated with the fader. The first approach had the transition at the same time the rudder was activated with a long (30-sec) time constant. The second approach delayed the transition as long as possible and had a short fader time constant. This technique also included Mach-dependent logic that used a combination of both signals if the product of the two signals was negative. The final technique selected, based on the SDSS flight control simulation in early 1979, was Mach 2.1 with a 10-sec fade time with the combination logic being I-loaded out. When these numbers were selected, it was recognized that the yaw RCS jets would be required to supplement the surface trim during the time required to change from aileron to rudder trim. (This concept would be completely reworked during the redesign effort.)

The decision on rudder activation criteria involved many hours of discussion and hundreds of time-domain simulation runs and linear stability analysis cases. Finally, the aerodynamic community was asked to determine the maximum Mach number, along the nominal entry trajectory, at which they could guarantee the "sign" on the rudder coefficients. The flight control community was very concerned that the rudder effectiveness could be reversed at high angles of attack and high Mach numbers. Bass Redd, the JSC lead for the Orbiter aerodynamic database, indicated that the aerodynamic community would stand behind the rudder at Mach numbers up to 3.5 for a nominal entry alpha-Mach profile. Therefore, Mach < 3.5 was the criterion used during early Space Shuttle flights. (Later flight test data would show that the rudder was effective up to Mach 5 and that no control reversal was found up to Mach 6. Mach 6 was the highest Mach number at which the rudder had been tested.)

After several unsuccessful attempts to define a discrete switch criterion to handle the transition from the high-Mach roll logic to the normal aircraft roll logic, Ray DeVall and Maury Fowler of McDonnell Douglas designed a fading logic using the entry flight control roll axis gain GALR, which is a function of Mach. This logic was baselined and is still used in the current entry DAP. To provide additional protection, the crew was given the capability to override the automatic transition logic using the entry roll mode switch. (This switch is the only four-contact switch in the Orbiter.) The nominal procedure was to place the switch in the AUTO position, which allowed the DAP to use the normal programmed logic. If the pilot placed the switch in the EARLY position, the entry roll logic (GALR = 1.1) would be maintained down to Mach 1. If the pilot placed the switch in the LATE position, the low-speed logic (GALR = 0) was used as soon as the Orbiter reached Mach 5. (This is the same switch that is currently used to select the no-yaw-jet mode.)

PIO Suppression Effort: After the PIO observed during the final ALT flight, several modifications were made to the entry FCS to minimize the probability of a PIO during Orbiter landing.

The first change was to the elevator PRL. The ALT PRL allowed either the aileron or elevator requirements to lock out surface motion to satisfy the other axis. (For example, a large elevator command would prevent any surface motion in response to a smaller aileron command.) The Entry 5 PRL included logic to prevent one axis from locking the other axis out. The PRL function is required to make the best use of the limited rate capability of the Orbiter actuator system.

The second change was to increase the sampling rate of the RHC from 12.5 to 25 sps. This change reduced the transport lag through the computer. Transport lag had been shown to be a major contributor to PIOs. The lower rate had been selected as part of a CPU scrub. The final change was to add a nonlinear filter on the RHC output to attenuate oscillatory inputs in the normal PIO frequency band. This nonlinear filter was designed by engineers at Dryden Flight Research Center (DFRC). As part of this change, the shaping of the RHC to pitch rate command function was modified. Finally, the pitch-forward loop gain was reduced.

An additional RHC-related modification was the elimination of doubling the pitch RHC output when the pilot pushed the RHC past the mechanical soft stop. (This was necessary because the pilots accidentally exceeded the soft-stop level several times and were surprised at the response.) These events, which tended to occur near touchdown, resulted in unacceptable landings. The value of the gain, GPX, was changed from 2.0 to 1.0. The code was not removed until the OI-8C scrub. (Extreme care should always be taken when discrete gain changes are used.)

An RHC hardware change made between the ALT flights and the first OFT modified the force gradients on the springs in the RHC. This change effectively doubled the feel characteristics of the RHC.

Flex Body Suppression: The final element of the Entry 5 DAP was the addition of a set of bending filters to suppress Orbiter bending modes that could corrupt RGA and AA measurements. In parallel with the work on the rigid body control requirements and basic DAP structure, a second group of engineers at JSC, Rockwell (RI), and Honeywell (HI) had been working on bending filter requirements. The assumption was that the frequency separation between rigid control frequencies and Orbiter bending modes was enough to allow parallel design activities. The normal rigid high-frequency crossing is about 10 rps. The basic empty Orbiter flex modes are 1) fin mode—24 rps (ground tests indicate actual frequency is lower), 2) Z-fuselage mode—30 rps, 3) wing symmetric modes—36 rps, and 4) wing antisymmetric mode—36 rps. Later it was found that payloads could have a significant effect on the mode shapes and frequencies, as illustrated in figure 3-5 (from reference 3-2). Very little of the SPS/SDSS simulation work or the rigid-body stability analysis at JSC, Honeywell, and Rockwell included the final set of bending filters because it was necessary to design the flex bending filters in parallel with the rigid-body design. This was largely due to the late maturity of the vehicle flexible dynamics database. This lack of coordination between the flex and rigid design efforts was the major error in the design process, and it would come back to haunt the entry FCS design community. (Because of computer speed limitations, no MIL simulation has ever included a flex body simulation; *however, some tests were conducted with second-order transfer functions inserted in control loops to assess limit cycle performance due to a low damped or unstable flex mode*) A detailed discussion of ground testing to determine the actual vehicle modes and frequencies is presented in Section 4.

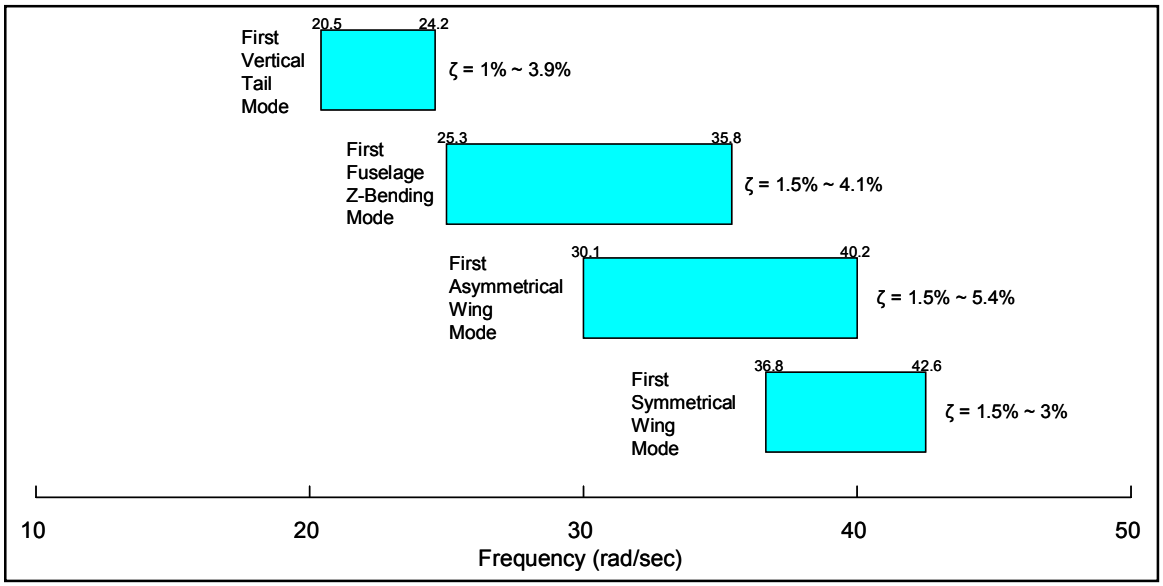

Figure 3-5. Frequency and Damping Ratio Ranges for Four Dominant Vehicle Modes

Downmoding Logic: Before STS-1, there was a lot of concern about the quality of data used to design bending filters and the magnitude of aerodynamic uncertainties. As a result, special switches were added to orbital vehicle (OV) 102 to allow the pilot to modify, or downmode, the entry FCS in real time. These were the four three-position downmoding switches below and to the left of the commander's attitude direction indicator (ADI) and the two pushbutton indicator (PBI) switches (one for pitch and one for roll) on the commander's and pilot's eyebrow panels that were required to activate the four downmoding switches. The positions on these four switches could do the following: 1) reduce or increase the aileron, rudder, and elevator forward loop gains, 2) stop the use of rate feedback in the stability loops, 3) add a bias to the angle of attack used in the turn coordination logic, 4) freeze all the aerodynamic surfaces, and 5) activate a no-yaw-jet lateral control law. It was agreed that no formal certification would be required for performance of the downmoding options. This direction was given by the Space Shuttle Program Office because of the magnitude of the work required to certify the nominal system, the known problems with the system, and the decision to increase the STS-1 RCS redlines to 2,200 lb. This higher limit would cover the worst-case failures or aerodynamic variations.

The primary individuals responsible for the development of these requirements were the flight crews. Ken Mattingly and Hank Hartsfield spent many hours in the SPS and the CPES developing crew procedures and pilot cues to use these switches safely. Because these switches were only put in OV-102, the capability

was intended to be temporary; however, crew and engineering inputs resulted in design of a reduced and simpler downmoding capability for operational flights. In 1985, an effort was started to develop a no-yaw-jet system that could be certified and could serve as a stepping stone in the development of minimum RCS entry control system. This effort resulted in the upgrade to the no-yaw-jet system that was incorporated in the OI-8A software, and analysis and simulations were completed to certify the upgraded no-yaw-jet system for emergency use. At this point, downmoding was added to the BFS for the first time.

3.2.3 Aborted Verification Attempt

The completed Entry 5 DAP design was given to IBM for implementation in the flight software that was to be used in the first STS-1 verification attempt at the Flight Simulation Laboratory (FSL) at Downey in the fall of 1979. A significant event that had occurred between the final SPS and SDSS simulations and the start of verification at FSL was the release of a new Orbiter Aerodynamic Data Book (the ADB, also known as the 1M book). This new database was implemented in parallel at the primary simulation facilities at JSC, Rockwell, and Honeywell. In an ideal world, the flight control design community would have taken the Entry 5 system through a complete stability analysis review and SPS simulation at JSC using the new database and bending filters, but the schedule did not allow this ideal process to be followed.

Before formal verification runs started at the FSL, an extensive site acceptance process was conducted that included these elements: 1) aero slices, 2) step responses, 3) frequency responses, 4) timing checks in effector and sensor loops, 5) model unit tests, 6) gain margin tests, and 7) full trajectory comparison tests. The original trajectory tests—common facility tests (CFTs)—were so complicated that they became almost useless. From this point on, CFTs were kept simple. At the first test readiness review in June 1979, the FSL was rejected with agreement of JSC and Rockwell sponsors, and a list of Category 1 (mandatory) changes was identified. This list included resolution of timing issues (especially in RCS), additional aerodynamic model tests, and improved data reduction capability. All issues were resolved, and testing was started in September 1979. *(In my opinion, not enough thought and resources are used to define test capability and data processing capability during the development of major test facilities. A second good example of this is the Shuttle Mission Simulator (SMS) at JSC.)*

The approach taken at the FSL was to verify the nominal configuration against Level I requirements (linear stability margins and handling qualities) and to ensure that the vehicle was flyable for the combination of worst-on-worst elliptical variations and sensor and effector uncertainties. This approach was a compromise because time and resources did not allow separate testing with all of the individual error sources. It would have required over a thousand runs at the FSL and approximately ten thousand stability and response cases at Honeywell. The formal runs were augmented by additional MIL cases on the SPS and batch trajectory runs on the Space Shuttle Functional Simulator (SSFS) and Shuttle Descent Analysis Program (SDAP). Trajectory points selected for the Honeywell verification tests were based on the results of Monte Carlo runs made at JSC. Figure 3-6 shows the range of dynamic pressures used in the analysis. The automatic and CSS systems were verified within the 3-sigma limits against Level I criteria, and the CSS system was formally evaluated between the 3- and 6-sigma limits. Level II criteria were used for these tests.

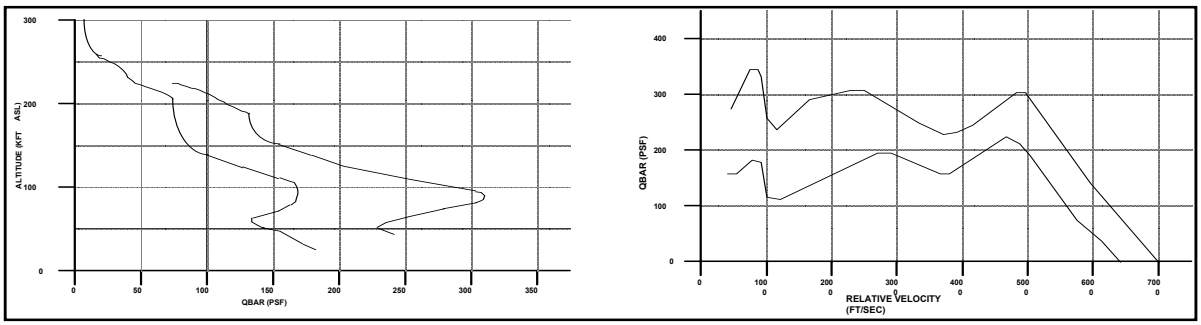

Figure 3-6. Entry/GRTLS Dynamic Pressure 3-Sigma Limits

For both NEOM and GRTLS, the angle of attack was varied ±4 deg from the nominal angle-of-attack profiles shown in figures 2-4 (NEOM) and 2-10 (GRTLS). In the definition of cases, limits such as the 2.5-g limit were used to restrict the selection of test points.

The formal process for completion of the entry verification process is shown in figure 3-7. “Uncertainties” refers to the combination of worst-case aerodynamic and LRU uncertainties at the variations level (large values in the database), and “tolerances” refers to the smaller level of the uncertainties in the aerodynamic database together with LRU uncertainties. Tools used in the formal flight control verification process were the FSL and the off-line tools at Honeywell in Clearwater, Florida. The FSL function was moved to the Shuttle Avionics Integration Laboratory (SAIL) in Houston starting with STS-41C. The SMS was never considered part of the verification or design process because of two generic problems: lack of a formal dynamics site acceptance program and lack of capability to record data for post-processing.

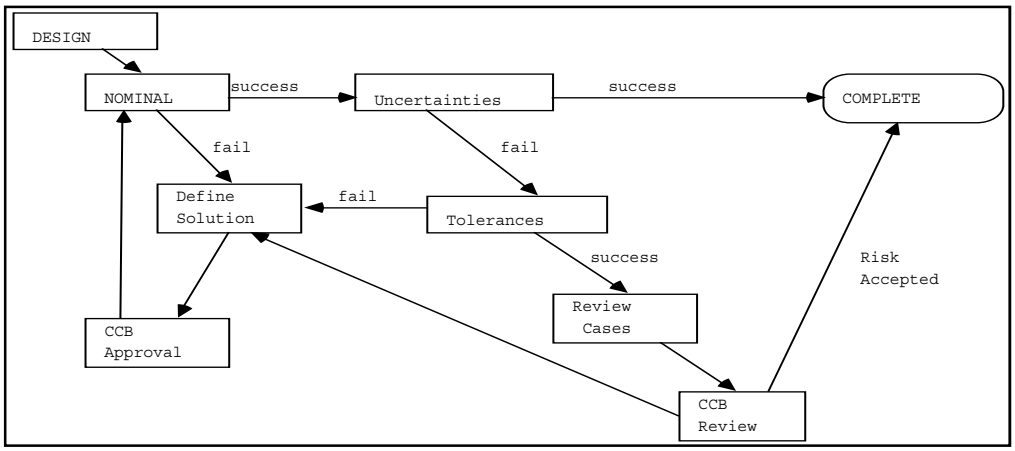

Figure 3-7. GN&C/FCS Verification Process

The verification attempt was stopped and a redesign "tiger team" was formed after the following conditions were observed. First, very low damping was seen for the nominal case during reversals in the Mach 2.5 to 5.0 region. The low level of margins was confirmed by linear stability analysis at Honeywell. Second, a low-amplitude, low-frequency oscillation was observed in the pitch axis in the 3 < Mach < 10 region. Third, complete loss of control was observed (high-frequency divergent oscillation) when the rudder was activated and LVAR 12 was included in the test configuration. The fourth and final problem was the excessive RCS requirement for the LVAR 9, 11, 19, and 20 cases. The combination of a new aerodynamic base and the new bending filters was the primary reason for the failure of the attempt to certify the Entry 5 DAP for flight.

The first and second problems were associated with the nominal case, whereas the others were associated with aerodynamic variations. As can be seen from the process diagram (figure 3-7), the first two problems had to be fixed. For this reason, tolerance cases associated with variation cases were not run as part of the aborted verification attempt. It was agreed to use these cases if the sensitivity to aerodynamic variations could not be fixed as part of the redesign to fix nominal problems. *After the entry flight test program began to produce updates to the aerodynamic database (STS-4/FAD 4), the concept of two levels of uncertainties was dropped from the program and replaced with uncertainties based on the spread of flight data.*

Doug Johnson, the Rockwell manager for entry flight control, presented the results to Aaron Cohen, Orbiter Project Manager, and other NASA and Rockwell managers at a meeting in Downey in late 1979, with a recommendation that the verification process be halted and the entry DAP be redesigned. The managers approved the recommendation and a tiger team was formed, with Guy Bayle of Rockwell and Larry McWhorter of JSC as team leaders.

One study that would be of historical interest to many engineers and program managers is evaluation of the Entry 5 DAP against the operational database after it has been updated to reflect the final results of the flight test program.

3.2.4 Tiger Team Activities for STS-1 (1979)

The STS-1 tiger team activity was one of the most intense periods of design and evaluation ever undertaken by any group with whom I have been associated. To form this team, Rockwell management selected some of their most experienced people and an outstanding support group including key

individuals from Honeywell in Clearwater, Florida. This group, with the support of JSC government and contractor personnel, had one goal: to upgrade the entry DAP to a commit-to-flight status.

As the process evolved, both the JSC team and the combined Rockwell-Honeywell team worked for about 2 months to develop changes to increase the robustness of the DAP, and at the same time to improve the margins for the nominal case in the Mach 2 to 5 region. The groups then held a joint meeting at Downey in building 4 to baseline a final configuration for continued evaluation and IBM implementation. In several cases, agreement could not be reached and dual paths were included in the software changes given to IBM for implementation.

Because of the compressed schedule for change implementation, it was decided to patch the redesign into version 16 of the flight software for STS-1 and to document the change sources in version 18 for STS-2 in parallel. Therefore, the emphasis was on making change requests (CRs) as easy as possible for IBM to implement. No attempt was made to remove excess code. (Much of the code that was removed via CR 79962 as part of the scrub effort to support OI-8C originated with the redesign effort.)

One unique characteristic of this process was that before the final software CR went to the software control board for approval, the change in the form of an IBM-developed patch had been tested at FSL in the actual flight software. This process removed the normal concern for the differences between the functional software emulations used to develop the final requirements change and the actual IBM implementation.

The redesign effort had the benefit of the site acceptance work that was done to validate the FSL for verification. For example, team members were able to compare the primary tools used. Figure 3-8 shows the tools and process used during the redesign effort. During the design phase, each group was always aware of what the other groups were doing. Close communication was maintained, using a combination of teleconferences and face-to-face meetings.

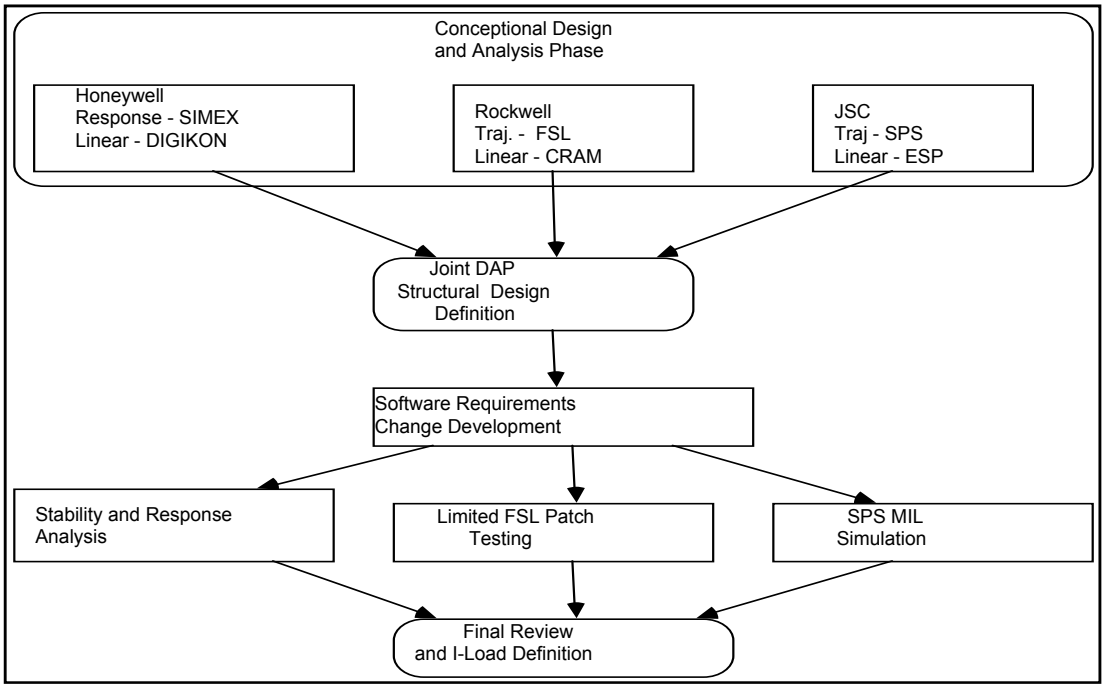

Figure 3-8. Redesign Process and Tools

One key ingredient in the success of this effort was Doug Johnson's coordination of the rigid and flex design efforts. Several meetings were held at Downey to identify where the bending filters could be modified to reduce the impact on the rigid body response. Early in the process, Rockwell, Honeywell, and JSC reached an agreement to employ a switchable filter approach *(similar to the ascent baseline DAP)* and establish the maximum phase lag and gain that could be induced by the bending filters at 10 rps. The value of the allowable lag was set at a *maximum* in the Mach 2 to 3 region in the lateral channel because of the low damping seen with the Entry 5 DAP. Meanwhile, the *maximum* lag was set at landing

in the pitch channel because of the PIO tendency at this point in the trajectory. The following paragraphs summarize changes made to the entry DAP as part of the redesign activity.

Attitude Processor Modifications: As part of the code review, an error was found in the definition of the prefilter coefficients in the rate fill algorithm. This error was made when the Euler angle computation frequency was reduced from 12.5 to 6.25 sps. As part of this CPU reduction, a second first-order filter, with a computation frequency of 12.5 sps, was cascaded with the existing first-order filter that had a computation frequency of 25 sps. The I-loads defined for these filters resulted in filters with break frequencies of 10 and 5 rps instead of the desired 20 rps. These I-loads were corrected in CR 29356A. This CR also reduced the gain on the rate gyro bias estimator by a factor of 10. These changes contributed significantly to the elimination of the ¼-Hz oscillation seen in the pitch axis AUTO mode performance testing.

The reduced frequency of computation for the Euler angles has been shown to cause a jitter on the heads-up display (HUD) that was added for STS-6. If a CPU is made available as part of a GPC upgrade, a return to the higher computation frequency should be reviewed.

GJET Modification: A study was performed by Ray DeVall on the SPS to optimize the pitch RCS to elevator trim interconnect gain, GJET, for the worst-case pitching moment and XCG conditions expected in STS-1. The results indicated that the gain should be reduced from 5 to 4, and used for dynamic pressures between 0.5 and 8.psf. Previously, the interconnect had been active until a dynamic pressure of 10 psf was reached. *(This interconnect was disabled via K-load changes in OI-22, primarily to facilitate thermal analysis.)*

Bending Filter Modifications: The bending filter structure that resulted from the redesign process was the largest structural change to the DAP. The pitch axis was the only axis that did not undergo a structural change, but the I-loads associated with these filters were changed. (As part of the IUS upgrade for STS-6, this loop would be restructured.) The pitch jet loop has a single second-order filter, whereas the elevator axis uses a sixth-order filter above Mach 1 and a second-order filter below Mach 1. Note that the subsonic second-order filter is the first stage of the sixth-order supersonic filter.

In the roll axis, two structural changes were made. The first was to add a separate fourth-order bending filter for the roll jets. The second was to increase the number of filters in the aileron loop. The Entry 5 DAP had a second-order filter in the subsonic regime and a sixth-order filter in the supersonic regime. The structure was changed to have three sets of aileron filters that would be used for these regimes: a second-order filter for subsonic, a sixth-order filter between Mach 1 and 3.5, and a different sixth-order filter above Mach 3.5. Two supersonic filters were used to take advantage of the reduced attenuation requirement in the lower supersonic regime, thus obtaining a reduction in the phase lag in the rigid body frequency range. In the lower dynamic pressure regime, it is necessary to have higher aileron forward loop gains to get the required transient response. These higher gains necessitate the increase in the filter attenuation of the flex modes.

In the yaw axis, one structural change was made. Provision was made for separate fourth-order bending filters for the yaw jets and the rudder. In the yaw jet loop, the coefficients of the bending filters are changed when the minimum ON time changes from 80 to 320 msec. This takes advantage of the reduced attenuation required because maximum limit cycle frequency has been reduced by at least a factor of two. In addition, the reduced phase lag was needed to stabilize the LVAR 12 high-frequency rigid body crossing. The rudder filter coefficients are changed at Mach 1.

Jet Hysteresis Changes: Although the error signal required to turn a jet on was not changed in any of the three jet loops, the level at which the jets would be turned off was changed. In all three cases, the turn-off values were set very close to the turn-on values: pitch .25/.245, roll .35/.33, and yaw .35/.33. Completely removing the hysteresis was discussed, but was not done because of code impact. The hysteresis is not necessary because the combination of the quantization level in the sensors and the mechanical delay in turning the jets off provides the desired effect. The remaining hysteresis computations are potential candidates for a software code scrub if one becomes necessary. They were missed during the definition of the OI-8C scrub. Figure 3-9 shows typical jet hysteresis configurations.

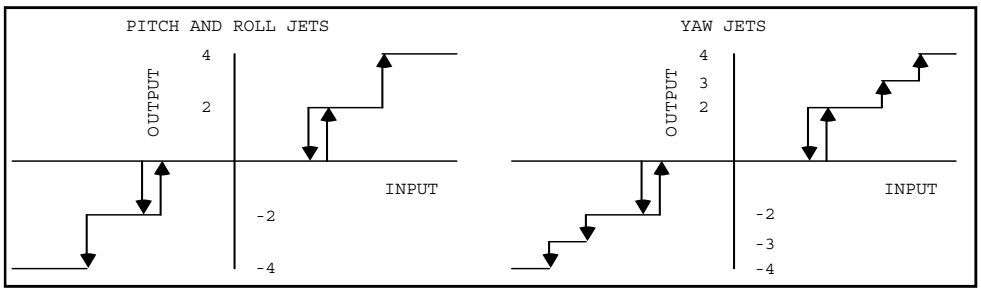

Figure 3-9. RCS Jet Hysteresis

One unique change that was evaluated as part of the redesign was a "reverse" or "smart" hysteresis. This approach had logic to turn off the yaw jets when the magnitude of the error signal was decreasing at an acceptable level and the magnitude of the error was less than a desired value. Since the turn-off level can be greater than the turn-on level, this approach provided significant phase lead, resulting in earlier jet turn-off and improved stability of several low gain LVARs. It was not used because of the complexity required to conduct a complete nonlinear analysis and because the related benefit from the reduced phase lag was already obtained from the bending filter redesign. It was implemented as part of the STS-1 patch (I-loaded out), but not sourced for STS-2. This technique might be useful on other projects where there is a considerable lag in executing jet commands.

Pitch Axis Unique Modifications: Two additional structural changes were made to the pitch axis. The first was the addition of a first-order lag-lead filter on the angle-of-attack error. The purpose of this filter was to increase the low-frequency gain margin during entry (especially for some PVAR cases) by attenuating the oscillatory components of the alpha error signal. Two side effects were an increased residual error in the alpha command loop and large overshoots in step responses. The response to large alpha errors as seen in GRTLS pull-up resulted in setting the filter to unity in GRTLS. Given the reduced PVARs, the filter may not be required in entry today. The OI-8C scrub removes the lag lead filter from the GRTLS DAP.

The second change was to add a Mach-scheduled gain option on the pitch rate feedback if the lag-lead approach did not work. But because the lag lead worked, the gain was set to unity for all Mach numbers. In addition, capability for separate gains for auto and CSS would have been required to make this approach work. This gain remained in the flight software until it was removed as part of the entry GRTLS scrub (CR 79662) in OI-8C.

The final elevator loop change was to modify the angle-of-attack error gain, GQAL (scheduled as a function of Mach), to be consistent with the lag-lead filter on alpha error. For the first two flights, the alpha error gain for the elevator and the corresponding gain for the pitch jets were slightly different (.25 and .33). This did not cause a problem, but was corrected as part of the TAL update for STS-3.

Lateral Trim Modifications: The aileron trim loop was simplified. The new logic simply switched the input to the trim integrator at Mach 3.5 by 1) grounding the signal (DRRCL) instead of setting it equal to the yaw rate error from the yaw channel and 2) setting the gain (GTRA) on the roll error signal (DCSP) to a nonzero value. The GTRA is scheduled with Mach number. The fader (the optimization of which had consumed much time during the design of Entry 5 DAP) was eliminated. In addition, the maximum rudder trim value was increased from 4 to 6 deg to handle the variations. The rudder trim integrator gain (GTRR) and the aileron trim integrator gain (GTRA) were also modified.

GDA Hump Addition: To stabilize the LVAR 9 case in the Mach 5 region, the aileron forward loop gain was increased in this region. The Entry 6 schedule was designed to provide an increase before activation of the rudder, but to return the gain to the Entry 5 level at rudder activation in order to prevent high-frequency problems in the Mach 3 region with LVAR 12. A second reason for not increasing the gain below Mach 3.5 was the light aileron bending filter in the Mach 1 to 3.5 region. An increase in GDA would have forced a redesign of the bending filter. The higher gain above Mach 3.5 could be accommodated with the heavy filter used above Mach 3.5. Even with the hump, the gain was still less than that used in the low dynamic pressure region of early entry. This region was the driver for the design of the heavy filters. Figure 3-10 presents the aileron gain schedules as used for STS-1 and as revised for STS-41C to fix the lateral ¼-Hz lateral oscillation in the Mach 1.5 to 2.0 region.

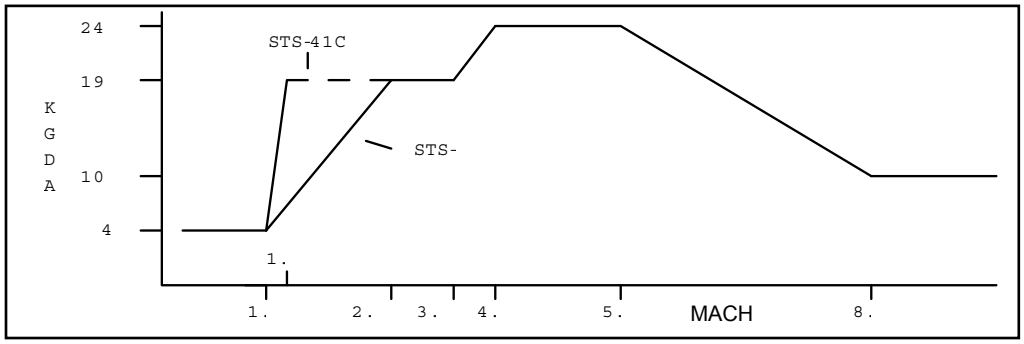

Figure 3-10. Aileron Gain Schedules

GDR Subsonic Increase: The rudder forward loop gain (GDR) was increased in the subsonic region to provide additional low-frequency gain margin. Figure 3-11 shows both the STS-1 and STS-51F rudder gain profiles.

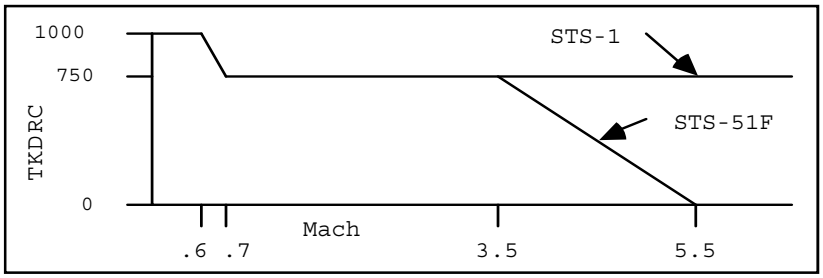

Figure 3-11. Rudder Forward Loop Gain

Ny Feedback Modifications: Changes to the Ny feedback were second in complexity only to restructuring the bending filter. Changes included removing the boosted signal from the yaw axis and the steady-state signal from the roll axis. Only the boosted signal was used in the roll channel to prevent a buildup of sideslip during a roll reversal, whereas only the steady signal was used in the yaw channel. Figure 3-12 shows the modified Ny structure without the dead code, which was I-loaded out. (The dead code removal was authorized by the OI-8C-scrub CR.) This change removed the nonlinear effects from the jets, thereby reducing their activity and the steady-state signal from the aileron when it wasn't needed to prevent excessive sideslip development.

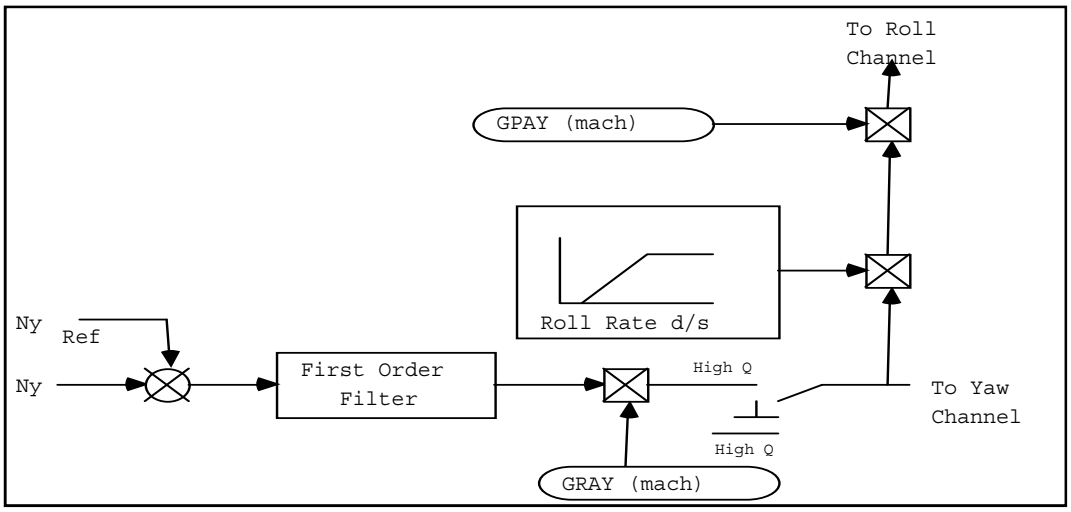

Figure 3-12. Modified Ny Feedback Diagram

In addition to the structural changes, the common gain on the Ny feedback (GRAY) was modified and the time constant of the first-order lag filter was reduced from 1.0 to 0.8 sec. This new time constant was a compromise between the need for a short time constant for some low-frequency LVARs (9, 11, 19, etc.) and the need for a longer time constant for high-frequency LVARs (10, 12, etc.).

Turn Coordination Modification: The FCS executive module (RECON) I-load, MACH_RRXF, was reduced from 0.9 to 0.6 as a result of the final SPS simulation. This I-load defines the Mach number at which yaw axis starts to follow the aileron-driven roll rate instead of matching the commanded body yaw rate. Little difference was seen in the SPS between the two values, but the change was made because most of the available data were obtained using 0.6. The minimum value is set by the transition to the approach and landing phase.

BANKERR Threshold Modification: The use of the nonlinear function BANKERR_THRESH was extended to GRTLS and to lower Mach numbers in OPS-3 to reduce the reaction to small changes in the commanded roll angle. Many I-load variations were evaluated during this period, but none could be found that were significantly better than the Entry 5 values. Figure 3-13 depicts the BANKERR_THRESH function that is in both the entry and GRTLS DAPs.

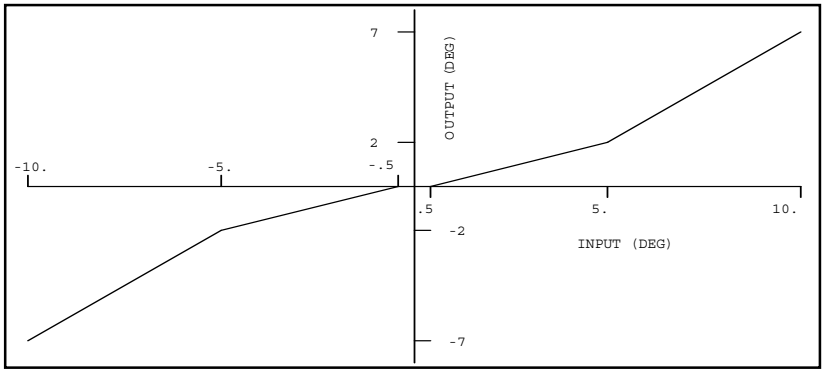

Figure 3-13. Nonlinear Bank Error Function Diagram

Speedbrake Modifications: For entry (OPS-3), the speedbrake channel was modified to use the Mach-scheduled speedbrake profile down to an I-loaded Mach number instead of automatically transitioning to the guidance-computed command at the start of TAEM (MM 305). The I-load for the transition was selected as 0.95, and the guidance I-loads were set to ensure a smooth transition. One oversight that has caused an excessive amount of paperwork (in IBM discrepancy reports [DRs]) is that the surface position indicator starts to use the guidance commands for display at the start of MM 304. This could be a problem only if the flight control I-loaded speedbrake schedule and the guidance-commanded position were allowed to be different.

The only modification for GRTLS was to change the high Mach speedbrake profile from 98 to 80 deg, thus reducing the maximum down-elevon during the pushover. This change, along with modifications to the elevator schedule in the bodyflap channel, prevents excessive hinge moments during this phase of GRTLS.

Elevator Schedule Changes: The elevator schedule in entry was changed to be at trail in the Mach 1.5 to 2 region to provide better lateral stability. In GRTLS, the elevator schedule was changed from 5- to 2-deg down in the Mach 4 to 6 region to reduce the maximum elevon hinge moments. During the pushover phase (IPHASE 5) of a GRTLS trajectory, the bodyflap cannot keep the elevator on schedule because of the rapid change in angle of attack. This results in a down-elevator position approximately 3 deg more than desired. The change in schedule was done to account for the overshoot tendency.

Formal Certification of Entry 6 DAP: Formal certification for the Entry 6 DAP consisted of two parts. The first was the trajectory work at the FSL at Downey. The combined NEOM and intact abort matrix consisted of over 150 trajectory runs, including both manual and automatic flight control modes. In a number of the manual cases, the pilots (at Rockwell and JSC) were asked to provide Cooper-Harper ratings for three tasks at various points in the profile. The tasks were 1) a medium-magnitude roll and/or pitch maneuver, 2) following the needles, and 3) roll reversals. An extensive post-run data evaluation was done for each case, both at Rockwell and at JSC. The final phase of data evaluation was a week-long review of the strip charts and other data products at Downey by 10 engineers (five from Rockwell and five from JSC). During this review, at least two engineers reviewed the data from each formal verification run.

The second part of formal certification was the stability and response assessment done by Honeywell at Clearwater, Florida, using SIMEX and DIGIKON. This matrix assessed both the rigid body and flex linear

margins/attenuation and the response of the system to step inputs. The extensive matrix (over 2,000 test cases) included test points from the nominal and a series of off-nominal trajectories, aerodynamic and RCS uncertainties, flex body tolerances, and 1- and 3-sigma sensors and effectors. At this time, Honeywell had the only flexible body time domain simulation capability; this was used to evaluate the possibility of RCS or aerodynamic surface limit cycles.

A set of 3-sigma composite flex tolerances was defined using 1.5-sigma tolerances combined to give the worst case effect on flex stability. This composite set and 3-sigma tolerances on individual parameters were used in defining the test matrix.

Describing-function techniques were extensively used to find points where limit cycles might be encountered. Once a point was found, the nonlinear time domain simulations (SIMEX and SIMFLEX) were used to evaluate the magnitude and effect of the limit cycle if it existed. It should be noted that describing functions only indicates where limit cycles might occur.

After the analyses were completed, Honeywell documented all anomalies in a series of flight control anomaly notices (FCANs), each of which was reviewed by the JSC and Rockwell flight control subsystem managers. Each was resolved by additional analysis or was formally documented and presented to the Orbiter Project Office. A final presentation was made to Aaron Cohen on the Saturday before the first launch attempt. This meeting focused on Doug Johnson's review of areas with low attenuation of structural modes, a subject of great interest because of hot-fire test results (discussed in Section 4).

3.2.5 STS-1 Results

Overall, systems performance of the entry flight control on STS-1 was very good. Only four problems were noted during the flight or during postflight review of the data: 1) low-frequency, high-amplitude lateral oscillation during the first roll maneuver, 2) more down-elevator required for trim during hypersonic flight than expected, 3) more up elevator required for trim in the Mach 1 to 2.5 region, and 4) ¼-Hz roll oscillation in the Mach 1.4 to 2.0 region.

As soon as flight data were available, the tiger team started a detailed review, with members assigned to work each issue. Following is a discussion of the resolution of each of the four issues.

First Roll Oscillation: The key parameter used in the analysis of first roll oscillation was lateral motion, as shown by the inertially computed sideslip angle. Figure 3-14 shows the oscillatory motion seen during the first roll maneuver.

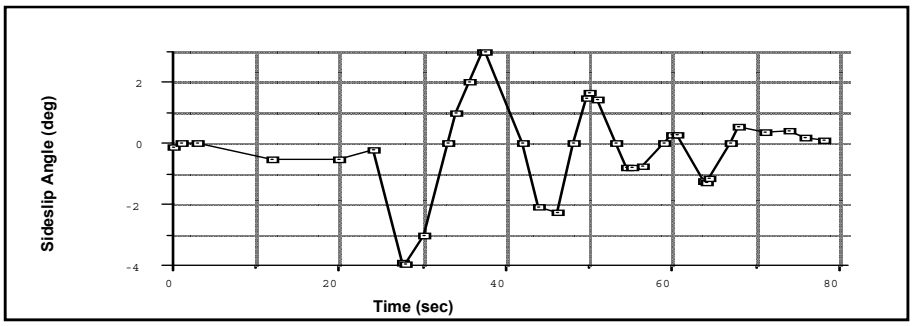

Figure 3-14. Sideslip (Beta) Motion During First Roll Maneuver

The cause of this unexpected motion was quickly identified. By accident, an SSFS run had been made before the first flight without setting the flag to include the RCS/aero interaction terms. This run showed the same type of motion seen in the first flight data. From this starting point, a series of entry profiles was run on the SPS with different yaw jet roll and yaw moments. Comparing SPS results to the flight data revealed that the roll moment from the yaw jets was almost at the variation level. (These results were slightly modified by data obtained from the flight test program.) Figure 3-15 compares the expected jet torques with the actual ones. The most significant item is the sign difference in roll torque.

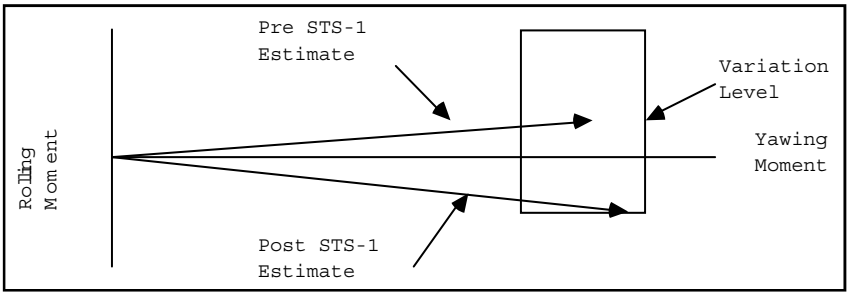

Figure 3-15. Comparison of Yaw Jet Moments

The software solution was identified within a month, and a proposed flight software change was written for Orbiter Avionics Software Control Board review and disposition. The solution was to put back into the software the beta washout filter that had been removed in an earlier scrub, and to reduce the maximum roll rate for automatic maneuvers above Mach 23 from 5 to 3 deg/sec. During the development of this change to the automatic system, it was found that the CSS mode did not have the same problems if the pilot rolled the Orbiter at the reduced rate. Because of schedule and resource issues, program management decided to use the manual technique until the software solution could be implemented in version 19 of the flight software for STS-5. No problem was seen with the manual technique on STS-2, -3, or -4, and flight test data from STS-5 showed that the software solution had solved the problem with the automatic system. Since STS-5, all initial roll maneuvers have been done in automatic control mode.

This problem and its solution showed the wisdom of designing the control system to handle large aerodynamic uncertainties.

High Mach Pitch Trim: The bodyflap was significantly farther down in the hypersonic flight region than expected during STS-1, reaching a maximum of 17 deg down. In response to this anomaly, the desired elevator schedules were redefined to prevent the excessive down bodyflap, and the flight test program was expanded to include flight test maneuvers on flights with 7-deg-down-elevator positions in this region.

Supersonic Pitch Trim: Elevator schedules were not changed in the supersonic region; a full up-bodyflap was accepted in this flight region. No thermal issues were involved; thus it was decided not to open the speedbrake more to get the elevator down. Opening the speedbrake would have reduced rudder effectiveness and resulted in higher hinge moments. On a number of flights, the bodyflap has gone either full up or very close. The flight test program would give priority to the evaluation of the effects of up-elevator on the aileron characteristic in the supersonic region. This issue was correlated with the ¼-Hz issue.

Quarter-Hz Oscillation: Of all the STS-1 anomalies, the ¼-Hz oscillation became the most difficult to solve, and this resulted in restrictions on the allowable XCG for several years. A software change was not implemented until STS-41C. Unlike the oscillation at the first roll maneuver, a single physical reason for the oscillatory motion could not be identified; the motion seen on each flight was different. A number of models (linear and nonlinear) were created that showed motion approaching the flight data. Several detailed Honeywell reports written by Robbie McAfoos discuss these models.

On STS-9, a special flight test, or detailed test objective (DTO), was done to investigate an aerodynamic theory on the cause of the oscillation. The theory dealt with the angle the speedbrake made with the flow coming off the front part of the vertical tail. According to the theory, the oscillation would decay if the speedbrake was reduced. At Mach 1.8, the pilot manually reduced the speedbrake to approximately 40 deg, but instead of being reduced, the oscillation increased. The problem with the test was the increase in up-elevator that resulted from the change in the speedbrake setting. For this reason, the validity of the theory is still unresolved.

Flight test data from the automated PTI logic showed that the aileron was less effective in this Mach region (near the variation level) than had been predicted by wind tunnel data. Finally, on STS-41C, these I-load software changes were incorporated: 1) aileron forward loop gain (GDA) reduction was delayed until Mach 1.6 (see figure 3-10), and 2) Ny gain (GRAY) was reduced. Subsequent flight data showed a significant reduction in the oscillatory motion, and the anomaly was closed. Residual motion can still be seen in this region, and occasionally a yaw jet will be commanded to fire. For this reason it was decided

to maintain the yaw jets down to Mach 1 for the duration of the program. There is no case in the FAD 26 database that will result in loss of control in this region.

3.2.6 Addition of Transatlantic Abort Landing (TAL) Mode

In the design of ascent profiles for high-performance missions, the need for a downrange intact TAL capability became evident. The design of this capability called for the direct transfer from MM 104 (post-ET-SEP) to MM 304 (entry) software, a transition that requires use of the Orbiter mass memory units to reload the primary computer system. During the loading of the computer with the entry software, the Orbiter is in a free-drift mode with no active attitude control.

This abort mode, which was added to the Space Shuttle system requirements to support STS-3, was to be considered an intact abort mode. In an entry sequence, there are three major differences between an AOA and a TAL. 1) Most TAL landing sites have shorter and narrower runways than AOA landing sites. (No special construction was done to extend or widen existing TAL runways.) 2) Attitude at the start of TAL entry is like a GRTLS attitude (low alpha); this requires a maneuver similar to the pull-up maneuver in GRTLS. 3) Buildup of dynamic pressure is faster in TAL because of the lower speed. Only item 2 required a change to the DAP.

The following changes were made to the entry DAP to handle a TAL: 1) GJET was disabled, 2) the alpha error lag-lead filter was bypassed until an I-loaded Mach number (normally Mach 20) was reached, 3) pitch rate control power was increased to handle the pull-up maneuver, and 4) capability for a separate alpha error gain was added. These changes were done to make the entry DAP functionally match the GRTLS DAP in the high Mach region. After the trajectory reaches Mach 20, the DAP reverts to the normal entry DAP. These changes are active only when a TAL has been declared by the crew before MECO. (Additional changes were made to the entry, TAEM, and approach and landing guidance techniques to accommodate TAL.)

The only special analyses required to commit the entry DAP for use in TAL were a small group of stability and response cases at Honeywell and a series of TAL trajectory runs at FSL.

A crew procedure had been developed for STS-2 to execute a manual TAL. It involved sequencing the BFS to MM 304 and flying the BFS guidance commands using the GRTLS DAP in MM 602 and 603. This procedure is still a possibility for some high-speed contingency aborts.

3.2.7 STS-6 Update

STS-6 was an extremely important flight for two reasons: it was the first flight of OV-099, and it carried the first heavy payload—the tracking data relay satellite (IUS-TDRS). Five major modifications were made to the DAP for this flight: 1) IUS-related changes, 2) a GRTLS aileron gain computation logic change, 3) implementation of the operational downmoding concept, 4) addition of the HUD, and 5) rudder/speedbrake limit change.

IUS-Required Modifications: Because of the unique characteristics of the IUS payload, extensive work was done before STS-6 to determine if modifications were required to the entry/GRTLS DAP. The IUS, a solid upper stage built by Boeing, was first used for the TDRS. Because this payload had to be rotated before deployment, it could not be solidly supported in the front. In addition, because of its structural load requirements, it had to be soft-mounted to the Orbiter. The combination of this first large payload's mass and mounting configuration resulted in a set of very strong low-frequency (3-Hz) flexible modes for the combined Orbiter-payload configuration. To avoid significant impact to the rigid stability and response characteristics, a combined hardware-software solution was developed (CR 39983).

The hardware part of the solution was to add a set of nonlinear coulomb dampers to the interface between the cradle and the Orbiter. These dampers were designed to reduce the impact of the payload motion on the Orbiter. It was assumed that they would limit the motion to a low-amplitude limit cycle. Analysis verified this assumption, but no entry flight data has been obtained to confirm it because the payloads have *always* been deployed as planned.

The software changes consisted of three parts: 1) the addition of two new crew-selectable sixth-order bending filters in the elevator loop, 2) an additional second-order bending filter (12.5 sps computation frequency) in the yaw jet loop, and 3) increase from first- to second-order of the ELERROR filter. The

new pitch bending filters could be selected by the crew via the keyboard, whereas the other two changes were made part of the nominal system.

In an attempt to make the CR as simple as possible, the selection of the alternate bending filter was tied to the selection of the alternate elevator schedule, which had been added to handle flights with a wide range of possible XCG during entry.

This decision would create problems for selection of I-loads for future flights. It wasn't until OI-5 that separate keyboard selection was available for the two items. This connection wasn't a problem for single payload flights, but could have been a serious problem for multipayload flights. I-loads were never defined to take advantage of the higher order filter in the ELERROR module because adequate bending frequency attenuation was achieved using the combination of bending filters and a forward loop pitch gain reduction. The filter was reduced to first order as part of the OI-8C scrub.

The magnitude of the analysis to support the commit-to-flight of STS-6 was second only to that of STS-1. Most of the work was associated with the flexible body dynamics and the possible limit cycles relating to the dynamics of the coulomb dampers. Describing-function techniques to estimate when a limit cycle could be expected were extensively used, as was the time domain simulation SIMFLEX at Honeywell. Most of the analyses centered on the early phases of GRTLS, TAL, and abort-from-orbit, all of which would involve landing with the payload in the cargo bay. Emphasis was placed on low dynamic pressure regions because of the high forward gains in the surface loops in these regions.

The two results needed from the analysis were the force level required to activate the dampers and the amount of free play that should be allowed. When the analyses and flight control stability ground tests (see Section 4) were completed, the system was ready for flight.

GRTLS GDA Logic Modification: One other software change for STS-6 was the addition of a new gain in the aileron loop that was a function of angle of attack. Figure 3-16 shows how the GRTLS GDA has been computed since the STS-6 modification. For NEOM, the computation is the same as GRTLS except for the angle-of-attack multiplier, KALPHA.

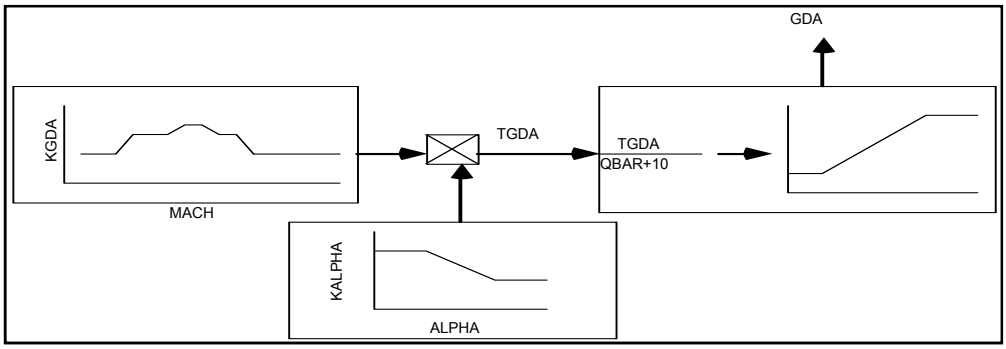

Figure 3-16. GRTLS GDA Computation

When the aft XCG associated with the IUS was analyzed in the alpha-hold and Nz-hold phases of a GRTLS profile, it was found that the high-frequency gain margin for the case with nominal aerodynamics, sensors, and effectors was less than 3 dB. When this was evaluated on the SPS, control was lost with a 4- to 5-dB increase in GDA. A review of the aerodynamic data showed that the rolling moment coefficient for the aileron increased by a factor of two between an angle of attack of 20 deg and 45 deg. The new gain was developed to reduce the forward loop gain by a factor of two at 45 deg and ramp to the nominal gain at 20 deg. With this change, the required gain and phase margins were achieved.

After STS-51L, as payloads with very forward longitudinal CGs were evaluated, it was found that the alpha-scheduled multiplier needed to be changed as a function of the expected CG at the start of MM 602. As the elevator goes up, the gain should increase to compensate for the loss in aileron effectiveness. To handle this case, two sets of I-loads were developed and selected based on the Orbiter CG. A review of the ADB shows the strong relationship between aileron effectiveness and the elevator position.

Operational Downmoding: During the definition phase of the operational downmoding system, a number of options were reviewed by the flight control community, flight crew, and program office personnel. These included 1) adding switches to the new vehicles, 2) eliminating downmoding

completely, 3) using the on-orbit flight control PBIs, and 4) using the entry roll mode switch to provide a limited capability.

For the first flight of OV-099, the software was modified to use the entry roll mode switch to select the low-surface-gain option or the no-yaw-jet option. The other downmoding capabilities were removed from the requirements, but IBM left the unused code in the flight software until the development of original OI-8 software. (This created a problem because the code did not agree with the documented requirements.) Option 4 was selected because OV-099 did not have the downmoding switches or the PBI switches needed to activate the logic. There was no room to add the PBI switches because of the addition of HUD hardware in the glare shield area; it was decided that the low-gain and no-yaw-jet modes were required for the operational phase. Still, the program office would not direct Rockwell to conduct a stability analysis of the downmoding system because of the heavy workload associated with the flight test program and resolution of various flight anomalies. It was known that the system would work well in the higher Mach number (Mach >10) regime, but was unstable and/or had poor response below Mach 7, depending on the aerodynamic data used and the pilot's level of training.

In the spring of 1985, the Orbiter Avionics Office directed the entry FCS community to start to work on an upgrade to the current no-yaw-jet mode. SES trajectory analysis and Honeywell stability analysis were to be included in this effort. After STS-51L, this upgraded no-yaw-jet system was incorporated into the software, and a certification-by-analysis program was conducted before STS-26. *Flight testing was carried out as part of the wraparound DAP flight test program described in the "Flight Test Program" paragraph of Section 6.4.*

HUD Addition: With the delivery of OV-099, an HUD was added to the vehicle configuration as a landing aid. It was set up to display a combination of guidance, navigation, and sensor information to the pilot. Changes made to the HUD for STS-8 included development of two display formats. The first was optimized to support manual landing, whereas the second was an attempt to provide an acceptable autoland monitoring capability. The autoland monitoring format was deleted in the OI-8A software release. The BFS does not support the HUD.

Rudder/Speedbrake Limits: For STS-1 through STS-5, the rudder and speedbrake limits were the same during the airborne and rollout flight phases. In the rudder and speedbrake assemblies delivered for OV-99, OV-103, and OV-104, a manufacturing error limited the amount the right or left panel could go past the center line. Because of the small changes in speedbrake effectiveness between 15 and 0 deg, it was decided to change the software limits and accept the assemblies as built; returning the units would have caused a major impact to the deliveries of these Orbiters. To provide maximum rudder effectiveness during rollout, the software limits were made a function of the weight on wheels (WOW) discrete by changing the associated I-load. The I-load was converted to a constant as part of CR 89674E in OI-20. No attempt has been made to take advantage of the correct hardware in OV-102.

3.2.8 Landing Rollout Upgrades

The evolution of upgrades in the landing rollout system for the Orbiter can be discussed in light of two incidents in flight. The first is the STS-3 "wheelie" and the second is the blown tire on STS-51D, both of which resulted in significant changes to the DAP. The resulting changes were first flown on STS-9 and STS-61A. The program did not include any of the normal taxi tests because of the lack of ability to get the Orbiter rolling at the high speeds (180 KEAS) required. In addition, only limited tire testing was done to determine the parameters of interest to the flight control designers. As will be seen during the following discussion of the nosewheel steering upgrade program, tire tests at Langley resulted in a revised tire model that was incorporated in subsequent Ames simulations.

STS-3 "Wheelie": STS-3 was a unique flight for several reasons: 1) use of autoland down to 100 ft, 2) landing at White Sands, 3) large steady-state winds and shears in the landing altitudes and in the higher altitudes, and 4) the pitch-up transient between main gear touchdown and slapdown. Although the others are interesting, the pitch-up was the only one that affected the design of the DAP.

The STS-3 landing events, as well as can be reconstructed from flight data and pilot comments, were as follows. When the pilot touched down at a higher-than-expected speed due to wind conditions, the RHC was temporarily pushed forward. This established a pitch response of less than 1 deg/sec., which the DAP was not able to stop when the RHC was returned to detent. When the local pitch angle reached approximately 2 deg, the pilot started pulling back on the RHC with increasingly larger deflection. His

initial inputs were not large enough to stop the nose from going down. Finally, the nose started up very rapidly and the pilot reacted by pushing the RHC almost full forward, driving the nose down on the runway. His hard response to the nose-up motion prevented the Orbiter from going airborne. The DAP drove the elevators at maximum rate in both directions during this transient. The pilot then completed the rollout without any additional problems.

Postflight analysis showed that the handling problem was due to the low gain in the elevator proportional loop. In CSS, unlike in the automatic mode, the elevator loop gains did not change when the vehicle touched down on its main gear. In comparison, the automatic system used the main gear proximity switches to change the mode to a new system with higher forward loop gains and an additional integral control term. Linear analysis showed that the system was actually unstable at the lower pitch angles reached on STS-3. The lower the speed, the higher the pitch angle at which the system became unstable. This incident set off a design and analysis effort with a smaller tiger team than that used in the pre-STS-1 redesign effort, but no less dedicated and resourceful. Within a couple of months, this team had completed a design and analysis effort that included simulation of an improved slapdown control system on the entry SES in JSC building 16. The new system was similar to the automatic logic that was a proportional-plus-*double integral system (i.e., a low rate and authority forward loop integrator along with the lagged position feedback*) with higher gains, which relied on the proximity switches or the crew to sequence the DAP to the correct mode. Figure 3-17 shows the original CSS logic and the revised logic.

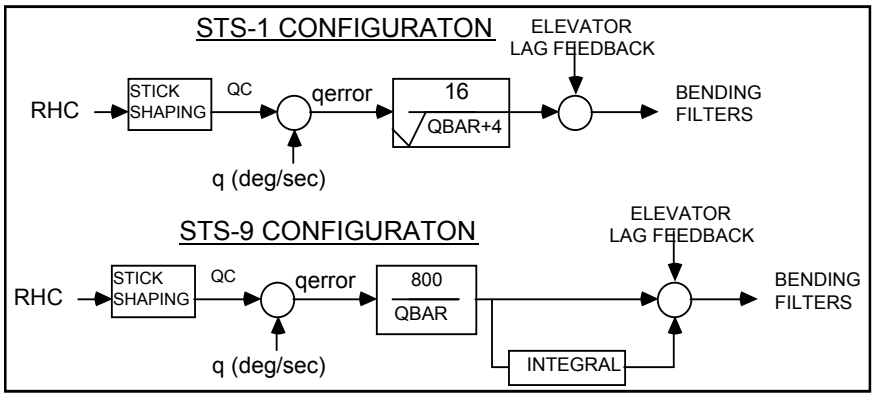

Figure 3-17. CSS Slapdown Control Logic

If the software does not receive signals (change of state of the proximity switches) showing that contact with the ground has been made within a set time, a WOW dilemma is declared. The crew must set the corresponding flag (WOWLON) in the software by depressing the ET-SEP switch or the solid rocket booster separation (SRB-SEP) switch. The set time was lengthened from 3 to 7 sec for later flights to ensure that the transition would be made. This increase was selected based on a review of flight data and simulation data to ensure that the WOWLON would be set in large crosswind cases.

It should be noted that there is only one proximity switch on each gear and only a single path into the computer. The required redundancy is provided by the crew. *When resources become available, upgrading the redundancy in the touchdown detection system should be considered. (Upgrades to main gear touchdown were approved as part of the Extended Duration Orbiter (EDO) program. Software upgrades are discussed in Section 3.2.12.)*

The new slapdown control system that was implemented for STS-9 has been used for all subsequent flights without any problems. For STS-9, the software that included the new DAP was not added to the SMS until late in the training flow, which allowed for only a limited amount of STS-9 crew training. In addition, a computer failed during landing. These combined problems resulted in a slow touchdown speed with a large pitch rate at slapdown. The pilot seemed to have reverted to the technique used to fly the old system. This is an example of what can happen when the flight crew does not get sufficient training for DAP changes.

The STS-41B crew was the first with a full training program using the new system. During the slapdown maneuver, Vance Brand, the commander, actually brought the nose to a stop at a pitch angle of between 0 and 1 deg without any problem. The old system did not have this capability. Unfortunately, there are a large number of data dropouts during this maneuver, thus preventing a detailed analysis of the flight maneuver.

One issue with the new system, first identified by Rockwell pilot Al Moyles, was a change in sensitivity to RHC inputs when the DAP is moded at main gear touchdown. A software change to modify the RHC sensitivity was developed before STS-41B and implemented as part of the OI-10 package. Although the change, which reduced the pitch RHC gain GPX to 0.5, was not originally scheduled for reimplementation in the OI-8 sequence of software deliveries, crew support led to its being incorporated in OI-20.

A second issue, identified as part of the analysis of the deflated strut on STS-41D, was the 10-rps gear-driven oscillation during slapdown. The increased amplitude of this mode can be attributed to the higher gain in the new slapdown system. A software change to eliminate this undesired motion was developed and incorporated in OI-8D. (Although this gear filter was considered for OI-8A and 8C, it was not implemented because of limited IBM resources in the flight control area.)

This gain increase has also resulted in the requirement for increased structural mode attenuation during the slapdown flight phase. Previously, this area was not an analysis driver.

Nosewheel Steering Upgrade: With the aerodynamic flight test program nearing completion, the flight control group's emphasis was shifting to upgrading the overall system for the long-term operational era. In early 1985, a meeting was held to discuss ways to upgrade the nosewheel steering system to a point at which the crew would be willing to use the nosewheel for steering. The nosewheel system had been used for only a short period on STS-9 as part of a DTO in which only the manual direct mode was used. The GPC modes had never been used in flight. Both the manual direct (no computer augmentation) and the manual GPC use the pilot's rudder pedal inputs to provide commands to the nosewheel control logic. The automatic GPC mode uses commands from the automatic rollout guidance based on lateral runway position and velocity, and includes a forward loop gain that is scheduled with Mach number.

For all flights before STS-61A, the primary lateral steering mode during rollout was differential braking. This procedure was consistent with the requirements documented in both the Shuttle Systems Specification (NSTS 07700, Vol. X) and the Orbiter End Item Specification (OVEI). (It should be noted that the older beryllium brakes used on these flights had caused problems or failed several times because of energy and/or dynamic problems.)

Between the first and second days of the nosewheel steering review meeting, STS-51D landed at Kennedy Space Center (KSC). On this flight, one of the main tires blew near the end of rollout. Overheating of the brakes caused by the need to accomplish steering with the brakes was identified as a major cause of the blown tire. This incident demonstrated the need for an operational nosewheel steering system; therefore a two-phase upgrade of the system was undertaken. The purpose of the first phase was to quickly design and certify a fail-safe manual GPC mode so that KSC landings could be resumed. For this design, fail-to-caster was defined as fail-safe.

The second phase plan was to develop a fail-operational/fail-safe system that would provide 1) redundancy in the command path, 2) the ability to withstand an APU failure, and 3) the ability to feed back to the pilot the system status. However, this upgrade has not been made because of time, resources, and program priorities.

One additional problem with the nosewheel steering system that was found and corrected was the positioning of the different modes (aft—manual direct, middle—off, fwd—GPC) on the three-position switch the pilot used to select the desired mode. With the off position in the middle, the crew could not quickly turn the system off when they detected a problem. Several times in simulations, the crew moved the switch too far, an action that could result in loss of control if it occurred in flight. The mode positions were rearranged to be (aft—off, middle—GPC, fwd—manual direct). With this positioning, the pilot could simply slap the switch to turn the system off. *This is a good example of what can happen if care is not taken in defining switch functions.*

Nosewheel Steering Phase I: The baseline nosewheel steering system was not considered acceptable by the flight crew and engineers because a failure in GPC 2 or multiplexer-demultiplexer (MDM) 2 could cause the nosewheel to be commanded to full deflection. This would cause the Orbiter to depart the runway before the crew could turn the system off. In addition, the manual direct mode was considered to have unacceptable handling qualities at higher speeds. Figure 3-18 is a diagram of the original manual GPC mode. (Note that a single MDM is used for output to the nosewheel steering actuator.)

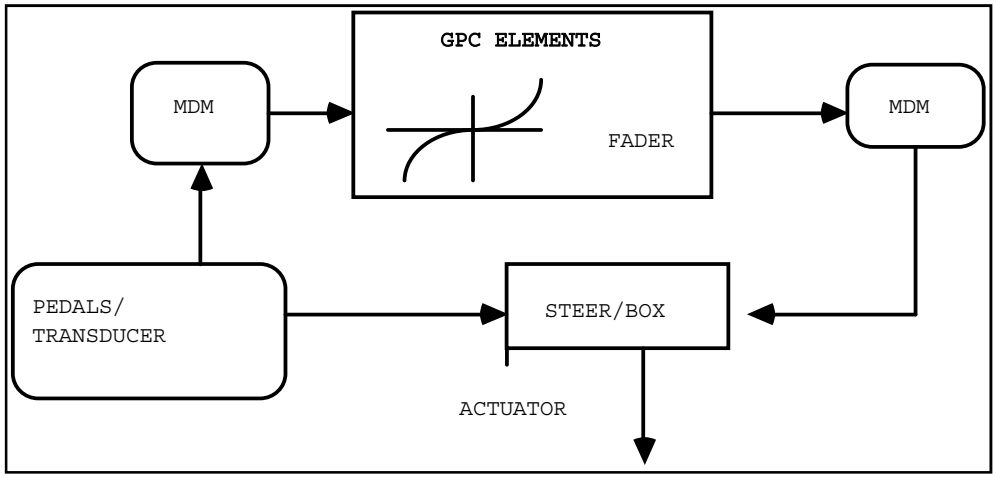

Figure 3-18. Original Manual GPC Mode

The requirements placed on the designers of the new system were to make the manual GPC mode fail-safe and to provide acceptable handling qualities for both manual systems. The need for redundant power was deferred to the second phase of the upgrade. Hydraulic system 1 is the only system capable of driving the nosewheel. Once again, the tiger team concept worked, enabling completion of this complex hardware and software change in only 5 months. The effort included development and integration of hardware, software, and test requirements, as well as math model execution (in SES and SAIL) and vehicle checkout tests (frequency and step).

A key effort during this period was the upgrade of models in the various simulations and analysis tools used to evaluate proposed nosewheel steering upgrades. New models of the tire dynamics (especially cornering forces and friction characteristics), the actuator dynamics, and the antiskid system were developed and implemented. *The antiskid is another off-the-shelf black box that has caused problems because of the proprietary nature of the design.*

The resulting redesign for the manual direct mode consisted of changing the transducers on the rudder pedals that converted the pedal deflection to nosewheel position commands from linear to quadratic transducers. This reduced the sensitivity of the system to small pedal deflections and still provided the required maximum deflections.

The resulting redesign of the manual GPC mode consisted of four individual parts that are shown in figure 3-19, which is a block diagram of the final result of the effort. The numbers refer to the discussion of changes that follows the diagram.

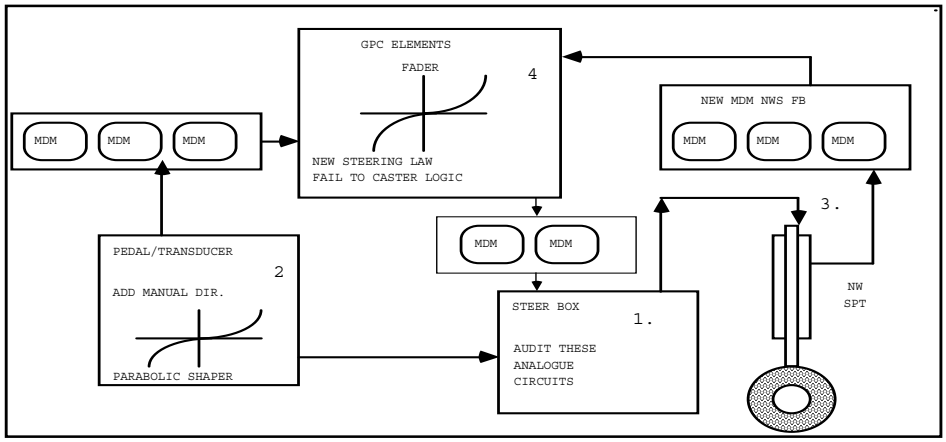

Figure 3-19. Upgraded Nosewheel Block Diagram

The first part of the redesign was a complete audit of circuits in the steering box. This was a problem because of the proprietary nature of the system being reviewed. *(NASA should be very careful in the future about the use of boxes for which it does not have complete access to the design diagrams.)* The

second part was making modifications to the transducer on the rudder pedals. The third part was the addition of new hardware to measure the nosewheel position and feed it back to the GPC. This was a new transducer that Honeywell built by modifying the existing rudder pedal transducer design. The feedback is triplex, even though the mechanical system used to measure the actual deflection is simplex. The feedbacks are through forward MDMs 1, 2, and 4. The fourth part was an extensive upgrade to the nosewheel steering software in the GPC that included the logic to detect a nosewheel steering failure. A failure was defined as a steady or increasing difference between the commanded position and the measured position. Logic was also included to detect reduced rates and to declare a failure if the rates were too low.

An upgraded algorithm to compute the desired command was also added. The system was changed from an open-loop to a closed-loop (Ny, lateral acceleration feedback) system. Further, a second discrete path was added through a second MDM to provide a redundant method of downmoding the system to caster if a failure was detected. Both the discrete through MDM 1 and the discrete through MDM 2 are required to have active GPC steering. The MDM 1 discrete is required to have manual direct steering. (Loss of GPC 1 or FWD MDM 1 will result in the loss of all nosewheel steering capability.)

This system was flight-tested on the Edwards Flight Center (EDW) lake bed during STS-61A with very good results. The system was also used during a nominal rollout profile on the EDW concrete runway (EDW 22) on STS-61C.

STS-30 Results: On STS-30, the first crosswind DTO, with a crosswind greater than 10 kts, was accomplished with a landing on the concrete runway at Edwards (EDW 22). The crew gave the system a Level I Cooper-Harper rating before the slapdown maneuver and a Level II rating post-slapdown. Initial efforts to extract wind magnitude from flight data indicated a wind level between 12 and 16 kts. An unexpected event during this landing was the weight-on-nosewheel dilemma. Two reasons for the dilemma were 1) the soft nosewheel touchdown (less than 1 deg/sec at initial nosewheel contact), and 2) out-of-specification action of the two proximity switches on the nosewheel. Postflight testing showed that one of the switches required 2.1 inches of deflection to indicate weight on wheels. The specification showed a rigging requirement of .875 inches to 1.75 inches. Actual data showed that the crew pushed the ET-SEP switch approximately 4 sec after the initial nosewheel touch. At this point, the software moded to the rollout configuration with its resulting automatic load relief and active nosewheel steering. When the nosewheel steering became active, the software, according to requirements, initially commanded the nosewheel to move from the caster position to a zero deflection in a step. It then ramped the command to the desired position. This transient in the nosewheel command resulted in a transient lateral acceleration of approximately 0.1g. This, combined with the response of the vehicle to the crosswind, resulted in a peak lateral acceleration of almost .25g.

To reduce the transient at nosewheel initiation, the software was changed for STS-28 to initialize the nosewheel command to the measured value of the nosewheel position instead of just setting the initial command to zero. The software was configured to initialize the command to zero because before the initial nosewheel upgrade for STS-61A, there was no sensor to measure the actual position of the nosewheel. The use of the measured nosewheel position to prevent mode switching transients had been included in Phase II of the nosewheel steering upgrade program.

STS-28 Results: Three items of interest occurred in the landing/rollout area on STS-28. The first was that in the initial use of software changes (CR 90060 and CR 90061) to the nosewheel steering on this flight, the software worked as expected. The second was the decision to launch, even though one of the main gear proximity switches had failed. The management team made this decision 2 days before launch based on the crew's training to land and accomplish the slapdown maneuver using the airborne control system. After launch, the question of patching the software to allow the transition based on the remaining proximity switch was discussed, but was discarded because of the undesirability of patching the flight software in a critical area without time to do a complete verification of the patch.

The final item of interest was the extremely slow landing. Touchdown occurred at approximately 160 kts and a pitch angle of almost 14 deg (tail scrape occurs at approximately 16 deg). The commander allowed the Orbiter to decelerate for several seconds with the main gear within a couple of feet of the ground by continuing to hold back stick, instead of letting it settle on the ground at the nominal airspeed. This resulted in a late nosewheel touchdown (140 kts) and a high pitch rate (approximately 9 deg/sec).

STS-37 Low-Energy Landing: The touchdown point on STS-37 was 600 ft short of the marked runway threshold, at a significantly low airspeed—166 KEAS. The cause of this short landing can be attributed to two things. The first was the large wind shear, 70 kts, in the 10,000-ft-altitude range. It should be noted that the pilot was never told of the large shear in the wind profile. The wind profile was outside the design profile (figure 3-20).

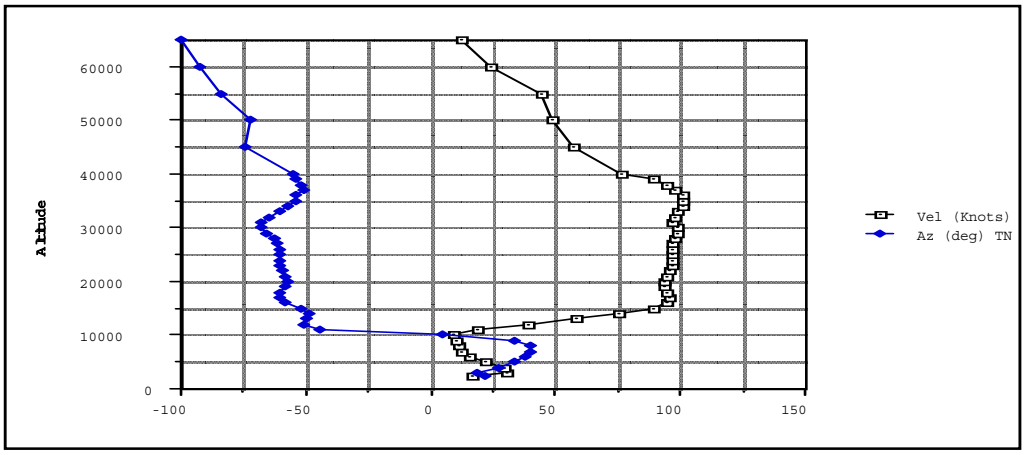

Figure 3-20. STS-37 Wind Profile

The second cause of the low energy was the piloting technique used in coming around the HAC. The commander did not follow the roll error needles, resulting in the vehicle ground track being longer than desired. The guidance attempted to compensate by shrinking the radius of the HAC. Before the shear, the pilot had the energy converging back to the desired level, but was unable to maintain the desired energy and correctly gave priority to establishing the necessary airspeed to allow a successful flare before landing. Postflight analysis has demonstrated that the automatic system would have successfully landed the Orbiter on the runway at the correct airspeed.

STS-39 High-Speed Touchdown: While the energy at touchdown was nominal on STS-39, the right main gear touched down only 170 ft past the runway threshold at KSC. The equivalent airspeed at this point was 218 kts. The primary reasons for the early touchdown were 1) the commander made a very shallow approach (well below the standard 1.5-deg inner glide slope), and 2) to stop a drift caused by a crosswind, he had to roll the vehicle near the ground. It should be noted that the pilot had not been told of the low-altitude crosswind because the 30-ft wind sensors did not record the data. It was only during postflight analysis that the data from the 500-ft tower was reviewed. This tower, located several miles away from the runway, showed a 10-kt crosswind at the time of landing. The landing occurred at the peak of a transient wind profile. Data 5 min before and after showed significantly lower crosswinds at the 500-ft tower.

3.2.9 Significant Analysis Efforts

Over the years, a number of analyses have been completed that may not have resulted in structural software changes but did extend the understanding of the system. Some of these major efforts will be discussed in the following paragraphs, and many more are recorded in the minutes of the joint JSC, Honeywell, and Rockwell flight control reviews.

Extended Pitch RCS Use: In the process of certifying the required longitudinal and lateral CG envelope, it was found that in the region between a dynamic pressure of 20 and 40 psf, the low-frequency gain margins did not meet the requirements in the auto pitch mode in both GRTLS and NEOM. After attempting to modify the forward-loop gains without success (because the gain would have to be increased, causing reductions in the flexible body mode attenuation), a plan was developed and executed to extend the use of the pitch jets to 40 psf.

The key feature in the plan was a series of pitch jet test inputs to obtain flight data on the effectiveness of the jets at the higher dynamic pressures. PTIs were executed at 20, 30, and 38 psf on several flights starting with STS-41B. The evaluation of the flight data showed that the jets were still effective; thus a significant reduction in the uncertainties was included in the resulting database update.

While the PTIs were accomplished by simply moving the HIGHQ flag from 20 to 40 psf, it was necessary to add a new pitch discrete to sequence the pitch axis and allow the yaw and roll axes to be sequenced at the 20-psf level. This change was first added to the software as part of OI-6. (During the period that the extended pitch jet PTIs were executed, only two yaw jets were available between 20 and 40 psf.)

STS-41C Aileron Trim Bias: A review of flight data from STS-13 revealed that the commander had maintained a steady-state roll RHC input during the flight around the HAC and during the approach and landing. Evaluation of flight data showed that the commander had moded to CSS after the roll to the HAC attitude had been started in auto. The aileron trim integrator is zero for subsonic flight in the CSS mode but not in the automatic mode. The zero value for the gain on the trim integrator during subsonic flight was selected based on the ALT design and flight experience, plus crew comments during MIL simulations on the SPS. Figure 3-21 shows the aileron trim integrator gain for the roll error signal.

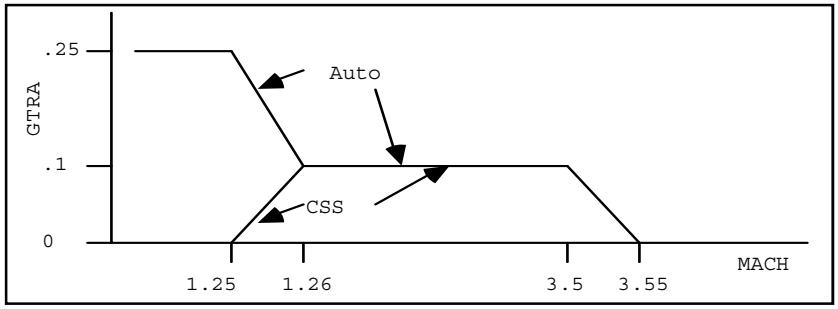

Figure 3-21. Aileron Trim Integrator Roll Error Gain

Normally, in a large subsonic automatic roll maneuver, *with active trim control*, the aileron trim integrator will build during the initial rate buildup and then return to the original value when the rate goes back to zero. Because only the first part of the maneuver was done in auto on STS-13, the normal operation of the trim loop was not available. This condition is still possible.

Manual Pitch Axis Upgrade Evaluation: At the request of the program office, an 18-month study was undertaken to develop an improved CSS pitch axis control system. The study included SES, Ames vehicle motion simulator (VMS), and Calspan total in-flight simulator (TIFS) evaluations and involved personnel from JSC, Rockwell, Honeywell, McDonnell Douglas, and DFRC. Twelve proposed systems were evaluated on the SES; the top performing changes were taken to Ames for evaluation in the moving base VMS simulator. Finally, the top two were put on the Calspan TIFS aircraft for an airborne evaluation. The final result was a decision to not change from the current system. This decision was a direct result of the JSC flight crew position that they preferred the current pitch rate system. Both Rockwell pilots and DRFC pilots preferred the CSTAR (C*), a control technique in shaped-pitch-rate type systems. JSC pilots have learned through hundreds of hours of simulator training and STA training flights and ALT and Orbital flight experience to use the current system. Other pilots, without the extensive training and experience base, preferred the systems that had better direct flight path control characteristics, but allowed larger pitch rate overshoot.

Centaur Evaluation: The magnitude of the Centaur upper stage evaluation was equivalent to that of the IUS evaluation. The two unique features of the Centaur were the liquid propellant and the abort dump requirements. The Centaur was powered by a combination of liquid oxygen and liquid hydrogen (LO_2 and LH_2). The interface control document (ICD) required that both be dumped overboard before landing with the payload still in the cargo bay. Until the cargo integration review (CIR), the formal program position was that no entry would ever have to be attempted without a successful dump of LO_2 and LH_2.

At the CIR for STS-51F, it was acknowledged that a single failure could prevent the dumping of either tank, but not both. Therefore an analysis was required of the effects of having a full or partially full LH_2 or LO_2 tank. The analysis centered on the slosh effects and on the effect of the resultant aft CG. Extensive flexible body stability analysis had been done before the CIR for all flight phases. Analyses at JSC and Honeywell showed that the mass in the LH_2 tank was not enough to affect the results, but the LO_2 tank had a major effect on the XCG. It was concluded that the slosh effects were not major (an excessive amount of analysis may have been done) and the stability analysis of XCG back to 1,125 inches showed a very high probability that the XCG envelope could be extended several inches in the aft direction. The

stability analysis conducted by Honeywell showed that the control system met Level II requirements with the XCG as far aft as 1,120 inches. Only minor violations were seen with the CG at 1,125 inches.

This extension would require additional structural and thermal analysis to clear the Orbiter aft limit from 1,109 to something between 1,115 and 1,120 inches.

Early Rudder Engagement: As discussed earlier, the Mach <3.5 criterion for activation of the rudder for STS-1 was set very conservatively. When data from the early automatic PTIs (STS-5 and STS-6) became available, it was found that the rudder was effective at higher Mach numbers. Rudder PTIs were executed at Mach numbers as high as 6 during the test program. Using these data, the flight control community started to evaluate the benefits and problems associated with earlier activation of the rudder. It was found that the lateral trim problems that occurred just before rudder activation could be reduced (Mach 3.5 to 5 had been the worst region for lateral trim), and the "black zone" (Mach 3.5 to 4) in the no-yaw-jet procedure could be eliminated. This problem region was created by scheduling the GALR gain for the nominal system to pass through 1.0 before activation of the rudder. No significant problems were found during the extensive fixed-point linear and time domain analyses.

Again, the conservative approach was taken: the rudder activation criterion was first moved to only Mach 4.2, with the intent of looking at flight data before moving the criteria to Mach 5. This change was made for STS-51F, which was the last flight with PTIs. Postflight data analyses were as expected; therefore, plans were made to change the criterion. The change had been scheduled for a flight in the summer of 1986, but because of the STL-51L accident, implementation of the change was delayed until STS-26. Mach 5 was picked as the final criterion based on the decrease in rudder effectiveness above this point.

As part of the STS-51F changes, two other I-load changes were made. The first was a change in the rudder forward loop gain, as shown earlier in figure 3-11. The ramp to zero was to provide the desired gain reduction at higher Mach numbers. In addition, the I-loads in the aileron bending filter used between Mach 1 and 3.5 were changed to be the same as the above-Mach-3.5 bending filter I-loads. The logic in the DAP to change aileron bending filters used the discrete that was also used to activate the rudder. Because of the GDA hump in the Mach 4 region, the bending filter with the higher Mach number coefficients was required. In addition, the reduction in aerodynamic uncertainties in the aileron stability derivatives allowed the increase in phase lag associated with the higher Mach number filter. The excess code and I-loads were not removed until the OI-8C software scrub.

Bending Filter I-Load Updates: Analysis of additional payloads showed that neither the current nominal STS-1 nor the IUS bending filters would be acceptable for some of the heavier, hard-mounted payloads. During the aerodynamic flight test program, it was observed that the pitch channel could absorb some additional phase lag at higher Mach numbers. The STS-1 filters had been designed to handle the empty Orbiter modes and had a notch at the Z-fuselage mode (30 rps), whereas the IUS filters were designed to handle the low-frequency (3 Hz) payload pitch and plunge modes. Many of the planned payloads caused the combined Z-fuselage mode frequency to be moved out of the notch provided in the existing filters.

As a result of parallel studies at Honeywell and JSC, new heavy weight bending filters were baselined and have been selected for use in non-IUS flights. The criteria for selection of new filters included constraints on the impact on step response in addition to the normal phase and gain constraints. The response constraint was especially important in the selection of the subsonic bending filter. With the move of the pitch filters to the feedback path in CSS in OI-8C, it may be possible to add attenuation in the pitch axis without significantly impacting the transient response and handling qualities in the landing phase.

In addition to evaluating new I-loads for the current sixth-order filters, Chaing Lin conducted an evaluation of the impacts and benefits of using higher order digital filters in the DAP. This work showed that additional attenuation could be obtained, but at the expense of additional delay in the transient response.

Analysis by Honeywell in early 1985 showed the need for additional attenuation in the pitch jet loop. The resulting redesigned filter has been used for all flights since STS-51J. As part of STS-51L return-to-flight activities, the bending filters were reevaluated. This resulted in the definition of new roll and yaw jet filters that were baselined for flights starting with STS-28. These filters have been referred to as the "n" and "w" filters.

GRTLS Forward Center-of-Gravity Evaluation: Evaluation of the GRTLS DAP for compliance with the OVEI specifications revealed that as the XCG moved forward, both the aileron and the elevator loop

automatic mode low-frequency stability margins were reduced below the required values in the alpha recovery phase (alpha = 50 deg) of the profile. This reduction is a direct result of the need for additional up-elevator for longitudinal trim after the bodyflap has saturated in its full up position. At the forward (65%) end of the required envelope, the elevator is in excess of 20 deg up for nominal aerodynamics.

These results were documented in the minutes of several joint JSC-Rockwell-Honeywell FCS reviews and were briefed to Frank Littleton in the Orbiter Project Office. As a result, a JSC memorandum was written in 1983 to temporarily constrain the flight planning process to the as-built Orbiter capability. It was hoped that a simple software change could be found to solve the problem.

Several joint studies were done, with Buddy Schubele of Honeywell taking the lead. Although a number of options were evaluated, no acceptable change was found. Changes to the flight profile were also evaluated. A reduction in the angle of attack during this phase would solve this flight control problem, but would result in unacceptable higher dynamic pressures during the Nz-hold phase; therefore, it was decided not to change the system. One key reason for this decision was the interaction between the Orbiter dump profile and the movement of the longitudinal CG. A detailed review of the baseline dump profile (excluding the FWD RCS dump) showed that the Orbiter could not have an extremely forward CG in this phase without violating the 65% criteria in the later phases of the profile. At the STS-26 Orbiter Design Certification Review, the Orbiter project manager directed the development of a change to the OVEI specifications and the Space Shuttle systems specifications, NSTS 07700 Vol. X, to make the requirements match the as-built system capabilities. The change was approved by the Level II Program Requirements Change Board (PRCB) in April 1989.

GRTLS GDQ Limit Reduction: To meet the low-frequency elevator loop margin requirements for STS-1, it was necessary to have a higher limit on the elevator forward loop gain, GDQ, during the alpha recovery phase. This limit was set to a value of 10 instead of the normal value of 5. This higher limit was a driver on the flex analysis and the design of elevator bending filters; therefore, the reduction of this gain was a priority as the flight test data became available. The resulting reduction in the pitch jet uncertainties allowed the limit to be first reduced to 7 on STS-6 and then to the standard 5 on STS-9. The software capability for a separate limit was removed as part of the OI-8C scrub.

GRTLS Beta Washout Initialization: Currently for entry and GRTLS, the beta washout filter is initialized to output zero (response to a steady-state input). Unlike entry, where the expected beta at washout activation (Qbar = 2 psf) is near zero, the beta at GTRLS washout activation (start of MM 602) may be significant. Although NSTS 07700, Vol. X, puts a requirement on the GRTLS ET-SEP DAP to maintain the computed beta to less than 2 deg, the actual number may be greater due to high-altitude winds.

In the early 1980s, Dale Bennett of Rockwell directed a study to evaluate the effect of initializing the output of washout to current input. The results of this study indicated that improvement was not worth the cost of changing existing flight software; therefore, the proposed change was dropped. (With the current emphasis on contingency aborts, this proposed change may need to be reevaluated.)

Entry Elevator Schedule Elimination: Elimination of the need to select the desired elevator schedules for each flight was approached in three ways: 1) three generic schedules (AFT, MID, and FWD) were defined and have been used for most flights since STS-51F; 2) a software change was defined to load all three generic schedules into the software at the same time instead of having to select two of the three for each flight; and 3) a software change was defined that would remove the need for a schedule. The three schedules that have become know as the “generic elevator schedules” are shown in figure 3-22.

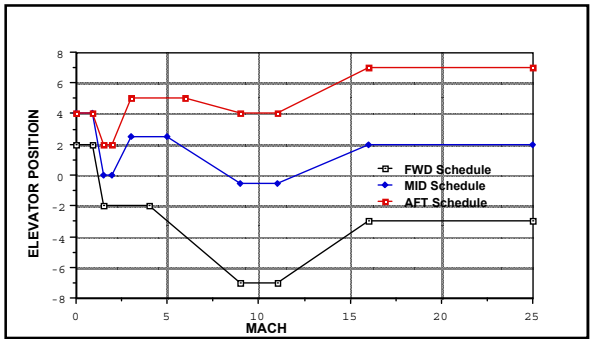

Figure 3-22. Generic Elevator Schedules

Mark Hammerschmidt defined a new set of logic that allowed the software to compute the desired bodyflap and elevator trim positions as a function of the actual bodyflap and elevator positions at any time in a trajectory. This logic has been documented and a software change request submitted. Before the change could be approved, a new Space Shuttle main engine (SSME) heating problem was found; therefore, the logic had to be modified to honor the constraints on elevator and bodyflap position imposed by the SSME project.

This proposed logic was functionally verified by running a series of SES and SDAP trajectories with various aerodynamic uncertainties and reductions in the bodyflap hysteresis logic. The purpose of the reductions was to ensure that a bodyflap limit cycle would not occur. *Additional discussion of this topic appears in the **"The Bodyflap Change"** paragraph of Section 3.2.12.6.*

Reaction Control System Redlines: The engineering and operations communities both recognize the need to reduce the current entry RCS redlines. Early in the program, the magnitude of the aerodynamic variations was the primary driver for the RCS redlines, but as data were obtained from the flight test program, variations were reduced drastically. This resulted in an initial reduction in the redlines, especially for aft CGs. When FAD 26 data became available, it was found that the baseline atmospheric turbulence model had become the driver for RCS usage.

Several approaches to further reduce the redlines include 1) going to a single yaw jet system, 2) opening the jet deadbands and relying more on the reverse aileron concept for control, and 3) updating the turbulence model. Analysis for the first two approaches has been accomplished. Development of a minimum RCS system appears feasible, but will require a considerable analysis and verification effort. After Marshall Space Flight Center completed development of a revised turbulence model for consumable analysis, a Monte Carlo version of the SES was used to define RCS redlines of various sigmas. The turbulence model was incorporated, along with a revised aerodynamic model and random Global Reference Atmosphere Model (GRAM) atmospheres obtained from Jim West of the JSC Flight Design and Dynamics Division to build the new redlines. Figure 3-23 shows the effects of variations in longitudinal CG, vehicle weight, and orbital inclination on RCS usage.

Based on these data, it was decided at the entry flight techniques meeting to go with a redline of 1,100 lb for 28-deg inclinations and 1,300 lb for 57-deg inclinations. The first use of these new numbers was on STS-34. The method of handling flights at other inclinations is still being worked.

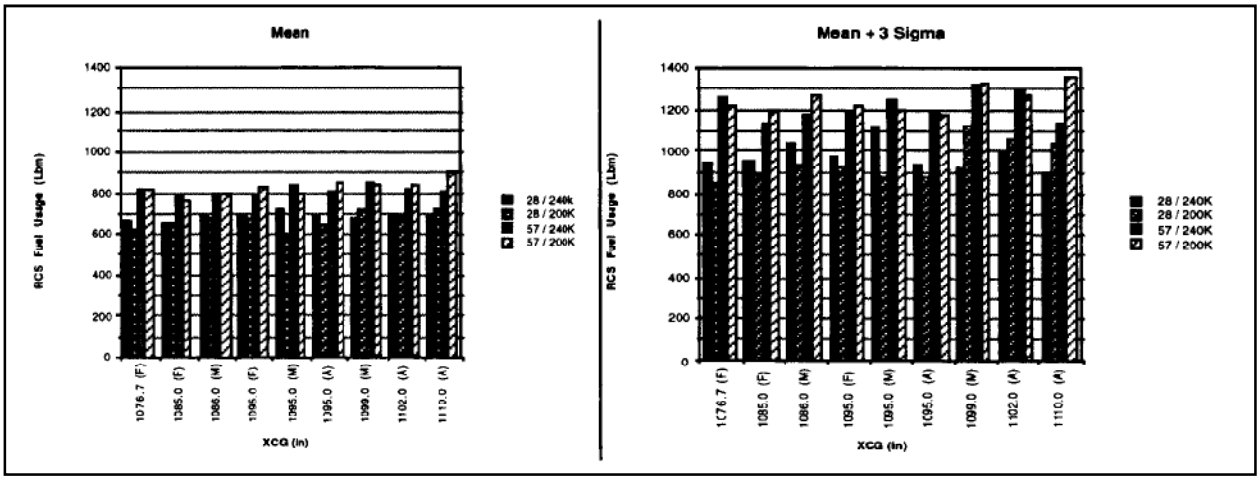

Figure 3-23. RCS Usage from Monte Carlo Analysis

3.2.10 Abort Dump Enhancements

In 1984 to early 1985, a major abort landing weight reduction program was undertaken for RTLS, TAL, and AOA. This program was required to accommodate the heavier payloads that were being manifested for future flights. At this time, the maximum certified abort landing weight was 240,000 lb. This program involved the design, analysis, and verification of a series of changes to dump as many liquids overboard as possible before landing. During this period, a number of new main propulsion system (MPS), Orbiter maneuvering system (OMS), and RCS dumps were added to TAL and GRTLS. The difficulty of the

analysis and verification of the different proposed dumps varied from very simple (aft RCS) to very complicated (forward RCS). The criteria for initiation of each dump were shown in tables 2-2 and 2-3.

Aft RCS: Early in the program (before STS-1), an aft (4 + X) RCS dump was baselined for GRTLS to meet the structural requirements of the aft RCS tanks for landing. The length of the dump was set to minimize the landing weight without moving the CG extremely forward. A similar dump, added to TAL as part of OI-5 to reduce the landing weight by about 2,000 lb, was scheduled to be executed at Mach 8 to ensure that enough propellant would be available for control during entry. It was found that because the +X aft RCS jets fire almost through the CG of the Orbiter, they have very little effect on the control system. The major effect of the dump is to add some energy to the trajectory, but analyses showed that the entry guidance and control system could handle the additional energy and still achieve the desired entry/TAEM interface conditions. Post-STS-51L, it was determined that continued firings in excess of 88 sec were not acceptable from an RCS subsystem point of view. In addition, some flights are being planned without aft dumps to prevent the XCG from moving forward.

Main Propulsion System Dumps: Additional capability to dump the MPS propellants (LH_2 and LO_2) trapped in the Orbiter feed lines after ET-SEP was added as part of OI-6. When the need for capability to minimize the amount of LH_2 and LO_2 was recognized, a 1.5-inch LH_2 RTLS dump valve was included in the design, along with the capability to dump a limited amount of LO_2 through the main oxidizer valves (MOVs) during an RTLS abort. For a normal mission, these propellants are vented during on-orbit operations. To ensure complete removal of these fluids, a vacuum-inerting dump was added to the process for both TAL and GRTLS using the 8-inch fill-and-drain valves on the sides of the Orbiter, and the current MOV dump was moved from MM 104 to MM 304 on a TAL abort. The MOV dump was moved to allow the crew to load the entry software earlier in the timeline and to ensure that the moments generated by the LO_2 fill-and-drain dump remained small.

In support of this effort, a flight test was defined and executed on STS-51D to validate the force and moment models being used to determine the effects of the fill-and-drain dump. The procedure used for this test was to close off the MPS system and then to open the 8-inch valves. When this was done, the Orbiter trans-DAP was not able to prevent the Orbiter from rolling to almost 90 deg. when the command was wings-level. Postflight analysis revealed that when the MPS system was closed, a rapid pressure rise resulted that caused excessive forces and moments on the Orbiter. As a result of this experience, a new test procedure was developed to better simulate the TAL and RTLS dump timeline. When this procedure was executed on STS-51J, the forces and moments were at the expected lower level.

The results of this test were used to partially validate the MPS force and moment model that was being used to assess the impact of the new dumps on the entry and GTRLS FCS. The model included 1) the jet effects of the LO_2 and LH_2 as it comes out of the valves, 2) the impingement effects of the plume on the wings, and 3) the effect of the flow out of the valves on the normal flow field about the Orbiter.

Using this model, it was determined that the best place to execute the dump is after the high-Qbar (dynamic pressure > 20 psf) flag has been set, but before the dynamic pressure has built up to higher levels. The first constraint was based on the desire to have all four yaw jets available for control, whereas the second constraint was imposed to minimize the flow field interaction. Therefore, the dump logic was designed to start the fill-and-drain dump when the dynamic pressure reached 20 psf in GRTLS and when the Mach number decreased to less than 20 in TAL. It should be noted that because of the length of time between opening the MOVs and Mach 20 on a TAL, it is expected that most of the LO_2 will have been dumped through the MOVs and that very little effect will be seen when the fill-and-drain valves are opened. In GRTLS, a small yaw upset with the yaw jets firing from 5 to 15 sec is expected.

OMS Dump: During the ascent phase of an abort, most of the OMS propellant is dumped by firing either the OMS engines only or a combination of OMS engines and the 24 aft RCS jets in an interconnected mode. All of the OMS cannot be dumped during ascent because of the requirement to provide single SSME roll control using the aft RCS jets. Therefore, this dump is stopped when the single engine roll control level (approximately 1,500 lb) is reached. For OI-7C (the Centaur load), it was decided to add the capability to dump the remaining OMS propellant during the early part of a TAL by firing the OMS engines. The analysis of this new capability did not show a control problem for either the nominal conditions or for any failure mode. The aft RCS is able to handle the moments generated by the dump.

It should be noted that no attempt was made to certify the interconnected dump logic that was also added to MM 304 or 602. There are known problems with the mirror image logic that is used during an

interconnected OMS dump. (The term “mirror image” refers to the concept of turning on all the aft jets and then turning off jets as required to produce the moments required for control.) A very limited database exists on the stability and response characteristics of this control mode.

The major problem noted during the analysis was the limited time available to accomplish the dump before the buildup of aerodynamic forces. These forces will move the OMS propellants away from the OMS tank screens and cause variations in the mixture ratios as the engines shut down because of the inability of the tanks to feed the engines.

Protection for the case where the dump is done using only the OMS engines was added in MM 304 as part of the OI-8A software build, as well as in MM 602 for OI-8C. The protection automatically turns the OMS engines off when the normal acceleration level reaches .05g. The only problem is that the screens will not be able to support the interconnected dump before .05g for a limited OMS fuel level.

Two other items were noted in OMS dump: 1) reduction in the plunge into the atmosphere because of the additional energy in the trajectory, and 2) the effect on computation of the estimate of dynamic pressure caused by the NAVDAD software assumption that the only forces on the Orbiter during entry are aerodynamic. The maximum error noted is about 6 psf; the major effect is to delay activation of the aerodynamic surfaces. The software could be modified to improve the estimate by adding logic to account for the OMS forces.

Forward RCS Dump: The final and most controversial element of the dump program was the addition of the capability to dump part of the forward RCS propellants during atmospheric flight (MM 304 in TAL and MM 602 in GRTLS). This dump was planned to be done by firing the opposing forward yaw jets for a defined length of time. A complete dump could not be accomplished because of the configuration of the tanks: they were not designed to operate in an entry-type force field. Because of the uncertainty of the effects these jets would have on the Orbiter flow field, a program combining wind tunnel and flight tests was defined to validate the models used to simulate the effects of this dump. It was agreed that completion of the flight test program would be a constraint on the use of this dump capability.

A model validation program led by David Kanipe (aerodynamics and wind tunnel tasks) and Mark Hammerschmidt (PTI design and effects on FCS) was planned to consist of three parts: 1) evaluation of an analytical model, 2) model update and analysis based on wind tunnel results, and 3) model assessment based on flight-derived data. The PTI program was designed to be accomplished in six flights with time to analyze the initial results (short pulses—1 to 5 sec) before longer pulses were tested to get the steady-state effects. The first flight planned to execute these PTIs was STS-61C. Just hours before entry, it was found that one of the forward yaw jets on OV-102 was of an older design, on which the effects of the planned PTIs had not been evaluated enough to guarantee safety; thus the maneuvers were cancelled. Currently, three sets of forward RCS PTIs have been completed with excellent results. Good agreement has been seen in comparisons of wind tunnel data and flight data. OI-23 software will improve the capability of the software to properly sequence the GRTLS MPS and RCS dumps.

During safety checking of the forward PTIs, forward RCS uncertainties from the wind tunnel program were increased by a factor of three in combination with the worst-case aerodynamic uncertainties. To provide an additional safety factor, logic to automatically stop the maneuvers if body rates exceeded a preflight set magnitude was added to the PTI logic.

Summary: A large effort was expended by the FCS community in support of the abort dump program. The key analysis tool was the entry SES. Early in this program, it was recognized that the dumps had little effect on the classical stability of the FCS. Their major effect was to temporarily change the lateral and longitudinal trim requirements. Therefore, most of the analysis was done in the time domain. A major problem created by the addition of the dumps was a large movement of the XCG between ET-SEP and landing; this continues to cause problems in the selection of elevator schedules.

3.2.11 Payload ICD Issues

Because of the effect that a payload’s structural characteristics have on the overall combined system characteristics, the need to control payload characteristics was recognized early in the program. The approach taken was to define conservative screening criteria and to plan on conducting detailed analysis on any payload that failed to pass. An assumption of the current criteria is that if a payload is acceptable for entry, it will be acceptable for ascent. (If the first stage ascent flight control requires use of Orbiter-mounted RGAs, this assumption will need to be reevaluated.)

Figure 3-24 shows the current screening criteria for ascent/entry. The inputs to the criteria are gross payload weight, payload structural damping, and payload frequencies. Given the required inputs, the minimum allowed frequency can be obtained using payload weight and damping (as shown in the figure). If the lowest payload frequency is greater than the minimum allowed frequency, the payload passes the screening and no payload unique analysis is required. If the payload fails the screening criteria, the payload supplier will be required to pay for detailed flight control evaluation (referred to as an optional service analysis). Examples of payloads that have paid for optional service analysis are Gamma Ray Observatory (GRO) and Shuttle Commercial Orbital Transfer Stage (SCOTS) upper stage. In addition, unique payloads such as Centaur required detailed analysis as a normal course of business.

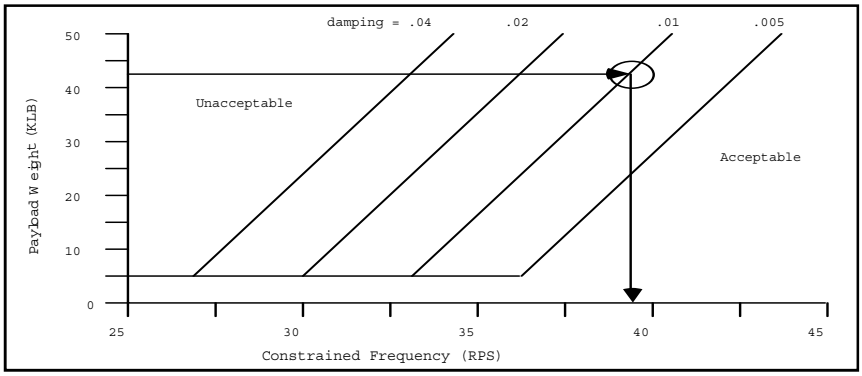

Figure 3-24. Ascent/Entry Payload Screening Criteria

The known problems with the current ICD are 1) no accounting for more than one payload on the same flight, 2) no accounting for the strength of the individual modes, and 3) no accounting for slosh modes.

An update to the current ICD was developed and submitted for approval, but was later withdrawn because additional changes were requested. The desire is to incorporate the mode strength data into the ICD. The approved ICD provided for a set of equations to estimate the effects of multiple payloads and has been used to assess several payloads to determine the level of analysis required for commit-to-flight.

In the 1991-through-1993 timeframe, flex enveloping analysis was performed for the mated coast (M/C) and ET-SEP RTLS flight phases to define payload envelopes within which commit-to-flight analysis would not be required. But because the yaw channel in the current mini-DAP has no bending filter to provide bending mode attenuation, the M/C RTLS yaw axis payload envelope is restrictive. Therefore, flight-by-flight analysis has to be performed for the M/C RTLS flight phases because a usable M/C RTLS FCS flex payload envelope would require implementation of a software change. To address this issue, Dzung Duong proposed CR 90706 ("M/C / ET Sep RTLS Mini-DAP Yaw Channel Bending Filter") in 1999, but the proposal never received funding to design and implement the change.

3.2.12 Post-STS-51L Software Modifications

After the STS-51L accident, a new software release sequence was defined to allow incorporation of mandatory return-to-flight changes. A key question discussed in this time period was which computers should be used for the return to flight. It was decided to continue to use the current (AP101B) computers and to delay the step-up to the new computers (AP101S).

Figure 3-25 shows the flow of software releases from STS-51L to projected first flight of the upgraded GPCs. It can be seen from this drawing that after STS-51L, a split developed in the flight software release sequence. The OI-8 leg was used to develop the return-to-flight software and will be used for all future flight software releases that are scheduled for actual flight usage. The OI-9, -10, and -11 leg was defined before STS-51L and was intended to result in the software release for the first flight of the upgraded GPCs. Many of the changes incorporated into the OI-10 and -11 releases have been moved to the OI-8X leg and incorporated in OI-8A, B, and C. Those requiring large amounts of additional memory, such as the additional displays in OPS-1 and -6, will have to wait for incorporation until after the OI-8F release (first flight load for new GPCs). Because of documentation development between the writing of these changes and the 8B FSSRs, the changes that were not incorporated in OI-8A or B are being rewritten for a new submittal and consideration for later releases.

To expedite testing of the upgraded GPCs, a version of the OI-8B STS-26 RECON-2 software that was compatible with the upgraded GPCs was developed. This software release, denoted OI-9B, was used in the JSC Avionics Engineering Laboratory (JAEL) and SAIL. The only CRs in OI-9B that were not in OI-8B are related to the new machine operating system.

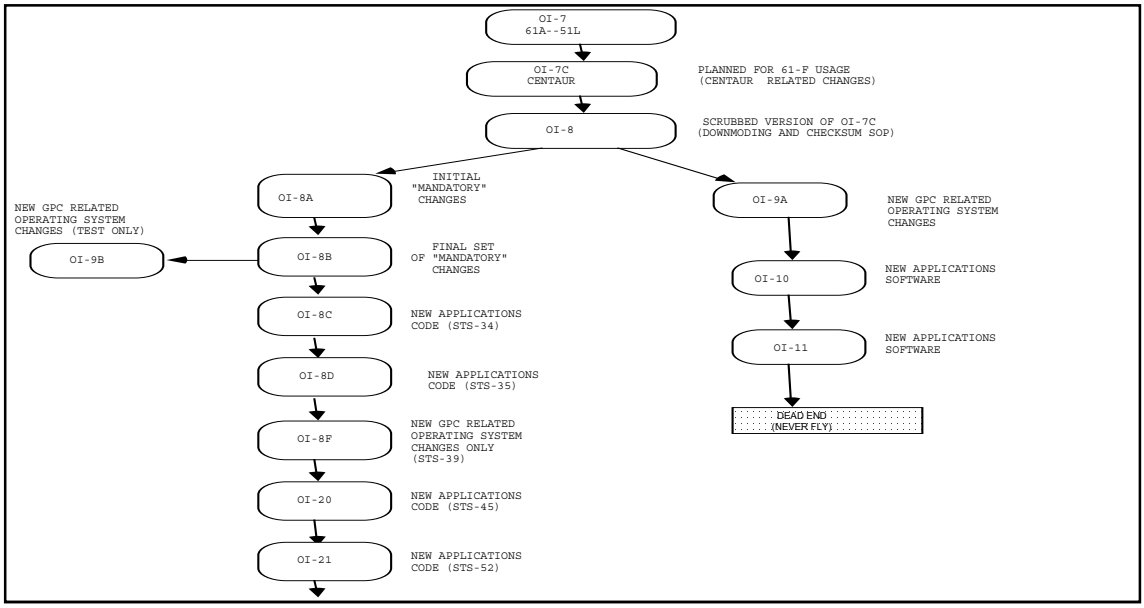

Figure 3-25. Current Software Release Sequences

3.2.12.1 OI-8A and -8B Approved Changes

As part of the new software release sequence definition, several major changes to the entry/GRTLS DAP were approved. The following paragraphs discuss each of the changes.

Nosewheel Steering Update: (CR 79946F) Between the baselining of the OI-7 release for STS-61A (Spring 1985) and the baselining of the OI-8A release for STS-26, it was found that a revision to the nosewheel steering logic was required to handle two blown tires at or near nose gear touchdown. Revisions to the tire model from the Langley track tests were the primary reason for the change in the results from previous Ames rollout simulations. The new change added a filter in the lateral acceleration feedback loop and increased the gain in the feedback loop by a factor of 2 (6 dB).

The last two flights (STS-30 and STS-33) using OI-8B software incorporated two additional changes, CR 90060 and CR 90061A, which resulted from the STS-28 flight results. Details about these changes were given earlier in the “STS-28 Results” paragraph of Section 3.2.8. These CRs were also approved for subsequent software releases.

Early WOW Protection: (CR 69089F) It had been found that a failure in the Orbiter wiring could cause all of the proximity switches (main gear and nose gear) to be set early. If this failure occurred between the transition to MM 305 (NEOM) or MM 603 (GRTLS) and touchdown, the flight control would mode to the rollout system. SES simulations showed that a total loss of control could result because there is no trim loop in the rollout pitch control system.

The software was programmed to not set the WOWLON flag until the crew pushed one of the SEP switches if the failure happened before the major mode transitions. The new software change inhibited the setting of the landing discretes, if one of the nose gear discretes and one of the main gear discretes were set at the same time.

No-Yaw-Jet Upgrade: (CR 79616G) The no-yaw-jet downmoding system was upgraded and certification analysis was completed as directed by the manager for National Space Transportation System (NSTS) engineering. The changes to the old system included 1) scheduling the GALR gain as a function of Mach number, 2) modifying the Ny feedback to the aileron channel for the no-yaw-jet system, and 3) activation of the rudder at Mach 5 (this change also was applied to the nominal system). A separate CR (79945D)

was written and approved to add the no-yaw-jet and low-gain modes to the BFS. It should be noted that the no-yaw-jet system is available only in the roll/yaw CSS control mode.

Auto Load Relief: (CR 89120A) To achieve minimum loads on the main gear during rollout, logic to automatically position the elevons during rollout was implemented in both the PFS and BFS software. The logic will mode the pitch axis to auto (.5 sec after weight on nosewheel is set) and then command the elevator to 10-deg down during the entire rollout phase. The pilot can get out of this logic by pushing the pitch CSS PBI or by using the hot stick option. A separate pitch axis deadband for hot stick logic was defined for rollout.

Split-S Modifications: (CR 79644C, CR 89256, and CR 89850) At the direction of the PRCB, the Shuttle Avionics Software Control Board (SASCB) approved a series of three CRs for OI-8A that were meant to provide a split-S abort capability. The first of these CRs added logic to the GRTLS DAP that would keep the yaw jets on if the altitude was above 80,000 ft, and would bypass the turn coordination logic if the magnitude of the pitch angle was greater than 80 deg. None of these changes had been evaluated in detail on the SES before approval. There was no aerodynamic or aerothermal database to support analysis of these GRTLS DAP changes. As soon as the GRTLS DAP change was put into the SES, it quickly became obvious that to make the system work, two additional changes would be required. The first was a change to prevent subsonic minimum dynamic pressure logic from becoming active if the altitude was above 80,000 ft. (This logic turned off the pitch/roll jets and prevented correct surface gains from being computed). The second was to reinitialize the bending filters if Mach went from below to above a value of 1.

Even with these additional changes, simulations have shown that further DAP changes are needed to make the split-S work. For some cases structural changes to the Space Shuttle system are required.

3.2.12.2 Entry/GRTLS DAP-Related Changes

Over the years, several changes have been made that affect the DAP operation and requirements that are not part of the DAP itself. Following is a discussion of some of the major changes.

Bailout Control System: (CR 89250 and CR 89272B) The capability for the crew to set the Orbiter up at a manually selected airspeed (guidance actually controls to a fixed dynamic pressure) and roll angle was added as part of the OI-8B system. The software changes were added to the GRTLS TAEM guidance to make use of existing airspeed control logic there. These changes required evaluation of the DAP at new subsonic flight conditions (alpha -15 to -20 deg and 100 KEAS).

Early TAL Transition Procedure: The change to the crew procedures to open up the criteria for the PRO to MM 304 on a TAL for STS-26 required a significant set of analysis cases, especially the late TAL (180-deg roll) configuration.

Nominal OMS Maneuver in MM 304: To ensure a sufficient distance between the Orbiter and the ET, a 100-ft/sec OMS burn was added to the nominal TAL profile in MM 304. As part of this change (CR 89142B), logic was added to stop the dump when the Nz level reaches .05 g. There is capability for either an OMS-only dump or an interconnected dump (24 RCS jets and mirror image jet selection logic). The OMS-only dump is considered an intact abort requirement, whereas the interconnected dump is considered a contingency case. *I wouldn't be surprised if the interconnected logic isn't upgraded as part of the contingency abort review.*

3.2.12.3 OI-8C Approved DAP Changes

Two significant software changes to the entry DAP as well as several related changes were approved for OI-8C. They are described as follows:

Elevator Bending Filter Move: The first change (per CR 89415A and CR 69870F) was to move the elevator bending filters from the forward loop to the pitch rate feedback path for the CSS mode. This change was designed to reduce the delay between RHC movement and response to that input, thereby improving handling qualities and PIO tolerance. The phase characteristics of the filters added the equivalent of approximately 40 msec transport delay in the overall vehicle response.

Scrub of Excess Code: The second change (CR 79962F) removed unused and excess code from the entry and GRTLS DAP to allow incorporation of other required changes. This CR removed approximately 350 words from the OPS-6 and OPS-3 software loads. Some changes were to 1) remove Entry 5 boosted

Ny logic, 2) remove soft stop logic, 3) remove pitch rate feedback gain, 4) reduce number of break points in a number of gain schedules, 5) simplify the aileron trim logic, 6) change bodyflap initialization and limit logics, 7) simplify supersonic aileron bending filter logic, 8) remove aileron deadband logic, 9) remove PRL acceleration limit logic, and 10) remove capability to use rudder in GRTLS ET-SEP DAP.

Discussed but not Approved: Two changes that were considered, but not baselined because of lack of IBM resources were 1) a rollout pitch notch filter designed to reduce the effects of the gear modes during slapdown (CR 79396D) and 2) a yaw rate filter designed to notch out the effects of the wing antisymmetric mode (CR 79630).

Related Changes: Two related significant changes and a number of smaller changes related to the entry/GRTLS DAP were approved for OI-8C. These are described as follows:

MM 601-602 Transition: CR 89413B modified the logic for the automatic transition from MM 601 to 602. This change added a new test to ensure that the angle of attack magnitude was less than 90 deg when the transition occurred. This change was developed to prevent loss of control in contingency aborts between powered pitch around and Vrel of zero. The navigation logic is such that the computed angle of attack is incorrect for angles greater than 90 deg. The ARCSIN function is used instead of the ATAN2 function.

Contingency Nz Automatic Logic: CR 89474B added an automatic capability for the open-loop phases (alpha hold and Nz hold) of contingency aborts. Logic was added to GRTLS guidance to automatically compute the desired angle-of-attack command and Nz command during a contingency abort and then automatically fly the desired profile. This change was the number one priority software change related to contingency abort. A byproduct of this change is the correct setting of the IPHASE flag used by the GRTLS DAP. Before this time, the IPHASE flag had been initialized to 6 and not changed during a contingency abort. This change allows the closure of an OI-8B Discrepancy Report (DR) caused by the use of the incorrect gains, when the BAILOUT logic is used in OPS-6.

In addition, several smaller changes were approved to fix problems found in executing contingency aborts that were related to the GRTLS control system: 1) CR 89229G added an automatic termination to the GRTLS OMS dump similar to the TAL OPS-3 protection; 2) CR 89465C provided a special LH_2 dump sequence for selected contingency abort (this sequence is manually initiated using the MPS switch); and 3) CR 89479 removed the automatic OMS initiation in MM 602 added at the crew's request to OI-8B. (The double toggle procedure will be required to initial OMS dumps in certain contingency cases.)

3.2.12.4 OI-8D Approved DAP Changes

Three changes were approved for the entry/GRTLS DAP as part of the OI-8D baselining process. Two of the changes were related to landing and rollout and the third is associated with expanding the GRTLS forward CG capability.

Two landing and rollout changes were 1) a rewritten version of the pitch notch filter, and 2) a new change to provide a separate up-elevator limit after WOWLON.

A rewrite of the previous notch filter change request (CR 79396) was required to make the documentation consistent with changes that had been approved for OI-8C. The rewrite (CR 89443D) provided for reduced interaction between the entry FCS and the dynamics of the gear modes by use of a digital second-order notch filter in the pitch rate feedback path.

The second landing and rollout change (CR 89442G) was to provide separate I-loads (before and after WOWLON) for the maximum allowed up-elevator command. The dual I-loads are required to allow the full up-elevator during the early part of various abort modes and to restrict the command during slapdown. The reduced slapdown limit is desirable because the slope of the pitching moment versus elevator curve changes signs between 20 and 25 deg elevator during the slapdown maneuver. This sign change causes a loss in desired nose-up moment instead of the desired increase when the elevator is commanded past the reflection point in the pitching moment versus elevator curve. It should be noted that the normal force vs. elevator curve does not have this reflection point; therefore, the main gear loads due to aerodynamics will continue to increase as the elevator continues up. Incorporation of this change will reduce peak main gear loads during the slapdown maneuver.

Expansion of GTRLS forward CG (CR 89678), the third OI-8D change, provided the capability to have different values of the I-loads in the aileron trim loop in GRTLS and ENTRY in the BFS. Higher gains were

needed in this path to react to rapidly changing trim requirements in GRTLS when the CG is forward and the elevator is up. The PFS already had this capability because the GRTLS and entry DAP are in separate overlays of the flight software. It was agreed that until OI-8D was available, the new GRTLS I-loads would be used in the PFS and the current I-loads in the BFS on flights projected to have forward CGs in GRTLS.

Three non-FCS changes in OI-8D affected the use of the DAP. These were 1) CR 89665B, which corrected the handling of the HUD velocity vector in extreme off-nominal cases; 2) CR 89665B, which allowed the crew to declare a post-MECO TAL selection capability; and 3) CR 89484C, which provided for entry/TAL guidance enhancements. This last CR corrected a number of minor problems with entry guidance operation that had been noted either in simulations or during the first 24 Orbiter flights. The major FCS-related change was correcting the PTI inhibit logic to make the pre-roll-reversal maximum allowed heading error a function of the number of roll reversals already executed. This change makes the software function according to the original design intent.

3.2.12.5 OI-8F Approved DAP Changes

No applications changes were allowed as part of the build of the first flight load for the new GPCs (AP101S machines).

3.2.12.6 OI-20 Approved DAP Changes

Several DAP-related changes were baselined for the first applications update for the new computers. Among these, the three key changes were 1) addition of the “smart” bodyflap, 2) half-gain RHC during rollout, and 3) redundant nosewheel steering related software.

The Bodyflap Change (CR 79844G) eliminated the need to select elevator schedules before flight. The new software contains an algorithm that computes the desired elevator and bodyflap positions to balance the load between the two surfaces. The final weighting factors (I-loads) to be used in the software in OPS-3 would be defined based on a combination of SSME and Orbiter heating constraints and flight control requirements. The OPS-6 values would be defined based on flight control requirements and surface hinge moment constraints. Originally the CR was an OP-3-only change, but it was expanded to include OPS-6 to aid the contingency abort upgrade effort. Excessive bodyflap hinge moments are a major cause of loss of control during contingency aborts at low Mach numbers. The smart bodyflap logic is shown in figure 3-26.

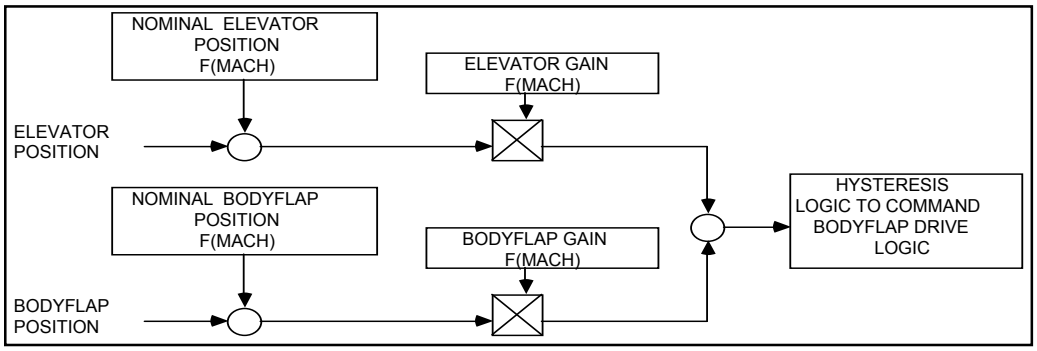

Figure 3-26. Smart Bodyflap Logic

As part of the I-load design process for STS-43 (first flight of OI-20), a set of smart bodyflap I-loads was designed to provide maximum protection for the SSMEs. Figure 3-27 shows the initial elevator/bodyflap profile and the profile that was used to protect the SSMEs.

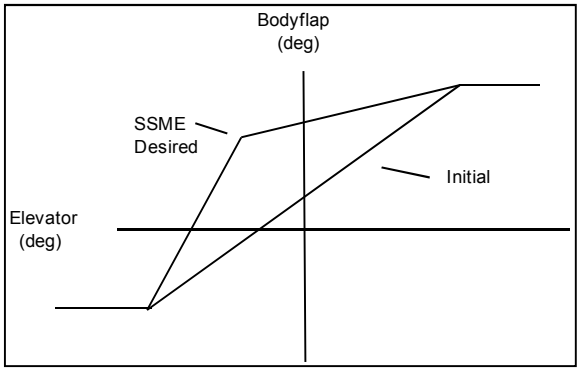

Figure 3-27. Elevator/Bodyflap Profiles

During the STS-48 entry, a bodyflap/elevator limit cycle was observed. The limit cycle lasted for 12 cycles with a 5-sec period in the Mach 23 area. Although the limit cycle did not cause problems (e.g., with control, hydraulic, or trajectory), it is not considered to be acceptable for the long term. The reason it was observed on STS-48 and not on STS-43 was the difference in XCG. The two flights were on different segments of the elevator/bodyflap desired profile. Rockwell, Honeywell, and JSC began an effort to understand the limit cycle and to design an I-load solution to eliminate the problem without compromising the SSME heating. *The solution was to reduce the deadband in the bodyflap command hysteresis. This causes the command to turn off sooner, thereby reducing the probability that the actuator will "coast" to the opposite turn-on value.*

The RHC Gain Change (CR 89680A) provided a separate I-loaded gain to convert the pitch RHC deflection to a desired pitch rate during slapdown (main gear touchdown to nose gear touchdown). This separate gain would allow the stick sensitivity to be reduced. The change in elevator deflection per degree of RHC deflection almost doubles at the transition to the slapdown system. This increased sensitivity has been shown to cause problems for some pilots, especially with the addition of the drag chute transient load.

The Nosewheel Steering Change (CR 89889H) provided the capability for the DAP to interface with the second nosewheel command path added as part of the nosewheel redundancy upgrade. The hardware change removed the manual direct mode and added a duplicate command path using MDMs 3 and 4. The pilot was given the capability to select the command path (MDMs 1 and 2 or MDMs 3 and 4) using a cockpit switch. Analysis showed that the pilot should not (although no inhibit was included in the software or hardware) change command paths during rollout without letting the system dynamics settle in the caster mode. Figure 3-28 shows the revised nosewheel steering system. During SAIL testing, it was found that a correction (CR 90439) was required to account for the dual output (25 Hz and 6.25 Hz) rates in the BFS software supporting system 2.

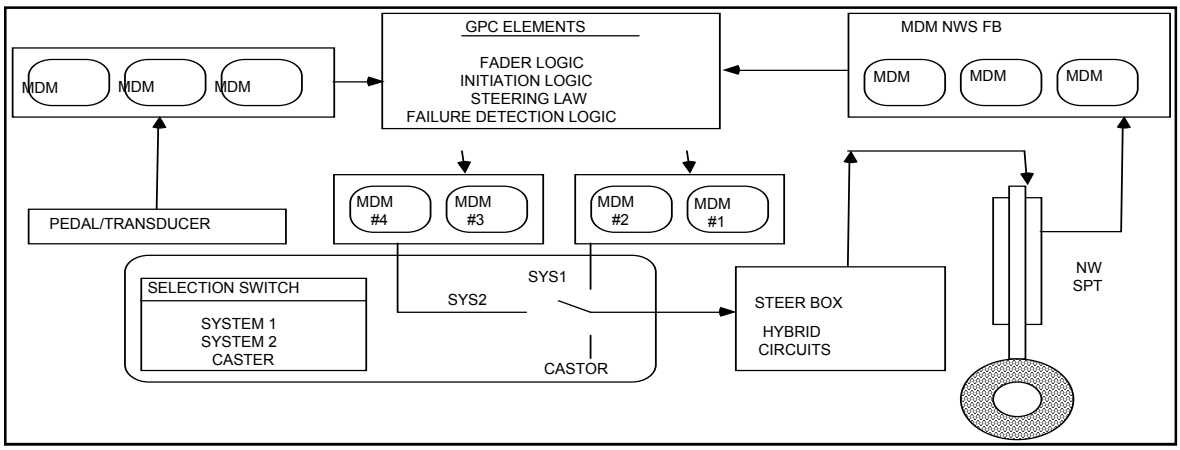

Figure 3-28. Revised Nosewheel Steering Logic

3.2.12.7 OI-21 Approved DAP Changes

No changes were made to the basic operation of the entry/GRTLS DAP as part of this software release, but four changes were made that have a direct effect of the operations of the entry/GRTLS FCS. Three of the changes were related to Orbiter hardware upgrades (drag chute, wheel speed sensors, and landing gear isolation valves), and the fourth was the upgrade of the abort and RCS/OMS sequencing software.

To improve the **landing capability** of the Orbiter, **a drag chute** was added to the basic configuration, with its deployment made a manual operation similar to deployment of the landing gear. To provide the necessary clearance above the SSMEs, the PRL logic was modified as part of CR 89991. This change accounted for the hydraulic flow required to move the engines down from the stow position to the new landing position. The key benefits of the drag chute are 1) reduced stopping distance, 2) reduced braking requirements, 3) lower main gear loads, *and 4) nose-up moment aero-effect*. Crew procedures were written to ensure that the WOWLON discrete is set before deploying the chute manually.

As part of the EDO program, it was decided to increase the redundancy of the **WOW sensor system**. The two primary approaches evaluated were 1) additional proximity sensors and data paths, and 2) incorporation of the antiskid wheel speed sensors into the landing subsystem operating program (SOP) logic. Because the wheel speed sensors were already on the Orbiter and there was insufficient room to add more proximity sensors, it was decided to use a mixture of proximity sensors and wheel speed sensors to determine when the main wheels were on the ground. CR 90112 was written to add the required logic to the landing SOP. This logic uses two proximity sensors and four wheel speed sensors to determine when the wheels are on the ground. Data from previous flights had shown that the wheel sensors would respond first and mode the software to the slapdown logic before the proximity sensors detected the ground. Figure 3-29 shows the revised logic for setting the WOWLON discrete.

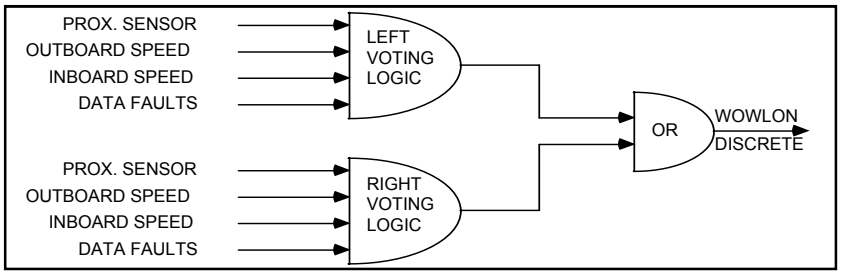

Figure 3-29. Revised WOWLON Discrete Logic

Another landing-related change was CR 90102, which revised the logic for opening the hydraulic system isolation valves associated with the brakes. The new hardware (a valve) and logic ensure that brake pressure has not been applied before getting the Orbiter nosewheel on the ground.

The final DAP-related change was CR 90114, a complete rewrite of the abort control and OMS/RCS interconnect logic. Two key additions affected the entry/GRTLS DAP operation: 1) the mirror image logic was changed to account for jets detected as failed by the RCS RM logic; and 2) Initiation of the OMS burn in MM 304 during a TAL abort was automated. This change was written as a replacement for CRs 89635, 89636, and 89637, which had been used to build OI-15 (a nonflight software release). This build was used to check out the logic in the three changes before committing them to an actual flight software build.

3.2.12.8 OI-22 Approved DAP Changes

The addition of the yaw rate filter (per CR 89679D) was the only structural change to the entry/GRTLS DAP, but a number of other changes were approved that affected the operation of the autopilot. The yaw rate filter change consisted of simply adding a second-order notch filter to attenuate the effects of the wing antisymmetric mode from the measured yaw rate signal. The addition of the filter reduced the amount of mission-specific analysis required by increasing the robustness of the flex-body dynamics of the entry/GRTLS DAP.

Other DAP-related changes included 1) redefinition of approximately 300 parameters from I-load to K-load categories (CR 89674E), 2) modification of the TAEM guidance speedbrake control law to base the command on energy and energy-rate errors instead of airspeed error (CR 89979F), 3) redesign of the

GRTLS ET-SEP jet selection logic to meet NSTS 07700 requirements (CR 90014G), and 4) provision for an automatic capability to fly a lower angle-of-attack profile during a low-energy TAL entry (CR 90152D).

3.2.12.9 OI-10 and OI-11 Approved DAP Changes

Four CRs affecting the entry DAP were approved as part of OI-10 and OI-11 updates. They were 1) I-load to K-load conversion (converting a large number of I-loads to K-loads constants) in the flight software (CR 79967G), 2) pitch notch filter to reduce interaction between gear modes and FCS (CR 79396D), 3) half gain on RHC to reduce the gain on pitch RHC inputs during slapdown phase (CRs 79397A and 79898), and 4) move of elevator bending filter to feedback path from the forward path for CSS mode (CR 69870F). The fourth change was baselined as part of the OI-8C system, and the second change was later approved for OI-8D. The first and third changes were baselined as part of OI-22 and OI-20, respectively. The half gain capability was verified, but not used on any OI-20 flight.

4.0 Test Program

Separate from the analytic/simulation test program, the entry flight control test program can be divided into a series of closed-loop stability tests on the ground to verify the structural and FCS margins and a series of flight tests to update the aerodynamic and thermal characteristics of the Orbiter.

4.1 Vehicle Tests

Of the numerous tests that were run on the Orbiter before flight, three dynamic stability tests (DSTs) have had a significant effect on the design and commit-to-flight process for the Orbiter FCS. The first two tests, "hot fire" in November 1979 and "entry dynamic stability test" (EDST) in August 1980, were part of the first flight effort. The third test, "IUS DST," was required to certify the unique properties of the IUS payload configuration before STS-6.

4.1.1 Hot Fire Test

The first Orbiter ground test to attempt to verify that the Orbiter entry FCS had the required 6-dB high-frequency gain margin was conducted at KSC in late 1979. The name "hot fire" came from the fact that the Orbiter APUs were used to power the Orbiter hydraulic systems. During this test, the aerodynamic surface gains were increased both 3 dB and 6 dB. When the gains were increased 6 dB, an instability was detected. As a result of this ground test, two changes were made to the FCS system. First, a new set of bending filters was developed as part of the STS-1 tiger team effort. The second change was a relocation of the Orbiter rate gyros on the 1307 bulkhead. Figure 4-1 shows both the hot fire and the later RGA configurations.

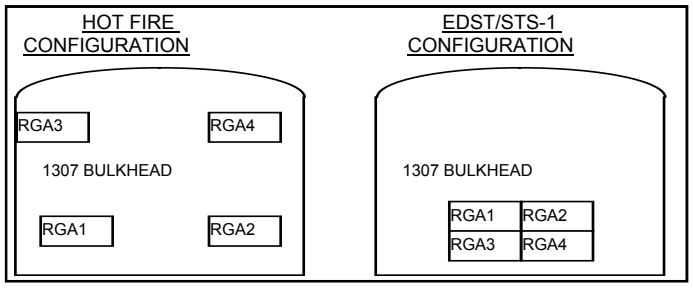

Figure 4-1. RGA Locations

The move was necessary because of the unpredicted "oil canning" motion of the 1307 bulkhead, which resulted in excessive structural vibration motion being picked up by the RGAs. Because of the results of this move and the necessary software and hardware changes, a more extensive ground test, the EDST, was required to certify the Orbiter entry FCS before commit-to-flight for STS-1.

4.1.2 Entry Dynamic Stability Test

The EDST was added after the problems encountered during the hot fire test to validate the analysis that indicated that the entry FCS was ready for flight. The original verification plan had not included a vehicle-

level ground test to verify the analysis models being used to certify that the FCS-structural interaction attenuation met the requirements.

Program management, at the urging of the FCS community, added the EDST to the STS-1 flow. This test differed from the hot fire test in three primary ways. 1) Ground carts were used to provide power for the Orbiter hydraulic systems; 2) both open- and closed-loop tests were included in the process; and 3) analysis was conducted using the planned test configuration of the Orbiter to develop accurate pretest predictions. It should be noted that no test could be defined for the RCS jet loops because of restrictions on use of the RCS jets on the ground.

Test Setup: To uncouple the rigid body modes associated with the suspension system from the vehicle flex modes, the tires were partly deflated and the strut oleos were pressurized to make them soft. The dynamics of this modified suspension system became a significant issue in the analysis and interpretation of the test results. The closed-loop test was conducted and monitored manually.

The closed-loop test was designed to demonstrate that the entry FCS had the required 6-dB margin by increasing the surface forward loop gains by 3 dB and 6 dB from the nominal value during simulated operation at two flight conditions (Mach 0.6 and Mach 3.4). This simulated flight was obtained by patching the flight software to force operation at the desired conditions. Figure 4-2 shows the vehicle test configuration in block diagram form. In this configuration, input stimuli were generated by the flight computer and applied to gyro torquers. The torque commands sent to the gyros were positive and negative 4 deg/sec with a duration of 0.2 sec in all three axes. The gyro outputs were processed in the computer using flight software to generate elevon and rudder commands that were applied to the actuation system. As a result, the gyro and accelerometers on the Orbiter react to the vehicle motion and send the measurements to the flight computers. The Shuttle modal test and analysis system (SMTAS) was used to provide rapid turnaround of data to allow near-real-time evaluation of the test results.

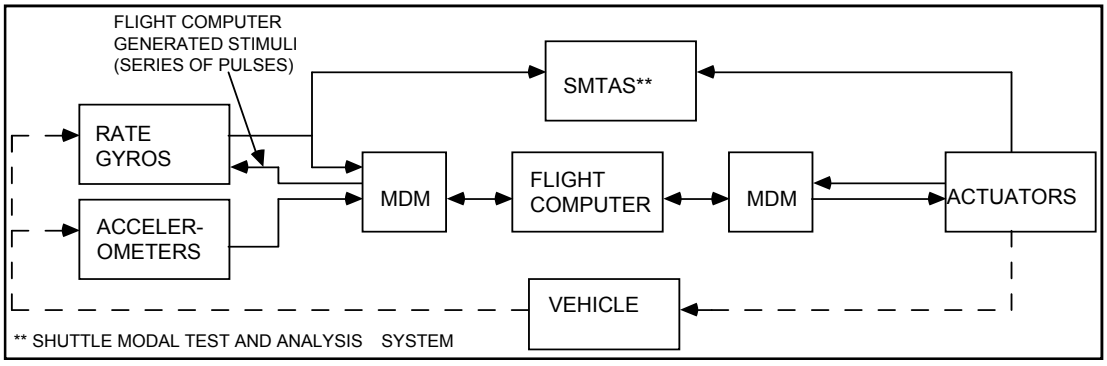

Figure 4-2. Closed-Loop Test Configuration

The open-loop test objective was to obtain the frequency response (gain and phase) of the FCS gyro and accelerometer outputs to aerodynamic surface actuator inputs. Figure 4-3 shows the vehicle configuration for this series of tests. The primary difference from the closed-loop test was that in this test, the flight computer generator commands were not used to drive the actuator system. The actuator system was driven by a series of sine waves at various frequencies and amplitudes. The frequencies ranged from 2 to 18 Hz and the amplitudes were designed to provide enough motion to provide acceptable test results and still be small enough to not saturate the surface rate capability.

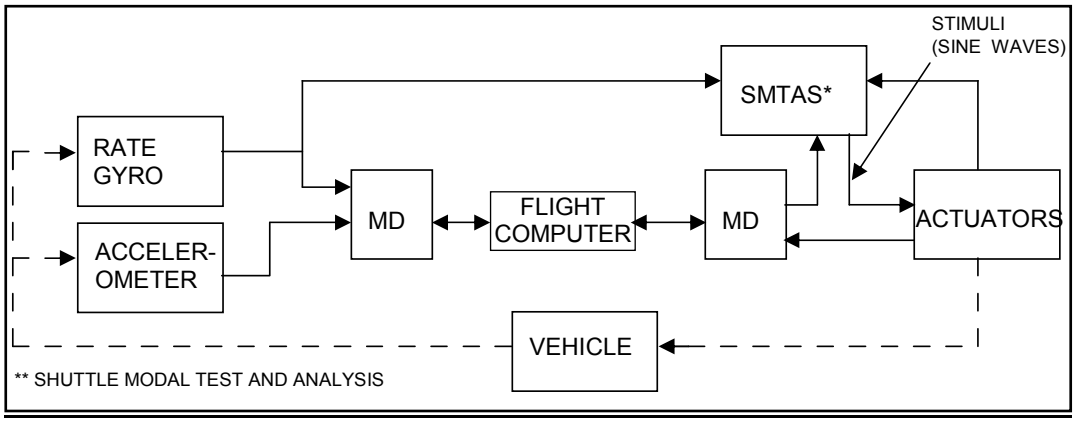

Figure 4-3. Open-Loop Test Configuration

Test Results: Closed-loop stability was not confirmed; a low-frequency instability was present. *During this test, the aerodynamic surface gains were increased both 3 dB and 6 dB. When the gains were increased 6 dB, an instability was detected*. Subsequently, *the planned open-loop testing, utilizing SMTAS*, found the following unpredicted results: 1) higher frequency and higher amplitude rigid body motion due to the landing gear configuration, 2) first fuselage bending mode at a significantly higher frequency (5.4 Hz vs. 4.7 Hz) because of friction between the payload bay doors (not included in the pretest model), 3) significantly lower frequency (6.4 Hz vs. 6.7 Hz) and modal strength for the wing symmetric mode, 4) reduced fin mode frequency (3.3 Hz vs. 3.7 Hz), and 5) lower strength in the higher frequency modes. (This fifth result could indicate higher structural damping than was used in the model.)

The results of the tests were incorporated in the analysis efforts in several ways. Some frequencies used in analysis were moved, and the uncertainties in modal strength were modified to cover the test results as well as the model-derived frequencies. An example of a change in the analysis due to the test results is that the tolerances on the first fuselage mode frequency were changed to 4.5 Hz, -0%, +20%. These one-sided tolerances are still used in the linear and nonlinear analysis done in support of new payloads.

Table 4-1 gives a summary of the results of the closed-loop test. The data in this summary table shows that the results did not give a clear validation of the required modal attenuation requirements.

Table 4-1. Closed-Loop Test Results

Test Gain	Prediction		EDST Results
	Linear	Nonlinear	
Nominal	Stable in all axes	Stable in all axes	2.4 Hz sustained symmetric elevon oscillation, 0.6 deg p-p
+3 dB	Stable, but lightly damped	Stable in all axes	2.4 Hz sustained symmetric elevon oscillation, 1.0 deg p-p
+6 dB	Unstable, slowly divergent 3.7 Hz lateral oscillation	2.7 Hz damped lateral oscillation	2.6 Hz sustained antisymmetric elevon oscillation, 3.0 deg p-p

The symmetric oscillations were a direct result of the way the landing gear had been configured for this set of tests. The closed-loop roll oscillation was found to be the result of a combination of the gear dynamics and the lower-than-expected fin mode (3.3 Hz vs. 3.6 Hz). The fin mode frequency was found as part of the open-loop testing.

A large amount of time and labor were devoted to the analysis of the results of the EDST test and to explaining the unexpected oscillations to both flight crews and program managers before STS-1. All anomalies were resolved and no flight anomalies have involved FCS-structural interaction dynamics.

4.1.3 IUS Dynamic Stability Test

The IUS DST was done to verify the safety of the entry FCS redesign for the first IUS flight (STS-6). This test was similar to the EDST with two primary exceptions. 1) A new gear support technique (soft airbag suspension system under each tire) was used to prevent the problems encountered during the EDST. 2) A pathfinder model of the Boeing IUS/TDRS was placed in the cargo bay to simulate the effects of the payload on the basic Orbiter dynamics. The primary reason for the ground test on this payload was the addition of the Coulomb dampers, which limit the amplitude of any payload-induced interaction of the Orbiter structural dynamics with the FCS and its redesigned entry bending filters. A secondary objective of this test was to develop data to support the addition of RGAs to the front of the Orbiter. In theory, these RGAs could be blended (weighted summation) to remove the requirement for the dampers.

Test Setup: The test setup for the IUS DST was similar to that for the entry DST before STS-1, with three exceptions: 1) use of the airbag suspension system to isolate the vehicle from the effects of being in contact with the ground, 2) addition of IUS payload simulator and associated airborne support equipment (ASE)—which included the IUS cradle and dampers, and 3) addition of forward RGAs at two different locations. Like the EDST, the IUS DST consisted of both open- and closed-loop tests using the ground software and the SMTAS test software and equipment. During the open-loop sweeps, the high-frequency (1.5 to 10 Hz) inputs were superimposed on a 0.05-Hz, 3.5-deg amplitude signal to prevent excessive operation at the null point.

Test Results: The closed-loop test verified that the Orbiter system had more than the required 6-dB gain margin. Unlike the previous ground tests (hot fire and EDST), the testing revealed no unexpected instabilities. The comparison between pretest predictions and test results was extremely good. The response to the pulses used to excite the system damped very well (6 to 8 sec in pitch and 3 to 6 sec in roll/yaw) at both the nominal and the +6-dB gain settings.

The open-loop test provided a set of test frequency response data for the combined Orbiter-IUS-payload system that could be used to validate the model being used in verification by analysis. The test included sweeps with amplitude both below and above the level at which pretest predictions had indicated the dampers would become active. Tests without the dampers were also included to verify the damper-failed models.

In general, the pretest predictions provided a good indication of the results, but in some cases the measured linear transfer function gain was higher than the predicted gain. The key differences were 1) the normal accelerometer response was larger than predicted at the payload plunge mode (4.4 Hz), 2) the payload pitch and plunge modes were at higher (3.2 Hz and 4.3 Hz vs. 2.7 Hz and 3.6 Hz) than expected frequencies for the dampers-out cases, 3) Orbiter roll RGA and lateral AA response to the first antisymmetric fin mode (3.29 Hz test value) was greater than predicted for both aileron and rudder excitation, and 4) the first fin mode was observed at 3.29 Hz instead of the predicted 3.6 Hz. As with the EDST, the test data were used in the selection of cases to be used in the commit-to-flight verification by analysis.

Analysis showed that the forward RGAs provided outputs of the same magnitude as the aft Orbiter RGAs and between 135 and 150 deg out of phase with the aft Orbiter RGAs. These measurements indicated that the concept of blending forward and aft rate data to suppress the primary flex modes is feasible. The general equation for blending is

$$\text{Rate} = K * \text{Rate}_{aft} + (1 - K) * \text{Rate}_{fwd}$$

The value of the blending constant (K) would have to be selected based on further analysis of the modal shapes of the primary bending modes. Considerable work was done on this concept in support of the Centaur and IUS programs, but it has never been implemented in the Orbiter flight software. If RGAs are ever moved to the front of the Orbiter for other reasons, it might be desirable to continue this design and analysis effort in support of future heavy payloads.

The data collected on the response of the dampers generally confirmed the math models being used, but the exact breakout forces could not be identified because of conflicts in the displacement data and the force data. Comparison of the rate data with and without dampers showed that the dampers were effective in dissipating energy in the 5 to 7 Hz range, but little activity indicating energy dissipation was seen in the payload plunge frequency range even though the force was slightly above the predicted breakout level required to activate the dampers. In addition, the forces in the dampers were observed to level off near

the predicted 200-lb-force level when displacement was above the level required to activate the damper. Therefore, it was concluded that the model of the damper being used for analysis was acceptable.

One item of note during the IUS DST was the procedural error in bringing up the system. During the IUS DST, the FCS and hydraulic systems were incorrectly activated before inflation of the suspension system. As expected, an instability (limit cycle) occurred. This result was consistent with pretest predictions. After the procedure was corrected, the tests proceeded as planned. The limit cycle was stopped by downmoding the FCS to a zero gain configuration.

In summary, the IUS DST was a very successful set of tests, and consideration should be given to repeating the tests when new types of heavy payloads are to be flown in the Orbiter.

4.2 Flight Tests

The Orbiter flight test program can be divided into three phases: 1) the initial (manual) flight test program, 2) the execution of the automatic tests, and 3) the manual pull-up/push-over maneuvers. The purpose of these maneuvers was to obtain flight test data from which the aerodynamic coefficients could be estimated. These data were used to update the original database derived from the extensive preflight wind tunnel program.

A number of very heated discussions took place between the proponents of an aggressive flight test program and the individuals in favor of proceeding slowly. The final decision was to reduce the number of tests on each flight from the original plan to about ten per flight. In addition, an intercenter panel was set up to oversee the implementation and execution of the flight test program. The most important consideration was safety. Several times, the number or magnitude of maneuvers planned for a flight was reduced to ensure safety. This resulted in an increase in the number of flights required to complete the program. (The last flight was STS-51F.) Also, groups at JSC, Rockwell, Langley, and DFRC were set up to reduce the flight data. All of these groups had an input into the updating of the aerodynamic database.

Although the original plan was to certify the entry aerodynamic database to support the original center-of-gravity requirements, in order to expand the database to support an expansion of the longitudinal CG capability, a new PTI program was started on STS-32. The approach in this new series was the same as that used in the original PTI program.

The original plan for the execution of the flight test program was to make maximum use of manual procedures. The original plan included a number of manual inputs using the RHC (referred to as aerodynamic stick inputs [ASI]), manual bodyflap pulses, and automatic pulses using the CSS mode of the DAP. After the flight crews had a chance to train with this system, they requested that the execution be automated so they could devote more time to monitoring the Orbiter system. This request resulted in the automatic PTI program starting with STS-5.

4.2.1 STS-2, STS-3, and STS-4 PTI Logic

The automatic part of the initial PTI program simulated pilot RHC and RPTA inputs. A roll input consisted of a series of roll rate commands that simulated a sharp series of pilot RHC inputs. The yaw inputs were a series of Ny commands that simulated a sharp series of pilot RPTA inputs. Figure 4-4 shows how the signals were input to the DAP.

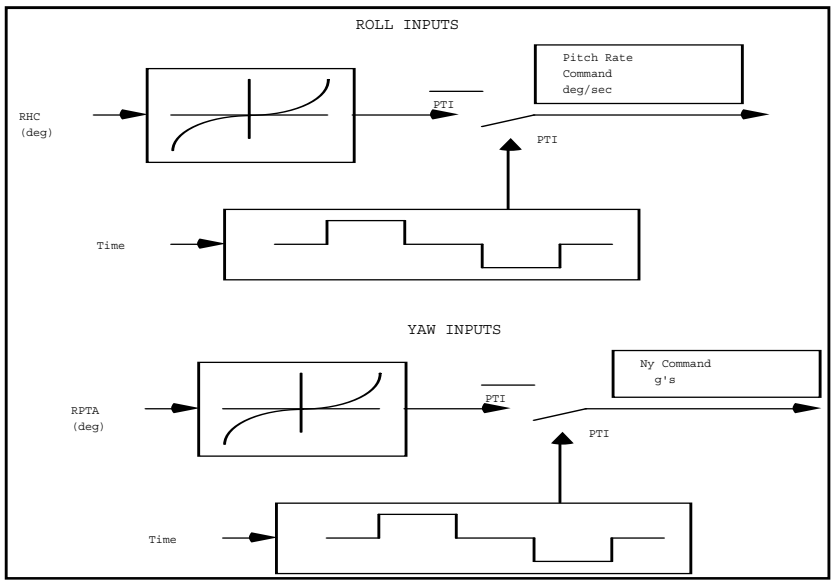

Figure 4-4. STS-2, STS-3, STS-4 PTI Logic

A PTI normally consisted of a series of these pulses that was automatically sequenced based on a set of I-loads that was loaded into the software before each flight.

The procedure for executing a PTI was as follows: 1) monitor the trajectory until the correct point (window) for a PTI to be executed was reached, 2) select the desired sequence using SPEC 50, 3) mode the flight control to CSS in both axes, 4) execute the PTI using SPEC 50, and 5) center the error needles and return to automatic in both axes. The pilot could execute the same PTI at different Mach numbers on the same flight.

The major problems with this technique were that 1) extensive pilot time was required to select and execute the desired maneuvers, and 2) several effectors (RCS jets and aerodynamic surfaces) were commanded to move at the same time. The combination of reduced PTI magnitudes and multiple effector action resulted in a reduced ability to extract the aerodynamic characteristics of the Orbiter. These problems resulted in a decision by the Orbiter Project Office to ask the PTI and flight control community to design a better system. This new system was targeted for STS-5 because that was the first flight scheduled to use a new primary software (release 19) drop.

On STS-3 and STS-4, a structural PTI was executed in the Mach 1.5 region to validate the flutter buffet data. This PTI consisted of a series of low-amplitude, high-frequency commands to the elevator actuators. These commands were superimposed on the normal flight control commands in the aerodynamic surface SOP.

4.2.2 Auto PTI Logic—STS-5

Development of the new software package was started between STS-1 and STS-2 as a result of heated discussions concerning the Orbiter flight test program. Doug Cooke, the JSC lead for the aerodynamic flight test program, took the lead in the design of the new system. The SES was the primary tool used in this design project.

The general requirements for the new software package were to 1) remove the extensive pilot interaction, 2) provide capability to command individual effectors, 3) provide pilot with override capability and a quick method to stop a PTI in progress, 4) ensure that the maneuver does not interfere with trajectory control, 5) ensure that the vehicle is in a quiescent condition before the maneuver is initiated, 6) provide positive indication to the crew when a PTI is in progress, 7) add no requirement for structural PTIs, and 8) give the crew responsibility for system monitoring. This major software design project had to be completed in 3 months to meet the deadline for inclusion in release 19 of the primary software.

A proposed software design was developed and incorporated into the SES for a MIL demonstration. Based on pilot observations, several proposed changes were incorporated and evaluated. The ability to make rapid changes for evaluation was the key to the success of this design process.

The final software design can be divided into four parts: 1) PTI window selection logic, 2) constraint checking logic, 3) PTI execution logic, and 4) crew controls and displays. The logic flow is shown in figure 4-5.

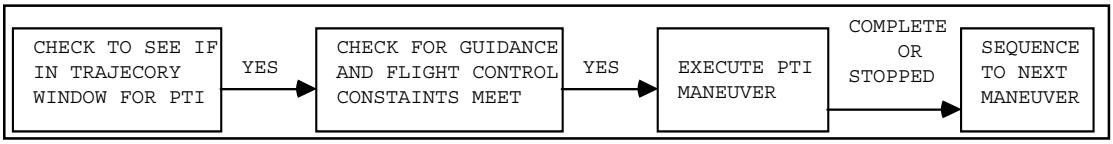

Figure 4-5. Automatic PTI Logic Flow

It should be noted that once a PTI starts to execute, it will continue until complete or stopped by the pilot, with the exception of the loss of air data information from the air data system below Mach 2.5.

PTI Window Selection Logic: While the earlier PTI software relied on the crew to execute the PTI at the correct time (window), the new software was required to select the window for execution of each maneuver. In a review of trajectory data, it was found that the best way to define windows was with a combination of dynamic pressure and Mach number. The software was configured to use dynamic pressure for the initial set of windows (in a flight region where dynamic pressure is normally increasing) and Mach number for the later set of windows (in a flight region where Mach number is normally decreasing).

The number of dynamic pressure and Mach windows can be changed from flight to flight using mission dependent I-loads. The original proposed sets included up to 20 windows, but flight crew desires and RCS propellant restrictions resulted in no more than 12 windows ever being scheduled for execution on any flight. For STS-5, STS-6, and STS-7, the lower priority maneuvers were disabled by making the opening of the window come after the close of the window (i.e., leading edge = 10 psf and trailing edge = 8 psf). The STS-5 software allowed up to 25 windows. As part of the OI-7C scrub, the number was reduced to 15 windows to provide room in the GPCs to add required Centaur-related changes. In addition, the maximum number of pulses that could be defined was reduced from 40 to 25. Table 4-2 gives an example of a possible set of windows. Note the reversal in the relative magnitudes of the leading and trailing edge values when the transition is made from dynamic pressure (Qbar) to Mach number for window definition. This was done to correspond to the normal trajectory characteristics of these parameters.

Table 4-2. Representative Set of PTI Windows

Window	Leading Edge		Trailing Edge	
1	Qbar	3	Qbar	6
2		20		25
3		35		38
4	Mach	20	Mach	19
5		14		12
6		8		7
7		4.1		3.2
8		2.2		1.7
9		1.5		1.3
10		0.9		0.8

Crew Controls and Displays: The crew controls provided the capability to monitor the status of a PTI on SPEC 50 and trajectory displays and the capability to inhibit and/or stop a PTI before it started execution or while it was in execution. To start the PTI execution process, the crew was required to enable PTI execution by entering an ITEM 2 on SPEC 50. To provide the required monitoring capability, the letters "PTI" started to flash when a trajectory window had been entered. These characters were displayed steadily and double-bright on the trajectory displays when a PTI was being executed.

The crew was provided with three ways to inhibit or stop the execution of PTIs. The first was to toggle the enable discrete by entering a second ITEM 2 on SPEC 50. The other two consisted of moding the flight control to CSS in either pitch or roll/yaw by use of the PBIs or the hot stick. Each time the pilot inhibits PTIs (keyboard entry or moding FCS), the PTIs must be re-enabled using the keyboard entry on SPEC 50.

In addition to monitoring the Orbiter systems, the pilot was responsible for monitoring RCS propellant levels to ensure that the highest priority maneuvers were executed if propellant levels would not allow all of the maneuvers to be executed. On several flights, the pilot inhibited maneuvers for this reason.

Constraint Checking Logic: In addition to the crew controls on SPEC 50, there were two groups of constraints on execution of a PTI after the window was entered. The first group, monitored in the entry and TAEM guidance modules, consisted of the following: 1) magnitude of the altitude acceleration (both entry and TAEM), 2) time until start of a roll reversal (entry), and 3) time from start of a roll reversal (entry). The purpose of these constraints was to ensure that a PTI did not interfere with the control of the flight profile. The second group, incorporated in the PTI sequencer, consisted of the following: 1) magnitude of the body rates, 2) pitch and lateral axes in automatic mode, and 3) measured air data in use below Mach 2.5. All constraints had to be met for four consecutive passes through the PTI sequencer (1.04 Hz execution rate) before a PTI could be started.

PTI Execution Logic: Once all the constraints have been met, the PTI Sequencer sets a "PTI_Execute" flag to mode the DAP and to start execution of the PTI_EXEC module. This module computes the signals that the DAP will integrate to set the magnitudes of the PTI signals to be used in each of the six effector (aileron, elevator, rudder, roll jet, pitch jet, and yaw jet) loops.

The changes in the DAP to support execution of the PTIs were to 1) set the stability roll command to zero, 2) set the inputs to the aileron and rudder trim integrators to zero, and 3) disable the GJET logic. The first change was made to prevent the DAP from responding to the large changes that occur in the entry and TAEM guidance roll angle commands. Because of transient changes that may occur in the measured drag, entry roll commands can change as much as ± 20 deg during a PTI. The second change was necessary to prevent the trim integrators from responding to the uncommanded body rates during a PTI. The initial design did not include this modification, and a string of yaw jet pulses was present at the end of each maneuver. The third change was incorporated to prevent the elevator and bodyflap from moving in response to low dynamic pressure pitch jet pulses.

The importance of a good simulation of a proposed software modification before submission as a CR was demonstrated by the fact that the second and third changes were found to be necessary during the SES evaluation of the proposed design. Extreme care should be taken in writing the software change as shown by the initial implementation of the PTI software. IBM initially implemented the rate check without the absolute value being considered. This error was found in the IBM testing before the first FSL testing.

During a PTI, the six signals from the PTI_EXEC module are integrated in the DAP to form the final command to be added to the normal signals in each of the six effector channels. It should be noted that only one of the signals being integrated at any time is nonzero. Each pulse has an associated I-load that specifies which of the six signals is nonzero. The outputs of the integrators in the surface loops are added directly to the surface commands ahead of the command limiters. The signals going to the jet loops are added to the error signals ahead of the respective jet hysteresis modules. (*Experience has shown that it would have been better to command a specific number of jets directly instead of using the biased error signals.*) Figure 4-6 illustrates the general process by which PTI commands are added to the normal effector command signals.

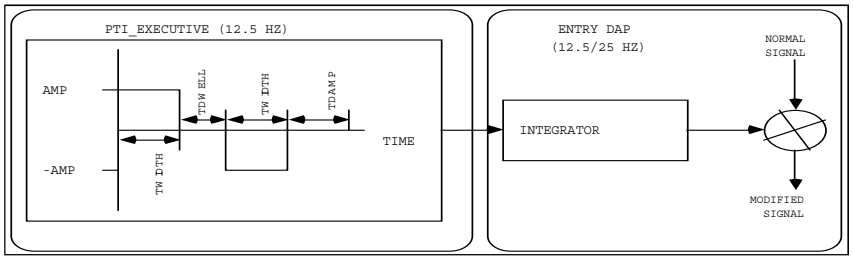

Figure 4-6. PTI Pulse Logic

The parameters used to define the form of the pulse were 1) AMP—the magnitude of the signal to be integrated, 2) TWIDTH—width of each of the two nonzero segments, 3) TDWELL—time between two segments, and 4) TDAMP—time at the end of the pulse to allow the FCS to damp the residual rates before the next pulse. The length of the timers was specified in the software as an integer number of 80-msec intervals. These intervals correspond to the frequency of execution of the PTI_EXEC module. Figure 4-7 illustrates several of the types of pulses that can be built from different sets of I-loads. The square wave was normally used for four-jet PTIs, whereas the triangular pulse was used for aileron and elevator pulses. The chopped triangular pulse was used for the rudder and the two-jet PTIs.

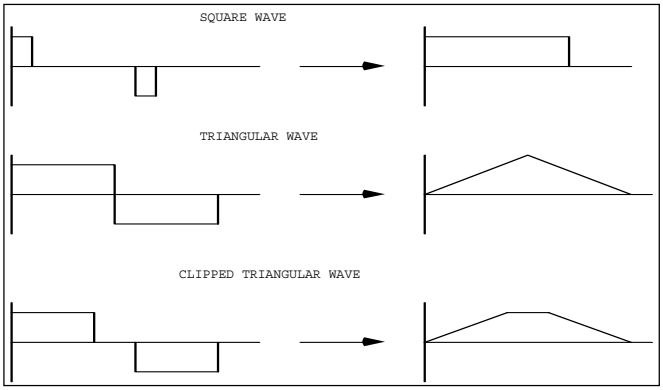

Figure 4-7. Typical PTI Pulses

There is no software limit on the number of pulses that can be sequenced to form a single maneuver. A typical example is rudder, aileron, yaw jet, elevator. The maximum number of pulses ever used in one maneuver was six in the Mach 1.5 region. This sequence was small rudder, small aileron, large rudder, large aileron, yaw jet, elevator. It is possible to sequence a series of pulses for the same effector to create a pulse train at a desired frequency.

I-Load Definition Constraints: Six ground rules were developed by the flight control community, flight crews, mission planning personnel, flight directors, and aerodynamic community for the selection of PTI l-loads. These were to 1) limit the length of the sequence of pulses to about 15 sec, 2) maintain maximum angular accelerations below 15 deg/sec² for roll and 5 deg/sec² in pitch and yaw, 3) maintain sideslip below 1 deg, except at high Mach where the limit was 2 deg, 4) maintain stability roll rate less than 5 deg/sec and body pitch rate less than 2 deg/sec, 5) keep nominal RCS propellant requirements for PTIs less than 400 lb, and 6) limit number of PTI maneuvers to 10.

PTI Verification Program: After a set of PTIs had been defined based on the expected trajectory and priority data needs of the aerodynamic community, a formal verification was executed. This process consisted of three steps: 1) SES evaluation that included a nominal run for fuel data, a run with double the planned amplitude pulses, and runs with each of the variation sets; 2) linear stability checks at each planned test point by Honeywell; and 3) FSL/SAIL runs with actual flight software. The SES evaluation was normally completed before the presentation of a set of l-loads to the Software Control Board (SCB) for implementation into the flight software. The other two steps were part of the formal commit-to-flight analysis process.

Flight Test Results: While the formal PTI data reduction responsibility belonged to the aerodynamic community at JSC, Rockwell, and DFRC, the flight control community conducted an independent assessment using the SES for several flights. Key members of the group that conducted this assessment were Joe Gamble, Scott Snyder, Robbie McAfoos, and Ray DeVall. The process simulated the actual flight profile using the best estimates of the Orbiter mass properties and trajectory parameters, and then varied the aerodynamic coefficients until an acceptable match was obtained between the simulation data and the flight data. Parameters of interest included body rates, lateral acceleration, estimated sideslip, and attitude changes. The SES results, while not as detailed as the results obtained using the MMLE program, provided a good cross-check.

The aerodynamic community released five official database updates based on the results of the flight test program. These updates comprised flight assessment deltas (FADs) to be added to the pre-operational (1L) data book, which had replaced the pre-STS-1 (1M) data book as the official aerodynamic database. The formal releases were FAD 4 (after STS-4), FAD 6 (after STS-6), FAD 9 (after STS-9), FAD 14 (after STS-41D), and FAD 26 (after STS-51F). Each release normally occurred about 6 months after the last flight used to define the data. The FADs were made up of deltas to the basic coefficients and updates to the uncertainties. These deltas were usually a function of Mach, alpha, and elevator. The uncertainties were reduced considerably in the regions of each independent variable for which flight data were available, but for some coefficients they remained at the pre-STS-1 level when a variable was outside the region covered by flight data. (A transition zone was included, which on some occasions caused strange results in both the stability analysis and the time domain simulations.)

The rapid feedback of flight results in the flight control development process was the key to steady improvements in the entry and GRTLS DAPs and the expansion of the flight envelope, especially the longitudinal CG expansion process.

4.2.3 Manual Alpha Sweep Maneuvers

To determine the variation in lift, drag, and pitching moment with angle of attack, a series of manual maneuvers was executed on STS-2, STS-3, STS-4, and STS-5. In these maneuvers, the pilot moded both the pitch and lateral axes to CSS and executed the following procedure. The pilot pitched the Orbiter up at 1 deg/sec until the desired angle of attack was reached, then pushed the Orbiter down at 1 deg/sec until the desired angle of attack was reached. Finally, the pilot returned to the commanded angle of attack to complete the maneuver. On most of the maneuvers in flight, the extreme angles were maintained for a couple of seconds. Typical maneuvers are shown in figure 4-8.

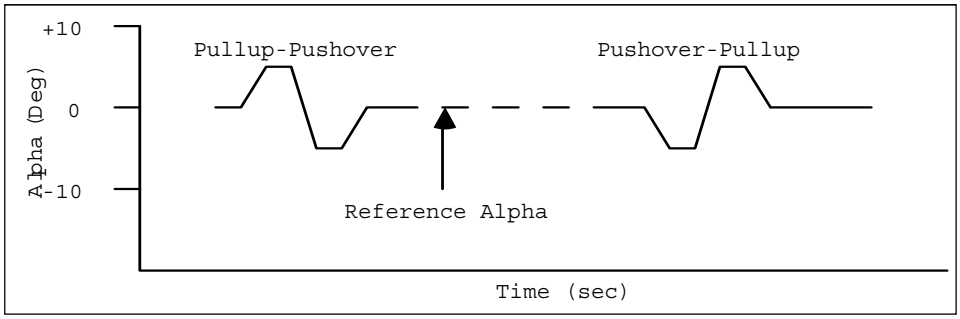

Figure 4-8. Typical Alpha Sweeps

This type of maneuver provided thermal and aerodynamic data as a function of angle of attack for comparison with the preflight models used to certify the Orbiter for the first few flights. Based on this and wind tunnel data, it has been decided to remove the requirement to have more than 1,000 nautical miles of crossrange capability. The Orbiter thermal protection system could not be certified for the lower angle-of-attack profile required to meet the original crossrange requirement.

There was at one time a plan to automate these maneuvers to obtain stability derivative data at angles of attack off the nominal profile. The effort was dropped when the crossrange requirement was reduced.

4.2.4 Bodyflap Pulses

On several flights, the crew was asked to manually maneuver the bodyflap up and down to provide data that would allow the estimation of the pitching moment, lift, and drag coefficients associated with the bodyflap. During a typical bodyflap pulse, the pilot manually maneuvered the surface along an up- and then down-profile, with the final position being the same as the position at the start of the pulse. A typical pulse could take 10 to 20 sec to execute. See figure 4-9 for a typical bodyflap pulse profile.

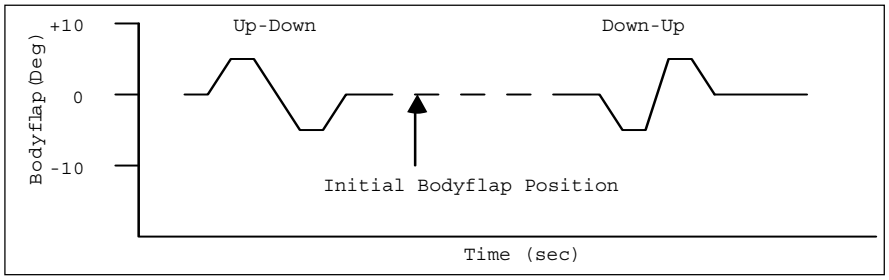

Figure 4-9. Typical Bodyflap Sweep

The lower drive rate in the down direction is due to the effect of hinge moments on the surface response to the moment applied by the actuator. With no hinge moment, the bodyflap typically drives at approximately 2.25 deg/sec.

The first and only bodyflap pulse during the initial flight test program, executed on STS-51F, did not show anything surprising. When the second phase of the flight test program was started after the return to flight,

a bodyflap pulse was included on each flight. Initial review of the STS-32 maneuver did not show anything unusual. However, the bodyflap pulse on STS-31 had a surprising result.

The STS-31 bodyflap pulse in the Mach 9 region resulted in a large pitch rate of 2.7 deg/sec and an up-elevon excursion to 27 deg (limit is 33 deg up). Postflight analysis, by Mark Hammerschmidt of JSC and Charlie Unger of Rockwell, provided a complete understanding of why the flight results did not match predictions.

A comparison of the STS-31 and STS-32 flight conditions shows that the STS-31 XCG was at 1091 inches, which is near the aft limit for using the forward CG elevon trim schedule (see figure 3-22), vs. 1,080 inches for STS-32. This difference accounts for the large down (70%) bodyflap position at the start of the STS-31 bodyflap pulse. The two key factors contributing to the STS-31 behavior were crew procedures and errors in bodyflap models. The crew procedures called for the crew to drive the bodyflap down for 3 sec and then up for 3 sec. During the actual flight, the crew drove the bodyflap down for 3.9 sec and up for 4 sec. This resulted in the bodyflap going almost full down (over 20 deg). When the bodyflap drive rate was compared to various actuator models used in SES, SDAP, and SAIL, it was found that none gave an exact match with the flight data. In the SES model, the effect of hinge moment on the drive rate was shown to be excessive, whereas the SDAP model underestimated the effect of hinge moment in the down direction and overestimated the effect in the up direction. The flight and simulation down drive rates were as follows: 1) STS-31 — > 1.9 deg/sec, 2) SES — > 1.7 deg/sec, and 3) SDAP — > 2.3 deg/sec. When the flight maneuver timing and drive rates were used in the SES, a good match was obtained with flight data using the nominal FAD 26 aerodynamic database.

The data obtained from this maneuver will be used to obtain estimates of $C_{m_{alpha}}$, $C_{m_{elevator}}$, and $C_{m_{bodyflap}}$. The data may be used to update the FAD 26 nominal database and the associated uncertainties. The up-elevator data will be extremely valuable in the CG expansion program.

5.0 Current Issues

While the current entry/GRTLS DAP has performed extremely well, there remain several issues associated with the FCS. The next few paragraphs address a number of the key remaining issues. *(These were identified in 1992; where subsequent developments or updates are discussed in this document, references to relevant sections are indicated in italics.)*

Landing System Automation: In support of long-duration flights (>16 days), it will be necessary to automate a number of critical crew procedures. The current criteria used to identify these procedures are 1) degree of crew interaction (manual flight, braking, etc.), and 2) time criticality of procedure (such as gear deploy and chute deploy).

Single APU Flight: After the STS-51L accident, the question of Orbiter capability to fly with two failed APUs was raised in several forums. Previous results had shown a high probability of success, but no comprehensive study has ever been completed. It is generally accepted that during entry the only significant probability of a problem is in landing and rollout because before landing, the surface rate requirements are within the capability of a single APU. As part of the PTI program, it was found that successful recovery could be achieved if a maneuver was started with two APUs operating, even if a second failure occurred anywhere during the maneuver. Based on this analysis, the flight rules allowed execution of PTIs with a failed APU.

The high rate requirements that the pilot may need to counteract high crosswinds or wind shears near landing present a problem. Past autoland analysis completed by Sperry has shown a high probability of success after two APUs have failed.

There is concern in some areas that the models available for single APU hydraulic flow capability may not be accurate because of the lack of test data, from either the Flight Control Hydraulic Laboratory (FCHL) or vehicle tests. One key assumption in the design of the PRL rate limits for single APU operation is that the pilot will manually mode the remaining APU to high pressure before activation of the rudder. If this is not done, the PRL may request more surface rate than the system is capable of providing. (*See the **"Single APU Studies and PRL Updates"** paragraph in Section 6.7.)*

Redundant Nosewheel Steering: At a meeting of the various JSC and Rockwell technical personnel working to improve the Orbiter landing systems, it was agreed that the highest priority should be given to the development of a redundant nosewheel steering system. Three areas were identified as candidate

areas for improvement: 1) getting a second hydraulic source (currently only hydraulic system 1 can be used to power the nosewheel actuation), 2) adding redundancy to the command paths (currently loss of string 1 or 2 will prevent the GPC mode from being used), and 3) redundancy in the actuator secondary servo systems (currently numerous single-point failures result in loss of nosewheel steering capability).

One related activity is continued testing at Langley to develop a realistic tire failure model for use in landing and rollout simulations at JSC and Ames. Current testing has shown that the models used previously were extremely conservative. Updated models are currently being evaluated at JSC and Rockwell. The result of this analysis will be used to define the models and tests to be performed at the upcoming simulation using the Ames VMS system.

Stopping on Short Runways: The need to gain more reliability in the Orbiter stopping system is being approached in two ways. The first is to enhance the current braking capability by going to carbon brakes; the second is to add a drag chute to the Orbiter. Currently both approaches are scheduled to be implemented.

Center of Gravity Expansion: The need to expand the Orbiter CG to provide additional payload manifesting capability has been documented by the Space Shuttle Level II Program Office at JSC. Currently, work is underway to estimate the cost and schedule to accommodate this request. In addition to supporting development of new flight rules to handle OMS tank failures, an effort is underway to define a contingency CG box. The activity to provide additional CG comprises the following tasks: 1) gathering of additional aerodynamic test data to reduce the aerodynamic variations, 2) structural analysis to allow landing with additional OMS propellant (original limit was 22%), 3) software changes to allow optional crew inhibit of the dump of the LO_2 trapped in the Orbiter during aborts, and 4) identification of other areas (such as venting and thermal) that could limit the expansion of the CG either forward or aft. (*See Section 6.5.)*

Contingency Aborts: After the STS-51L accident, contingency aborts assessment became a program priority. Before this time, the official program position was that work could be done to support crew procedures in this area as long as it could be accomplished without impact to normal activities and funding. The official position stated in NSTS 07700, Vol. X, can be summarized as follows: hardware and software changes may be included with program approval but will not be considered design drivers.

Currently, the Space Shuttle Program is involved in the third phase of three evaluations of systems contingency abort capability. The first phase involved 1) evaluation of fast separation capability in ascent, 2) definition of required database updates, 3) assessment of the crew procedures on the SAIL and SES, and 4) assessment by various subsystems (e.g., structures and venting) of selected SAIL trajectories. Cases involving multiple SSME failures in first stage were run on SES because SAIL was using the OI-7D flight software without autoloft capability.

The second phase was an expansion of the first to include additional trajectories, the evaluation of new crew procedures, and development of proposed software changes for future releases. In this phase, an updated Orbiter high-alpha, low-Mach assessment aerodynamic database was used in the evaluation.

The third and final phase was intended to develop a final set of proposed software changes and a candidate list of vehicle modifications that would improve the chances of the crew and/or Orbiter surviving a contingency abort.

Wraparound Control System: To reduce RCS use during entry to a minimum, an effort was made to complete the design and analysis of the wraparound entry control system. This design is a derivative of several proposed pre-STS-1 entry systems. It uses the reverse aileron concept to handle all the small inputs, and the yaw jets to aid in the execution of large maneuvers such as roll reversals. The design effort was started in the fall of 1985 and was carried to the point of writing a software change draft. The two main segments of the analysis were 1) a frequency domain stability analysis effort led by Milt Reed at Honeywell, and 2) an SES trajectory analysis effort led by Mark Hammerschmidt. The plan was to 1) complete the analysis, 2) get the software change approved and implemented in the flight software, and 3) conduct a flight test program to obtain high quality aileron data and handling qualities ratings. The design was completed and a software CR was submitted in April 1991. Implementation is dependent upon IBM resources and program priorities. *(See Section 6.4.)*

Heavyweight Aborts: With the development of the advanced solid rocket system, the ascent flight system will be able to launch more payload than the Orbiter is currently certified to land. The ascent

capability will require the ability to land 256,000 lb for an RTLS abort (ET-SEP weight could be as high as 263,000 lb). To complete a GRTLS abort, changes will be required in the GN&C system to allow the system to fly the pullout phase successfully. The planned approach includes the following options: 1) increase the normal acceleration limit, 2) increase the separation dynamic pressure, and 3) increase the maximum dynamic pressure during the pullout maneuver. The final solution probably will include some combination of two or more of the areas under evaluation. (*See Section 6.3.)*

Global Positioning System (GPS): While not directly a part of the FCS, this new sensor would simplify the Orbiter GN&C system by eliminating the need for TACANs and possibly MSBLS. In addition, the need to update drag might be eliminated if flight data indicates the capability to obtain sufficient data during the blackout period of the entry profile. During earlier upgrades to the Orbiters, GPS antennas were added to the Orbiters to allow this upgrade to be made at a later date. *(See Section 2.1.1.)*

6.0 Major FCS Studies and Updates Since June 1992

The Entry FCS has continued to evolve over the years, resulting in expanded mission capability. In many cases, expanded capability resulted from DAP modifications that made the FCS more tolerant of aerodynamic and environmental extremes. In other cases, additional capability was discovered or demonstrated by analysis and simulation of performance characteristics under extreme conditions using the then-existing DAPs. These successes must be attributed largely to the reduction in aerodynamic coefficient uncertainties resulting from the PTI test programs. The following sections describe a few of the studies and DAP updates done since the first edition of this document was published in June 1992.

6.1 DAP Reconfiguration Switches and Events

Several tables (2-1, 2-3, and 2-4) and figures (2-14 and 2-16) in Section 2 show early program values of some DAP reconfiguration events that were later changed. Specifically, the bodyflap is shown to be activated at Qbar = 0.5 psf, rather than the current value of 2.0 psf, and some HIGHQ transitions are shown to occur at Qbar = 20 psf instead of 40 psf.

Bodyflap Activation: The bodyflap channel has always provided manual control capability via the cockpit bodyflap slew switches whenever the entry or GRTLS DAP is on. The bodyflap position is set to an initial position depending on XCG at DAP-engage. Furthermore, until OI-26, active (dynamic) control of the bodyflap also began at DAP-engage because there was no switch or RECON logic to inhibit automatic control. This was not a significant concern before OI-20 because the elevon was initialized to the elevon trim schedule value, resulting in zero error to drive the bodyflap until active elevon control began at Qbar = 2 psf. Because there is no Qbar = 0.5 psf flag in the DAP RECON logic, historical use of this value for indicating bodyflap activation probably stems from the pitch RCS to elevon trim interconnect, GJET. This interconnect commanded incremental changes in elevon trim position in response to pitch RCS commands when Qbar was between 0.5 and 8.0 psf, which could result in bodyflap motion if pitch jet activity caused elevon trim deflection to deviate by more than 1.0 deg from the trim schedule.

Section 3.2.12.6 describes the smart bodyflap changes that were made in OI-20 to provide automatic balancing of elevon and bodyflap deflections and to mitigate SSME heating. Because the bodyflap still had no discrete activation switch, the smart bodyflap bias logic drove the bodyflap to approximately 12 deg at DAP-engage regardless of the initialization value. This was fixed (per CR 90711D) in OI-26 by the addition of a LOWQ (Qbar = 2 psf) switch in the bodyflap channel upstream of the bodyflap position command integrator. Independent of the bodyflap changes, the GJET interconnect was deactivated in OI-22 by changing the Qbar K-load values to 1,000 and 2,000 psf (per CR 90518A) to facilitate thermal analysis by reducing the amount of elevon and bodyflap motion at high Mach numbers.

HIGHQ Transitions: The flag HIGHQ, computed by RECON module QBAR_REGIME, is used for

1) Maximum yaw jet command limit transition from 2 jets to 4 jets (Aerojet and GRTLS DAPs)
2) Coordination feedback transition from sideslip to lateral acceleration (Aerojet and GRTLS DAPs)
3) Pitch trim transition from forward loop integrator to lagged elevon feedback (Aerojet DAP)
4) A variable in the high-Mach TAL configuration logic (Aerojet DAP)
5) Turning off the pitch jets (Aerojet and GRTLS DAPs through STS-41 only)

From STS-1 through STS-41, HIGHQ was set at 20 psf in both the Aerojet and GRTLS DAPs. When studies determined the desirability and feasibility of extending pitch RCS usage to 40 psf (see Section 3.2.9), logic

was added in RECON to generate the flag ZERO_PITCH_JET. This flag is now used to turn off the pitch jets at Qbar = 40 psf in both the Aerojet and GRTLS DAPs. When additional studies determined that it was either advantageous or not detrimental to have all HIGHQ transitions occur at 40 psf, the QBAR_REGIME I-loads were changed accordingly for both DAPs. (I-loads for ZERO_PITCH_JET are common for OPS-3 and OPS-6. Although the HIGHQ I-loads may be assigned independently for OPS-3 and OPS-6, they are currently set to the same values.) As a result of these efforts, no DAP RECON flags are operative at Qbar = 20 psf.

6.2 Ny Feedback Modification

Before 1990, the entry/GRTLS FCS had been formally verified for landing weights up to 240,000 lb. Loads structural certification expanded this capability to 256,000 lb for GRTLS, 250,000 lb for TAL, and 248,000 lb for AOA. With the 240,000-lb landing weight, GRTLS trajectory simulations exhibited peak Qbar values up to 375 psf during the pullout phase, which was the design limit. Increasing the GRTLS landing weight while maintaining existing constraints on ET-SEP Qbar and maximum load factor will cause the pullout Qbar to increase. FCS stability with the 240,000-lb weight and nominal aerodynamics generally satisfied Level 1 requirements at 375 psf. However, linear analyses and trajectory tests with worst-on-worst aerodynamic uncertainties and other dispersions exhibited marginally acceptable performance at 375 psf and unstable characteristics for higher values of Qbar.

Previous engineering evaluations during the Space Shuttle Program had demonstrated that lateral stability could be improved if sideslip feedback could be used during most of the entry phase instead of just in the region with Qbar < 40 psf. This was also found to be true in the GRTLS high-Qbar region. However, concern for errors in the NAV-derived beta feedback has always precluded its use beyond 40 psf. As an alternate approach, the possibility of modifying the Ny feedback to emulate the low-frequency gain and phase characteristics of beta feedback was examined. This effort was successful enough to stabilize the worst-case uncertainties for Qbar up to 450 psf, with no destabilizing effects for any other uncertainties. Furthermore, the improved performance was accomplished by only modifying the values of several I-loads. (Because some of these I-loads had been changed to K-loads in OI-22, the OI-23 effort required software modifications to reset them to I-loads.) Subsequent studies showed that the same changes could be used during NEOM entries as well, precluding the need for separate I-loads in OPS-3 and OPS-6. No negative effects were observed in the approach/landing region, or in flexible mode stability.

Figure 6-1 shows the original GRTLS DAP Ny feedback configuration and a root locus plot illustrating the effect of Ny feedback on system stability for a generic flight case at Qbar = 420 psf with LVAR 11 aero uncertainties. With the Ny feedback gain at zero, the closed-loop system is essentially neutrally stable, with roots very near the imaginary (jω) axis. As soon as the Ny feedback gain starts to increase, the system becomes unstable, with closed-loop roots moving into the right-half plane.

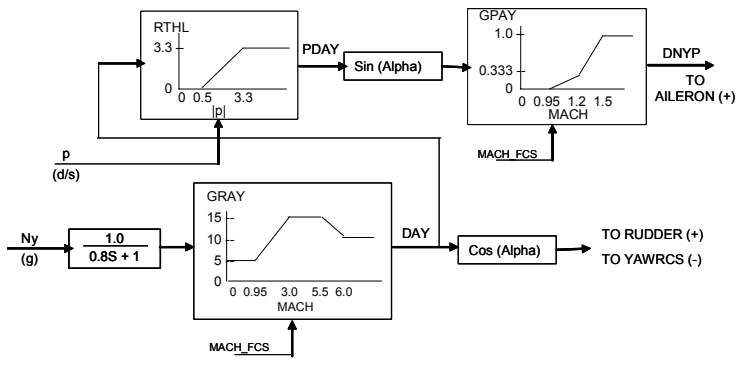

OI-22 GRTLS BASELINE DAP NY FEEDBACK CONFIGURATION

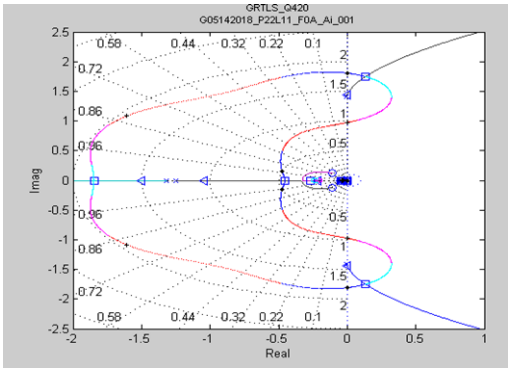

Root Locus for OI-22 Ny Feedback

Figure 6-1. Original GRTLS DAP Ny Feedback Configuration and Response

The beta feedback test configuration and root locus response for the same flight case are illustrated in figure 6-2. Here it can be seen that increasing the feedback gain improves system stability, with the closed-loop roots moving into the left-half plane.

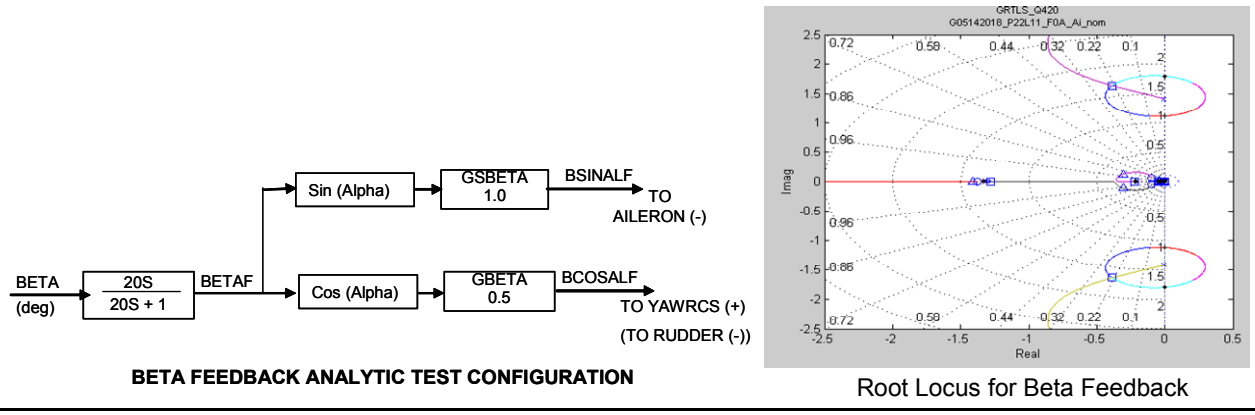

Figure 6-2. Beta Feedback Test Configuration and Response

The DAP modifications implemented to shape the Ny feedback root locus in the direction of the beta response are shown in figure 6-3, along with the root locus plot for the Qbar = 420 psf, LVAR 11 case. Changing the filter time constant from 0.8 sec to 0.2 sec reduces the phase lag at the zero-gain root location by about 35 deg, resulting in the locus departing into the left-half plane. Further reduction in the lag time constant would improve stability even more, but raises concerns about accelerometer noise and bending mode attenuation. Since the locus still moves into the right-half plane for higher gains, the scheduled gain GRAY was reduced 12 dB for Mach ≥ 3 to ensure stability at worst-case conditions. This also preserves the baseline gain level at high frequencies. To minimize impact of the changes on approach and landing handling qualities, the gain was not reduced in the subsonic region. The boosted gain feature of the original Ny-to-aileron path was replaced with a fixed value for the gain RTHL because stability and response tests indicated negligible degradation due to using the large-signal gain at low signal levels.

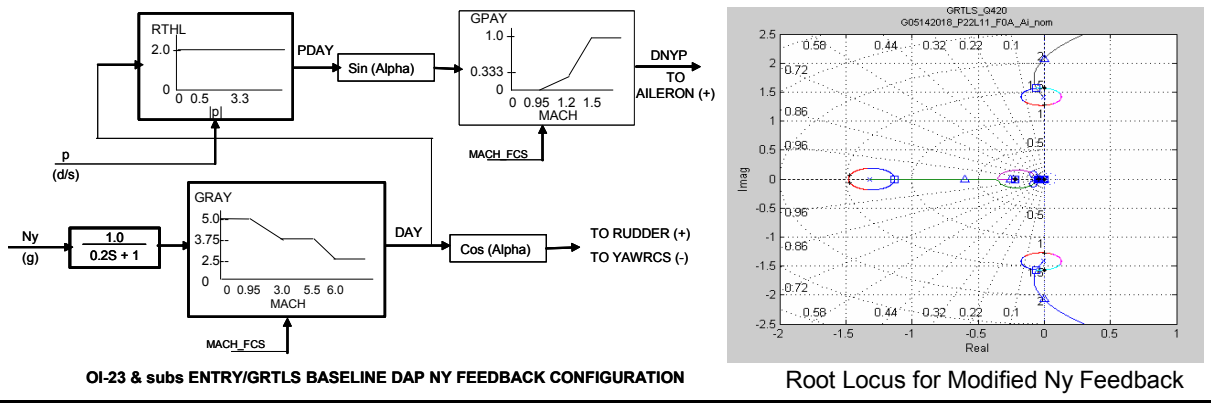

Figure 6-3. Modified Entry/GRTLS Baseline DAP Ny Feedback Configuration and Response

6.3 Descent Abort Heavyweight Verification

With DAP modifications defined that expand the maximum GRTLS Qbar capability, a task was initiated in 1992 to formally verify an increase in the landing weight limit to 248,000 lb for GRTLS, TAL, AOA, and NEOM. Successful completion of this task in early 1993 was followed by expansion of the certified Qbar envelopes in the Shuttle Operational Data Book (SODB), Vol. V, “Orbiter Flight Capability Envelopes,” to encompass the higher Qbar values associated with the increased Orbiter weight limit. This study was a cooperative effort involving Honeywell/Clearwater (fixed-point trim and linear stability), Rockwell/Downey (linear stability and non-real-time trajectory simulation), NASA JSC (real-time MIL trajectory simulation), and NASA Ames (real-time moving base approach and landing and rollout simulation).

Flight cases used for stability and response evaluation were selected from SVDS Monte Carlo data provided by NASA JSC Mission Operations Directorate (MOD) for GRTLS, TAL, and AOA with forward

and aft CG locations. Figure 6-4 illustrates Qbar vs. Mach for GRTLS analysis cases representing a composite of nominal, ±3σ, and ±6σ trajectories. Stability was evaluated using the 248,000-lb maximum landing weight for flight cases below Mach 3.5. Higher-Mach cases were evaluated with 254,000 lb, which is representative of the corresponding weight at GRTLS DAP-engage. All cases were evaluated with aft CG (1,110 inches) and forward CG (1,078 inches if Mach > 3.5 and alpha > 30 deg, otherwise 1,075.7 inches). The Honeywell and Rockwell studies are documented in References 6-1 and 6-2, respectively.

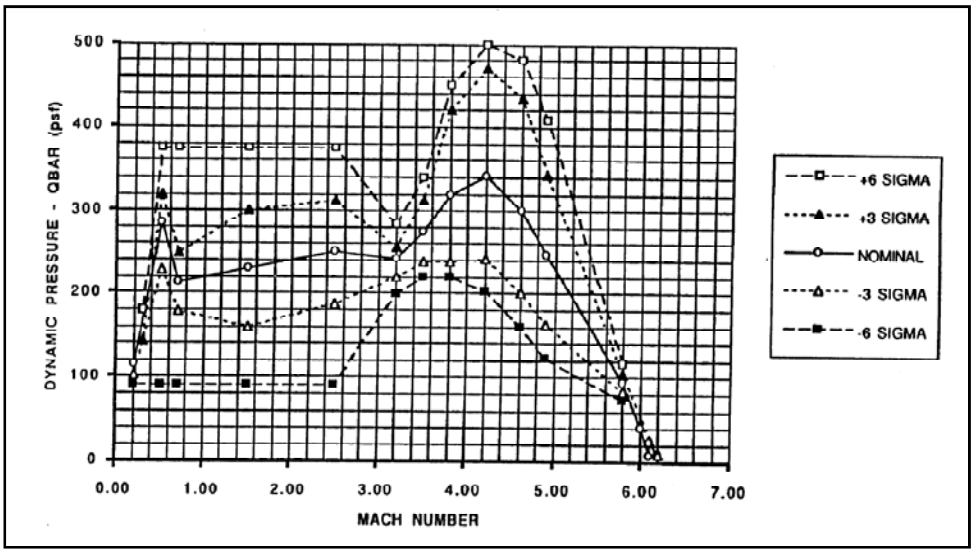

Figure 6-4. Composite GRTLS Qbar vs. Mach Analysis Envelope

The Rockwell heavyweight verification final report states that the RTLS, TAL, and AOA pitch axis and roll/yaw axis stability analyses study results meet the requirements for heavyweight verification. Although there are some differences in the Honeywell and Rockwell detailed results, both agree that all cases with nominal aero are stable, whereas some RTLS cases with PVAR 4 and LVAR 9 aero uncertainty sets are unstable. Regression tests with approved back-offs on uncertainties and/or other dispersions, as well as trajectory simulation tests, provided the rationale for accepting the linear stability characteristics of these cases. The same methodology was applied to other RTLS cases with nominal and off-nominal aero sets that are stable but exhibit stability margins below the requirements applicable to their particular combination of uncertainties and dispersions. The TAL and AOA cases are all stable with satisfactory margins even for worst-on-worst uncertainties and dispersions. Although a few cases exhibit stability margins below applicable Level 1 or Level 2 requirements, the deviations are small enough to be considered acceptable, and trajectory simulations indicate no anomalies.

The updated SODB, Vol. V, Qbar envelopes for OPS-6 and OPS-3 with landing weight up to 248,000 lb are shown in parts a and b, respectively, of figure 6-5.

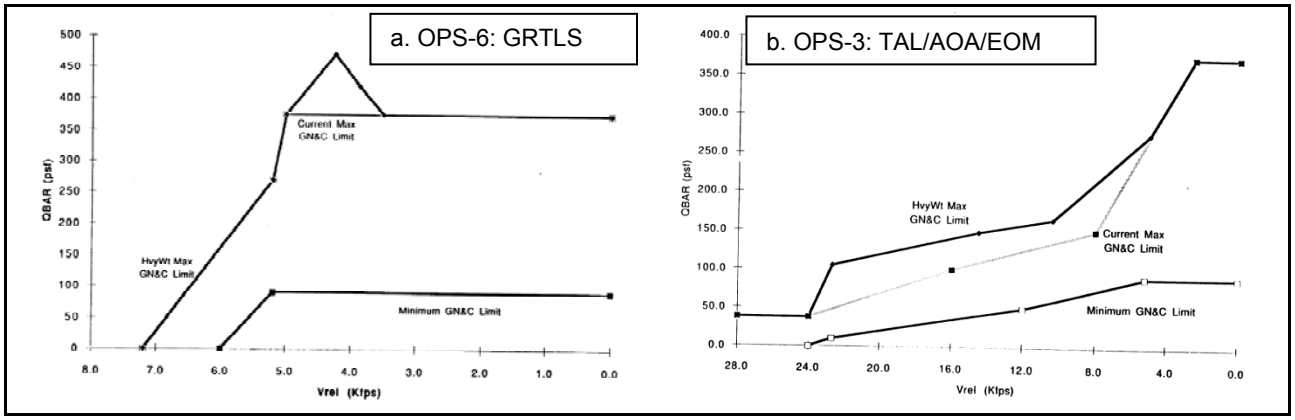

Figure 6-5. SODB Dynamic Pressure Envelopes for Increased Landing Weight

6.4 Wraparound DAP

Background: In August 1983, Paul W. Kirsten of the Air Force Flight Test Center Research Projects Office published a memo entitled "A Proposed Fuel-Saving Reentry Flight Control System for the Space Shuttle Orbiter." That memo presented DAP modifications, with supporting simulation results, which offered several advantages over the existing baseline entry DAP. These advantages included reduced RCS propellant usage during entry, an optimized pure aerodynamic control configuration for situations with limited or no yaw RCS capability, and lower RCS propellant reserve requirements for aerodynamic asymmetries. The proposed DAP modifications and their purposes are described in table 6-1.

Table 6-1. Proposed Modifications for Fuel-Saving Entry DAP

Change No.	Change	Reason for change
1	Aileron blending gain, GALR	Implements reverse aileron concept, improves aileron roll control, replaces fixed no-yaw-jet downmode gain
2	Lateral acceleration to aileron feedback	Provides artificial Cl_β which augments dynamic Cn_β; suppresses oscillatory and PIO tendencies for Mach 3.5 to 7 and above Mach 15
3	BANKERR_THRESH shaping (gain on roll angle error)	Suppresses lateral phugoid tendencies at high Mach
4	Yaw RCS switching deadbands	Widened deadbands at higher Qbar reduce RCS propellant usage during entry, and I-loads permit selection of one yaw jet minimum
5	Mach 5 rudder engage	Augments yaw stability and control for no-yaw-jet downmode and for large lateral asymmetries

A three-phase program was begun in February 1985 by NASA JSC, Rockwell, and Honeywell with the following objectives:

1) Phase 1: DFRC concept evaluation for CSS mode
2) Phase 2: "No Yaw Jet" CSS mode with yaw jet wraparound
3) Phase 3: "No Yaw Jet" Auto mode with yaw jet wraparound

The 1985 emphasis was on Phases 1 and 2, primarily without yaw jet wraparound, with concentration on changes 1, 2, and 5. This effort, which used FAD 14 aero data, involved numerous fixed-point stability and response studies by Honeywell, as well as four SES trajectory simulation studies comprising a total of 191 MIL (CSS) trajectories piloted by 16 different astronauts, and 169 auto mode tests. The later SES sessions included GRTLS as well as entry trajectories. Significant modifications to the originally proposed GALR schedule and Ny-to-Da feedback path resulted from these studies. Additional analyses and simulations were performed in 1986 using FAD 26 aero data to refine and validate the CR. The final configuration was implemented via CR 79616G ("No-Yaw-Jet Downmode") in OI-8A/B for the STS-26 post-*Challenger* return-to-flight mission. A brief overview of that development was given in the paragraph "No-Yaw-Jet Upgrade" of Section 3.2.12 of this document. Change 5 was discussed in the paragraph "Early Rudder Engagement" in Section 3.2.9. Since the no-yaw-jet downmode configuration, also known as the reverse aileron DAP, provides the inner loop of the wraparound RCS DAP, more details about its development and configuration are presented in the following paragraphs.

Reverse Aileron DAP: The baseline DAP originally had an uncertified no-yaw-jet downmode capability that could be enabled by moving the ENTRY MODE panel switch to the NO Y JET position. This selected a fixed high value of GALR, forced the roll/yaw axis into CSS mode, and opened the yaw RCS command path. The high value of GALR provided good reverse aileron characteristics suitable for no-yaw-jet control at high Mach, but it caused increasingly poor stability as Mach dropped below 6 (where the aerodynamics begin transitioning to normal aileron characteristics). Thus, in the event of a low RCS propellant situation, the crew procedure would have been to select no-yaw-jet downmode early in the trajectory, and then revert to baseline DAP control below Mach 7, where the remaining RCS propellant would augment either CSS or auto mode control. In the event of total yaw RCS failure, the procedure would be similar, except CSS control would be maintained until Mach 2.5 or lower, where stability and control characteristics of both CSS and auto are generally adequate without yaw jets.

Benefits of the reverse aileron DAP result primarily from the modified GALR schedule, and are most evident between Mach 6 and Mach 3. Above Mach 7, where the new and old GALR values are 1.7 and 1.8, respectively, stability of the reverse aileron DAP is very similar to that of the original no-yaw-jet downmode. At Mach 7, the modified schedule begins ramping down, becoming similar to the baseline schedule below Mach 4, where the aileron control characteristics are in transition. Engaging the rudder at Mach 5 maintains crew command capability as GALR goes through 1.0. Figure 6-6 compares the final reverse aileron DAP GALR schedule with the baseline DAP GALR schedule and the fixed downmode value of GALR.

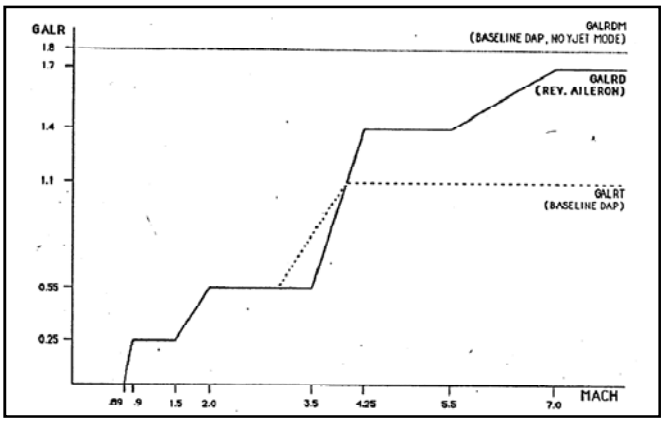

Figure 6-6. GALR (Aileron Blending Gain) Schedules

Lateral acceleration feedback in the aileron channel provides additional stability augmentation in some parts of the flight envelope, particularly above Mach 15 and below Mach 5. It also reduces the magnitude of sideslip transients during roll maneuvers. After several iterations, the baseline Ny-to-Da feedback shown in figure 6-1 was modified to the final reverse aileron DAP configuration shown in figure 6-7. A major change is that the new feedback utilizes the lateral acceleration feedback directly, rather than the output of the yaw channel NYCOMP module. This allows the gain to be tailored explicitly for aileron loop requirements, without having to factor in the GRAY schedule. Other changes from the configuration shown in figure 6-1 are the elimination of roll-rate-scheduled gain boost and sin(α) scaling, and the addition of a 20-sec high-pass to the 0.8-sec lag filter. The high-pass prevents steady-state lateral acceleration required for aerodynamic trim from opposing the aileron trim deflection, while allowing full gain during maneuvers and transients. It also improves trim performance when the rudder is active. Simulations and analyses showed no benefit to retaining the sin(α) scaling. It should be noted that when the baseline DAP yaw channel Ny lag filter time constant and gain (GRAY) were changed as part of the subsequent Ny feedback modification study described above, the reverse aileron DAP Ny-to-Da feedback gain and filter were not changed.

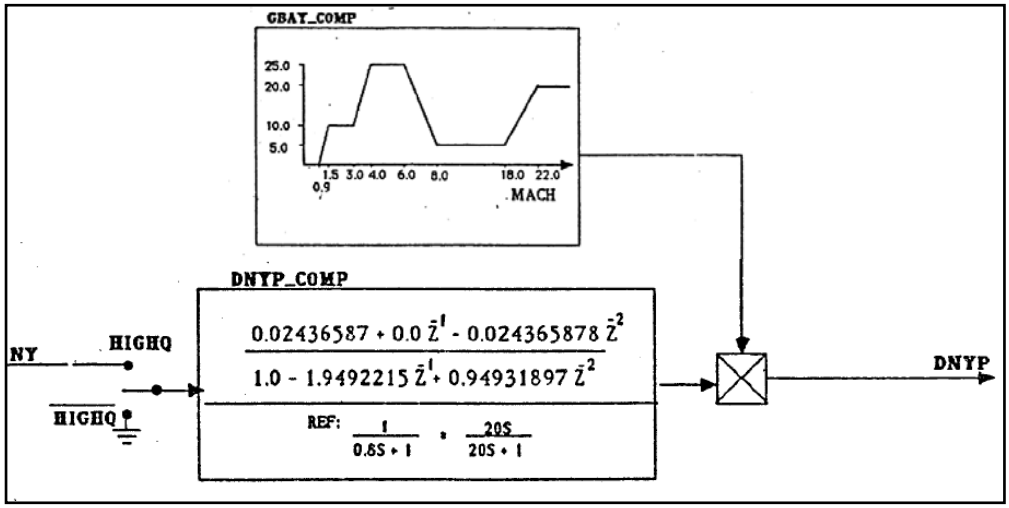

Figure 6-7. Reverse Aileron DAP Lateral Acceleration Feedback to Aileron

Wraparound Yaw Jets: The second major component of the proposed fuel-saving reentry FCS, after GALR modification, is widened yaw-RCS switching deadbands. While the reverse aileron DAP GALR schedule provides a stable aerodynamic system for most of the entry flight envelope and dispersions in CSS, the auto mode remains unstable with aerodynamic control for some worst-on-worst dispersion cases, and responses to roll commands often lack the briskness that the crew and the guidance system expect. Consequently, the yaw-RCS switching logic was redesigned so that the yaw jets will fire only for relatively large yaw channel errors: e.g., those due to roll commands, significant disturbances and oscillations, or large lateral mistrim conditions. The baseline and wraparound RCS switching logic configurations are shown for comparison in figure 6-8. Wraparound RCS was not incorporated in the reverse aileron DAP itself, but was included later with the full wraparound DAP.

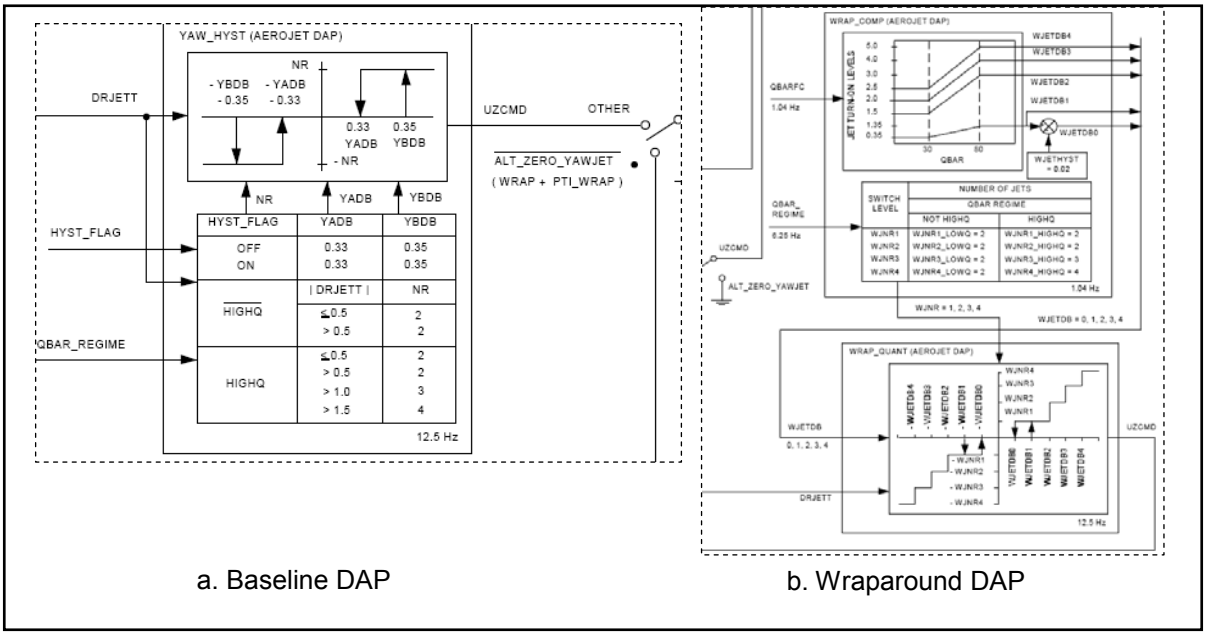

Figure 6-8. Baseline and Wraparound Yaw-RCS Switching Logic

Five items to note about the wraparound RCS are

1) The configuration allows a minimum firing command of one jet. However, flight I-loads have always been set to command two jets when the minimum switching level is exceeded.
2) In common with the baseline DAP, the maximum firing command will be two jets regardless of yaw channel error in the NOT-HIGHQ region (Qbar < 40 psf).
3) As a result of items 1 and 2, when Qbar is less than 30 psf, wraparound RCS switching is identical to baseline.
4) As Qbar increases from 30 to 80 psf, the switching levels increase linearly so that above 80 psf, the yaw channel error magnitudes needed to fire two, three, and four jets are three to four times greater than for the baseline DAP.
5) Turn-on/turn-off hysteresis for the minimum firing command retains the baseline value, 0.02, even as the minimum turn-on level increases.

No-Yaw-Jet and Wraparound RCS Auto Mode: During reverse aileron DAP development, studies were made of no-yaw-jet AUTO mode performance and of AUTO and CSS mode performance with yaw jets active. Even with change 3 (BANKERR_THRESH mod) implemented, no-yaw-jet AUTO mode performance was unacceptable at high Mach due to sluggish roll responses causing guidance-control interaction. The Mach 5 region experienced stability and trim problems with worst-on-worst uncertainties, although implementing change 5 (Mach 5 rudder) helped trim, especially in GRTLS. Activating baseline yaw jets with the other changes resulted in acceptable stability and control characteristics, as well as in significant reduction in RCS propellant consumption. However, crew evaluators were unenthusiastic about CSS or AUTO mode performance with the change 4 wide yaw-RCS switching deadbands. Although CR 90476, "Wraparound Yaw Jet System with PTI Effector," was written during this time, further development of no-yaw-jet AUTO mode and wide-deadband wraparound RCS was discontinued in early 1986 to permit completion of the reverse aileron DAP for CSS.

Interest in the wraparound RCS configuration resurged in late 1989 with considerations of providing a safe platform for actually flight testing the reverse aileron DAP, potential reductions in entry RCS propellant availability for extended-duration missions, and implementation of a single-yaw-jet DTO. Although analyses and simulations led to some refinements in the AUTO mode configuration, wraparound RCS DAP completion was again deferred due to higher priority program needs.

The impetus to finally complete development and implementation of the wraparound DAP resulted from two Space Shuttle flights that consumed excessive RCS propellant and exhibited abnormal aileron trim deflections during entry. STS-50, in July of 1992, experienced an asymmetric boundary layer transition (ABLT) that generated rolling and yawing moments requiring significant changes in aileron deflection and sideslip angle for aerodynamic trim. Since the baseline DAP aileron trim rate is very slow, yaw jet firings were necessary to balance these moments while re-trimming. Density shears during STS-57 entry in June 1993 caused drag errors resulting in large roll attitude corrections, with a significant increase in total RCS propellant consumption. In August 1993, the Shuttle Program Office initiated an investigation that would lead to the implementation of an operational wraparound DAP based on CR 90476, with any changes necessary to bring it up to operational standards and to provide adequate integrated guidance and control performance. The design team included personnel from NASA JSC (EG and DM divisions), United Space Alliance, and Honeywell. It was expected that the wraparound DAP would mitigate increased RCS propellant usage resulting from ABLT and density shear phenomena, as well as provide an increased margin of safety in the Orbiter's guidance and control function.

Roll Angle Error Path: Figure 2-11, Simplified Roll Axis Block Diagram, showed that the primary difference between roll/yaw axis CSS and AUTO modes is the replacement of roll rate commands caused by crew roll RHC inputs with roll rate commands caused by the error between guidance roll command and actual (NAV) roll angle. The reverse aileron DAP forms the wraparound DAP inner loop, and together with modified yaw-RCS switching logic, provides the wraparound CSS mode specified in the Phase 2 program objective. Figure 6-9 provides more details of the AUTO mode roll command path. The BANKERR_THRESH block is expanded in figure 6-10, which shows baseline and modified versions of this function. The purpose of the nonlinearity is to maximize the roll rate command for large roll commands and errors, while providing a low gain for small values of roll error to minimize the destabilizing effect of positive roll feedback that occurs when GALR > 1. Note that the effective linear roll error gain through this block is the slope of BKERR vs. BANKERR at a particular operating point. For the baseline system, the inner and outer slopes are 0.444 and 1.0, respectively. The output BKERR is multiplied by the gain GPBANK and then clamped by PCLIM so that over most of entry, the maximum stability axis roll rate command is 5 deg/sec.

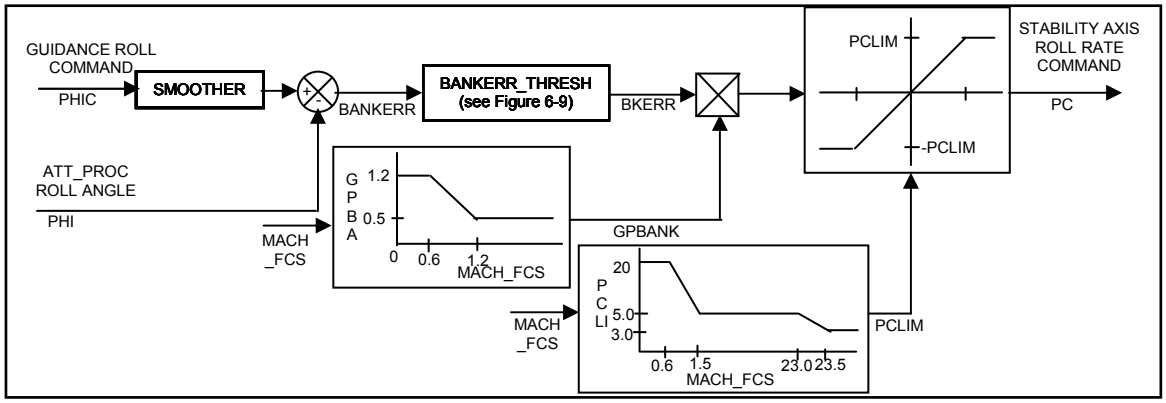

Figure 6-9. Auto Mode Roll Command Logic

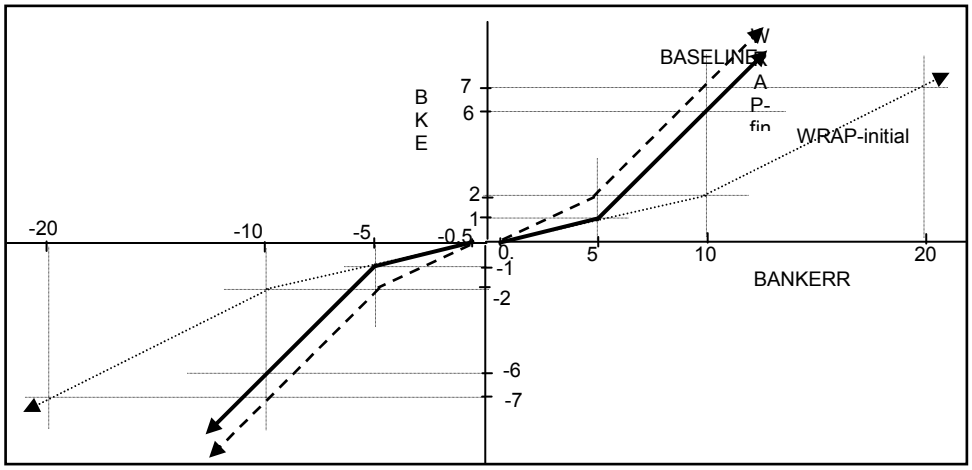

Figure 6-10. BANKERR_THRESH Nonlinear Roll Gain Function

In the original proposal, the only change unique to the AUTO mode was a 50% reduction in the roll angle error gains provided by the module BANKERR_THRESH (change 3). This reduction was accomplished by moving the BANKERR breakpoints out to double their baseline values, while keeping the BKERR breakpoints at baseline values, resulting in slopes of 0.211 and 0.5. This change improves AUTO mode low-frequency stability when the system is operating inside the yaw jet deadbands, or when the yaw jets are disabled. However, trajectory performance suffered due to sluggish responses to guidance bank reversal commands and excessive roll error standoff. Analysis of this behavior was facilitated by running roll command step responses in STAMPS, as illustrated in figure 6-11 (extracted from reference 6-3). Sluggish responses tended to cause excessive roll angle overshoot, which in turn caused more occurrences of guidance minimum roll commands with this wraparound DAP configuration than typically occur with the baseline DAP. The top part of figure 6-12 (also from reference 6-3) shows an example of minimum roll command during the first bank reversal of a typical trajectory.

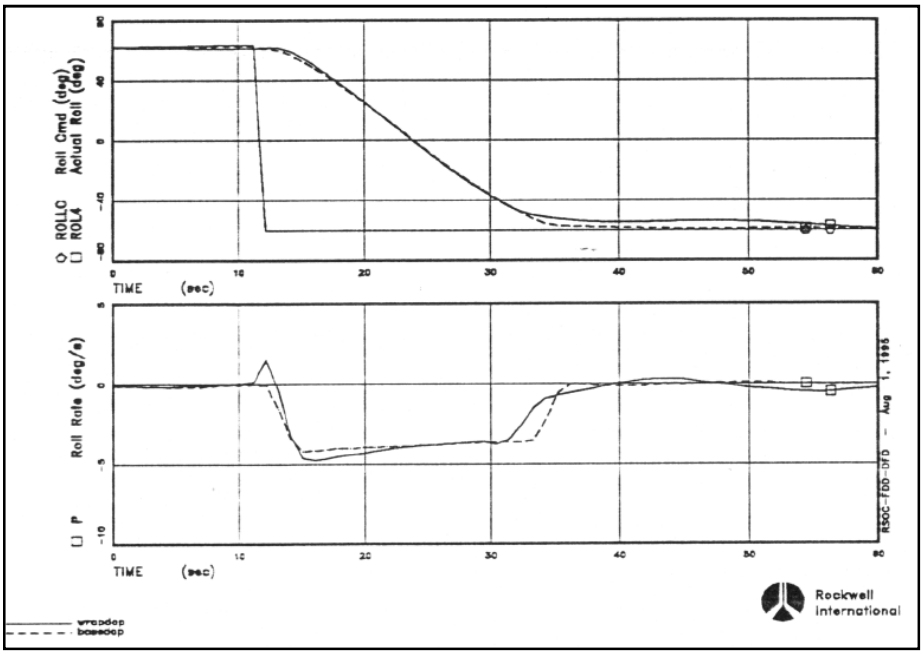

Figure 6-11. Roll Step Command Response Comparison: Initial Wrap vs. Baseline DAP

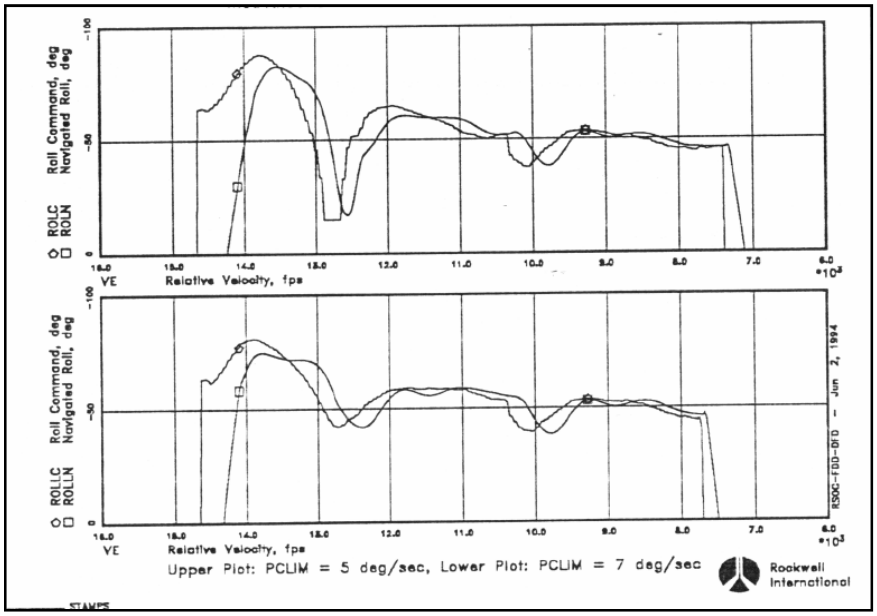

Figure 6-12. Example of Minimum Roll Command

The undesirable roll characteristics were found to be the result of early roll rate termination. With the baseline DAP, the roll rate command, PC, remains at 5 deg/sec until roll error drops below 13 deg, when it decreases linearly to 1 deg/sec for 5-deg roll error. With the initial wraparound BANKERR_THRESH function, however, PC starts dropping when roll error is 26 deg, decreasing linearly to 1 deg/sec for 10-deg roll error. The combination of reduced low and high gains, low gain extending out to 10-deg roll error, and Qbar-scheduled yaw-RCS switching, results in relatively little control power to expeditiously reduce roll error below 10 deg. Various trade studies were conducted to improve this performance. Increasing the roll rate command limit helped reduce the tendency for minimum roll commands, as shown in the lower part of figure 6-12, but was not implemented because of concerns about increased pitching moment induced by inertial coupling at the higher roll rate.

In the final wraparound DAP configuration, BANKERR_THRESH was changed to the curve labeled "WRAP-final" in figure 6-10, resulting in the improved roll command response illustrated in figure 6-13.

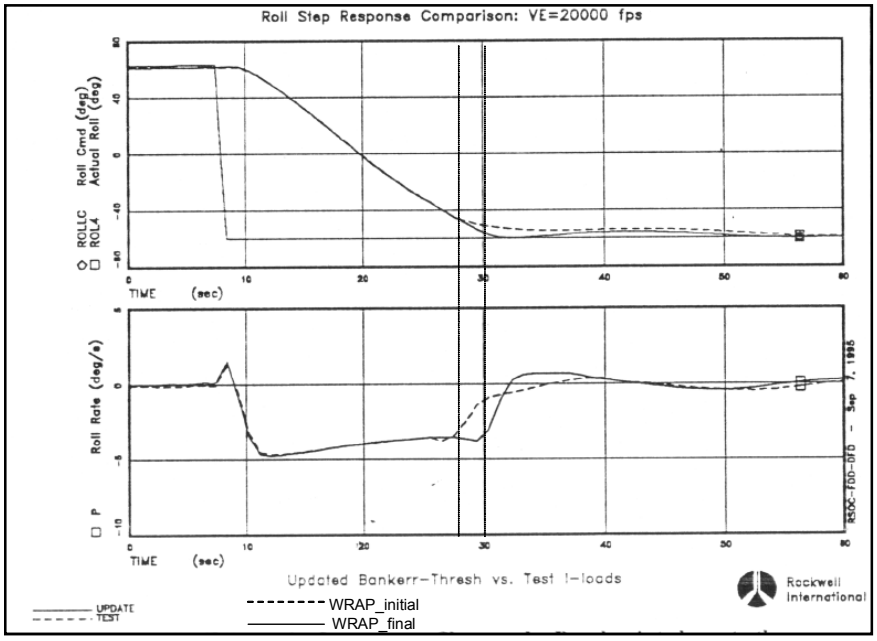

Figure 6-13. Roll Step Command Response Comparison: Final vs. Initial Wrap BANKERR_THRESH

Here the roll rate command does not start dropping until roll error is close to the computed value of 14 deg. Furthermore, with the steep slope gain applying until roll error drops to 5 deg, the steady-state roll error is less and is reduced faster. The unity gain steep slope and 5-deg roll error breakpoint between shallow and steep slopes of the final BANKERR_THRESH function result in greater susceptibility to auto mode roll loop instabilities when operating within the yaw-RCS deadbands. Oscillatory behavior may be expected when the average roll error is between 5 and 14 deg, e.g., when roll angle is approaching the roll command. However, the yaw jets as well as aileron will be forcing the error down towards the shallow slope region, where stable operation can be expected. The yaw jets will also constrain the amplitude of any oscillation. If yaw jets are not available, selecting the CSS mode will remove the roll loop from the system, ensuring stability and controllability

Angle-of-Attack Loop: To further improve roll command responses, the pitch axis alpha error filter and gain were modified as shown in figure 6-14 to tighten the alpha command response.

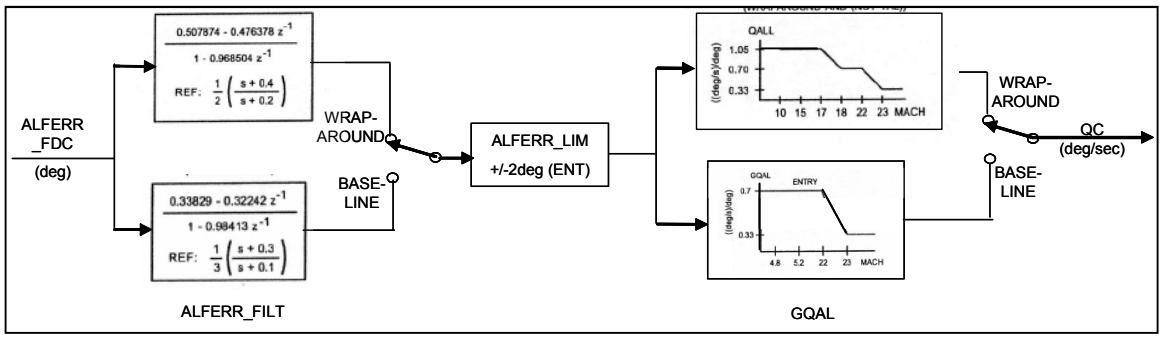

Figure 6-14. Alpha Error Filter and Gain Modifications for Wraparound DAP (Entry Only)

Aileron Trim Modifications: Two changes were made in the wraparound DAP yaw-to-aileron trim path to improve aerodynamic trim capability for extreme lateral asymmetries, e.g., those caused by ABLT. The first change was an increase in aileron trim limits from 3 to 5 deg, which improves the aerodynamic trim capability for large ABLT or other lateral asymmetries. The second change relates to the need to trim fast enough for the larger limits to be beneficial, and to un-trim rapidly if the asymmetry fades or disappears. Since this trim loop is destabilizing in the AUTO mode because of positive roll feedback, increasing the gain GTRIMB was quickly determined to be unacceptable. However, increasing the limit on the yaw channel error from 0.175 to 0.7 deg/sec (the second change) provides a maximum trim rate capability that is four times faster than that of the baseline DAP without compromising linear stability.

Flexible Body Stability: The implementation of the wraparound DAP had no significant impact on the flexible body margins and did not require any body bending filter redesign. Preflight flex performance was assessed before STS-85, which was the first full flight of the wraparound DAP. Comparison linear frequency response plots between the OI-25 wraparound and baseline DAP were produced in support of this assessment.

Wraparound DAP Applicability: Wraparound DAP is available between Qbar = 10 psf and Mach = 1 for all OPS-3 missions, and is normally the default DAP configuration via an I-load setting. If TAL is declared before OPS-3, the default configuration will be baseline DAP. However, the crew can use the override display to engage wraparound DAP anytime after Qbar = 10 psf. Wraparound DAP is not available in GRTLS, although the reverse aileron DAP no-yaw-jet downmode configuration may be selected.

Wraparound DAP is not engaged until Qbar > 10 psf because the large value of wraparound GALR would cause reverse roll RCS jet firings as well as reverse aileron deflections in response to roll angle commands. This type of problem did not occur in NEOM testing, but TAL simulations exhibited excessive roll angle divergence when roll angle commands were induced by large sideslip errors. With baseline DAP, GALR = 1.0 when Qbar < 10 psf; thus the ailerons and roll jets only provide coordination of the roll response. Excluding wraparound DAP below Mach 1 ensures that the CSS mode always has historic handling qualities during approach and landing.

Wraparound DAP Wobble Oscillations: Trajectory simulation tests of the wraparound DAP have exhibited two types of unexpected oscillatory activity, which have been named “TAEM wobble” and “TAL wobble.” TAEM wobble was first observed in an STS-79 SAIL test while the Orbiter was rolling from the fourth bank reversal toward wings-level during TAEM IPHASE 1 (Acquisition). TAL wobble was observed

during STAMPS tests of several missions during the first roll maneuver while the Orbiter was rolling back from maximum angles near 90 deg to the nominal 50- to 60-deg range. In all cases, roll angle command was changing at rates of 0.5 to 1.5 deg/sec, while roll angle was following with an error (BANKERR) between 13 deg and 5 deg; i.e., it was in the steep slope range of BANKERR_THRESH. This destabilized the aileron loop, allowing oscillations to build up until their magnitude caused yaw jets to fire. Because the FCS always drives roll error towards zero, the oscillations damp out when the average error drops into the shallow slope region. Because of smaller yaw jet deadbands, tests with the baseline DAP exhibit no significant similar oscillations. This observation was a major factor in the decision to use baseline as the default DAP for TAL. TAEM wobble has been observed in a few actual flights, but has not caused any concern for the wraparound DAP.

Most missions using the wraparound DAP for entry have exhibited activity within various intervals between Mach 7 and 2 that has been named "entry wobble." This has typically manifested itself as two to three cycles of irregular shape, periods of 10 to 20 sec, peak-to-peak roll rate amplitude increasing to 2 deg/sec, and occasional yaw jet pulses coincident with oscillation peaks. Trajectory simulations have not adequately demonstrated similar characteristics, although several mechanisms have been proposed and/or tested. Increasing selected aerodynamic coefficient uncertainties above ADB values increases cyclic activity, but the results tend to be more uniform and of frequencies different from those in flight. Modifying sensor and actuator nonlinearities improves correlation with flight, but only with nonlinearity values greater than current 3-sigma specifications. Perhaps the best correlations with flight were obtained by adding turbulence tuned to the natural modal characteristics of the Orbiter/DAP system, and by using reconstructed flight atmospheres with appropriate density changes. There have been no studies of entry wobble since mid-1999 because of other task priorities and lack of available budget and personnel.

Flight Test Program: In flight-testing the wraparound DAP, the OI-25 flight software had available three different DAP configurations that the crew could select (see table 6-2). The baseline DAP was the operational system; it had built a track record of dependable and predictable flight performance. The no-yaw-jet (reverse aileron) DAP had never been flight-tested despite efforts to gain Space Shuttle Program Office approval. The arguments used against spending resources on a no-yaw-jet flight test were that it was an emergency downmode and that it would involve manual flying because it did not have an AUTO mode.

Table 6-2. DAP Mode Comparison

DAP	History	Small Perturbations / Commands	Large Perturbations / Commands
Baseline	Operational STS-1	Yaw jets assisted by minimal reverse aileron	Yaw jets assisted by minimal reverse aileron
No-yaw-jet	Upgraded OI-8C	Reverse aileron	Reverse aileron
Wraparound	Added with OI-25	Reverse aileron	Reverse aileron assisted by yaw jets

With the implementation of the wraparound DAP and the plan to eventually make it the default selection for nominal entry, a flight test plan had to be defined and implemented. Because the I-loads for the wraparound DAP yaw-RCS loop could be configured independently of the I-loads for the baseline DAP yaw-RCS loop, the opportunity to flight-test some alternate configurations without impacting the baseline DAP now existed. Because the wraparound DAP was built on top of the no-yaw-jet mode, the no-yaw-jet DAP could effectively be flight-tested by zeroing out the yaw RCS deadband I-loads in the wraparound DAP. In addition, flight test data on single-yaw-jet firing levels could be flight tested by changing the yaw RCS deadband I-loads in the wraparound DAP from a two-jet-minimum firing level to a one-jet-minimum firing level. However, the Orbiter Project Office's priority was to get the wraparound DAP operational as soon as possible so that they could take advantage of its increased aileron trim capability, which was needed to certify an increased forward CG capability. To shorten the flight test, the single-yaw-jet firing configuration was dropped from the test plan.

The software change request (CR 90476) that added the wraparound DAP to the Shuttle flight software also modified the PTI software (described in Section 4.2) to allow automated testing of the wraparound DAP. The original version of the PTI software could send stimulus signals to the aerosurfaces and RCS jets for the primary purpose of obtaining aerodynamic flight test data. CR 90476 added a stimulus signal to represent an RHC roll rate command (Pc) doublet so that the end-to-end FCS response could be tested. The other change to the PTI software was to allow it to automatically switch between the baseline and

wraparound DAP modes during the PTI maneuver. If any PTI constraints were violated (e.g., excessive roll rate), the existing PTI logic would automatically terminate the PTI maneuver and revert to the baseline DAP.

The final version of the flight test plan is shown in table 6-3. Test parts 1 through 4 consisted of performing PTI maneuvers at five different flight conditions. Each PTI maneuver consisted of two back-to-back roll command doublets, the first using the wraparound DAP and the second using the baseline DAP. (The fifth maneuver added an aileron and rudder pulse to collect some additional aerodynamic flight data). In addition, the first two flights had the wraparound DAP yaw RCS jet I-loads zeroed out so that the no-yaw-jet DAP could be flight tested. The first flights performed the roll command doublets at 2 deg/sec with subsequent flights stepping up to 4 deg/sec. Parts 5 and 6 did not use the PTI software but actually had the crew mode to the wraparound DAP. For Part 5 the crew switched to the wraparound DAP for just the duration of the first roll reversal, but for Part 6 they flew the entire entry trajectory using the wraparound DAP.

Table 6-3. Wraparound DAP Flight Test Plan

Test Part	Flight	Roll Rate (deg/sec)	Description
1	STS-79	2	Reverse aileron: PTIs
2	STS-80	4	Reverse aileron: PTIs
3	STS-81	2	Wraparound DAP: PTIs
4	STS-82	4	Wraparound DAP: PTIs
4	STS-83	4	Wraparound DAP: PTIs
5	STS-84	5	Wraparound DAP: first roll reversal
6	STS-94	5	Wraparound DAP: entire trajectory
6	STS-85	5	Wraparound DAP: entire trajectory

After STS-79 landed, the flight control community began evaluating the flight test results and comparing the flight test data to the preflight predictions. Rockwell quickly noticed a significant discrepancy with PTI 1. Table 6-4 shows the PTI maneuvers flown on STS-79. Although PTI 1 executed the planned doublets, the yaw RCS jets fired during the wraparound DAP part of the maneuver. Because the yaw RCS jets were supposed to have been I-loaded to zero, they should not have fired. This software error was not observed during SAIL flight software verification testing because of the peculiarities in the way these specific I-loads are initialized when the DAP is first scheduled to run and then reinitialized when Qbar = 40 psf.

Table 6-4. PTI Maneuvers for STS-79

PTI #	Qbar/Mach Window	Pulse Summary	Time
1	Qbar = 35.0 - 50.0	Pc (wrap) - Pc (base)	14.4
2	Mach = 17.5 - 16.0	Pc (wrap) - Pc (base)	14.4
3	Mach = 12.0 - 10.0	Pc (wrap) - Pc (base)	14.4
4	Mach = 7.0 - 5.5	Pc (wrap) - Pc (base)	14.4
5	Mach = 4.5 - 3.0	Pc (wrap) - Pc (base) - aileron (wrap) - rudder (wrap)	17.1

The software error only affected the first initialization of the I-loads by incorrectly initializing them to the default firing levels. At Qbar = 40 psf, the I-loads were correctly re-initialized to prevent jet firing. Thus if the PTI started executing after Qbar = 40 psf, the I-loads would have the expected values and the jets would not fire. It happened that in all the SAIL tests, the PTI maneuver started after Qbar = 40 psf; thus it executed correctly with no jets firing. On the actual flight of STS-79, however, the PTI started executing just before Qbar = 40 psf; thus the PTI maneuver was affected by the I-load software error and the yaw jets fired. After the flight software community identified the root cause of the I-load error, they reviewed CR 90476 to see if the same type of software error might have affected any other I-loads. They concluded that no other I-loads were susceptible to this error and decided that the flight test program could continue.

During this time, Honeywell was comparing the signatures of the flight test maneuver responses with their preflight predictions. They got very good matches on all the PTI maneuvers except PTI 4. It was a close match, but not as close as the other PTIs. Because the Shuttle doesn't have an air data system available above Mach 5, sometimes postflight analysis discrepancies are simply due to unmeasured winds and turbulence. But Honeywell started playing "what if" games. When they assumed that a software change

might have been omitted in an “if” statement that switches which Ny feedback path is used, their comparison between flight data and their preflight prediction improved considerably! Figure 6-15 illustrates this with plots generated by Honeywell’s fixed-point 6-degree-of-freedom (DOF) time-domain tool, SIMEX. The flight responses were reproduced using downloaded flight data. In part A of figure 6-15, SIMEX utilizes the expected DAP configuration, whereas in part B, the SIMEX DAP is modified to emulate the suspected flight software error. Although the part B SIMEX responses don’t overlay flight, the peak amplitudes have increased. It is particularly noteworthy that in Part B, the SIMEX roll rate (PBODY, PGYRO) response shapes are more similar to flight than in part A as they approach the “bump” (due to roll rate reversal as the PTI reverses) and then decrease from the peak.

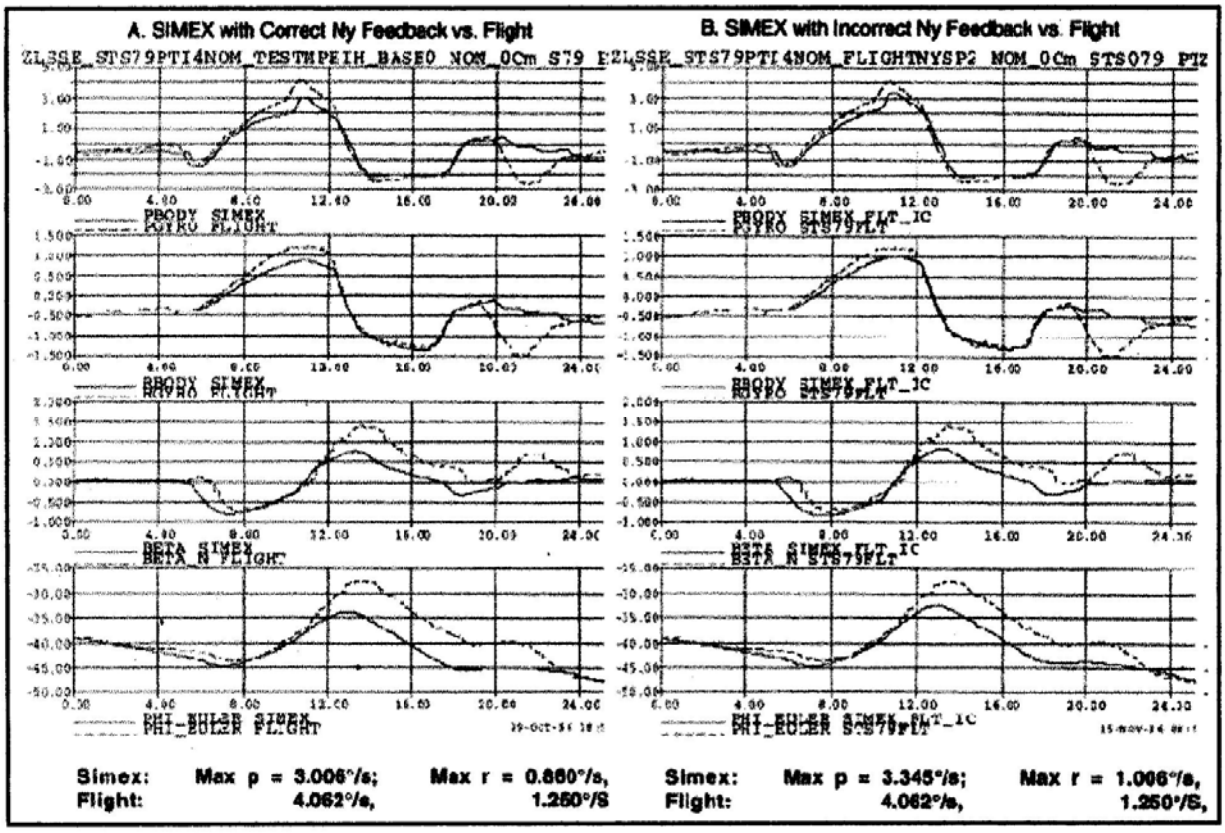

Figure 6-15. STS-79 PTI 4 Response Plots

At this point, Rockwell obtained a copy of the flight software source code and looked at the “if” statement that Honeywell had suspicions might be in error. They confirmed that there was an error in the source code and reported this to the manager of the Space Shuttle Flight Software Office, who then ordered the flight software contractor to do an exhaustive code audit of CR 90476. The contractor subsequently uncovered several more software errors, which are listed in table 6-5. These errors had small effects on the nominal system performance and so would have been very difficult to observe in SAIL testing. However, these errors should have been discovered in lower level software testing.

Once the software DRs had been dispositioned, the wraparound DAP flight test continued smoothly. With the completion of the flight test, the wraparound DAP was certified as the default operational mode. Subsequent flights have demonstrated that in terms of RCS propellant usage, the wraparound DAP is indeed more robust than the baseline DAP to dispersions such as density shears and asymmetric boundary layer transition.

Table 6-5. CR 90476 Flight Software Implementation Errors

DR Number	DR Title
110271	Incorrect initialization of number of jets for PTI
110286	Missing PSF cards for tabulated QBARFC I-loads
110287	Roll cmd PTI pulse not immediately zeroed when PTI terminated
110288	Incorrect switch conditions for DNYP
110291	WRAP_QUANT code does not provide for zero jet level
110292	BANKERR_LIMITER And ALFLOOP inputs do not switch simultaneously on WRAP transitions
110293	Aileron trim cmd may be incorrectly limited during a PTI
110294	WRAP_QUANT executes before parameter initialization
110299	Undesired initialization of ALFERR_FILT_NYJET and DNYP_COMP

6.5 Forward XCG Expansion

Expanding the Orbiter's CG capability forward of the original entry limit of 1076.7 inches has been a long-standing program goal in order to provide manifesting flexibility. This became especially important for Space Station assembly flights to ensure flight safety during the entry phase for cases where payload elements might still be in the cargo bay. In April 1997, NASA's Orbiter Program Office authorized Boeing North American (BNA) to perform a study to evaluate the feasibility of expanding the forward XCG limit by 1 to 2 inches. Honeywell was appointed the task of evaluating fixed-point trim and flight control stability and response characteristics. Successful certification of a forward CG limit of 1,075.2 inches for entry and AOA was made possible by the expanded aileron trim capability provided by the wraparound DAP, as well as by the reduction in aileron derivative uncertainties resulting from analysis of flight data. Documentation of this effort is provided in References 6-4, 6-5, and 6-6.

The overall FCS verification methodology and effort was comparable to that of the STS-26 return-to-flight and heavyweight Orbiter verification efforts. It included cross-functional studies in the following areas:

1) Aerodynamics analysis to reduce aileron derivative uncertainties in critical flight regions
2) Aeroheating analysis to verify compliance with entry heating envelope and temperature constraints
3) Fixed-point trim analysis to verify compliance with elevon and aileron trim deflection limits
4) Fixed-point rigid body stability analysis to verify stability margin compliance with current certification requirements (reference 6-7)
5) Fixed-point flexible body analysis to verify that no significant payload-Orbiter coupling occurred that would affect the FCS
6) Ames VMS tests to evaluate effects on approach and landing constraints
7) Structural analysis to identify any flight restrictions necessary to maintain loads within the current certification limit.

The ground rules and constraints imposed on this study included the following:

1) Stay within existing certification databases:
   a. SODB, Vol. V, environment
   b. Verified aeroheating thermal limits
   c. Existing alpha profile
   d. Nominal venting and dispersed Qbar envelopes
   e. 16.4-deg up-elevon limit (elevon cove thermal requirement)
   f. ± 5-deg aileron trim limits (with wraparound DAP)
   g. Operational aero database with updates through July 1997 (includes up-elevon DTO 251 data).
2) Use the wraparound DAP as defined in flight software release OI-25.
3) No hardware or software modifications shall be required.
4) Trade YCG for XCG as necessary to maximize XCG expansion.

The initial goal of this effort was a 2-inch XCG expansion, to 1,074.7 inches, with YCG ± 0.5 inch and 233,000-lb vehicle weight. Preliminary studies using heavyweight certification OPS-3 and STS-73 flight cases indicated acceptable trim, stability, and response characteristics at these limits, even with worst-on-worst uncertainties and dispersions. However, applying CG tolerances (XCG 1,073.7, YCG ±1.0) degraded

performance characteristics, particularly between Mach 9.5 and 7.5, where pitch and lateral stability issues were evident, yaw jets were required for lateral trim, and up-elevon deflections greater than the 16.4-deg thermal limit were required for trim. These issues were evident in trajectory simulations as well as in fixed-point results. Subsequent exploratory studies using Monte Carlo data specifically applicable to this effort and 248,000-lb weight revealed additional obstacles to the 2-inch XCG expansion; therefore, the certification objectives were reduced to a 1.5-inch XCG expansion, to 1,075.2 inches, with YCG limited to 1.0 inch in the expansion region. All evaluations were then done with tolerance values of XCG 1074.2 and YCG ±1.5.

Database, FCS Configuration, and Requirements: Flight cases for NEOM fixed-point stability and response evaluation were based on 50-cycle Monte Carlo data sets for entry trajectories run on the United Space Alliance Spacecraft Trajectory and Mission Planning (USA/STAMPS) facility for NASA-JSC Flight Design and Dynamics Division. These were run using the wraparound DAP with XCG 1,075.2, YCG 1.5, bent airframe, no ABLT, and weights of 248,000 and 233,000 lb. Twenty-two reference points ("slices") from Qbar = 2 psf to Mach 0.4 were selected for evaluation, with three to seven flight cases defined for each slice: nominal per cycle 0, ± 4-deg alpha about nominal, ± 3-sigma from correlated alpha-Qbar ellipses, and ± 6-sigma, based on doubling the correlated 3-sigma dispersions. The alpha and Qbar dispersions were generally limited to stay within the SODB alpha and Qbar envelope boundaries. TAL flight cases were based on 100-cycle Monte Carlo data sets for TAL run on the USA/STAMPS facility with XCG and YCG as for entry, 248,000-lb weight, bent airframe, and baseline DAP. Only those cases with 43-deg alpha and in transition to the nominal entry envelopes were chosen for evaluation. Flight cases for AOA evaluation were selected from the 1992 OPS-3 heavyweight certification matrix. Figure 6-16 presents an overview of the flight cases used for stability assessment.

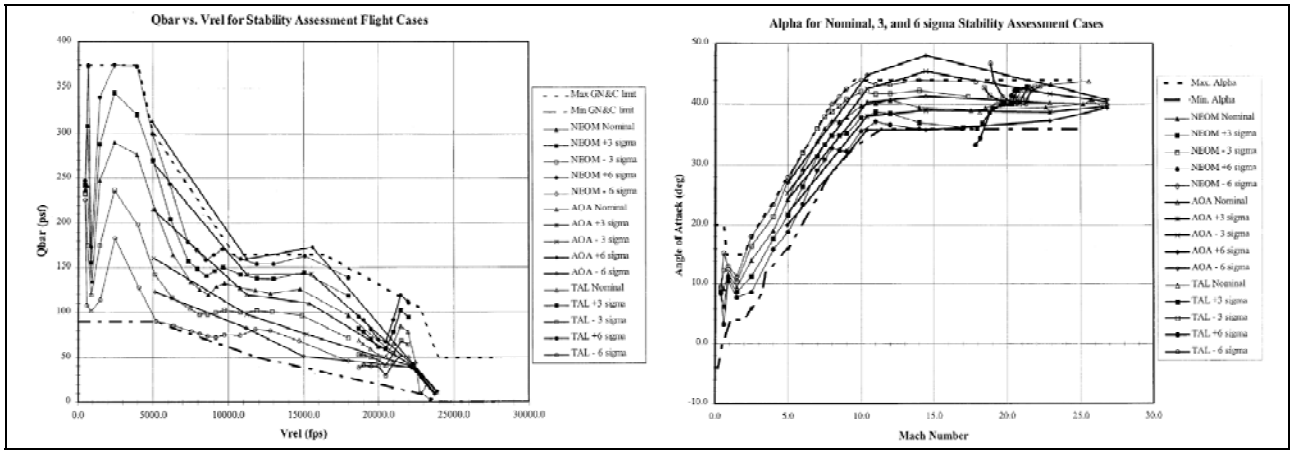

Figure 6-16. Flight Cases for Forward CG Expansion Analytic Assessment

Flight case data were computed using the 1962 Standard Atmosphere together with the Operational Aero Data Base (OADB) with updates and corrections through July 1997. In addition to nominal aero, stability was evaluated for pitch short-period aero uncertainty sets (PVARs) 1, 2, 3, and 4, and for roll/yaw aero uncertainty sets (LVARs) 2, 9, 10, 11, 19, and 20, with appropriate pitching moment uncertainties. Lateral asymmetries due to bent airframe coefficients of CLBA/CNBA = -/+0.00025 and full OADB ABLT values were included to stress trim. Selected cases were also evaluated with sensor and actuator (line replaceable units, or LRUs) tolerances applied to their gain and frequency characteristics. The OV-105 Orbiter vehicle, *Endeavour*, with the mass properties shown in table 6-6, was employed for stability and response evaluations.

Table 6-6. Forward XCG Evaluation Mass Properties

Weight (lb)	XCG (in)	YCG (in)	ZCG (in)	Ixx (slug-ft^2)	Iyy (slug-ft^2)	Izz (slug-ft^2)	Ixz (slug-ft^2)
248,000	1074.2	-1.5	372.4	964,253	7,319,980	7,605,583	176,349

This study was performed using the DAP configuration as implemented in flight software release OI-25, with the wraparound DAP employed for all NEOM, AOA, and TAL cases with Qbar > 10 psf and Mach > 1.0. The baseline DAP was used outside this region, and later for selected TAL cases, because wraparound was not certified for TAL. Where relevant, effects of the OI-26 Qbar = 2 switch in the bodyflap channel

were included. The AUTO mode was used for evaluating stability and response for all cases except those with ± 6-sigma Qbar dispersions, which were evaluated only for the CSS mode.

Evaluation of stability characteristics for this task was based on historical procedures and requirements used since STS-1, with relevant modifications to reflect updated values of aerodynamic coefficient uncertainties and actual flight performance. The requirements waterfall and numerical stability margin requirements are shown in table 6-7.

Table 6-7. Stability Requirements for Forward CG Assessment

STABILITY REQUIREMENTS WATERFALL

TRAJECTORY	DISPERSION	AERO	LEVEL
Nominal	None	Nominal	I
		FAD Unc.	I
		Pre-Op Unc.	II
Nominal	+/- Alpha Disp.	Nominal	I
		FAD Unc.	II
		Pre-Op Unc.	DA
+/- 3 Sigma	None	Nominal	I
		FAD Unc.	II
		Pre-Op Unc.	DA
+/ 6 Sigma (CSS Mode)	None	Nominal	I
		FAD Unc.	II
		Pre-Op Unc.	DA

The Stability levels are defined in the "SDM", Rockwell document SD72-SH-0105, Vol. 1, Book 2, Part 1B, dated 5 December 1980, with some page change updates.

STABILITY LEVELS TABLE

	Gain Margin (dB)	Phase Margin (deg)
Level I	GM >= 6	PM >= 30
Level II	4 <= GM < 6	20 <= PM < 30
Design Assessment	0 <= GM < 4	0 <= PM < 20
Unstable	GM < 0	PM < 0

Aero Uncertainties Reduction: Aileron derivative uncertainties have a major effect on lateral trim capability, affecting both the aileron deflection needed for aerodynamic trim of lateral asymmetries and the elevon deflection needed to null pitch angular acceleration. Sufficient flight data from up-elevon DTO 251 were available to permit refinement of the aileron derivative uncertainties into smaller Mach ranges. Figure 6-17 illustrates the results of this refinement on the rolling moment due to aileron derivative uncertainty for Mach 7.5 to 8.5. Flight-derived uncertainties are now applied for up-elevon deflections to -10 deg, with the uncertainty values ramping to preflight levels at -14 deg. The uncertainties ramp to original OADB96 values for Mach < 7 and Mach > 10.

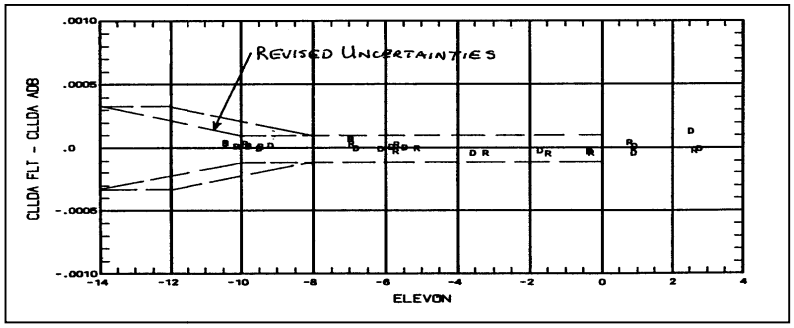

Figure 6-17. Revised Aileron Rolling Moment Derivative Uncertainty

Trim Results: The Honeywell TRIM program served two purposes: 1) to provide initial conditions and aero data for fixed-point stability and response evaluations, and 2) to provide aerosurface deflection and RCS duty cycle data for the fixed-point evaluation cases.

A number of flight cases between Mach 5 and 14 with worst-on-worst combinations of uncertainties and dispersions, including LVARs 10 and 19, exhibited aileron and elevon deflections greater than the ± 5 deg and -16.4 deg limits, respectively. Figure 6-18 illustrates elevon static trim deflections for all fixed-point flight cases and the corresponding up-elevon deflections with aileron trim added. Elevator static trim (average of right and left elevon positions) is between -16.4 deg and -17.3 deg for about 36 cases between Mach 7 and 10, all from the +4-deg alpha or -6-sigma Qbar dispersion sets. However, when aileron trim is taken into account, the right elevon deflection exceeds -16.4 deg for more than 100 cases.

Aileron trim deflections for all fixed-point test cases, and yaw RCS duty cycles for cases with aileron trim greater than 5 deg, are shown in figure 6-19. Nearly 150 cases between Mach 5 and 18 exhibit aileron trim greater than 5 deg. The majority of these cases have LVARs 10 or 19, as well as ABLT, and exceedances occur for the nominal trajectory and all trajectory dispersion sets. Computed yaw RCS duty cycles needed to achieve lateral trim are greater than 50% (2 jets on for 50% of the time) for a number of these cases, and in the Mach 8 region the duty cycle exceeds 100% (2 jets on continuously).

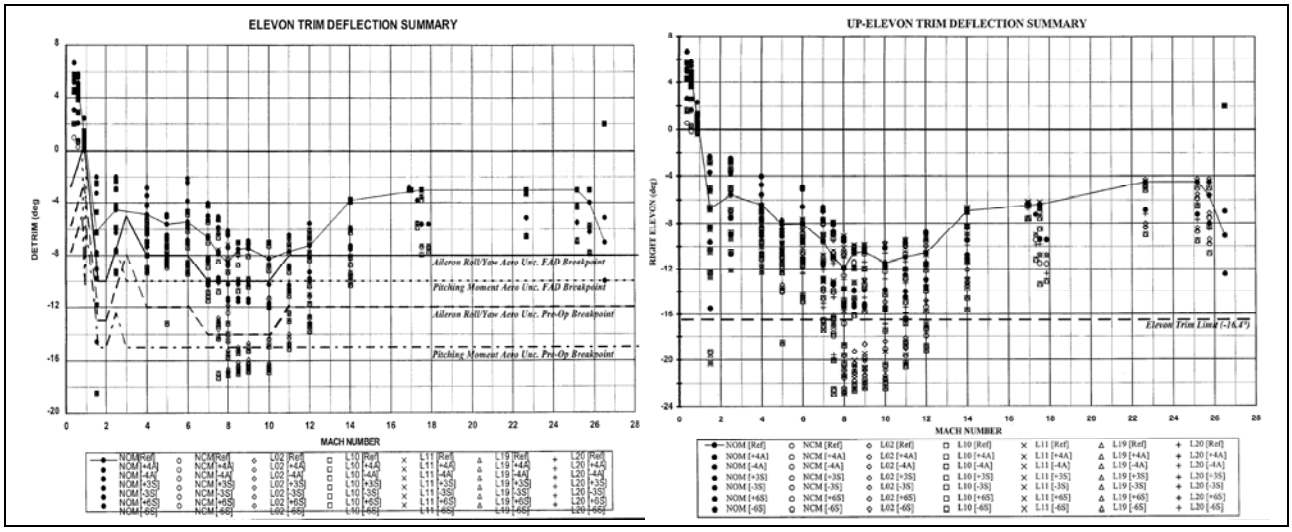

Figure 6-18. Elevon Trim and Up-Elevon for Fixed-Point Cases

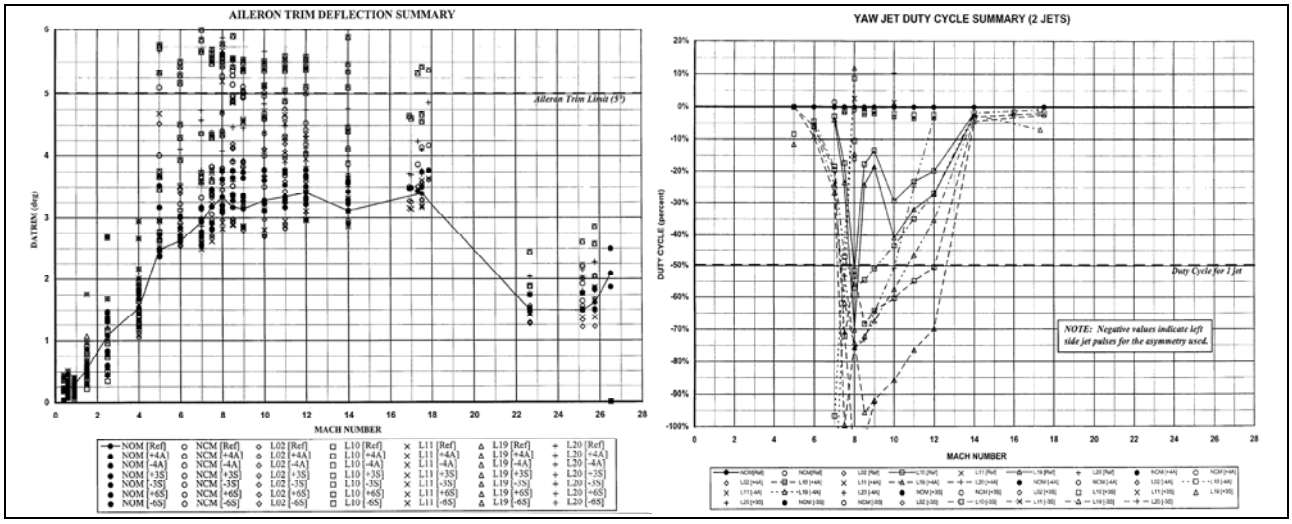

Figure 6-19. Aileron Trim and Yaw RCS Duty Cycle for Fixed-Point Cases

Monte Carlo runs using the BNA SDAP trajectory simulation program were made to evaluate elevon and aileron trim characteristics with statistical application of uncertainties and dispersions. The results, shown in figure 6-20, exhibit 3-sigma maximum up-elevon and aileron deflections of -13 deg and 4.7 deg, respectively, demonstrating compliance with the study ground rules.

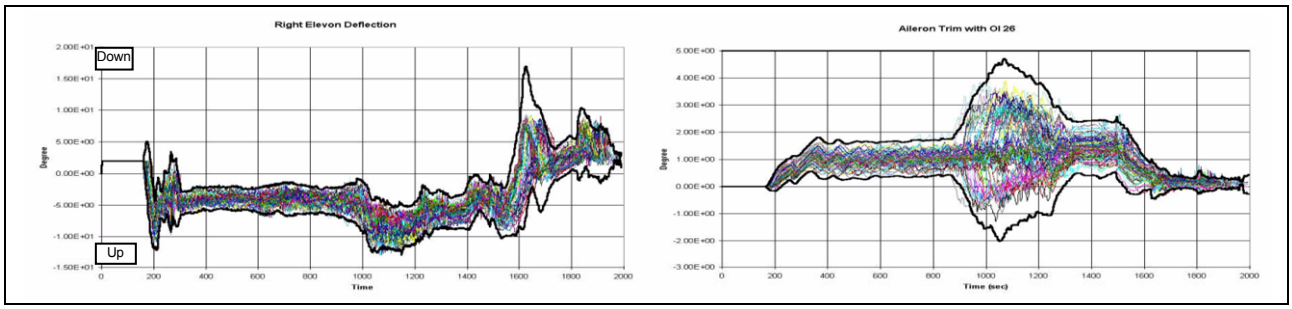

Figure 6-20. SDAP Monte Carlo Results for Right Elevon Deflection and Aileron Trim

Fixed-Point Stability and Response Results Summary: The overall study conclusion, as stated in Reference 6-4 is, "Fixed-point stability and response test results support certification of the wraparound DAP for the entry flight phase (including AOA and TAL) with a design XCG limit of 1,075.2 inches and a YCG limit of ± 1.0 inch when the XCG is forward of 1,076.7 inches."

This conclusion was supported by stability margins showing high compliance with defined requirements, as well as by fixed-point step responses that are consistent with linear stability results and demonstrate adequate performance characteristics for the entry mission. Most cases in both the pitch and roll/yaw axes exhibit Level 1 stability margins even when the requirement is Level 2 or DA. The few cases that failed to meet required stability levels on initial assessment were determined to be acceptable by regression analyses, trajectory simulation, or engineering judgment. Stability results for AOA and TAL were similar to those for NEOM, with no additional problem regions encountered or types of regression analyses required.

Seven cases were linearly unstable with the original uncertainties and dispersions. Of these, one pitch axis case, with PVAR 4, and four roll/yaw axis cases, with LVARs 10, 11, 19, and 20, occurred at Mach 5.0 with negative alpha dispersion. The dispersed alpha value was initially set to 17.0 deg, corresponding to the lower boundary of the SODB alpha envelope, rather than 4.0 deg below the nominal alpha value of 24.27 deg. Increasing alpha to 18.0 deg stabilized the roll/yaw cases, bringing their margins to Level 2 or better. The pitch axis case could be stabilized with DA margins either by increasing alpha to 21.0 deg (3.27-deg α dispersion), or by reducing the pitch uncertainty scale factors 50% and increasing alpha to at least 18.0 deg (6.27-deg α dispersion). The remaining two instabilities occurred for roll/yaw axis cases with LVARs 11 and 20 at Mach 0.4 with alpha dispersed to the SODB envelope upper limit (20.0 vs. 8.878 deg nominal). These were stabilized with DA margins when alpha was reduced to 18 deg.

Regression analyses were also performed for several cases that were stable but failed Level 1 or Level 2 requirements. These included PVAR 4 cases that were brought into compliance with required stability levels when 50% PVAR uncertainties were used, and additional roll/yaw cases with alpha dispersions on the SOD B envelope boundaries, which were improved by reducing the alpha dispersions (which were still at least 4.0 deg). Reducing weight to 233,000 lb or moving XCG aft to 1075.7 inches (nominal forward limit with tolerance) had only minor effect on resolving noncompliant stability margins; therefore, results of these regression tests were not used in final data tabulations.

With regression test results included in the stability margin tabulations, all 1,836 test cases are stable, and only 14 fail to meet stability level requirements defined per the waterfall chart in table 6-7. Six of these have PVAR 1, 3, and 4 uncertainties, and exhibit Level 2 margins of at least 5.5 dB and 24 deg vs. Level 1 requirements. The remaining failures are DA margins of at least 1.32 dB and 10.6 deg for PVAR 4 and LVAR 11 cases vs. Level 2 or (in one case) Level 1 requirements. All of these failures were accepted by the entry community during various meetings and reviews. (If the requirements had been defined per the waterfall developed during the post-*Columbia* recertification effort, the number of failures would be reduced to six.)

Figure 6-21 contains representative pitch axis (elevon loop) stability margin plots from Reference 6-4. Specifically shown are worst-case low-frequency gain margins (LFGMs), which occur for PVAR 4, and high-frequency gain margins (HFGMs), which tend toward minimum values with PVAR 1 (illustrated) and PVAR 3. Some of the PVAR 4 minimum LFGM values between Mach 4 and 8 reflect results of regression tests on cases that were unstable when evaluated along the lower boundary of the SODB alpha envelope. It should be noted that the ± 6-sigma cases were evaluated with the CSS mode,

resulting in generally better gain margins than for 3-sigma and alpha dispersion cases, which were evaluated with the AUTO mode.

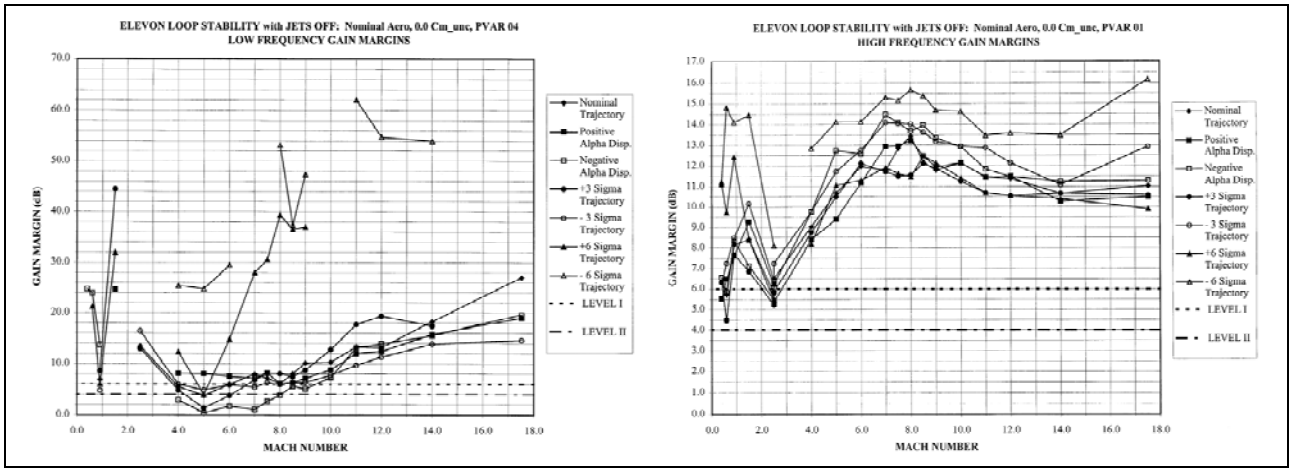

Figure 6-21. Representative Elevon Loop Stability Margins

Representative roll/yaw axis stability plots are shown in figure 6-22 for aileron loop LFGM with LVAR 11 and aileron loop HFGM with LVAR 10. These uncertainty sets exhibit the lowest margins of the sets evaluated. Again, the displayed results reflect the effects of approved regression back-offs for some worst cases. However, the very small LFGM (0.216 dB) shown for LVAR 11 at the Mach 6 negative alpha case is the result for alpha on the SODB envelope lower boundary (dispersed alpha 21.3 deg vs. nominal alpha 29.32 deg), and meets the DA requirement. If alpha is increased to the actual -4 deg dispersion (25.32 deg), the LFGM improves into the Level 2 range.

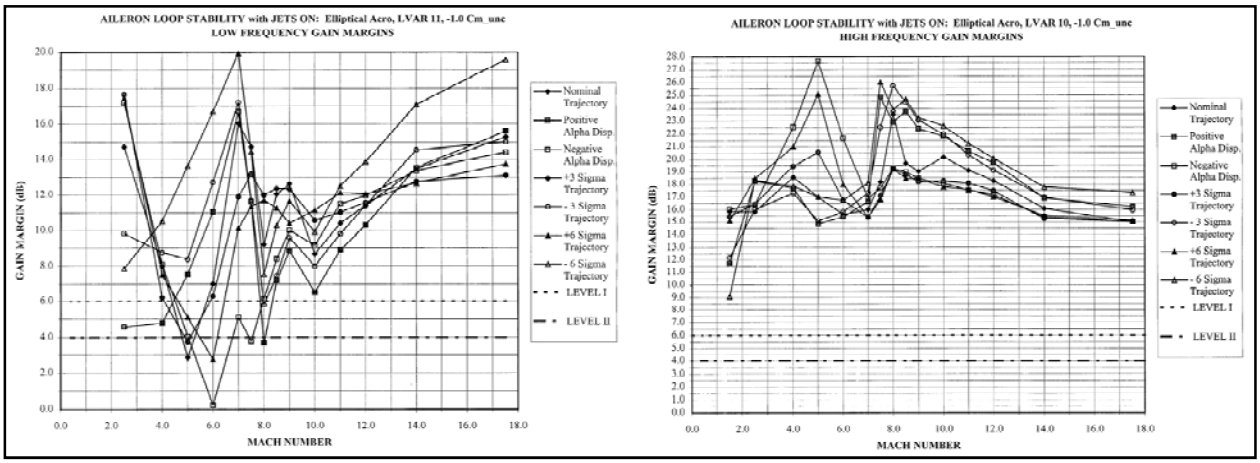

Figure 6-22. Representative Aileron Loop Stability Margins

Figure 6-23 illustrates typical fixed-point nonlinear FCS responses for a 2.0-deg angle-of-attack command and a 30-deg roll angle command. The alpha response remains well within the applicable envelope except for the small acceptable reversal in the first 3 sec. Because of the wraparound DAP reverse aileron control design, however, the roll angle response has significant reversal below the initial slope, and the wide yaw jet control deadbands allow the steady-state value to be about 6 deg below the roll command. These characteristics are consistent with observed flight results for entries flown with the wraparound DAP.

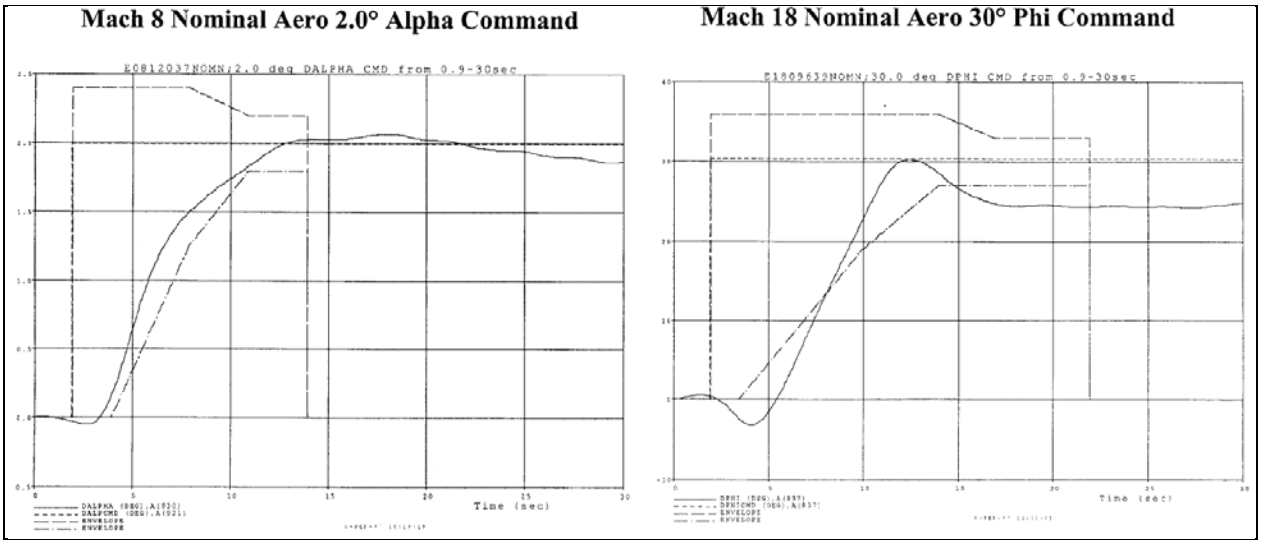

Figure 6-23. Representative Fixed-Flight-Case Step Responses with Nominal Aero

Examples of fixed-flight-case step responses with oscillatory characteristics caused by aero uncertainties are shown in figure 6-24. Because these cases have Level 2 or DA performance requirements, the step response envelopes are provided only for reference; they are not performance specifications. However, the envelopes help demonstrate adequate speed of response, that the responses are in the direction of the commands, and that oscillations converge towards the step command values.

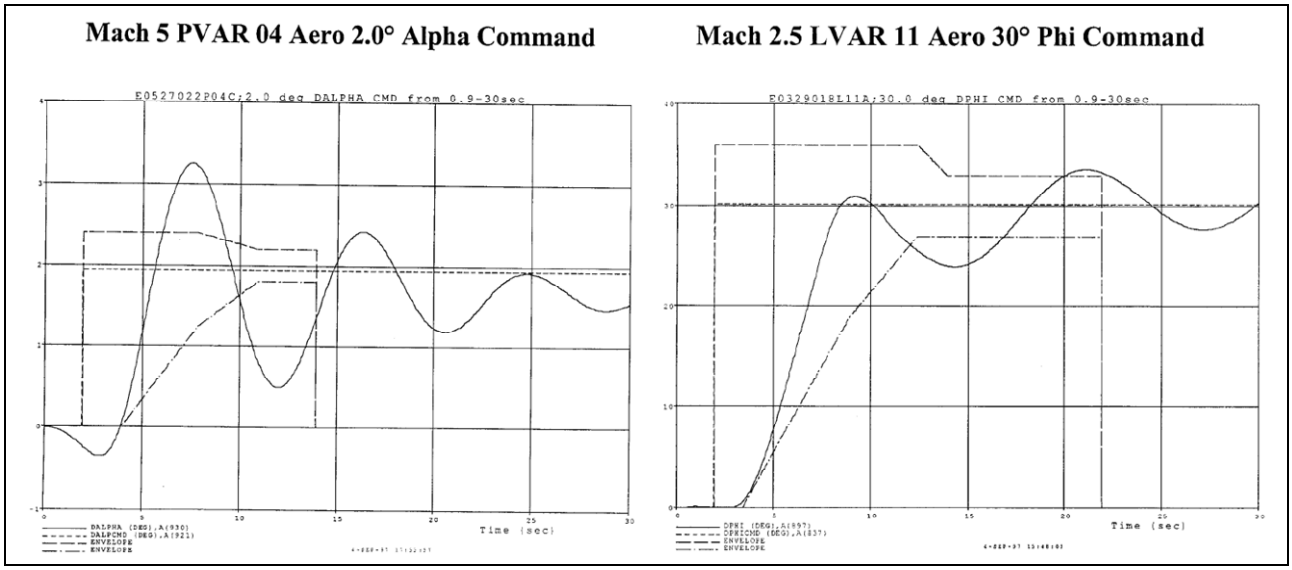

Figure 6-24. Representative Step Responses for Fixed-Flight-Cases with Aero Uncertainties

In keeping with Honeywell's traditional stability evaluation process, open-loop stability margins were obtained for aerosurface paths with RCS paths open—i.e., elevon open-loop margins with pitch jets off for Qbar = 2 to 40 psf, and aileron open-loop margins with yaw jets off for Qbar = 2 psf to Mach 1. These evaluations show FCS stability characteristics for operation within the RCS jet deadbands, where the elevon and aileron loops are linearly unstable for some flight regions and aero data sets. The results are consistent with flight data showing elevon and aileron oscillations between Qbar = 2 and 40 psf as well as with simulation data showing aileron oscillations between Mach 14 and 7 with LVARs 10 and 19. In all flight results and simulation tests, oscillations are bounded and constrained when amplitudes reach RCS jet turn-on levels.

Flexible Body Stability: It was determined that the range of XCG values analyzed during the 1992 flex enveloping effort covered the proposed 1.5-inch forward-XCG expansion; thus no further flex body analysis was required.

Ames VMS Evaluation: Multiple astronaut pilots evaluated landing and rollout performance with expanded XCG in the Ames Vehicle Motion (moving base) Simulator, with no major landing/rollout issues indicated. Landing subsystem performance requirements were met for all cases that had no subsystem failures, and handling qualities ratings were not significantly impacted by the forward XCG. The maximum slapdown rate exceeded SODB limits in some cases with combinations of 248,000-lb vehicle weight, manual derotation (beep trim switch failure), aero uncertainties, winds, and no drag chute; but loads analyses verified that gear loads were not exceeded. Tire failure effects were magnified by the forward CG, but there is no specific applicable requirement. The OCCB and Flight Techniques Panel determined that all observed exceedances were acceptable.

Structural Loads Analysis: Forward XCG flight restrictions, which included modifications to the maximum Nz and maximum main gear sink rate constraints, were developed using the M6.0 Loads Cycle, and were approved by the June 30, 1997, Loads Panel. Descent flight loads were then calculated for steady and abrupt pitch maneuvers, abrupt roll/yaw maneuvers, and lateral gusts at points on the V-N diagram for weights from 187,000 to 256,000 lb with XCG 2 inches forward of the current limit. Landing loads were calculated for main gear impact, nose gear slapdown, taxi, and braking conditions using the same weights and XCG. The analysis results supported 2 inches of forward CG expansion by verifying that positive margins were maintained for all critical loads and that fuselage down-bending moments remained within prescribed limits.

Thermal Analysis: Certified aerodynamic heating thermal limits for trajectory design are defined in Vol. V of the SODB. Trajectory evaluations using MOD's Thermal/Structural Envelope Program (TSEP) demonstrated that entry trajectories that are on the boundary of thermal envelope limits with the proposed forward XCG could be developed. Detailed analysis of trajectories with the most forward XCG determined that thermal performance was acceptable, thus supporting the proposed 1.5-inch forward XCG expansion.

6.6 RCS Redline Reduction

The following paragraphs are based on information contained in three presentations on the wraparound DAP RCS by B. Bihari of Lockheed-Martin (References 6-8, 6-9, and 6-10).

Because the Orbiter relies on RCS jets for control and stabilization during most of the entry phase of the mission, it is imperative that adequate RCS propellant is available at the beginning of entry to meet FCS needs until Mach 1. For early flights, this "redline" quantity was based on mission-specific trajectory simulations run with the full gamut of dispersions and uncertainties. It was initially set at 2,200 lb to cover effects of the large aerodynamic variations. Section 3.2.9, paragraph "RCS Redlines," discusses data and procedures that allowed redline reduction to 1,100 and 1,300 lb for entries from low inclination (<30 deg) and high-inclination (>30 deg) orbits, respectively, starting with STS-34. Since most flights used between 600 and 900 lb, unless responses to flight DTO PTIs consumed more, these redline values were considered to provide adequate margins of safety. However, STS-57 (a low-inclination flight) used approximately 1,430 lb of propellant during entry, 330 lb more than the redline value. Density shears were the major contributor to this increase, causing excessive roll command activity. Previously, STS-50 had used approximately 1,300 lb of propellant because of lateral trim changes induced by ABLT in addition to density shears. Figure 6-25 shows how RCS propellant usage for these two flights compares with that of other low-inclination flights through STS-69. As a result of these instances of high propellant use, the redline values were increased by 330 lb—to 1,430 and 1,630 lb, respectively—for low- and high-inclination orbits.

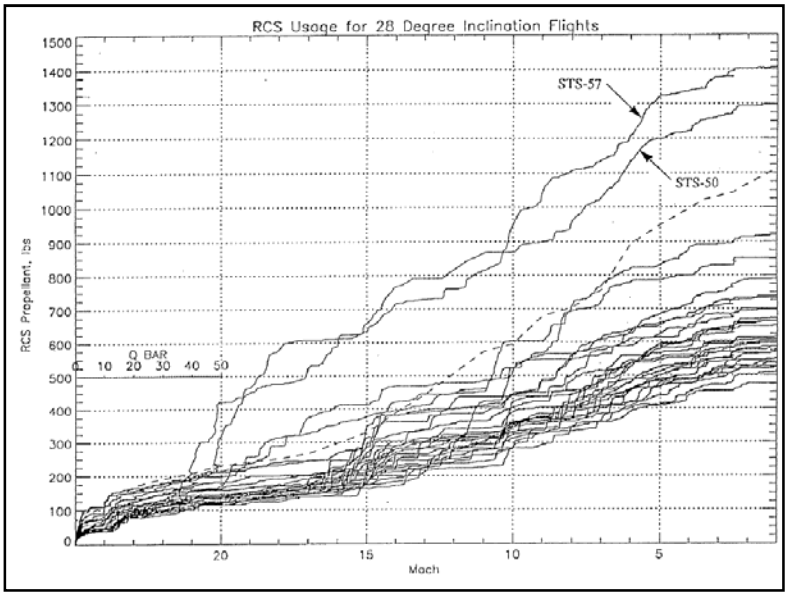

Figure 6-25. Entry RCS Propellant Usage for Low-Inclination Missions

As the wraparound DAP became operational following STS-94, there was again the opportunity and impetus to reduce the RCS redlines. Actual RCS propellant consumption from entry interface (EI) to Mach 1 averaged 349 lb for the first five missions employing wraparound DAP for the full entry phase, compared with 670 lb average for all previous flights using the baseline DAP. (PTI effects are excluded from these averages.) A valid statistical basis for reducing the redline was obtained through a combination of 1) deterministic trajectory runs using reconstructions of 88 entry missions, 2) Monte Carlo trajectory runs using worst-case mass properties for propellant usage as defined by MOD together with 86 reconstructed atmospheres from the deterministic runs. All tests were run on both the SDAP and SES, and with both the baseline and wraparound DAPs. Additional Monte Carlo runs were made on the SES using GRAM 95 and GRAM 97 atmospheres instead of the reconstructed flight atmospheres. Since previous studies had shown correlation between XCG and propellant consumption, these Monte Carlo cases were run with XCG 1,109.0 and 1,095.0 inches.

Figure 6-26 presents a comparison of wraparound DAP vs. baseline DAP RCS propellant consumption for the 88 deterministic cases. The SDAP values tend to be slightly greater than SES values, although baseline DAP values for both simulations are generally close to those for actual flight. Notable exceptions occur for STS-50 and STS-57, where values for the baseline DAP reconstructions are considerably less than the actual flight values. Overall, wraparound DAP propellant consumption is shown to be between ⅓ and ⅔ that of the baseline DAP.

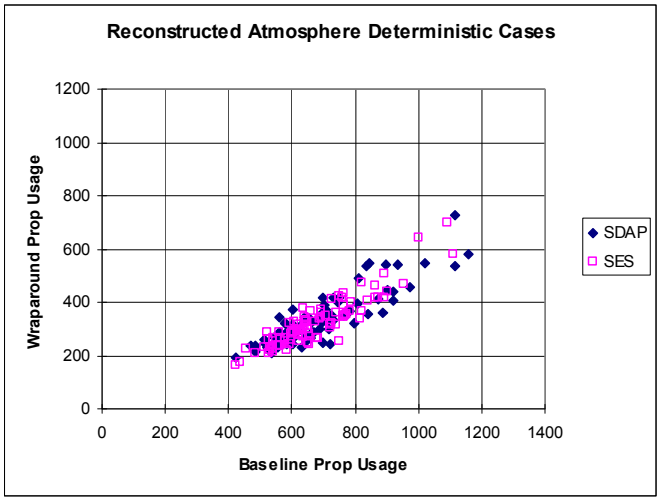

Figure 6-26. Comparison of Wraparound DAP and Baseline DAP RCS Propellant Consumption

Early in this effort, a redline reduction of 255 lb was proposed based on the available statistical results—i.e., to redline values of 1,175 and 1,375 lb, respectively—for the low- and high-inclination orbits. Subsequent analyses showed that there was very little correlation between RCS propellant usage and orbit inclination, as shown in the left plot of figure 6-27, which compares statistical RCS propellant estimates for SDAP and SES Monte Carlo cases with low- and high-orbit inclinations. However, significant correlation with XCG was observed, as illustrated in the right plot of figure 6-27, which shows that propellant consumption increased considerably as the CG location moved from full forward to full aft. (Points in these plots are the Weissman estimates, as described below, of propellant usage for each Monte Carlo set using the wraparound DAP.) Propellant usage sensitivities to Orbiter weight, orbit apogee, and ABLT were also evaluated, and found to be statistically insignificant. Therefore, the proposed redlines were changed to 1,175 lb for XCG <1,095 inches, and 1,375 lb for XCG > 1,095 inches.

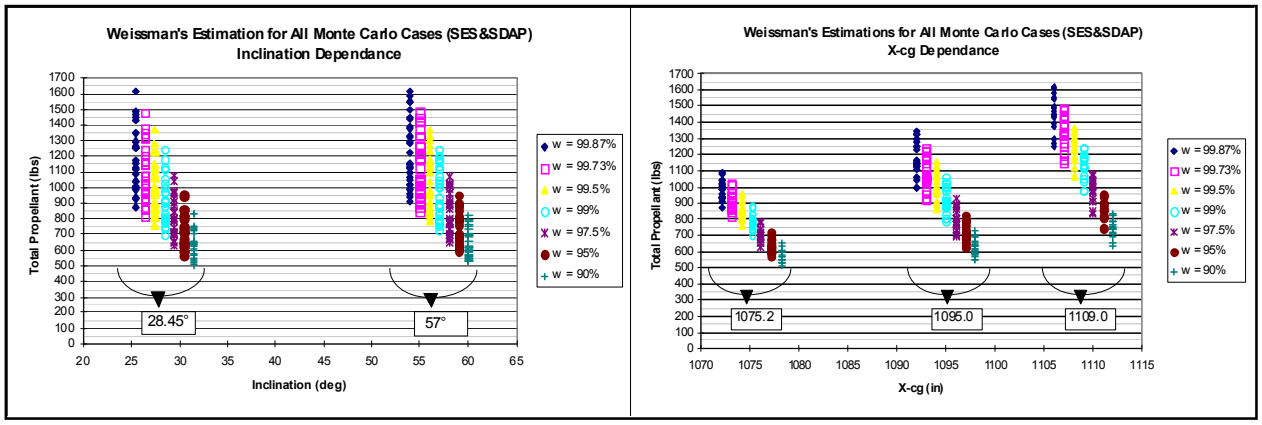

Figure 6-27. Effect of Orbit Inclination and Orbiter XCG on RCS Usage

A major factor that had to be considered in the statistical analysis is that RCS propellant is not normally distributed, but instead has significant high-consumption "outliers," or one-sided tails. This is illustrated in the histograms of figure 6-28, which show the old and new redlines applied to the baseline DAP and wraparound DAP distributions, respectively, for Monte Carlo cases with aft CG and the SES GRAM 97 atmosphere.

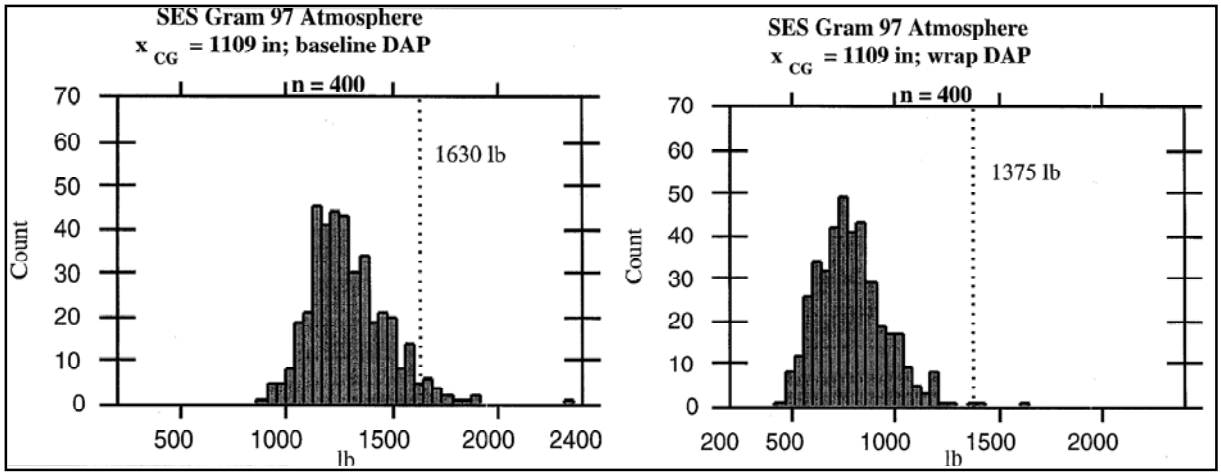

Figure 6-28. Representative RCS Propellant Distributions from Monte Carlo Runs

Since the distributions have large outliers, the conventional method of using the mean-plus-3-sigma value to determine the 99.87% protection level is not applicable. A statistical tool known as the Weissman Estimator was employed to account for the outliers by using order statistics methodology to compute RCS propellant values that provide the desired protection level with 95% certainty. Table 6-8 lists representative Monte Carlo statistics, and specific data for the SES cases are illustrated in figure 6-28. It can be seen from the figures that the GRAM 97 mean + 3σ values of 1,853 lb for baseline and 1,296 for wraparound miss several of the high propellant outliers. While the 99.87% protection Weissman values exclude only one case for each DAP, they do not represent any reduction in redlines. Table 6-9 shows how changing

the protection level affects the Weissman estimate for the same cases shown in table 6-8. With 99.5% protection, the Weissman value of 1,396 lb for wraparound DAP with XCG = 1,109 and GRAM 97 is only slightly larger than that of the proposed redline (1,375 lb), although the baseline DAP value of 1,947 lb is significantly higher than that of the old redline (1,630 lb).

Table 6-8. SES Monte Carlo Statistics for EI to Mach 1 with XCG 1,109 and GRAM Atmospheres

	GRAM95 Base	GRAM95 Wrap	GRAM97 Base	GRAM97 Wrap
Min	833	428	878	452
Max	2,287	1,679	2,341	1,610
Average	1,401	859	1,293	786
Stdevp	249	219	186	170
Mean + 3s	2,147	1,517	1,853	1,296
weisman	2,381	1,812	2,133	1,573

Table 6-9. Effect of Protection Percentile on Weissman Estimate

1109cg	GRAM95 Base	GRAM95 Wrap	GRAM97 Base	GRAM97 Wrap
-3sig 99.87	**2381**	**1812**	**2133**	**1573**
99.73	2271	1701	2032	1477
99.5	2178	1607	1947	1396
99	2074	1502	1852	1305
-2sig 97.5	1936	1362	1726	1185
95	1831	1257	1630	1094
90	1727	1151	1535	1003

Another factor considered during the RCS redline reduction task is that flight rules require a minimum of 880 lb of RCS propellant in the tanks until Nz exceeds 0.05g. This typically occurs about 4 to 5 minutes after EI, before the first roll maneuver (which is triggered when total load factor reaches 0.12g). Monte Carlo run data for the EI to 0.05g trajectory segment provided a maximum 3-sigma level Weissman propellant usage estimate of 193 lb. Thus any of the proposed redline values at EI will ensure more than 880 lb of propellant remaining at Nz 0.05g.

Because Monte Carlo results show that the 99.5% Weissman estimates are exceeded for a small number of cases, there is a remote possibility of RCS propellant being exhausted before Mach 1. A short study was made using the SES forward cockpit to evaluate crew control capability for 17 outlier cases using the no-yaw-jet downmode system. The four participating pilots used consistent control techniques to fly no-yaw-jet, and gave the handling qualities Level II ratings (Cooper-Harper values of 4 to 6, improving as Mach decreased). No cases experienced loss of control, and all runs made the runway or were terminated when control was no longer an issue.

The proposed RCS redlines for the wraparound DAP, 1,175 lb for XCG <1,095 inches, and 1,375 lb for XCG > 1,095 inches, were approved at the Ascent/Entry Flight Techniques Panel No. 150 in June 1998. In wraparound DAP flights to date, RCS propellant usage has been far below these numbers. For the first 38 flights (STS-94 through STS-124), the average RCS propellant consumption was 322 lb, with a maximum of 497 lb and a minimum of 235 lb. Figure 6-29 shows the RCS propellant used for each wraparound DAP entry and a histogram of the propellant distribution.

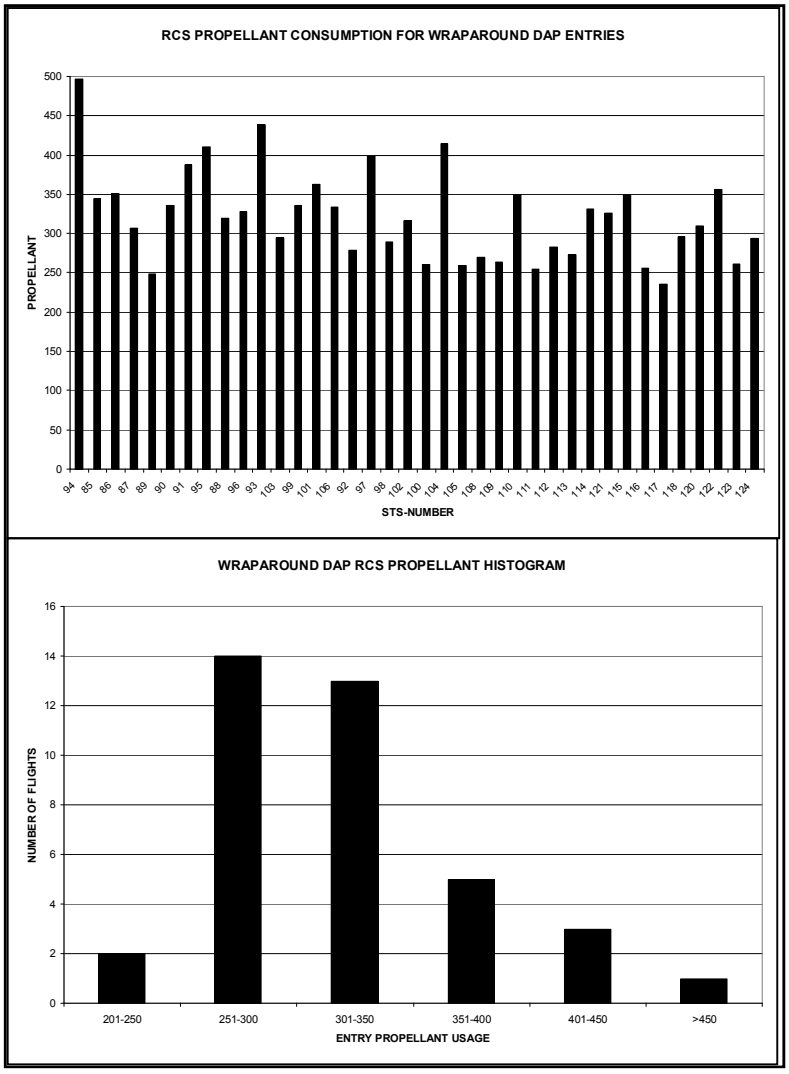

Figure 6-29. Wraparound DAP RCS Propellant Usage History

6.7 Miscellaneous Studies and Updates

Electric Auxiliary Power Unit Upgrade: The electric APU system was designed to replace the Orbiter's existing hydrazine-powered APUs with battery-powered systems. The electric APU would have consisted of a battery, a 270-volt power distribution and control system, an electrohydraulic drive unit, and a cooling system. The electrical system was intended to meet all of the existing performance requirements of the hydrazine system while avoiding the use of highly toxic hydrazine and high-speed machinery. The electric APU would have theoretically provided a 15% reduction in mission risk.

Despite the significant risk reduction that would have been afforded by this upgrade, the system was not technically feasible at the time. Due to these technical and associated budget issues, the upgrade was deferred in June 2001.

Single APU Studies and PRL Updates: In April 1998, studies were conducted in the Ames VMS to support the electric APU upgrades. During these studies, serious flaws were discovered in the current PRL software for the existing hydraulic APUs. Specifically, during single-APU operation, the software would consistently allow APU over-demands in excess of 20 gpm during certain flight phases. Severe hydraulic pressure drops and probable loss of vehicle control were expected under these circumstances. Over-demands would mostly occur post-WOW, but some problems were also noted during gear deploy. The primary causes of the over-demands were a sluggish speedbrake, a lack of accounting of postlanding flow demands, and an underestimation of in-air landing gear deploy flow.

While there is always some lag between the speedbrake command and position even under three-APU operation, speedbrake responsiveness was significantly reduced under single-APU operation, which became an issue. In this condition, when the PRL commanded a given rate, the speedbrake took 1 to 2 sec to achieve the rate, resulting in a delta between the commanded and actual positions. The delta caused the speedbrake to continue moving for 1 to 2 sec after the software command stopped in order to catch up. Because the PRL is not a feedback system, it does not take into account the extra 18 gpm required to drive the speedbrake in this 1- to 2-sec period. The speedbrake lag was further exacerbated by the fact that the speedbrake could not always achieve the drive rate commanded by the PRL when only one APU was operating. The PRL would drive the speedbrake at the same rate regardless of the number of systems operating. It should be noted that other aerosurfaces also experience lag under single-APU operation, but to a much smaller degree—on the order of 0.3 sec or less.

Several demands on the hydraulic system during landing and rollout were not being taken into account, including post-weight-on-nose-gear (WONG) leakage, nosewheel steering flow, and brake flow. These factors amounted to about 6 gpm of demand on the hydraulic system. These demands, coupled with active aerosurfaces and a sluggish opening speedbrake, would frequently cause over-demands in single-APU operation. While less common, an over-demand situation was also possible during gear deploy with a single APU, provided the speedbrake was moving and the vehicle was encountering a sufficiently dynamic situation to significantly drive the elevons and rudder.

In response to these issues, the following changes were made to the PRL for OI-29 in PASS SCR 92384 and BFS SCR 92422.

1) Gear deploy hydraulic flow was increased from 6.64 gpm to 12.75 gpm
2) Flows were added to account for
   a) Post-WONG leakage (2.93 gpm)
   b) Nosewheel steering flow (1.50 gpm)
   c) Brake flow (1.60 gpm)
3) Post-WONG elevator and aileron surface drive rate limits were reduced from 13.9 deg/sec to 10.5 deg/sec
4) New speedbrake drive rate I-loads were created for single-APU operation (5.43 deg/sec open and 6.06 deg/sec close)

Table 6-10 presents the revised aerosurface drive rate limits.

Table 6-10. Updated Aerosurface Drive Rate Limits

Aerosurface	Drive Rate (deg/sec)			
	3 APUs	2 APUs	1 APU	1 APU post-GSENBL
Elevator	20	20	13.9	10.5
Aileron	20	20	13.9	10.5
Rudder	14	12	7	7
Rudder (sumlim)	5.43	5.43	1.9	1.9
Speedbrake close	10.86	10.86	6.06	6.06
Speedbrake open	6.1	6.1	5.43	5.43

The increase in gear deploy flow is now in line with flight experience. In flight, the gear typically takes 5.6 sec to deploy. Because a fixed quantity of fluid is required for gear deploy, the flow rate during gear deploy is dependent on the speed of deployment. The original flow rate value of 6.64 gpm was believed to be based on a spec-gear-deploy time of 10 sec. Because the actual gear deploy time is less, the flow demanded will be greater during that time.

The addition of the post-WONG, nosewheel steering, and brake terms account for terms that were either overlooked or did not exist when the PRL software was written.

The reduction of post-WONG elevator and aileron surface drive rates serves to reduce elevon demand and reserve greater flow for rudder activity. The rudder is extremely important for control authority during rollout because nosewheel steering may not be available with a single APU, depending on which APU systems have failed. This reduction was found to have a slightly negative but acceptable increase in tire and nose gear landing loads. Table 6-11 shows the effects of specific APU failures on nosewheel steering and braking capability.

Table 6-11. Effects of Specific APU Failures

APU Status			NWS	% Braking	Pre-Deorbit No NWS Brake Energy Limit (million ft-lb)	Crosswind Limit (ft/sec)
1	2	3				
OK	OK	OK	YES	100	70	12, 15, or 17
OK	OK	FAIL	YES	100	70	**10**
OK	FAIL	OK	YES	100	70	**10**
FAIL	OK	OK	YES	100	70	**10**
OK	FAIL	FAIL	YES	**50**	70	**10**
FAIL	OK	FAIL	YES	**50**	70	**10**
FAIL	FAIL	OK	**NO**	100	**42**	**10**
FAIL	FAIL	FAIL	**NO**	**0**	**N/A**	**N/A**

The primary reason for reducing the speedbrake drive rate was to protect the hardware. Creation of new speedbrake drive rate I-loads was driven by competing factors: providing reasonable hardware protection and ensuring acceptable landing energy conditions.

An additional change for OI-29 was evaluated to reduce flow demands between WOW and WONG. A 2.93-gpm leakage term and a reduction in aileron and elevon rates from 13.9 to 10.5 deg/sec was proposed, but the changes were ultimately dropped because they aggravated an undesirable bounce/oscillation condition at WOW. It was determined that it was safer to risk some over-demand between WOW and WONG rather than to adversely impact handling.

The single-APU studies also had an impact on crew training and procedures. Commanders are told to expect a lag in control response based on lower surface rates in single-APU operation. They are also instructed to not cross-couple inputs (making adjustments in both roll and pitch simultaneously) and to accept small misalignments. At 3,000 ft, the speedbrake is to be set manually in a position determined by the Flight Dynamics Officer (FDO), and the crew is instructed to leave it in that position until wheel stop. Overall, in single-APU operation, the crew is instructed to fly normally with smooth inputs.

7.0 Post-*Columbia* (STS-107) Recertification

After the STS-107 *Columbia* tragedy on February 1, 2003, several ensuing activities culminated in the complete recertification of descent flight control performance and flight envelopes for International Space Station (ISS) missions. These activities, described in the following sections, included 1) reconstruction of the STS-107 entry trajectory and FCS performance, 2) an attempt to certify expanded GRTLS envelopes, 3) a technical interchange meeting (TIM) called to resolve questions on flight control stability requirements and analysis procedures, 4) creation of a new entry flight control requirements document, 5) flight-specific FCS certification for the first few post-*Columbia* missions, and 6) generic FCS certification covering all remaining ISS flights. Because of its lower orbit inclination, flight-specific certification was planned for the Hubble Space Telescope repair mission, STS-125.

7.1 Columbia *Accident Investigation*

The following paragraphs, quoted from Reference 7-1, summarize the entry flight control community's contributions to the *Columbia* accident investigation.

> The Integrated Entry Environment (IEE) Team was created in support of the STS-107 Orbiter Vehicle Engineering (OVE) investigation effort. The primary team objectives were to evaluate the preflight and real-time entry design and verification processes to ensure they were adequate and properly executed, examine flight data for any indications of off-nominal vehicle performance and perform the analysis necessary to identify the potential causes for any such observed flight performance. The scope of these efforts was limited to the Guidance, Navigation and Control (GN&C) systems, Flight Control effectors and the aerodynamic analysis required to accomplish the objectives.
>
> A review of the preflight and real-time design and verification processes used on STS-107 did not reveal any discrepancies. The preflight entry design was correct for the mission conditions. All ground and onboard actions performed on the day of entry were appropriate and did not contribute to the loss of the vehicle and crew. Furthermore, there

were no non-standard crew actions that had any appreciable effect on vehicle performance.

The GN&C systems, including control effectors, performed nominally during the STS-107 entry. Flight control responded properly to all commands and was operating within limits until loss of signal (LOS) plus five seconds (GMT 13:59:37). The first off-nominal signature observable in the telemetry data occurred at approximately GMT 13:53:38, or 569 sec after Entry Interface (EI). It was at this point that the inertial sideslip angle exceeded previous flight experience. Shortly after, at GMT 13:54:20 (EI + 611 sec), the aileron required to trim the vehicle began to diverge from the expected value based on preflight predictions. The Flight Control system was approaching lateral trim saturation at LOS + 5 sec. Analysis of reconstructed telemetry data from approximately 26 sec later in the flight indicates that the vehicle was in an uncommanded attitude and was experiencing uncontrolled rates.

Identification of possible vehicle aerodynamic configuration changes that could explain the above performance was accomplished via detailed reconstructions of the entry trajectory. These reconstructions required accounting for all known conditions such as environmental factors and expected nominal performance, then deriving the off-nominal vehicle aerodynamics required to produce an acceptable match with flight data. The result was a set of aerodynamic force and moment increments that were then used to evaluate the reasonableness of results from wind tunnel and computational fluid dynamics analyses performed on various vehicle configuration changes (reference Aero/Thermal team report). This analysis suggests that the effect of any vehicle damage on the overall vehicle aerodynamics was small until very late in flight. In addition, three distinct aerodynamic configuration changes can be identified that correlate well with the observed GN&C response from telemetry. While the uncertainties on the off-nominal aerodynamics are large, the team is confident that the final increments can be used to identify significant changes in the vehicle aerodynamic configuration that occurred during the entry.

The IEE team has concluded that the GN&C and Flight Control Hardware subsystems performed as designed during the STS-107 Entry, and that the current subsystem designs are adequate. There are no recommended changes to these subsystems required for Return-To-Flight.

7.2 GRTLS Envelope Expansion

In January 1996, the RSOC Descent Flight Design Group gave a presentation to the entry FCS community that requested expansion of the certified GN&C and structural GRTLS dynamic pressure envelopes (Reference 7-2). The current SODB envelope, shown previously in figure 6-4, was defined in 1993 based on results of the descent abort heavyweight verification task. However, many subsequent missions had lighter weight, higher ET-SEP velocity, and lower ET-SEP Qbar, all of which resulted in violations of this envelope during Monte Carlo evaluations. The requested envelope expansion was designed to encompass these violations and thus eliminate the need for flight-specific assessments to clear them.

Because of higher-priority tasks and reduced budgets, no significant progress was made toward certifying expanded GRTLS envelopes until a new request was approved in June 2002 and given authorization to proceed in October of the same year (Reference 7-3). In addition to flight control, the expansion effort was to include loads, stress, and aerothermal analyses to confirm that the expanded envelopes were within current hardware certification constraints. Figure 7-1 compares the proposed envelopes used for this study with the 1993 certified envelopes. The most significant difference in the two is along the right-hand Qbar boundary, which provides coverage for ramp-up Qbar values at the higher velocities resulting from lighter-weight Orbiters.

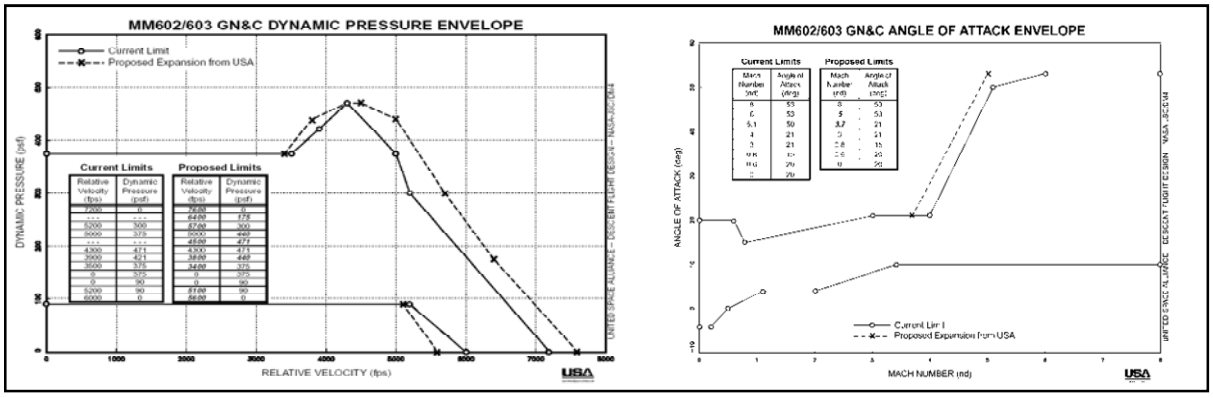

Figure 7-1. Proposed GRTLS Qbar and Alpha Envelopes

Sixteen flight cases along the Qbar vs. Vrel boundaries, each with two values of alpha, were defined by USA. Because no single trajectory or Monte Carlo run will encompass all boundary points, these cases were based on data for five trajectory profiles: lightweight (Lwt), heavyweight (Hwt), heavyweight fast (HwtFast), heavyweight slow on top boundary (HwtSlowTop), and heavyweight slow on bottom boundary (HwtSlowBtm). All 32 cases were evaluated for two sets of mass properties: heavyweight with forward CG, and lightweight with aft CG. Basic flight case parameters and mass properties are listed in tables 7-1 and 7-2, respectively. Figure 7-2 shows the locations of these cases on the Qbar vs. Vrel envelope boundaries.

Table 7-1. GRTLS Envelope Expansion Test Cases

Flight case number	Velr	qbar	alphalo	alphahi	IPHASE
qbarLwt01	7400	42	50.10	51.10	6
qbarLwt02	7000	92	49.50	50.02	6
qbarLwt03	6700	130	40.60	43.00	5
qbarLwt04	5700	300	21.80	24.00	5
qbarLwt05	5500	340	21.10	21.10	4
qbarHwtFast01	5400	360	21.60	23.20	5
qbarHwtFast02	5100	420	19.60	21.32	5
qbarHwtFast03	5000	440	18.89	20.53	5
qbarHwtFast04	4700	459	13.40	17.60	4
qbarHwt01	4500	471	17.30	18.75	5
qbarHwt02	4300	471	13.30	17.50	4
qbarHwtSlowTop01	4000	452	16.64	18.39	5
qbarHwtSlowTop02	3800	440	12.10	17.20	4
qbarHwtSlowTop03	3400	375	14.89	15.16	4
qbarHwtSlowBtm01	5500	42	49.78	50.29	6
qbarHwtSlowBtm02	5100	90	49.42	50.70	5

Table 7-2. GRTLS Envelope Expansion Mass Properties

	HU - Heavy Wt	LU - Light Wt
Weight	248000.0	195000.0
X-cg	1074.2	1110.0
Y-cg	-1.5	-1.5
Z-cg	372.4	360.0
Ixx	964253.0	888077.8
Iyy	7319980.0	6684037.1
Izz	7605583.0	6975688.1
Ixz	176349.0	167081.9

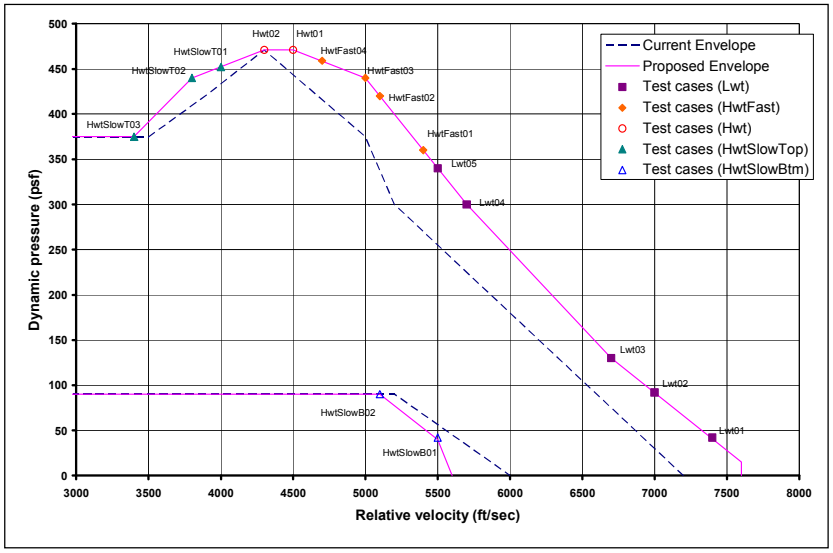

Figure 7-2. GRTLS Envelope Expansion Flight Cases

FCS performance was evaluated using the stability requirements waterfall and numerical stability margin requirements shown previously in table 6-7. Detailed results are presented in Reference 7-4. Using the traditional worst-on-worst combinations and pass-fail criteria used in previous certification and validation efforts, stability margins along the expansion boundaries were found to be generally not acceptable. In the pitch axis, seven flight cases (Vrel-Qbar points) are unstable for at least one combination of mass properties, alpha, and aero uncertainties. The corresponding number for the lateral axis is nine cases. With nominal aero, all lateral axis cases exhibit Level 1 stability for every combination of mass properties and alpha. However, the pitch axis shows Level 1 stability for only six nominal aero cases, and one nominal aero case is unstable. Table 7-3 summarizes the worst-case stability levels, and figure 7-3 illustrates these results graphically.

Table 7-3. Stability Level Summary for GRTLS Expansion Cases

Worst result at each flight case

Flight case number	PIT-NOM	PVARS	LAT-NOM	LVARS
qbarLwt01	DA	Unstable	Level 1	Unstable
qbarLwt02	Level 1	Unstable	Level 1	Unstable
qbarLwt03	Level 2	DA	Level 1	Unstable
qbarLwt04	Level 1	DA	Level 1	DA
qbarLwt05	Level 1	DA	Level 1	DA
qbarHwtFast01	Level 1	Level 2	Level 1	DA
qbarHwtFast02	Level 2	DA	Level 1	DA
qbarHwtFast03	Level 2	DA	Level 1	Unstable
qbarHwtFast04	Level 2	Unstable	Level 1	Unstable
qbarHwt01	DA	DA	Level 1	Unstable
qbarHwt02	Level 2	Unstable	Level 1	Unstable
qbarHwtSlowTop01	Level 2	DA	Level 1	DA
qbarHwtSlowTop02	Level 1	Unstable	Level 1	DA
qbarHwtSlowTop03	Level 1	Level 2	Level 1	Level 1
qbarHwtSlowBtm01	Unstable	Unstable	Level 1	Unstable
qbarHwtSlowBtm02	DA	Unstable	Level 1	Unstable

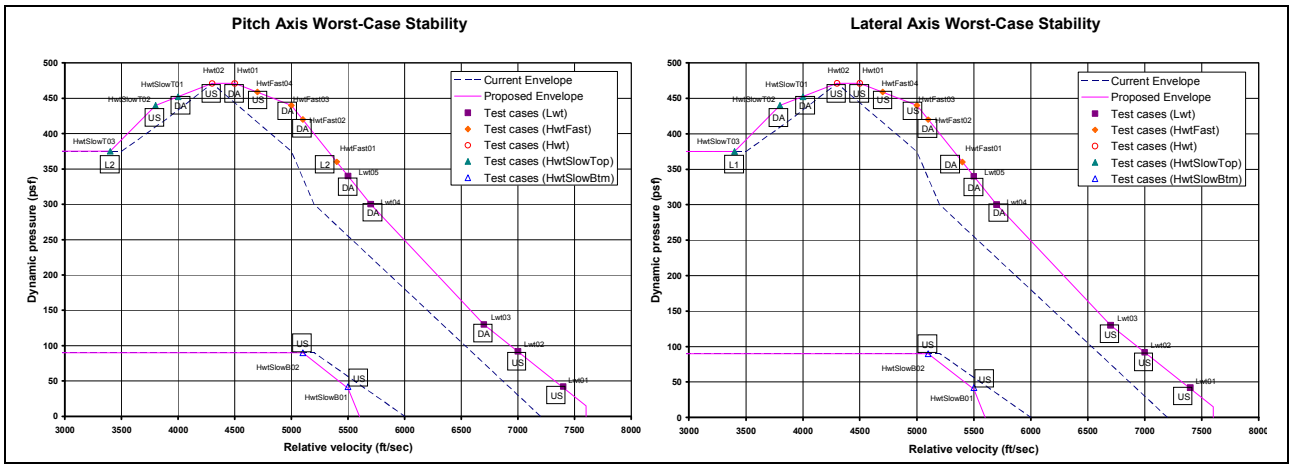

Figure 7-3. Worst-Case Stability on GRTLS Expanded Envelope Boundaries

Several factors contributed to these poor stability results:

1) Elevon deflections approach and exceed 20 deg up for HwtSlowBtm cases and the fastest Lwt cases. This reduces nominal values of elevon and aileron moment derivatives and drives pitching moment and aileron derivative uncertainties to the large pre-op values. Limiting up-elevon to 20 or even 25 deg, however, would preclude consideration of some envelope expansion.
2) Angle of attack for the same flight cases exceeds the flight test DTO experience range, driving elevon and aileron derivative uncertainties to the large pre-op values. Even without expansion, however, the large alpha values in early GRTLS require use of the pre-op uncertainties.
3) Stability for all test cases was evaluated with both sets of mass properties specified in table 7-2. Thus an XCG of 1,074.2 was always used as forward CG, whereas a more reasonable value above Mach 3.5 would be 1,078.0. Also, flight cases derived from lightweight trajectory profiles were evaluated with heavyweight mass properties, which might be considered inappropriate.

While these results obviously raised questions about the feasibility of certifying the desired GRTLS envelope expansion, particular concerns arose because two of the points exhibiting instabilities (Hwt02 and HwtSlowBtm02) are on the SODB envelope boundaries certified by the 1993 heavyweight verification task (see Section 6.3 above). In addition, several other failed points are on or within the trajectory envelopes evaluated during the 1993 task. The heavyweight verification reports (References 6-1 and 6-2) show that several cases were unstable or otherwise failed stability level requirements. These were all declared acceptable based on stability margins with approved regression from worst-on-worst conditions, or on nonlinear time-domain simulation results that demonstrated acceptable trajectory performance. Although it is likely that these dispositions were reviewed with the GN&C community, the simulation test procedures and results are not documented in the verification reports.

Figure 7-4 shows the 1993 verification flight cases along with the certified and proposed GRTLS Qbar envelopes. This figure also indicates which flight cases exhibited worst-case stability characteristics when rerun using 2004 aerodynamics and tools. As a result of the apparent violations of standard stability certification requirements identified during this effort and the lack of adequate disposition documentation in the 1993 verification, the task direction was changed from certifying expanded GRTLS envelopes to confirming the validity of the current SODB envelopes.

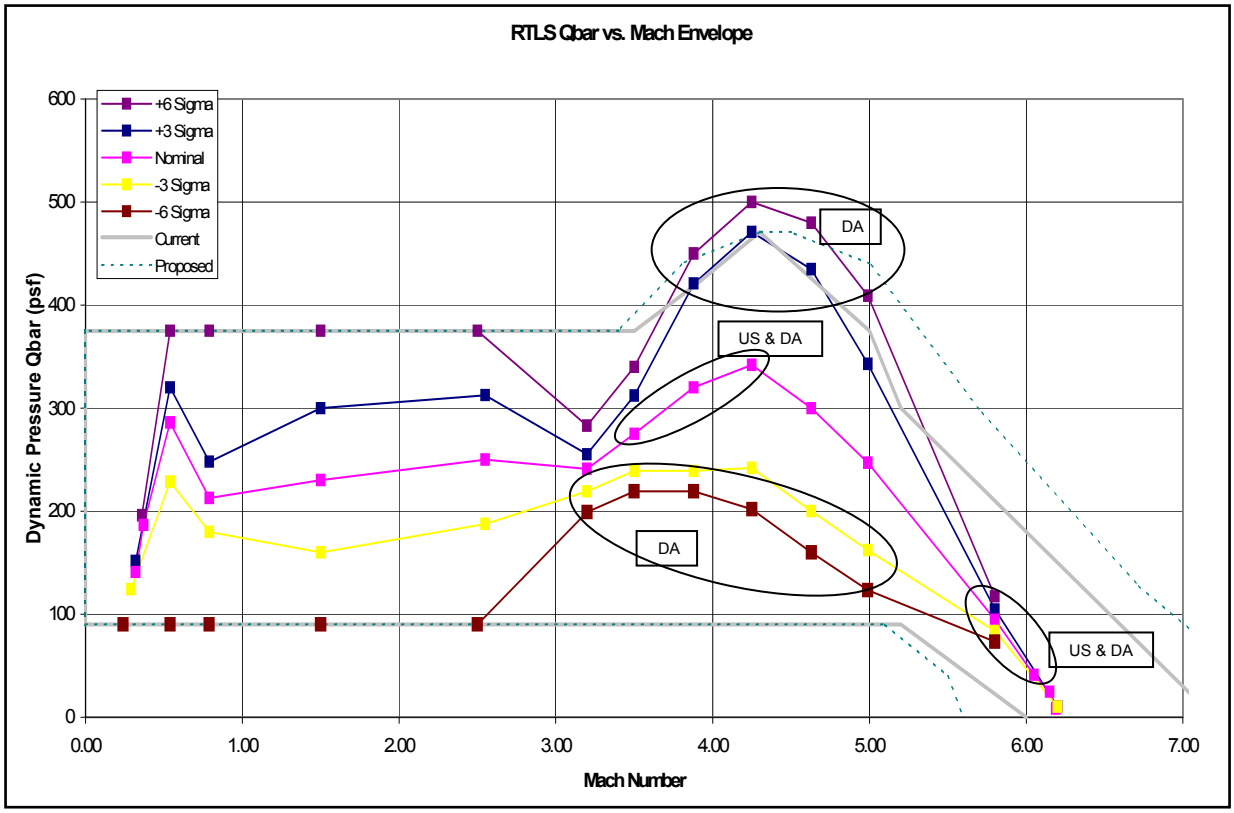

Figure 7-4. 1993 Verification Flight Cases with 2004 Stability Rerun

7.3 Technical Interchange Meeting

The task to reconfirm the existing SODB GRTLS Qbar envelope quickly expanded into a directive to recertify all descent Qbar and angle-of-attack envelopes for GRTLS, NEOM, TAL, and AOA. A review of the 1993 heavyweight verification results revealed numerous inconsistencies between Rockwell and Honeywell stability margins, and the 2004 rerun of the same flight cases yielded a third set of results. Table 7-4 shows a sample comparison of pitch axis stability margin differences for a flight case at Mach 5.8. (It should be noted the unstable margin [US] shown for the Honeywell 1993 -3-sigma PVAR 04 case is actually due to an error in the processing program, and the DA value of LFGM for the Honeywell +3-sigma PVAR 04 case is probably due to using an IPHASE different from that of the other programs.)

As this recertification task and a simultaneous effort to certify STS-114 for return to flight got underway, a number of concerns arose because of apparent violations of standard certification requirements in previous studies. These included definition of actual certification requirements and how they should be applied, clarification of methods used to disposition apparent violations, and selection of certification flight cases relative to SODB envelope boundaries. Other concerns included the need to identify regions of marginal controllability and trim capability, and possible errors in the aerodynamic coefficient uncertainty algorithms and tables. References 7-5, 7-6, and 7-7 address these issues and plans for their resolution and for ongoing certification efforts.

Table 7-4. Sample Stability Comparison for Analysis Tool Sets

Mach 5.80 Cases - Stability Comparisons									OPEN-LOOP ELEVON STABILITY (AT GDQ)						
									Low-Freq Gain Margin		Phase Margin		High-Freq Gain Margin		
CaseID	Weight	Xcg	Zcg	Traj	Disp	Aero	FCSmode	DataSet	Gain(db)	Freq(r/s)	Phase(deg)	Freq(r/s)	Gain(db)	Freq(r/s)	MSTB
G05809449N	254000	1078.0		NOM	None	Nom	Auto	HI 1993	15.98	0.41	45.48	1.35	13.23	6.75	L1
								RI 1993	19.62	0.30	61.15	1.32	11.34	7.30	L1
			384.5					BA 2004	27.10	0.20	68.56	1.35	11.75	7.33	L1
G05810449D	254000	1078.0		+3sig	None	Nom	Auto	HI 1993			60.88	1.38	11.15	7.28	L1
								RI 1993	21.50	0.03	60.79	1.39	11.14	7.30	L1
			384.5					BA 2004			68.40	1.43	11.53	7.33	L1
G05808350C	254000	1078.0		-3sig	None	Nom	Auto	HI 1993	12.34	0.29	60.78	1.20	11.65	7.29	L1
								RI 1993	12.25	0.29	60.82	1.21	11.63	7.31	L1
			384.5					BA 2004	12.90	0.22	67.73	1.22	12.03	7.33	L1
G05810449D	254000	1078.0	384.5	+3sig	None	Pvar01	Auto	HI 1993	13.99	0.39	59.87	1.68	9.19	7.26	L1
								RI 1993	15.33	0.38	61.41	2.20	7.17	7.36	L1
			384.5					BA 2004	17.67	0.22	64.46	2.20	8.11	7.31	L1
G05808350C	254000	1078.0	384.5	-3sig	None	Pvar01	Auto	HI 1993	9.86	0.34	60.63	1.47	9.87	7.26	L1
								RI 1993	11.21	0.34	63.62	1.94	7.83	7.37	L1
			384.5					BA 2004	11.29	0.22	66.84	1.94	8.76	7.32	L1
G05810449D	254000	1078.0	384.5	+3sig	None	Pvar04	Auto	HI 1993	2.65	0.29	13.21	0.37	22.30	7.27	DA
								RI 1993	7.21	0.30	35.57	0.61	18.67	7.02	L1
			384.5					BA 2004	8.09	0.22	47.79	0.58	17.39	7.35	L1
G05808350C	254000	1078.0	384.5	-3sig	None	Pvar04	Auto	HI 1993	25.40	0.04	-13.69	0.19	-1.77	0.26	US
								RI 1993	6.23	0.24	55.28	0.79	13.16	7.39	L1
			384.5					BA 2004	2.33	0.22	28.01	0.38	17.43	7.36	DA

A major event in the forward action plan was the calling together of active and retired members of the entry aerodynamics and GN&C communities for an "Entry Aerodynamics/Flight Control Technical Interchange Meeting (TIM)." This meeting was held July 21 and 22, 2004, at the Boeing Space Park facility in Nassau Bay, Texas, with splinter meetings on July 20 and 21. The purpose was to resolve open issues regarding requirements, analysis methods and disposition rationale. The four planned topics of discussion, with major recommendations resulting from each, follow.

1) Orbiter Entry Phase Stability Requirements
   a) Use new waterfall charts for OPS-3 and OPS-6 as proposed by L. McWhorter
   b) Document and use 6-dB Level 1 LFGM requirement
   c) Resurrect time-domain step response capability
   d) Define minimum frequency for applying waterfall requirements as 0.1 rad/sec
   e) Create a new entry FCS requirements document to replace Reference 6-7
   f) Document the Boeing stability analysis process in an internal letter
2) Aerodynamic Uncertainties
   a) Expand the elliptical uncertainty tables to cover the GRTLS del-alpha and del-elev ranges
   b) Avoid use of the may97 lateral elliptical uncertainty tables until corrected
   c) Correct lateral elliptical uncertainty tables and the LATGEN tool
   d) Assess impact of elliptical uncertainty table updates on results of previous studies
3) Stability Analysis Methodology
   a) Modify the standard stability analysis process to use the most meaningful combinations of uncertainties and dispersions
   b) Use perfect navigation state parameters in stability analyses but verify margin acceptability by applying known effects from NAV sensitivity studies
   c) Redevelop capability to do step responses in both rigid and flex domain analysis
   d) Improve fidelity/accuracy of the subroutines used to extract stability margins from MATCRAM stability analysis results
4) Disposition Rationale and Methodology
   a) Reinstate the stability analysis and verification process flow diagram as revised by L. McWhorter to accommodate current aero uncertainties
   b) Develop capability to generate cold start/restart initial conditions for time-domain simulations
   c) Develop standard set of accepted methods to support disposition of cases not meeting standard stability margin requirements

d) Reinstate the FCAN process for reporting and tracking the disposition of cases that fail to meet FCS requirements

Table 7-5 lists meeting attendees who signed the recommendations and action Items document.

Table 7-5. Entry Aerodynamics/Flight Control TIM Attendees

Sergio C. Carrion	James R. Harder	Milton W. Reed
Olman Carvajal	Gordon C. Kafer	Robert G. Reitz
Kyle W. Cason	Vincent M. Levy	Jeffrey S. Stone
Milton C. Contella	Pamela L. Madera	Tuan H. Truong
Olin Ray DeVall	Larry B. McWhorter	Thomas T. Tanita
Joe D. Gamble	Viet H. Nguyen	Charlie Unger
Mark M. Hammerschmidt		

7.4 Entry Flight Control Requirements Document

Reference 6-7 (the SDM) presents flight control subsystem performance and functional requirements across all mission phases for both ALT and OFT, including aborts. Although this document served well for entry and GRTLS performance assessment during the OFT program phase and for many years thereafter, TIM members determined that it was out of date. They decided that a new document should be created to capture the currently accepted stability requirements and processes, specifically addressing the entry (including TAL and AOA) and GRTLS flight phases. They also noted that in more recent studies, waterfall charts relating uncertainties and dispersions to stability level requirements were modified from the SDM originals and/or applied inconsistently, and undocumented changes in the pitch LFGM value and in PVAR scaling had been employed. Other topics determined to need attention included the following:

1) Statistical methods relating Monte Carlo data to protection levels and flight case selection
2) Definition of aero data uncertainty boundaries (flight-derived [FD] vs. preflight)
3) Correlation of stability level requirements with aero uncertainty levels and other dispersions
4) Agreement on stability margin values corresponding to Level 1 and Level 2 performance

Reference 7-8 is the new entry FCS requirements document. The first release (dated December 22, 2004), prepared by M. C. Contella, G. C. Kafer, and L. B. McWhorter, was applied during all subsequent mission-specific and generic certification tasks. Revision A, prepared by G. C. Kafer, L. B. McWhorter, and M. W. Reed, cleaned up, reformatted, and clarified text, figures, and tables to provide more accurate and meaningful descriptions of the entry FCS analytic requirements. It did not change numerical values of the original release.

Significant Changes: Among the more significant changes that this new SDM made to the original document were new waterfall charts or waterfall matrices that defined required combinations of system degradation, failures, and environmental uncertainties corresponding to FCS performance requirements. Figure 7-5 reproduces the entry and GRTLS waterfall matrices (tables 8-1 and 8-2) of Reference 7-8 that apply for rigid-body stability and response evaluations. Reference 7-8 also includes waterfall matrices for flexible-body stability and response evaluation and for trajectory performance evaluation. The following definitions apply for the “Aero/RCS Unc” levels:

1) “None” corresponds to the latest published nominal data in the Aerodynamics Data Book, RSS99D0001, April 2000.
2) “FD” (flight-derived) refers to the aero and RCS interaction data and associated uncertainties extracted from vehicle responses to numerous PTIs applied during several Shuttle flights. Specifically, FD refers to the tabulated aero uncertainties within a band of alpha and elevon (typically ± 5 to ± 8 deg) about reference trajectory schedules that are defined in the ADB.
3) “Pre-Flight” refers to wind-tunnel-derived data and uncertainties that have not been augmented with flight data, and thus correspond to the original preoperational aero used from STS-1. Specifically, Pre-Flight refers to tabulated uncertainties for large values of delta-alpha and delta-elevon relative to the reference schedules (typically ± 10 deg to ± 14 deg and greater), representing alpha and elevon values that were not experienced during the PTI DTO flights.
4) The established convention for FCS performance evaluation is to apply the Pre-Flight requirement level whenever delta-alpha or delta-elevon exceeds the FD band and the uncertainty starts ramping up towards the Pre-Flight value.

Table 8-1: Entry OPS3 Waterfall Requirements

Trajectory	Aero/RCS Unc	LRU (FCS-1, FCS-2)	Requirements*
Nominal	None	None	Level 1
Nominal	FD	3 sigma	Level 2
Nominal	Pre-Flight	3 sigma	DA
+/- 4 deg Alpha Dispersion	FD	None	Level 2
+/- 4 deg Alpha Dispersion	Pre-Flight	None	DA
+/- 3 Sigma	FD	3 sigma	Level 2
+/- 3 Sigma	Pre-Flight	3 sigma	DA
+/- 3 Sigma	None	Default Air Data	DA
+/- 6 Sigma (CSS)	FD	3 sigma	DA
+/- 6 Sigma (CSS)	Pre-Flight	3 sigma	DA

Note: FD requirements applicable when Delta Elevator and Delta Alpha are within "FD" envelope, when either or both are outside, use Pre-Flight requirements.
Note: 6 Sigma requires CSS only, all others require both Auto and CSS
*Requirements applicable for two jets failed and failures in Table 4-1

Table 8-2: GRTLS OPS6 Waterfall Requirements

Trajectory	Aero/RCS Unc	LRU (FCS-1, FCS-2)	Requirements*
Nominal	None	None	Level 1
Nominal	FD	3 sigma	Level 2
Nominal	Pre-Flight	3 sigma	DA
+/- 2 deg Alpha Dispersion	FD	None	Level 2
+/- 2 deg Alpha Dispersion	Pre-Flight	None	DA
+/- 2 Sigma	FD	3 sigma	Level 2
+/- 2 Sigma	Pre-Flight	3 sigma	DA
+/- 4 Sigma (CSS)	FD	3 sigma	DA
+/- 4 Sigma (CSS)	Pre-Flight	3 sigma	DA

Note: Alpha dispersions applied only in IPHASE 6 and 4
Note: FD requirements applicable when Delta Elevator and Delta Alpha are within "FD" envelope, when either or both are outside, use Pre-Flight requirements.
Note: +/-4 Sigma requires CSS only, all others require both
*Requirements applicable for one jet/pod failed and failures in Table 4-1

Figure 7-5. Entry and GRTLS Waterfall Charts from Reference 7-8

Other significant changes from the original SDM contained in the new SDM include the following:

1) The Level 1 LFGM requirement is specified as 6 dB for all mission phases and control loops (was 12 dB).
2) Step response envelope requirements are divided at Qbar = 40 psf corresponding to the current HIGHQ reconfiguration change point (was 20 psf).
3) Cooper-Harper rating scale and associated handling qualities definitions are added (previously only referenced the relevant NASA document).

Step Responses: Although this new document contains step-response envelope requirements, none of the recent certification tasks have included such tests for the following reasons:

1) A suitable tool for creating nonlinear fixed-point step responses is not currently available.
2) Trajectory simulations show that the FCS responds adequately to guidance and pilot inputs throughout the flight envelopes, even for cases where stability margins do not meet requirements.
3) From past experience, it can be expected that step responses for Level 1 cases, as well as for Level 2 and DA dispersed cases that have Level 1, and possibly Level 2 stability margins, would comply adequately with envelope requirements. (The step-response envelopes apply only to cases that have Level 1 performance requirements.)

FCANs: The new entry FCS specification contains the following statements in Section 8.0, “Waterfall.”

1) When a case doesn’t meet the waterfall requirements, a formal FCAN should be written to document the requirements violation.

2) When a DA case doesn't meet the next higher level of requirements (i.e., Level 2 or 1), an information FCAN should be written to document the results.

FCANs are flight control anomaly notices originally used by Honeywell from STS-1 through STS-26 to document FCS verification cases that did not meet standard stability and response requirements. The FCAN form provided the following information:

1) Detailed description of the anomaly (e.g., flight case, nature of failure) and the facility where it occurred
2) Description of the processes and methods used to investigate and clear the violation
3) Detailed results of the investigation and other supporting evidence (attached to the form)

In response to direction from the Aero/FC TIM, the FCAN process was reinstated. A new form, illustrated in figure 7-6, was developed using Microsoft Access, which allows storing and tracking of all FCANs in a convenient database. The TIM also provided for creation of a new entry FCS Data Review Board (DRB) that would bring together Boeing, JSC, and contractor personnel directly involved with the entry FCS to discuss progress of certification analyses, review FCANs, and consider other flight control issues that did not require input from the larger GN&C community.

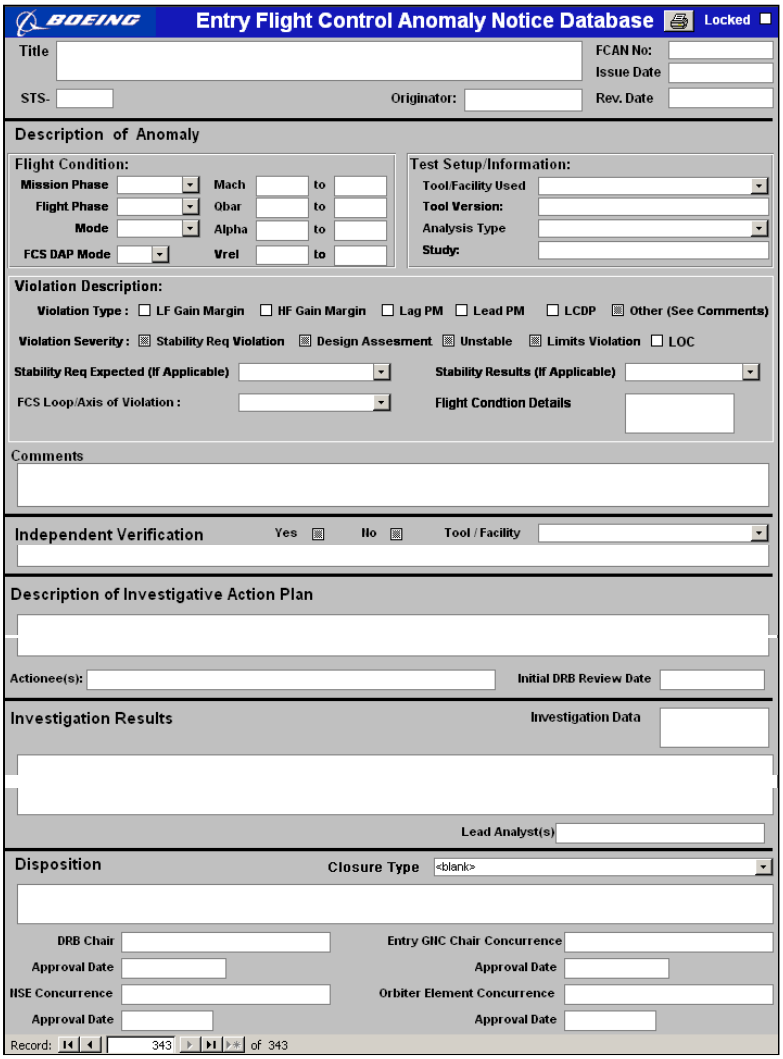

Figure 7-6. New FCAN Form

The general procedure called for each FCAN to be presented to the FCS DRB twice, the first time with the first four major blocks filled out. Block 1 contains the title, number, and other identifying data. Block 2, "Description of Anomaly," provides for detailed database information about the anomaly, including flight conditions involved and the nature of the violation, as well as a link in "Flight Condition Details" to spreadsheets providing numerical details. Comments can contain a verbal description of the cases and

violations. Block 3, “Independent Verification,” can include references to previous similar FCANs, as well as information on whether stability analyses and trajectory simulations exhibit correlating characteristics. Block 4, “Description of Investigative Action Plan,” proposes the plan and methodology for investigating and dispositioning the anomaly, and assigns personnel and a milestone for the task (these items may be augmented or revised at the first DRB).

At the second DRB presentation, Block 5, “Investigation Results,” can include a verbal description of the anomaly investigation and results, and “Investigation Data” provides for a link to more detailed documentation. Block 6, “Disposition,” contains a summary and rationale for the recommended disposition of the FCAN and the necessary approval signatures, and “Closure Type” designates the applicable type of FCAN closure. Disposition methods agreed on at the TIM to determine whether a given deficient margin constitutes a control issue include the following:

1) *Tools reassessment* – FCAN withdrawn and case reevaluated because of incorrect input data or tool configuration
2) *Engineering judgment* – Stability margin violation considered minor enough to dismiss; e.g., 0.1 dB or 1 deg
3) *PVAR correlation* – 0.8 scale factor on pitch short period uncertainties to represent a 3-sigma dispersion of the group (analogous to roll/yaw elliptical uncertainties)
4) *Time-domain simulation* – Nonlinear trajectory simulation characteristics in affected region can be used to show acceptable performance—e.g., negligible oscillation or divergence—and also to verify linear stability predictions. The SES provides similar capability for the CSS mode, and also for evaluating possible downmoding techniques for extreme cases
5) *SAIL testing* – For confirming acceptable performance when flight hardware is used
6) *Flight history evaluation* – Failures at test points well outside flight history may be considered insignificant flight risks. Conversely, some failures at cases inside flight history may be considered improbable flight risks
7) *PVAR set simulation* – Because trajectory simulations (e.g., SDAP, SES) have no capability to represent pitch short period uncertainties, a first-order approximation to their effects may be obtained by appropriate adjustments of the elevon loop gain
8) *Application of a missed GPC cycle* – Determination of stability margins with equivalent phase lag added at frequency of concern
9) *Similarity* – Apply analysis results from a previous FCAN with identical failure type and similar flight conditions

The available Closure Type statements include

1) *Acceptable Risk*—Depending on the risk level, may require approval at higher board levels than the DRB
2) *Acceptable Margin* (essentially an engineering judgment): applicable to cases that fail Level 1 or Level 2 requirements by small amounts, and to DA-dispersed cases that exhibit DA margins
3) *No Violation*—Higher fidelity analyses result in acceptable characteristics
4) *Withdrawn*—Applicable to FCANs written in error (e.g., because of faulty data) or combined with other FCANS
5) *Ignored*. Closure statements for very serious violations at flight cases that must be available: e.g., along the expected trajectory, include *Design Change Required—I-Loads* and *Design Change Required—Software.* (These have never been used in the current certification tasks.)

At the time this section was written, the FCAN database contained 353 records (although some were marked “Withdrawn”), covering STS-114, STS-121, and STS-300 (rescue mission) return-to-flight certification, and generic certification for OPS-3 and OPS-6.

7.5 Mission-Specific FCS Certification

During the TIM, reviews of the GRTLS envelope expansion task, re-run of the 1993 heavyweight verification flight cases, and preliminary STS-114 GRTLS assessment, revealed numerous flight cases within the current SODB OPS-6 flight envelope that did not satisfy standard stability margin requirements. It was agreed that these results indicated that the rigor used in the development of the SODB, Vol. V, flight envelopes was not sufficient to certify the current range of mission profiles, and that mission-to-mission flight control assessment would be necessary for the indefinite future. This decision included

OPS-3 as well as OPS-6, because similar analysis methods had been used to certify the SODB OPS-3 envelopes. The mission-to-mission process continued until a concurrent generic certification task provided Qbar and alpha envelopes covering all planned missions to the ISS.

STS-114 mission performance was investigated in the latter half of 2004; the associated launch-on-need (LON) mission STS-300 was investigated in the first half of 2005. Reference 7-9 summarizes this task as follows:

> This memorandum describes work performed to recertify the Orbiter Entry Flight Control System in support of STS-114 Return to Flight. Pertinent requirements documents were revisited and revised, analysis methods were updated and modernized, and tools were developed and/or modified as required to support the planned analysis. Analysis performed in support of this recertification effort included trim and controllability assessments, linear point stability analysis in the frequency domain, and time-domain simulation assessments. Both Control Stick Steering and AUTO flight modes were evaluated for nominal End of Mission and all intact abort mission phases. Both rigid and flex body requirements were verified with all requirements violations being documented and cleared with further analysis. Based on these results and with concurrence from the Entry Guidance Navigation and Control (GN&C) community as well as the Orbiter Project Office, the Entry GN&C subsystem was cleared for flight for both STS-114 and its associated rescue mission STS-300.

7.5.1 Preliminary Tasks

As a prelude to STS-114 FCS certification, a brief assessment was made of the effect of NAV-derived (NAVDAD) air data (Mach, Qbar, and alpha) errors on GRTLS FCS stability margins. STS-1 verification included NAVDAD errors, but their effect has been neglected in most if not all studies since then. The results of this assessment show that stability margin degradations caused by 10% errors in Mach and Qbar are no more than 2.5 dB in gain and 4 deg in phase for flight cases above Mach 2.5. Flight cases below Mach 2.5 and on or near ramps in the gain vs. Mach schedules can experience up to 6-dB-gain-margin degradation for 10% errors. However, flight rules would likely disallow landing in winds high enough to introduce errors of this magnitude in Mach and Qbar. Maximum stability margin changes of 1 dB gain and 1 deg phase occur for 2 deg NAV alpha errors, and only in the lateral axis. In a discussion of this study at the October 20, 2004, DRB (Reference 7-10), a rationale was presented that justifies the omission of air data error effects from the current requirements waterfall. It was also determined that at speeds above Mach 2.5, the assumption of perfect NAV is acceptable for the initial screening of stability results, and the effects of NAV errors need be considered only for particularly low-margin cases during requirements failure analysis.

Other tasks accomplished before or concurrent with STS-114 certification included the following:

1) Updating and correcting tools and procedures for computing elliptical aero uncertainties
2) Resolution of SDAP, SES and SAIL inter-facility inconsistencies and discrepancies
3) Enhancement of the flight case selection process
4) Improving the stability margin determination program to eliminate previous ambiguities
5) Adding coupled iterative pitch and lateral axis trim capability to the static trim program
6) Developing lateral control departure parameter (LCDP) computations

7.5.2 STS-114/STS-300 Scope

Figure 7-7 reproduces tables 7 and 8 from Reference 7-9, which illustrate 1) the scope of the STS-114 analysis effort, which encompassed 190,544 stability data sets, and 2) the small number of cases—less than 0.6%—that either failed requirements (755 cases) or had sufficiently low stability margins (DA values) that additional analyses for risk assessment were considered (321 cases).

Table 7. Number of Input Files for Each Mission

Mission	STS-114		STS-300	
	STRIM	MATCRAM	STRIM	MATCRAM
EOM (wrapDAP)	2782	19372	2873	19822
EOM (baseline DAP)	702	5504	624	4712
AOA	2093	14380	-	-
TAL	2964	20462	3068	20510
large HAC (EOM, AOA, and RTLS mp)	1183 (x3)	7824 (x3)	1131 (x3)	7646 (x3)
GRTLS (inc. TAEM)	2483	18024	2847	21348
Total	14573	101214	12805	89330

Table 8. Number of Cases which Failed Requirements or Achieved Design Assessment Level Margins

Mission	STS-114				STS-300			
	Failures		DA		Failures		DA	
	Number	%	Number	%	Number	%	Number	%
EOM (wrapDAP) + HAC with EOM mp	127	0.47	4	0.01	51	0.19	2	0.01
EOM (baseline DAP)	0	0.00	0	0.00	0	0.00	0	0.00
AOA (STS-114 only) + HAC with AOA mp	55	0.25	2	0.01	26	0.34	2	0.03
TAL	43	0.21	6	0.03	44	0.21	4	0.02
GRTLS	208	1.15	149	0.83	202	0.95	152	0.71

Figure 7-7. Statistics of STS-114 Stability Analysis Scope and Results

7.5.3 Stability Results

The regions in which requirements failures and DA margins were observed for STS-114 NEOM and GRTLS are shown in Figure 7-8, which reproduces figures 13 and 16 of Reference 7-9. Data points on these plots show the environment alpha and Mach number for the test flight conditions. Circles represent points along the nominal trajectory, and the remaining shapes represent environment dispersions. Squares, diamonds, and triangles, respectively, represent 3-sigma, 6-sigma, and ± 4-deg alpha cases for NEOM, and 2-sigma, 4-sigma, and ± 2-deg alpha cases for GRTLS. Points highlighted in red indicate flight conditions where requirements failures or design-assessment-level margins were observed for some combination of dispersions tested. The upper and lower SODB, Vol. V, envelope limits for each mission are shown as dashed lines, and the nominal SDAP runs associated with the given missions are represented by the solid grey line within the envelope. Groups of flight conditions in which issues were observed are enclosed by outlines with colors and shading representing the loop and type of margin of interest, respectively. Each of these groups corresponds to one or more FCANs, depending on the issues involved.

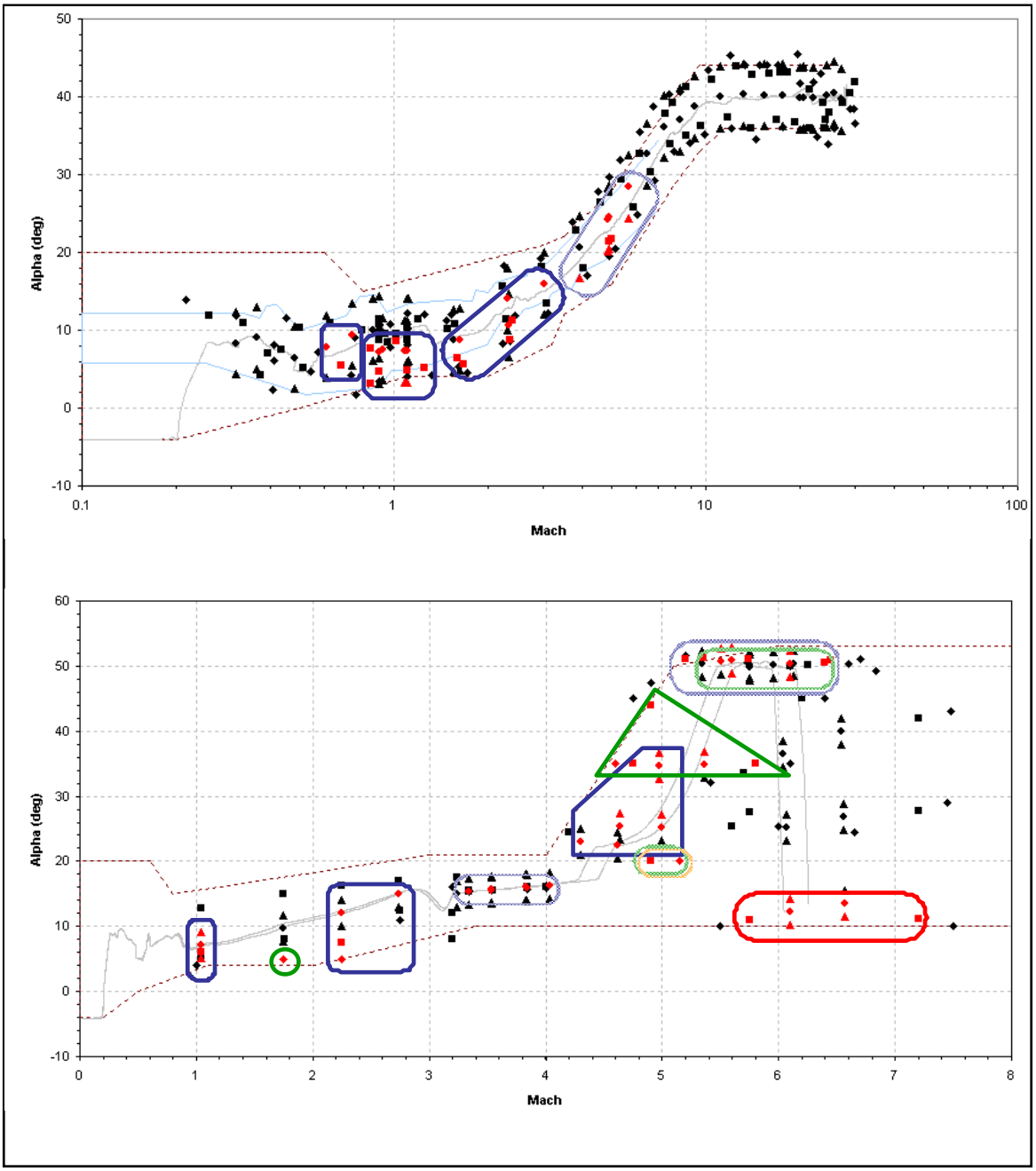

Figure 7-8. STS-114 NEOM and GRTLS Flight Cases and Regions of Stability Issues

Numerical data corresponding to the above figures are presented in figure 7-9, which reproduces table 9, for STS-114 NEOM, and table 13, for STS-114 GRTLS, from Reference 7-9. These tables summarize the regions in which requirements failures and DA level margins were observed, as well as the minimum stability margins for each region and the corresponding FCANs that document those cases. Similar figures and tables for STS-114 TAL and AOA, as well as corresponding figures and tables for STS-300 OPS-3 and OPS-6 missions, can be found in Reference 7-9.

All OPS-3 flight cases for both STS-114 and STS-300 were stable. As the reproduced table 9 in figure 7-9 shows, the worst case for STS-114 NEOM was a 1.2-dB LFGM in the elevon loop, occurring in the Mach 5 region with PVAR 4. For similar regions in AOA and TAL, the minimum elevon loop LFGM values were 1.0 and 0.1 dB, respectively. STS-300 NEOM and TAL exhibited minimum elevon loop margins of 0.98 and 0.8 dB, respectively, also in the Mach 5 region. (STS-300 AOA was not evaluated in this region.) For the lateral axis, OPS-3 minimum values of 3.4-dB HFGM and 27-deg high-frequency phase margin (HFPM) occurred in the aileron loop, both for STS-300. The GRTLS results show that both STS-114 and

STS-300 exhibit linear instabilities at many cases in the ET-SEP/IPHASE-6-INIT region. All remaining GRTLS cases are stable, although the elevon loop exhibits a minimum LFGM of 0.13 dB and a minimum phase margin of 0.81 deg, and the aileron loop shows a minimum HFGM of 1.6 dB.

Table 9. STS-114 EOM (wrapDAP) Requirements Failures and Design Assessment FCANs

Violation		Region						FCAN	Lowest failed (DA) margin			
		Mach		Qbar		Alpha			AUTO		CSS	
Loop	Margin	lo	hi	lo	hi	lo	hi		Nom traj	all	Nom traj	all
Elevon	HFGM	0.61	0.74	256	324	5.5	9.4	40, 44	5.8 dB	3.9 dB	-	-
		0.84	1.3	202	326	3.1	8.5	22, 41, 24, 45	4.7 dB	3.2 dB	-	-
		1.6	3.0	237	327	5.6	16	23, 42, 25, 46, 47	3.8 dB (-)	3.2 dB (3.8 dB)	5.0 dB (-)	3.7 dB (-)
	LFGM/ HFPM	4.0	5.7	154	238	17	28	26, 27, 89	4.4 dB	1.2 dB	-	-

Table 13. STS-114 GRTLS (Nov and Jun) Requirements Failures and Design Assessment FCANs

Violation		Region						FCAN	Lowest failed (DA) margin			
		Mach		Qbar		Alpha			AUTO		CSS	
Loop	Margin	lo	hi	lo	hi	lo	hi		Nom traj	all	Nom traj	all
Elevon	HFGM	1.0	1.0	232	249	5.1	9.1	16, 17, 18	3.1 dB	2.9 dB	-	-
		2.3	2.7	241	360	5.0	15	20, 21	4.8 dB (-)	4.8 dB (3.3 dB)	5.3 dB (-)	5.3 dB (2.8 dB)
		4.3	5.0	174	329	23	37	11, 12, 13	3.7 dB (3.7 dB)	3.7 dB (3.7 dB)	4.7 dB (-)	4.7 dB (-)
	LFGM / HFPM	5.2	6.5	39	60	48	53	14, 15	29 deg (8.8 deg)	27 deg (0.8 deg)	- (-)	- (-)
		3.3	4.0	223	294	15	16	10	25 deg	25 deg	-	-
Aileron	HFGM	1.8	1.8	330	330	5	5	19	(-)	(3.6 dB)	(-)	(-)
		4.6	5.8	110	190	35	44	3, 4	5.3 dB (3.1 dB)	5.3 dB (3.1 dB)	5.3 dB (3.2 dB)	5.3 dB (3.2 dB)
	LFGM / HFPM	5.4	6.5	39	40	48	52	5	(2.9 dB)	(2.9 dB)	(-)	(-)
		4.9	5.2	425	450	20	20	6, 8	- (-)	3.3 dB (-)	- (-)	- (3.3 dB)
Yaw Jet	all	4.9	5.2	425	450	20	20	7, 9	- (-)	3.3 dB (-)	- (-)	- (3.3 dB)
Lateral		5.8	7.2	7.5	9.5	10	14	1, 2	US (x)	US (x)	- (-)	- (-)

Figure 7-9. STS-114 NEOM and GRTLS Stability Summary and FCAN Assignments

7.5.4 STS-114 Anomalies

The STS-114 flight cases which failed stability requirements or passed with DA margins were grouped into 40 OPS-3 and 21 OPS-6 FCANs. These groups were based on variables such as control loop, type of violation, control mode, and similarity of flight cases. For STS-300, 41 OPS-3 and 44 OPS-6 FCANs were considered. In addition, an FCAN was written based on STS-114 SDAP trajectory oscillations that were not predicted by linear stability results. These FCANs all have DRB-approved dispositions, with concurrence where required by the Entry GN&C Panel and Orbiter Configuration Control Board (OCCB). Three of these FCANs are discussed below to illustrate examples of various disposition methods.

FCAN 26: Figure 7-10 shows the anomaly description section of FCAN 26, which comprises eleven NEOM flight cases within the indicated Mach, Qbar, and alpha ranges that exhibit elevon loop LFGM failures when run with PVAR 4. These cases either have -4-deg alpha or +3-sigma Qbar (with low alpha)

dispersions. Because actual alpha and elevon are within 5 deg of the alpha and elevon reference profiles defined in the ADB, aerodynamic uncertainties will have FD values. With these dispersions, then, the OPS-3 waterfall chart shown in figure 7-5 indicates that stability must meet Level 2 requirements. However, the actual LFGM values for all cases, and phase margins for most, are in the DA range, with the worst case having LFGM = 1.2 dB and Lag PM = 7.9 deg.

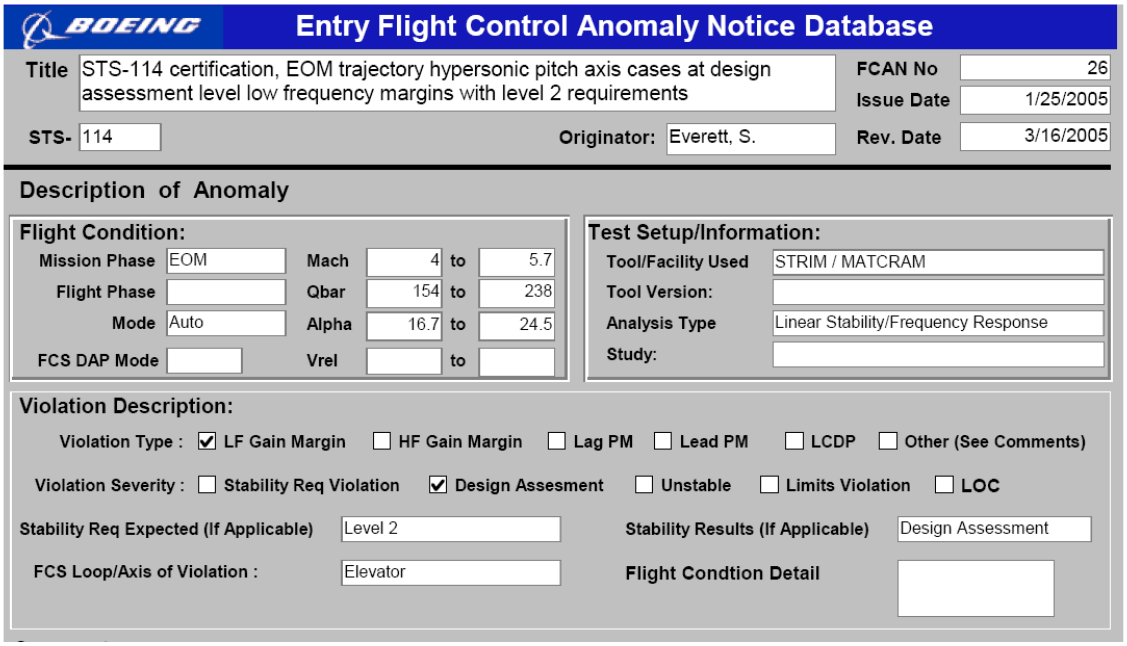

Figure 7-10. FCAN 26 Anomaly Description

The first disposition method applied to this FCAN was PVAR correlation. With 0.8 scale factors on the pitch short-period uncertainties, the worst-case LFGM increased to 2.9 dB and lag PM to 16.8 deg. These values are large enough to accommodate additional degradation due to NAV errors and FCS LRU tolerances. SDAP time-domain simulation was also used to disposition this FCAN. The region of concern was obtained by using an AOA trajectory with hot atmosphere, headwind, and -Cm uncertainty. The effect of PVAR 4 was evaluated by reducing the elevon gain by 6 dB. Figure 7-11 illustrates SDAP performance for this trajectory with the 6-dB elevon gain reduction and with nominal elevon gain. Linear stability results for PVAR 4 indicate modal damping ratio and frequency of approximately 0.065 and 0.7 rad/sec (9-sec period), respectively. The SDAP gain reduction run shows that disturbances cause damped pitch axis oscillations with period about 8.5 sec and not quite 2 cycles to half-amplitude, reasonably consistent with the linear PVAR 4 characteristics. With nominal gain, there is no significant oscillatory activity.

The investigation and disposition sections of FCAN 26 are shown in figure 7-12, which also records that this FCAN was closed with the statement “Acceptable Risk.”

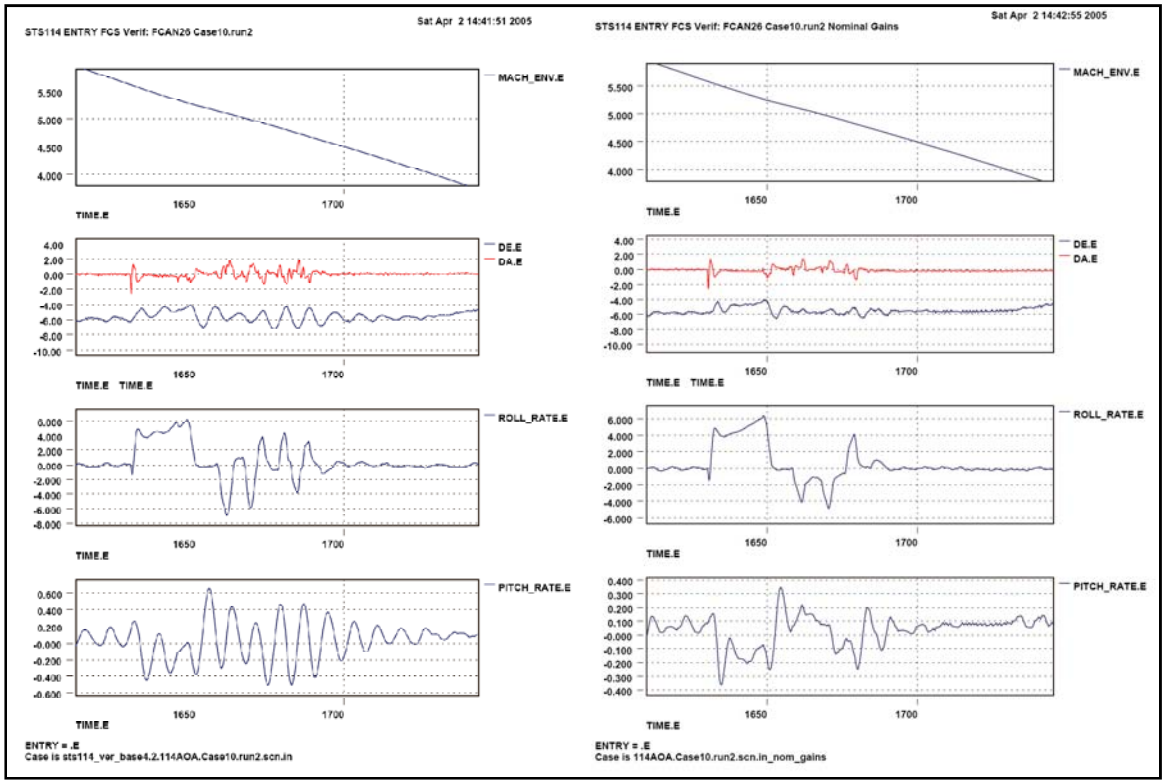

Figure 7-11. FCAN 26 SDAP Tests

Investigation Results **Investigation Data**

The aerodynamic uncertainties comprising the PVAR 4 set typically are all applied simultaneously. However, a scale factor of 0.8 on each uncertainty may be applied to represent the statistical reduction when the dispersion level is to be applied to the group as a whole. When selected runs in the Mach 5 region were made with this reduction on aerodynamic uncertainties, an increase of at least 1.4 dB was seen in the low frequency gain margin. If this improvement is included in the margins generated in this FCAN, some will be pushed into the Level 2 requriement region.

Linear analysis of cases in the range of Mach 0.7 to 5.1 revealed a close correlation between the value of PCMPDE and the elevon loop margin when PVARs are applied. In these cases, PCMPDE decreased by a factor of around 3 dB for PVAR 2 and 4. Thus, time domain runs in which GDQ is decreased for PVAR 2 and 4 by a factor of 4 to 6 dB should reveal any margin deficiencies which would have been caused by PVARs in the linear analysis.

Time domain run showed low amplitude low frequency oscillations in elevon and pitch that are characteristic of a reduction in elevon gains. This signature went away with nominal gains. Overall performance is acceptable and within expectations for this configuration.

Lead Analyst(s) Thomas Tanita

Disposition ***Closure Type*** Accepted Risk - Level 2 (Entry GN&C Concurrence Req'd)

Time domain analysis shows no unacceptable performance and is well within expected results. Linear analysis shows a 2.8 dB delta from the Level 2 requirements. It is concluded that this FCAN poses no risk to flight and should be closed with concurrence from GNC community

Figure 7-12. FCAN 26 Investigation and Closure

FCAN 1: FCAN 1 dispositions the only cases that exhibited linear instabilities during the STS-114 return-to-flight certification (similar unstable cases from STS-300 are covered in FCAN 150). Figure 7-13 shows the anomaly description. This FCAN comprises 75 GRTLS cases at the beginning of IPHASE 6, with Qbar less than 10 psf and before the alpha pitch-up maneuver is underway. All unstable cases have LVAR 2, 9, 10, 11, 19, or 20 uncertainties applied, These LVARs are characterized by roll jet aero/RCS interaction uncertainties that nearly null out the roll jet rolling moment and produce large adverse yawing moments, resulting in destabilizing tendencies when the roll jets fire. Some nearby cases with the same LVARs are stable, but with DA margins. Cases with nominal aero and LVAR 12 are all stable with Level 1 margins.

Entry Flight Control Anomaly Notice Database

Title	STS-114 GRTLS certification, instabilities at MM602 initialization	FCAN No	1
		Issue Date	11/4/2004
STS-	114	Originator: Everett, S.	Rev. Date	

Description of Anomaly

Flight Condition:

Mission Phase	GRTLS	Mach	5.75	to	7.2
Flight Phase	IPHASE6	Qbar	7.5	to	9.5
Mode	Auto	Alpha	10.3	to	14.3
FCS DAP Mode	WRAP/B	Vrel		to	

Test Setup/Information:

Tool/Facility Used	STRIM / MATCRAM
Tool Version:	
Analysis Type	Linear Stability/Frequency Response
Study:	

Violation Description:

Violation Type : ☐ LF Gain Margin ☐ HF Gain Margin ☐ Lag PM ☐ Lead PM ☐ LCDP ☑ Other (See Comments)

Violation Severity : ☐ Stability Req Violation ☐ Design Assesment ☑ Unstable ☐ Limits Violation ☐ LOC

Stability Req Expected (If Applicable)	Level 2	Stability Results (If Applicable)	Unstable
FCS Loop/Axis of Violation :	Roll/Yaw	Flight Condtion Detail	

Figure 7-13. FCAN 1 Anomaly Description

This FCAN was dispositioned by use of time-domain simulation. SDAP trajectory runs with initial conditions and aero uncertainties corresponding to the linearly unstable cases produced no indications of stability problems. This was expected because the predicted period and time to double amplitude of the unstable oscillations are typically around 50 and 30 sec, respectively, while Qbar usually reaches 10 psf within 20 sec, turning off the roll jets and stabilizing the system. In addition, alpha increases at about 2 deg/sec toward the 50-deg command, which generally improves the aerodynamic characteristics as they enter the reverse aileron region. A representative GRTLS trajectory with LVAR 10, illustrated in figure 7-14, shows no evidence of divergent characteristics during alpha recovery.

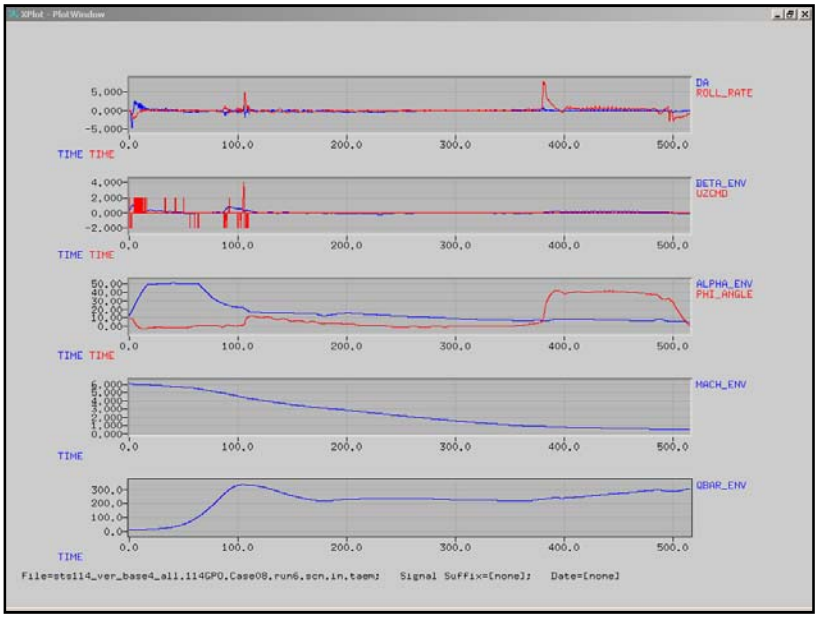

Figure 7-14. FCAN 1 STS-114 GRTLS SDAP Trajectory with LVAR 10

The FCAN 1 investigation included a “box corner” evaluation, in which trajectory initial conditions were varied to cover the NSTS-07700, Vol. X, MM 602 requirements. The FCS remained in control, exhibiting adequate performance for all cases, although for one case with +30-deg roll IC, the vehicle rolled off to -50 deg before recovering to wings-level. This occurred because prioritized combined pitch and roll jet commands limited the yaw RCS capability to one jet until the roll jets turned off at Qbar = 10 psf.

Subsequently, CR 93086A was written and implemented in OI-33 to increase from four to seven the number of jets per pod allowed to fire simultaneously during GRTLS. Figure 7-15 presents the disposition and closure statements for FCAN 1.

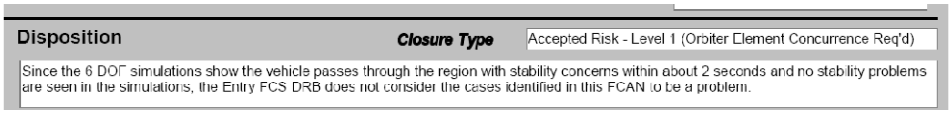

Figure 7-15. FCAN 1 Disposition and Closure

FCAN 90: FCAN 90 was written to document oscillatory characteristics that were observed during several SDAP OPS-3 time-domain screening runs but were not predicted by linear stability results. These oscillations occurred simultaneously in the pitch and roll/yaw axes for trajectories with wraparound DAP, hot atmosphere, OVEI spec headwind, and -Cm uncertainty, plus either nominal roll/yaw aero with -6-dB elevon loop gain, or LVAR 11 roll/yaw aero with -4-dB aileron loop gain. Figure 7-16 illustrates the worst case encountered, and shows that the oscillation initially increases to ± 7 deg/sec roll rate, but is completely damped out about 100 sec after its onset. However, RCS propellant consumption is almost 1,200 lb, encroaching on the redline value. Detailed analysis of simulation results shows that coupling between the pitch and roll/yaw axes through the guidance alpha and bank angle commands is exacerbated by the large error (>2 deg) between environment and GN&C alpha. The oscillation tendency can be mitigated by applying more realistic (GRAM) winds, using nominal gains, using nominal roll/yaw aero (with reduced aileron gain), or running with the baseline DAP. Because the conditions causing these oscillations are considered highly unlikely, and the overall performance impact is minimal (except for potential RCS propellant consumption), this FCAN was dispositioned and closed as indicated in Figure 7-17.

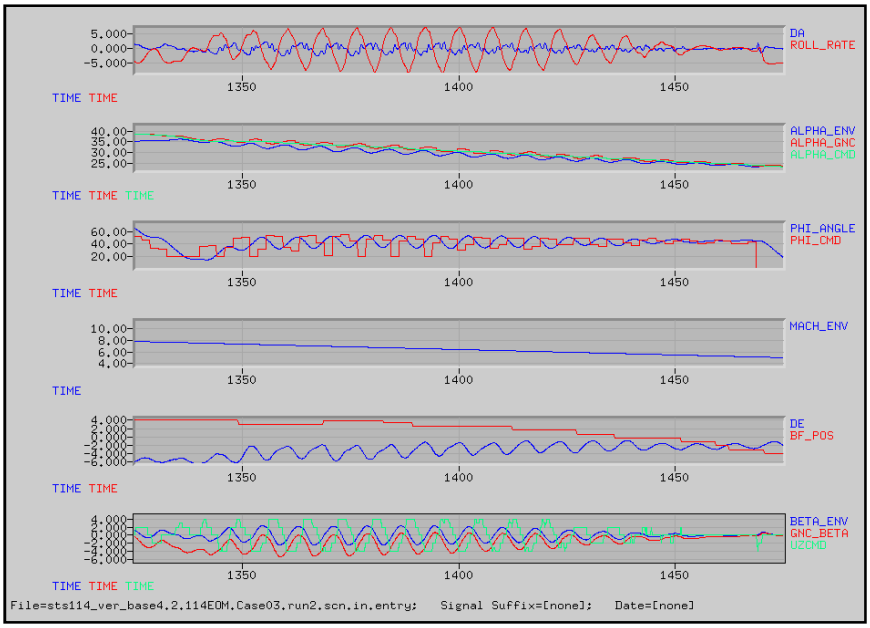

Figure 7-16. Worst-Case FCAN 90 SDAP Run

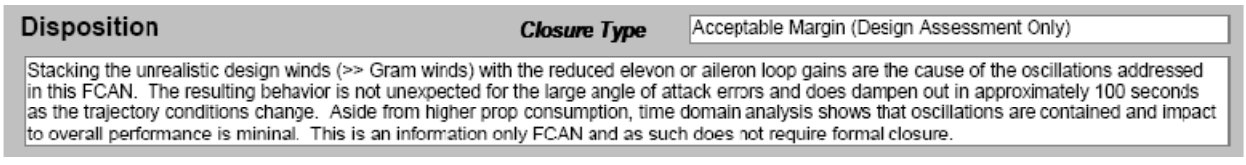

Figure 7-17. FCAN 90 Disposition and Closure

7.5.5 Additional ISS Missions

References 7-11, 7-12, 7-13, 7-14, and 7-15 document the mission-specific assessments for STS-121, STS-115, STS-116, STS-117, and STS-118, respectively, including any associated LON missions. STS-121 flight control issue dispositions were presented to the community in September and October 2005. STS-115

was cleared based on the proximity of its mass properties to those from previously cleared flights. A comparison of the dispersed trajectories for STS-301 (the LON mission associated with STS-121 and STS-115) with those from STS-300 showed no significant differences; therefore, STS-301 was cleared by virtue of similarity. By October 2006, the generic OPS-6 certification had been completed, allowing STS-116 OPS-6 to be certified implicitly. But because the generic OPS-3 certification was still in work, a limited set of generic OPS-3 flight conditions with anticipated STS-116 mass properties was analyzed and dispositioned by the community in October 2006. STS-117 and STS-118 were both cleared primarily by comparison to the then-near-complete generic certification database; thus no new analysis was planned. However, some mission-specific work was required after USA Flight Dynamics and Design (FDD) identified potential exceedances of the upper alpha limit using a new, more robust commit-to-flight (CTF) process. These exceedances were reviewed and dispositioned through the Entry GN&C Panel.

7.5.6 STS-125, Hubble Space Telescope Servicing Mission

The Hubble Space Telescope orbit inclination and altitude are 28.5 deg and 304 NM, respectively, significantly different from the ISS orbit characteristics. Since the resulting STS-125/*Atlantis* descent trajectories were not generically covered by the SODB Vol. V commit-to-flight envelopes, mission-specific entry FCS assessments were required. Although the SODB envelopes are certified only for 51.6 deg inclination missions, they are considered valid for assessment of non-51.6 deg inclinations. Therefore, since all OPS-3 and OPS-6 mass properties and trajectories provided by USA FDD for STS-125 were within the entry FCS generic certification mass property boxes and Qbar-alpha envelopes, no additional entry FCS analyses were required for STS-125, even though the launch date slipped several times.

As the launch date slipped, however, changes in mass properties and guidance I-loads were introduced for the STS-125 LON mission, STS-400. These changes resulted in STS-400 TAL and GRTLS weight vs. XCG combinations significantly outside of previous experience, as well as violations of the GRTLS SODB Vol. V Qbar and alpha envelopes for STS-400 trajectories. Several FCANs were opened covering STS-400 GRTLS stability margin failures and DA cases, all of which were cleared using accepted methodology. Two TAL FCANs were opened for points within the SODB envelopes, and were cleared by similarity to generic certification FCANs covering the same region and failures.

References 7-18 and 7-19 document the STS-125 and STS-400 FCS assessments, respectively. STS-125 launched on May 11, 2009, and landed at Edwards Air Force Base on May 24, 2009, after successfully servicing the Hubble Space Telescope

7.6 Generic FCS Recertification

Serious consideration of the merits of performing a generic entry FCS certification that would provide performance envelopes covering most, if not all, remaining Space Shuttle flights, began in March 2005. It was evident that continuing the approach used to certify STS-114 would be difficult because of schedule and resource constraints. Particular concerns were that there would be little or no time available for other flight control work, and continued reliance on resources outside the Boeing FCS group would be necessary. On the other hand, it would not be cost effective to spend more resources on generic certification than to certify each of the remaining 16 to 19 missions individually. Funding was approved in May 2005 to begin a generic recertification of the Orbiter entry operational GN&C angle of attack and dynamic pressure envelopes. Coverage was included for mission-specific analyses of STS-121, STS-115, STS-116, STS-117, and their respective LON flights. Detailed plans for OPS-6 and OPS-3 generic certification were approved by the OCCB in March and June 2006, respectively. The required project deliverables were

1) Updates to the NSTS 08934 (SODB), Vol. V, weight/CG constraints, alpha and Qbar envelopes, and Nz constraint wording
2) Refined wording for the NSTS 07700, Vol. X, Book 1, certified weight/CG limit
3) A generic certification final report

The generic certification final report, Reference 7-16, summarizes the task as follows:

> This memorandum describes work performed to generically recertify the Orbiter Entry Guidance, Navigation and Control (GN&C) Subsystem following the *Columbia* tragedy and subsequent Return to Flight (RTF) and mission specific analyses. Analysis

performed in support of this recertification effort included trim and controllability assessments, linear point stability analysis in the frequency domain, time-domain simulation assessments, and some thermal evaluations. Both Control Stick Steering (CSS) and AUTO flight modes were evaluated for nominal End of Mission and all intact abort mission phases. Results generally reconfirmed the known regions of poor margins within the flight envelope. Low margins of all types were observed in the AUTO mode at the initiation of Operational Sequence (OPS) 6 in several control loops, but which were not declared a safety of flight issue because of the speed with which the vehicle passes through this region. AUTO and CSS modes had low margins in both pitch and lateral axes during the alpha pullout region, a condition which led to the constraint on the lower alpha boundary. Poor low-frequency gain margins were also observed briefly after the pitch jets are deactivated at a dynamic pressure of 40 psf. In OPS 3, a region of poor AUTO low-frequency margins was noted between Mach 2 and Mach 9. There were also scattered instances of poor high-frequency gain margin in the transonic and low supersonic regions.

Based on the above results and the subsequent dispositions and with concurrence from the entry GN&C community as well as the Orbiter Project Office, new generic operational envelopes were established to replace those documented in NSTS-08934, Shuttle Operational Data Book (SODB) Vol. V. These constraints are applicable to all nominal NEOM and certified intact abort mode trajectories and eliminate the requirement for mission specific assessments to clear the Entry GN&C subsystem for flight.

Reference 7-17 is a briefing that presented final FCS generic certification results to the OCCB to obtain concurrence with the study results and conclusions and approval of proposed documentation updates.

Major ground rules and assumptions governing the generic certification task included the following:

1) Linear stability margin and waterfall requirements as defined in NS05HOU151 (Reference 7-8) (Exceptions: no NAVDAD or LRU errors, no PVARs in time domain, no flex body analysis [thus flight-specific flex analysis continues to be required for each mission])
2) Analysis concentration on regions of poor stability identified in mission-specific analyses
3) Airborne flight cases only (ground simulations at such facilities as Ames VMS and the SES provide adequate landing and rollout data)
4) OI-30 DAP configuration (changes in OI-32 and OI-33 should not affect certification results)
5 Planned ISS manifest only (rescue and non-ISS flights may require mission-specific analysis)

Generic certification used the same basic tools and techniques as the STS-114 certification, although with some improvements (e.g., automation of the flight case selection tool and coupled pitch/lateral trim capability). All tools used the 1997 baseline aerodynamic data with the December 2004 updated aerodynamic and RCS uncertainties. Flight cases were selected to satisfy the configurations defined in the waterfall charts shown in figure 7-5, and stability was evaluated according to the indicated requirements. FCANs were written to document all requirements failures and DA results, and were dispositioned using the methods and closure statements described in Section 7.4.

7.6.1 Monte Carlo Trajectory Selection

The overall scope of the generic certification task was approximately equivalent to that of four mission-specific certifications. Orbiter certification mass properties were defined by plotting weight vs. CG values at the beginning of each mission phase (EI for NEOM and AOA, post-ET-SEP for TAL, and MM 602 INIT for GRTLS) for all previous and anticipated 51.6-deg-inclination missions. The resultant weight vs. XCG certification boxes are shown in figures 7-18, 7-19, 7-20, and 7-21 for NEOM, AOA, TAL, and GRTLS, respectively, along with the selected certification points (numbered green circles). These points include 1-inch XCG, 0.5-inch YCG, and 1-inch ZCG pads. References 7-16 and 7-17 contain corresponding plots of weight vs. YCG and ZCG. Note that the selected points represent the initial mass properties for each Monte Carlo run set that will be generated. Aft RCS jet usage, propellant dumps, and forward OMS XCG shift will cause XCG to move forward by at least 1 inch in NEOM and AOA, 9 inches in TAL, and 4.3 inches in GRTLS, thus approaching or exceeding defined forward CG limits.

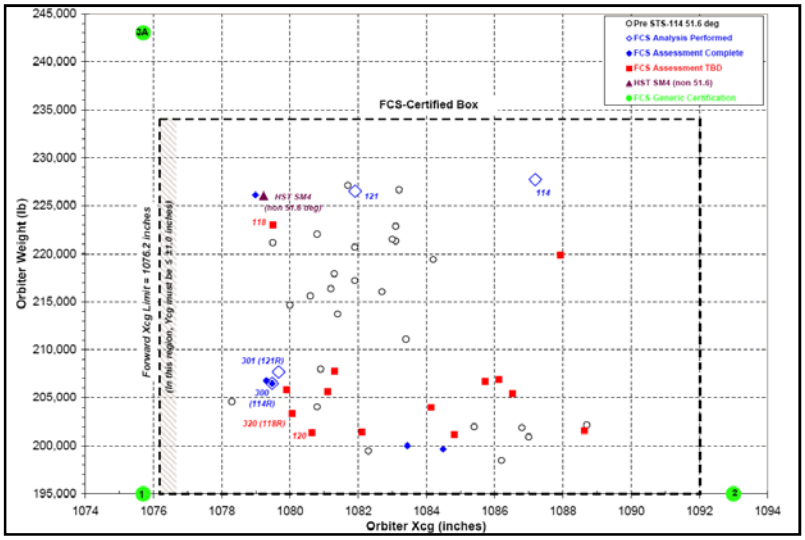

Figure 7-18. NEOM Entry Interface Orbiter Weight vs. XCG for Selected Missions

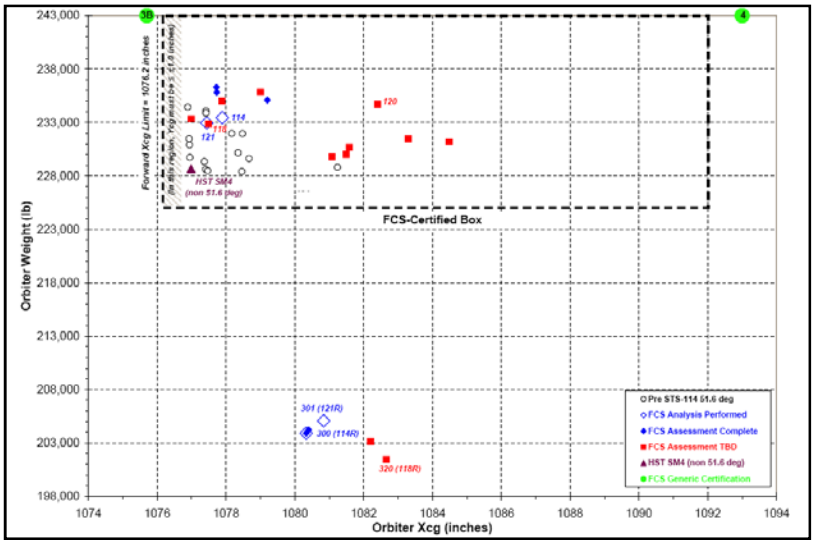

Figure 7-19. AOA Entry Interface Orbiter Weight vs. XCG for Selected Missions

The three certification cases defined for NEOM and two for AOA have a common point, 3A and 3B, with 243,000-lb weight at XCG = 1,075.7. Although this weight is greater than the certified NEOM maximum of 234,000 lb, weight sensitivity studies show that weight differences of this magnitude have little impact on elevator trim position or FCS stability, allowing this point to be used for a heavyweight, forward-CG case in both NEOM and AOA. Since the months specified for NEOM and AOA Monte Carlos are not the same, trajectory and aerodynamic differences can be expected to produce different stability characteristics.

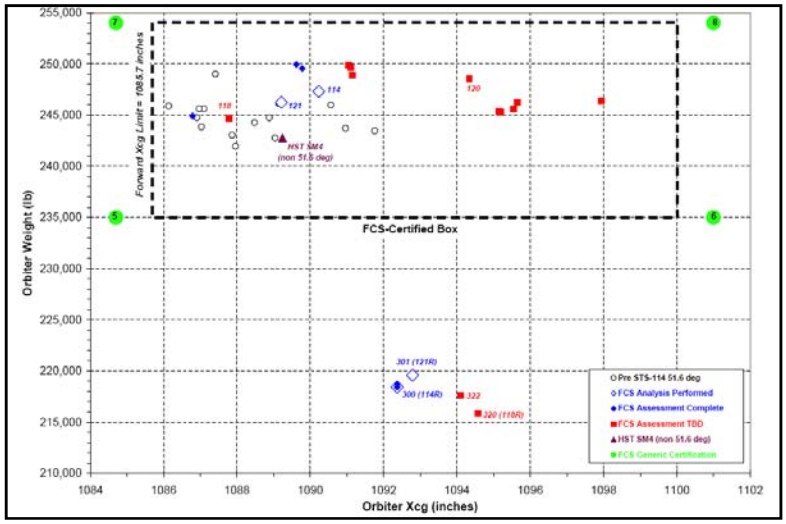

Figure 7-20. TAL Post-ETSEP Monte Carlo Case Weight vs. XCG for Selected Missions

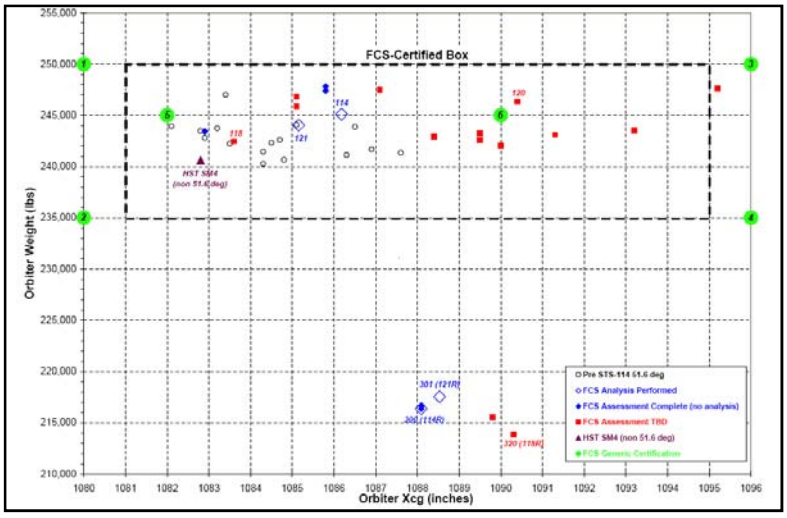

Figure 7-21. GRTLS MM 602 INIT Monte Carlo Case Weight vs. XCG for Selected Missions

The TAL and GRTLS selections each consist of four mass properties sets located at the corners of the weight vs. XCG boxes, with required X, Y, and Z CG uncertainties applied. Two additional cases with mid-range weights are defined for GRTLS to cover representative CG locations as well as to evaluate the effect on stability of applying an incorrect I-load value for the alpha-scheduled component of aileron gain.

Table 7-6 lists the initial orbiter weight and CG values, as well as the atmosphere models, for the requested 21 Monte Carlo run sets. A February model was used with NEOM and TAL trajectories because it contains the greatest dispersion in atmosphere and winds. The July model was selected for AOA to include a summer month for OPS-3. Two atmosphere models were used for GRTLS trajectories to create two different sets of extreme conditions. The 1995 GRAM for November is the most dispersed, pushing the expected trajectory nearer to the upper boundary of the dynamic pressure envelope. The June atmosphere shifts the trajectory toward the upper boundary of the ramp-down side of the angle-of-attack envelope. Subsonic Monte Carlo data were requested for four of these cases: NEOM 2, NEOM 3, TAL 8, and GRTLS 1N.

Table 7-6. Initial Mass Properties and Atmospheres for Requested Monte Carlo Data

Case		Weight	XCG	YCG	ZCG	Atmos Month
EOM	1	195000	1075.7	-1.5	385.5	February
	2	195000	1093.0	+2.0	359.0	February
	3A	243000	1075.7	+1.5	385.5	February
AOA	3B	243000	1075.7	+1.5	385.5	July
	4	243000	1093.0	-2.0	359.0	July
TAL	5	235000	1084.7	-2.0	385.5	February
	6	235000	1101.0	+2.0	359.0	February
	7	254000	1084.7	+2.0	385.5	February
	8	254000	1101.0	-2.0	359.0	February
GRTLS	1	250000	1080.0	-2.0	385.5	June & Nov
	2	235000	1080.0	+2.0	385.5	June & Nov
	3	250300	1096.0	+2.0	359.0	June & Nov
	4	235300	1096.0	-2.0	359.0	June & Nov
	5	245300	1082.0	-0.5	375.0	June & Nov
	6	245300	1090.0	-0.5	375.0	June & Nov

7.6.2 Support Studies

Several small studies were performed to confirm that the proposed weight and CG combinations to be used for the Monte Carlo trajectories were adequate and that no unexpected FCS performance characteristics would occur for intermediate values. Weight sensitivity studies were performed for OPS-3 and OPS-6, and XCG and ZCG sensitivity studies were conducted for OPS-6. Another study focused on the OPS-6 FWD RCS and OMS dumps to determine if additional dump variables were required in the Monte Carlo runs.

The weight sensitivity study evaluated elevon trim position and FCS stability at flight cases generated from four OPS-3 trajectories with 1,076.2 inches XCG and weights of 195,000, 210,000, 225,000 and 243,000 lb, and three OPS-6 trajectories with 1,080.5 inches XCG and weights of 213,000, 235,000 and 250,000 lb. As expected, differences in pitch FCS surface positions were minimal between weight increments, and no significant sensitivities in stability margins were noted in either set. Based on these results, it was determined that no intermediate weight test points were necessary.

The XCG sensitivity study consisted of a series of SDAP GRTLS trajectories with 245,000 lb weight and eight values of XCG ranging from 1,080.5 to 1,100 inches, plus a 250,000-lb case with 1,080.5 XCG. Results were as expected, with roughly linear correlation between XCG and elevon position. For the most forward XCG cases, up-elevon deflection briefly exceeded 20 deg during IPHASE 6, and all trajectories with XCG at or forward of 1,090 inches exhibited some bodyflap saturation. ZCG sensitivity was evaluated by comparing FCS stability at both forward and aft XCG with highest and lowest ZCG values. The absence of any significant margin differences due to high and low ZCG values, together with the expected XCG sensitivity results, supported the CG values proposed for the Monte Carlo trajectories defined above.

The goal of the GRTLS dump study was to determine if off-nominal dump configurations or dump failures had sufficient impact on FCS performance that additional Monte Carlo data and SDAP time-domain matrix cases were needed. Two basic dump configurations are available for GRTLS trajectories. The main dump configuration is the nominal dump, consisting of a 25-sec forward RCS dump combined with an MPS dump (which contains the LH_2 1.5-inch port dump, the LH_2 and LO_2 8-inch fill/drain valve dumps, and the LO_2 main oxidizer valve (MOV) dumps). The second, or off-nominal, dump configuration consists of a nominal dump coupled with an aft RCS dump. Failures can occur for any of these dump elements. Results showed that off-nominal dump configurations, as well as most failures with either dump configuration, do not pose a risk because they move the XCG further aft, which is usually beneficial to FCS stability. The “1 aft RCS jet” failure causes a YCG offset due to one-sided yaw RCS propellant used for trimming, but the FCS was able to handle that effect. However, with the “1 forward RCS jet” failure, XCG moves aft less rapidly than with no failure, resulting in slightly more up-elevon deflection during alpha pull-up. Although stability margins remained adequate even at the maximum elevon position, it was decided to include the “1 forward RCS jet” failure in GRTLS Monte Carlo trajectories with the most forward XCG.

7.6.3 Flight Case (Test Point) Selection

The flight cases used for trim, controllability, and stability evaluation were based on the Monte Carlo data provided by USA FDD for the trajectories defined in table 7-6. The goal of the point selection process was to select points that

1) Adequately described the proposed boundary and waterfall analysis requirements
2) Represented all weight-CG combinations throughout the envelopes
3) Covered both sides of flight control transitions (M5, M1, q2, q10, q40)
4) Were representative of the underlying Monte Carlo data as much as possible

A secondary goal was to keep the number of points small while still providing adequate coverage, considering factors such as aero table breakpoints, time spent in a region, and previous analysis results.

For each Monte Carlo trajectory set, values of various vehicle and atmosphere parameters were provided at specified "slices" (i.e., at discrete values of trajectory variables such as Qbar, Mach, velocity, angle of attack, altitude, or GRTLS IPHASE transition). In order to select test points, ellipses that quantify dispersions of Mach vs. Vrel, Mach vs. alpha, Qbar vs. Vrel, and Qbar vs. alpha were generated for each slice based on the required protection defined by the FCS analysis requirements document and the Level B Ground Rules and Constraints. Seven points were required for each slice: 1) nominal—based on the nominal Monte Carlo trajectory, 2 & 3) two alpha dispersion points—either ± 2 deg about the nominal point for OPS-6 or ± 4 deg about the OPS-3 nominal point, 4 & 5) two low-sigma dispersion points describing the widest possible range of dynamic pressure on the 2-σ ellipse for OPS-6 or the 3-σ ellipse for OPS-3, and 6 & 7) two high-sigma CSS dispersion points describing the widest possible range of dynamic pressure on the 4-σ ellipse for OPS-6 or the 5-σ ellipse for OPS-3. (For slices in which Qbar was constant, points associated with the largest Mach dispersion were chosen on the low- and high-sigma ellipses.) All points were required to be within structural boundaries established by the SODB, Vol. V, and to be reachable by the Shuttle FCS and guidance system, although CSS mode points could be outside reasonable AUTO mode dispersions. An automated tool was developed that selects the specified points for a given slice, based on the ellipse data and waterfall assessment requirements, and presents the chosen points for analyst review to ensure that structural constraints are met and that they are valid, reachable conditions. Figure 7-22 shows an example of the selection tool output for a representative slice.

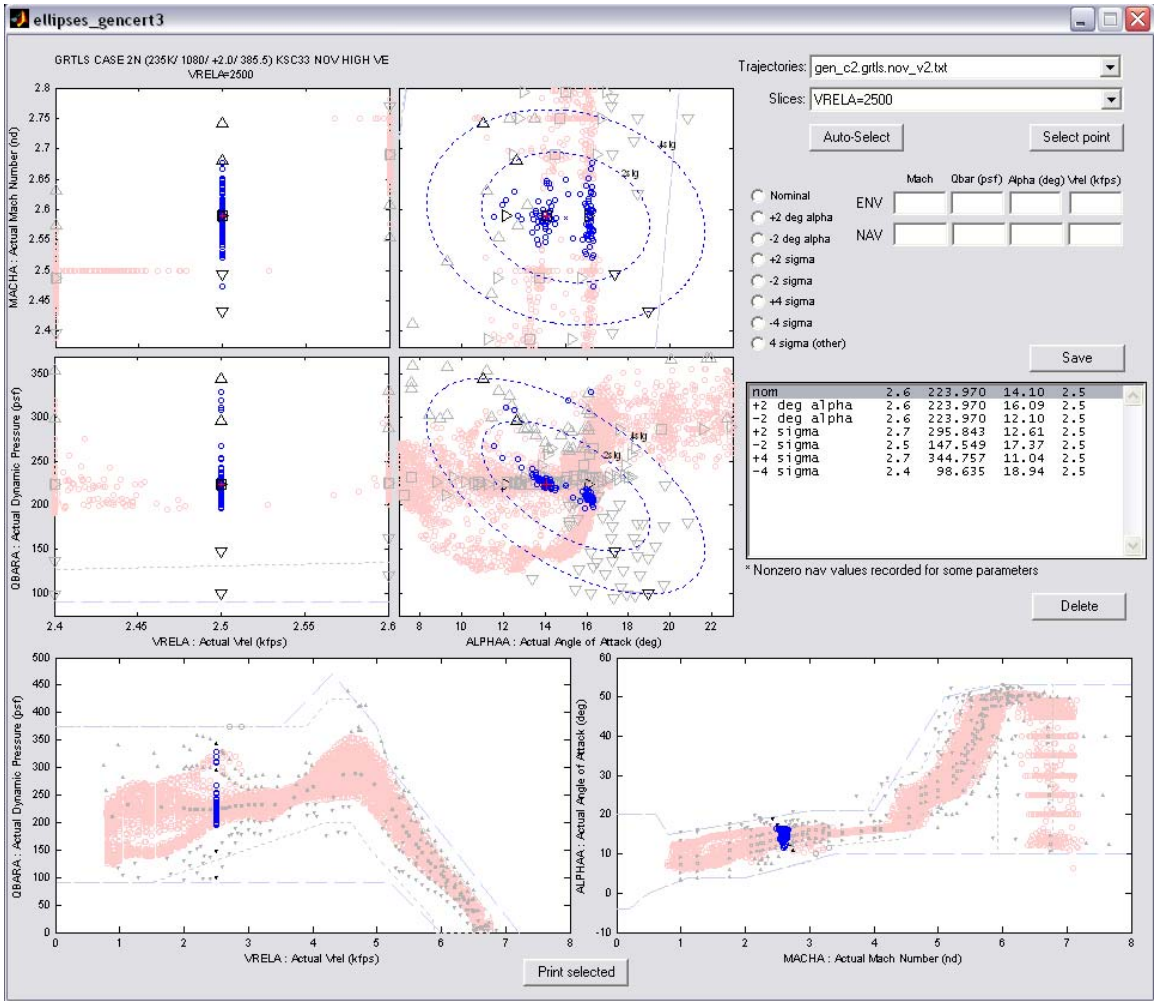

Figure 7-22. Example of Point Selection Tool Output

Altogether, 4,914 discrete flight cases were selected early on, resulting in 67,119 STRIM input files and 251,547 MATCRAM input files. Subsequent task additions resulted in slight increases in these numbers. The Qbar vs. Vrel and alpha vs. Vrel plots in figure 7-23 depict the flight cases initially selected for OPS-3 analytic evaluation. It should be noted that the SODB OPS-3 alpha envelope is plotted against environmental Mach number, rather than relative velocity. In figure 7-23, however, the alpha envelope is plotted using the approximation Vrel = 1000*Mach for convenience in showing the alpha variation and correlation with Qbar at each Vrel slice.

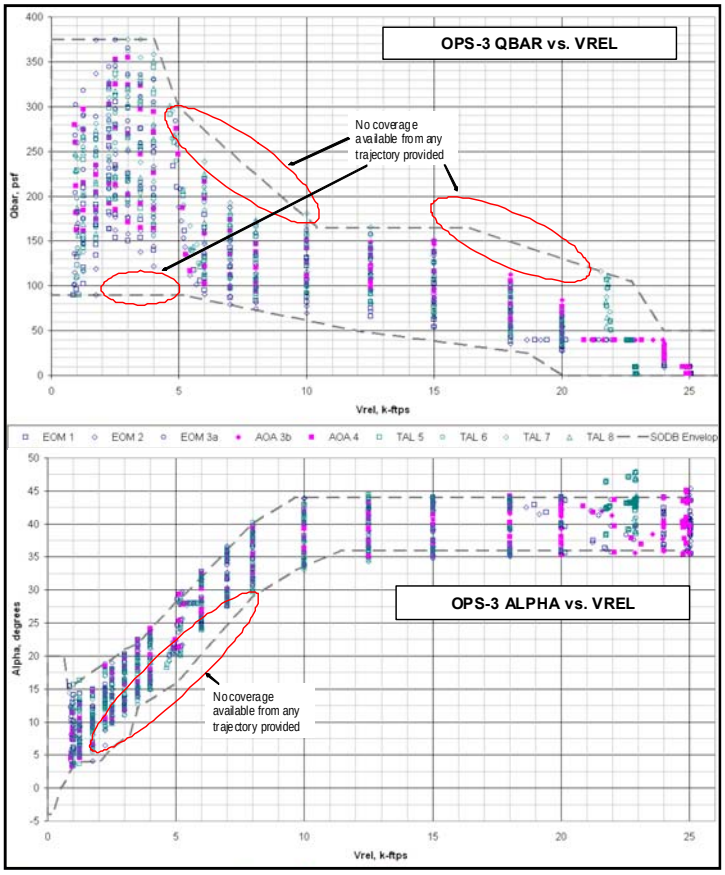

Figure 7-23. Selected Flight Cases for OPS-3 Generic Certification

When alpha was correctly plotted against Mach rather than Vrel, it was discovered that the SODB envelopes did not encompass the expected range of angle of attack between Mach 9 and Mach 4. This is illustrated in figure 7-24. Additional analysis points were selected using extreme values from the 3σ and 5σ ellipses for slices in this region where the original 3σ and 5σ points represented intersections of the envelope and ellipses. Points were chosen from NEOM sets 1 and 2 and TAL sets 5, 6, 7, and 8.

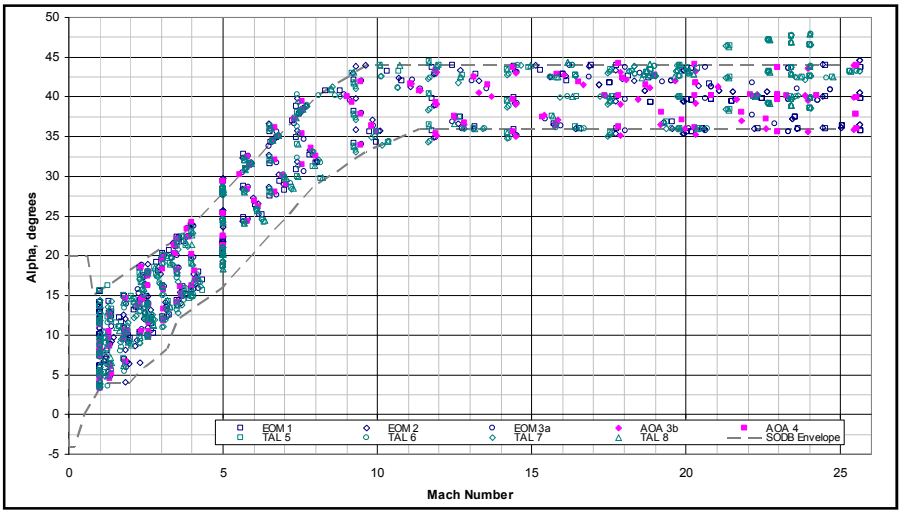

Figure 7-24. OPS-3 Flight Cases Alpha vs. Mach

Figure 7-25 shows Qbar vs. Vrel and alpha vs. Vrel plots for the flight cases selected for OPS-6 analytic evaluation. Qbar and alpha plots for selected subsonic flight cases are shown in figure 7-26.

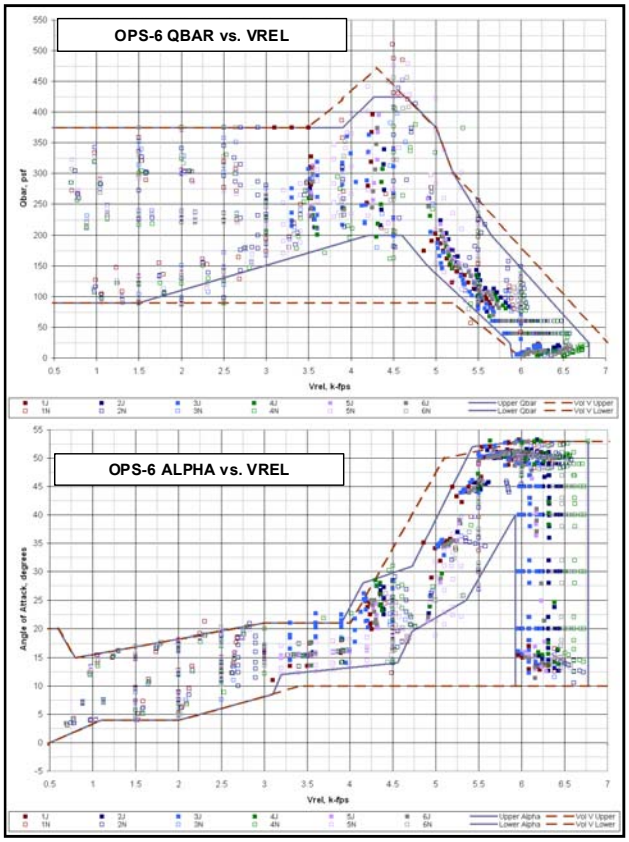

Figure 7-25. Selected Flight Cases for OPS-6 Generic Certification

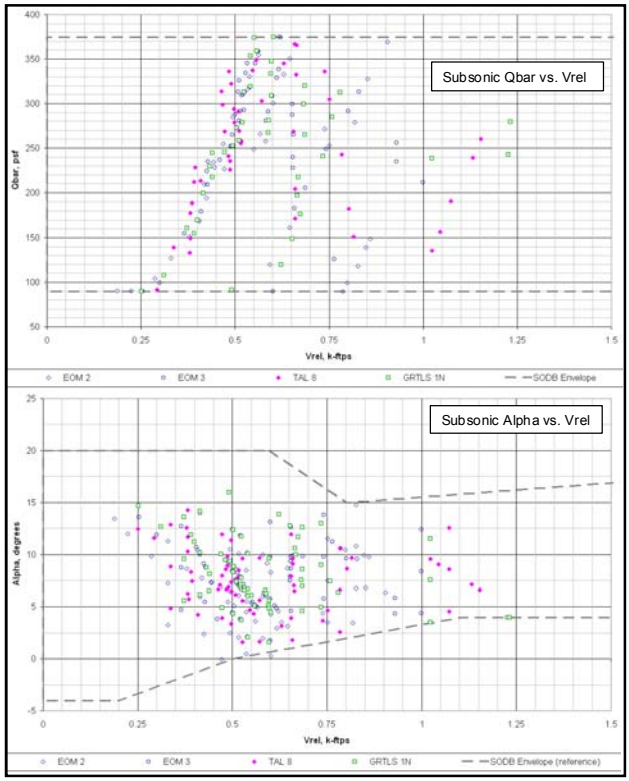

Figure 7-26. Selected Subsonic Flight Cases for Generic Certification

The program STRIM provided the data required by MATCRAM for linear stability analysis of each test case corresponding to the selected flight cases. STRIM input files (also called IC files) were created based on the following ground rules:

1) Environment Mach, Qbar, Vrel and alpha values selected from ellipses
2) Remaining required inputs (mass properties, phi, gamma, IPHASE) taken from nominal cycle of corresponding slice in Monte Carlo data
3) XCG shifted -1.5 inches from Monte Carlo XCG in forward CG NEOM and AOA sets with Monte Carlo YCG
4) YCG shifted ± 0.5 inches from Monte Carlo YCG in forward CG NEOM and AOA sets with Monte Carlo XCG
5) No XCG or YCG shifts in GRTLS or TAL
6) Speedbrake set at Monte Carlo values
7) For MM602 INIT slice, aero surfaces fixed at Monte Carlo values
8) Bent airframe and ABLT signs assigned to exacerbate moments due to YCG offset
9) Heavyweight filter active only for cases with weights greater than 220,000 lb
10) L/D uncertainty disabled when P21 or P22 used (+ or – Cmo uncertainty)
11) EOM cases run with Wrap and baseline DAPs, AOA with Wrap, TAL and GRTLS with baseline
12) 13 aero sets: Nominal; P22 (-Cmo unc); PVARs 1, 2, 3, and 4; LVARs 2, 10, 12, 19, and 20 with P21 (+Cmo unc); LVARS 9 and 11 with P22 (LVAR 23 not evaluated because it is similar to 9 and 11)
13) Both sides of control effector transitions—e.g., Mach_NAV=5.1 and 4.9 for rudder off and rudder on

The STRIM output files contain the data (mass properties, flight case parameters, aero and RCS coefficients and derivatives, and various flags) needed by MATCRAM to create sets of MATLAB files for evaluating the stability of each flight case. The following options are available via one-line MATCRAM input files for each test case.

1) DAP control mode—auto or CSS

Control loops—aileron and elevator for Qbar > 2, rudder for Mach < 5, roll jets for Qbar < 10, pitch jets for Qbar < 40, and yaw jets for Mach > 1

LRU uncertainties—FCS-0 (nominal), FCS-1 (low gain, low bandwidth), and FCS-2 (high gain, low bandwidth)

FCS-1 combined with LVARs 2, 9, 11, 19, and 20 (also with LVAR 23 if used)

FCS-2 combined with all PVARs and LVARs 10 and 12

The MATCRAM test cases were created to correspond with the new waterfall charts shown in figure 7-5. Reference 7-17 states that linear stability was evaluated for 267,757 test points, of which 99.5% passed requirements. In addition to the fixed points selected for linear stability evaluation, ICs were created for 1,169 SDAP trajectory screening runs for assessment of integrated GN&C (IGN&C) vehicle performance, including time-varying and nonlinear effects. Additional SDAP trajectories were run for dispositioning FCANs. The ascent/entry (A/E) SES was also used to help disposition FCANs, especially those relating to the CSS mode and others where crew involvement was desirable, and for independent verification of SDAP analysis.

7.6.4 Stability Results

Table 7-7 presents statistics of the generic certification stability results based on data in Reference 7-17. Out of 267,757 cases analyzed, only 1,211, or 0.45%, failed to meet the specific waterfall matrix requirements. Another 944 cases (0.35%) had DA level margins as well as DA requirements, so were not failures but generally received additional analysis to verify adequate FCS performance. The failure and DA cases were grouped into 73 FCANs based on similarity of DAP configuration, control loop, type of failure, and proximity of flight condition. Table 7-8 shows a top-level distribution of the FCAN failures and DA cases based on Reference 7-16 tables.

Table 7-7. Generic Certification Stability Evaluation Statistics

	OPS-3	OPS-6	SubSonic	Total	Percent
Number of Stability Results	139,619	114,520	13,618	267,757	100.00%
Number of Level 1 Margins	137,323	109,159	13,204	259,686	96.99%
Number of Level 2 Margins	1,804	3,814	342	5,960	2.23%
Number of Failures (i.e. Req is Level 1)	10	34	0	44	0.02%
Number of DA Margins	479	1,103	50	1,632	0.61%
Number of Failures (i.e. Req is Level 1 or Level 2)	408	235	45	688	0.26%
Number of Unstable Margins	13	444	22	479	0.18%
Overall Number of Failures	**431**	**713**	**67**	**1,211**	**0.45%**

Table 7-8. Generic Certification FCAN Failure and DA Case Distribution

	PITCH AXIS CASES			LATERAL AXIS CASES			COMBINED CASES		
TYPE	No. FCANS	Failures	Non-fail DA	No. FCANS	Failures	Non-fail DA	No. FCANS	Failures	Non-fail DA
OPS-3 Original	12	256	41	13	100	81			
OPS-3 High-Alpha	4	1	21						
OPS-3 Subsonic	4	63	8						
OPS-3 Total	20	320	70	13	100	81	33	420	151
OPS-6	15	206	339	25	405	450	40	611	789
Stability total	35	526	409	38	505	531	**73**	**1031**	**940**

Most of the generic certification FCANs document cases similar to ones observed during mission-specific certification; however, more complete coverage of the operational envelopes revealed some new regions of low stability margins. All of the documented violations to linear stability requirements were dispositioned with appropriate methods, and no changes to the flight software were recommended.

Five specific areas of low stability were identified in this task, most of which have been observed before.

At the initiation of MM 602 in OPS-6, low angle of attack and roll jet uncertainties produced AUTO mode instabilities and poor margins in the roll/yaw axis. These deficiencies were not declared a flight safety issue because of the speed at which the trajectory proceeds through and beyond these conditions. (See Section 6.7.5, paragraph FCAN 1, for the similar STS-114 situation.)

Poor HFGMs occurred in both the pitch and lateral loops during OPS-6 pullout, while poor LFGMs occurred in both axes later on, as illustrated for the aileron loop in figure 7-27.

- Deficiencies at both high and low frequencies in overlapping Mach regions preclude increasing or decreasing the DAP gains during this phase to improve stability.
- These low margins also constrained the lower boundary of the angle-of-attack envelope.
- Based on stability with PVAR reductions and SDAP/SES performance with stressed pitch and lateral axis gains, these margins were declared to not represent a risk to flight.

Poor LFGMs occurred in both the pitch and lateral axes as the dynamic pressure crossed 40 psf in OPS-6 and the pitch jets were turned off. This was also declared not to be a safety of flight issue because elevon effectiveness increases rapidly as dynamic pressure continues to rise.

A region of poor pitch and lateral axis LFGMs and pitch axis instabilities occurred between Mach 2 and 9 for the OPS-3 AUTO mode. Improved pitch axis stability with PVAR reductions, acceptable SDAP and SES trajectory performance with stressed gains, and desk analysis conclusions allowed these cases to be considered acceptable risks.

Scattered instances of poor HFGMs occurred in the transonic and low supersonic region for both OPS-3 and OPS-6.

- Poor margins in the transonic region were not unexpected based on FCS design features to ensure acceptable trajectory performance, and thus were generally not considered a flight safety issue.
- The results of PVAR reductions and SDAP/SES trajectory simulations with stressed FCS gains provided additional bases for viewing these cases acceptable risks.

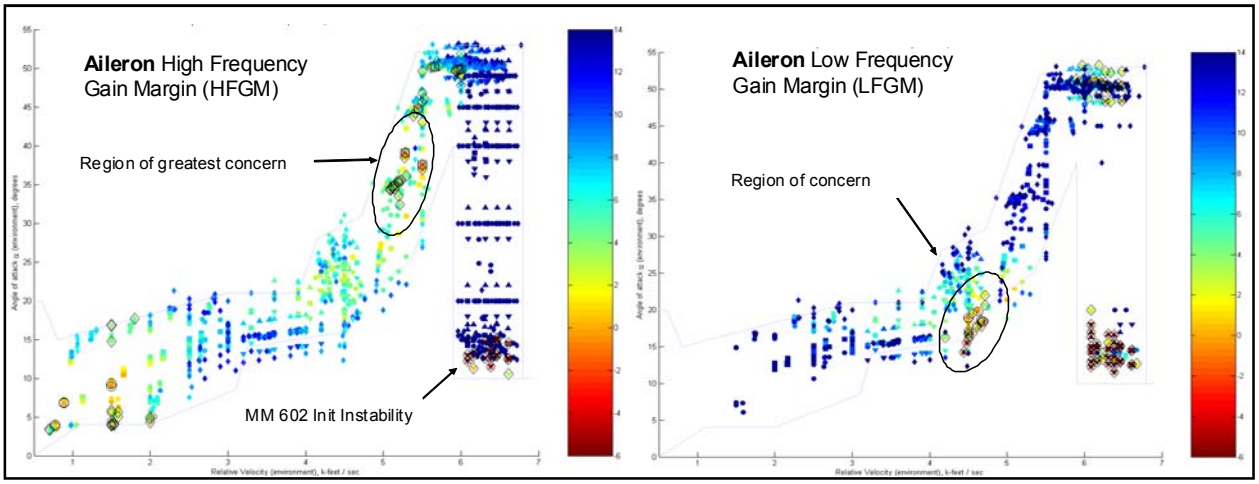

Figure 7-27. OPS-6 Aileron Loop Gain Margins Relative to Requirement

7.6.5 Trim and Controllability Analysis

In addition to providing all data required to generate MATCRAM files for linear stability analysis, the STRIM output files contained data permitting a comparison of static trim and controllability characteristics against design goals and requirements. Sufficient authority is required to maintain control, to maneuver, and to recover from disturbances in the lateral-directional and longitudinal axes throughout the entire entry without violating appropriate OVEI aerosurface position and rate limits. For OPS-3 and OPS-6 analysis, these requirements were interpreted as requiring all cases above Mach 1 to trim with no more than two yaw jets, and subsonic cases to trim with aileron and rudder alone. Although thermal and structural constraints were not a focus of this investigation, brief analyses were performed to assess compliance with elevon cove heating and SSME bluing requirements because the data were available.

Figures 7-28 and 7-29 show elevator trim deflections for all OPS-3 and OPS-6 flight cases. The maximum up-elevator trim deflections were 18 deg for OPS-3 and 21 deg for OPS-6. Subsonic elevator trim deflections ranged from -4 deg to +8 deg.

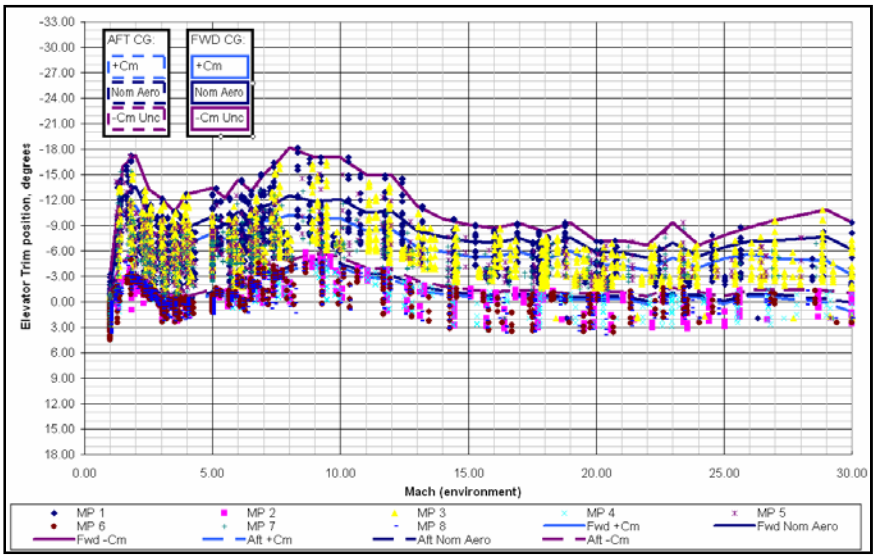

Figure 7-28. Elevator Trim Deflection for OPS-3 Flight Cases

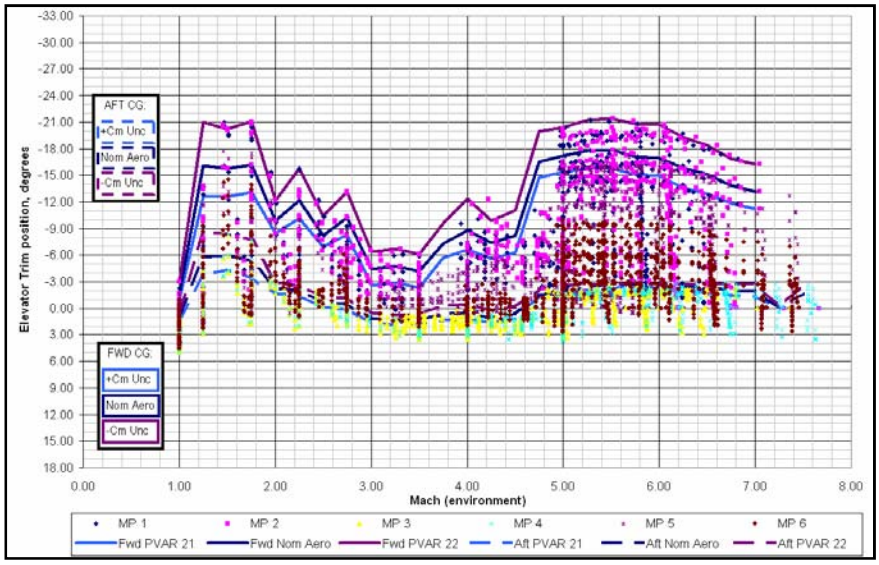

Figure 7-29. Elevator Trim Deflection for OPS-6 Flight Cases

Lateral axis trim and controllability analysis showed only localized issues in GRTLS and OPS 3. No trim concerns were found in the subsonic region. Although numerous test cases had saturated aileron trim deflections (± 3 deg for baseline DAP and ± 5 deg for wraparound), only 18 cases in the OPS-3 original data set and 39 cases in OPS-6 required more than two yaw jets for trim. Four FCANs were written based on these violations, two for GRTLS and one each for TAL and NEOM. All cases in one GRTLS FCAN were outside the proposed SODB, Vol. V, envelope boundaries. This FCAN was dispositioned by an SDAP run showing adequate trim and control authority for a trajectory that closely followed the low-alpha and high-Qbar boundaries in the region. The second GRTLS FCAN was dispositioned by an SDAP trajectory that demonstrated adequate trim and control authority at the cases of concern in the IPHASE 5 initialization region. The OPS-3 TAL FCAN was dispositioned by applying 81% scale factors to the "disturbance vector" components—ABLT, lateral CG offset, and bent airframe—to simulate an elliptical distribution. This reduced the yaw RCS trim requirement from 2.2 jets to 1.1 jets; it also lowered SDAP trajectory RCS propellant usage by more than 50%. The remaining FCAN resulted from SDAP NEOM trajectories showing loss of control for the worst-case combination of aero uncertainties. These failures were cleared by runs using 81% scale factors on the beta, aileron, and pitching moment uncertainties to model a statistically more realistic dispersion combination of three variables. An additional trim FCAN resulting from the delta certifications (discussed below) documented high-alpha cases that required more than two yaw jets for trim. The results were similar to those observed in the original set of data. Reduction of the disturbance vector lowered the number of required jets to below two, as expected.

Elevon Cove Heating: To protect the region between the wing trailing edge and the elevon leading edge (known as the elevon cove) from damage due to extreme heating, the Entry Aerothermal Group determined that total elevon deflection should not exceed -16.4 deg during entry. An assessment of STRIM elevator and aileron trim values for nominal aero (roll-yaw aero uncertainties were not applied per prior program decision) showed that 941 cases (2% of the total set assessed) had an elevon deflection farther up than -16.4 deg solely for trim, with some cases exceeding -20 deg of up-elevon deflection. These failures occurred in the high alpha side of the envelope for Mach 10 to 7. Assessment of OPS-3 Monte Carlo data showed that with statistically random dispersions (as opposed to the worst-on-worst sets used in generic certification frequency-domain analysis), elevon deflections did not exceed the cove heating limit.

SSME Bluing ("Ink Spots"): NSTS-07700, Vol. X, Book 1 details requirements on elevon and body flap deflections for NEOM entries to protect the SSME engine bells. Both STRIM results and Monte Carlo data showed violations of the acceptable regions; most were associated with extreme forward XCG values where full-up body flap is required to maintain elevon deflection near its schedule. Because further adjustments to the current body flap and elevon schedules would not be acceptable to GN&C, the violations have been accepted.

7.6.6 Trajectory Studies

SDAP Time-Domain Analysis: The entry FCS requirements document calls for a time-domain analysis of generic OPS-3 and OPS-6 mission scenarios to screen for unacceptable IGN&C performance characteristics that the linear analysis might not identify. To perform this analysis, 1,169 SDAP trajectory simulations were performed with specific combinations of FCS, aerodynamic, trajectory, and vehicle parameter variations. Included in these variations were changes to the pitch and lateral DAP channel gains and aerodynamic coefficient uncertainty combinations. In addition, different trajectory and vehicle parameter combinations were employed with these FCS and aerodynamic variations to further stress the FCS. Table 7-9 shows the ten unique combinations of independent FCS and aerodynamic parameters that constituted the OPS-3 FCS core matrix. The OPS-6 core matrix was identical to that of OPS-3, except that ABLT was not considered and only one yaw jet was failed. The environmental parameters that were varied to affect trajectory characteristics are identified in table 7-10.

Table 7-9. OPS-3 Time-Domain Core FCS Matrix

Core FCS Matrix										
RUN	LVAR	ΔCM	B/A	DXCG	DYCG	Failed Jets+	LRU++	ABLT+++	Gains	Notes
0	Nom	0	0	0	0	0	0	0	Nom	
1	Nom	+1	0	+1	0	0	0	0	+6db Dele	Screens for Pvars 1,3
2	Nom	-1	0	-1	0	2 pit	0	0	-6db Dele	Screens for Pvars 2,4
3	Nom	+1	0	+1	0	0	0	0	+6db Dela,Yjet,Delr	Screens lat hi-freq gain
4	Nom	-1	0	-1	0	2 yaw,rol	0	0	-6db Dela,Yjet,Delr	Screens lat lo-freq gain
5	19	-1	+1	-1	+1	2 yaw,rol	0	-1	Nom	Worst-case lat trim
6	10	+1	0	+1	0	0	0	0	+4db Dela	Optional: Nominal gains
7	11	-1	0	-1	0	2 yaw,rol	0	0	-4db Dela	Optional: Nominal gains
8	12	+1	0	+1	0	0	0	0	+4db Dela	Optional: Nominal gains
9	20	+1	0	+1	0	0	0	0	+4db Dela	Optional: Nominal gains

+ Pitch jets failed are R1U, R2U, R2D, R3D, L1U, L2U, L2D, L3D. Yaw/Roll jets are same as pitch jets plus L1L, L3L, R1R, R3R
++ LRU uncertainties not modeled in SDAP. Uncertainties will be simulated by SES if necessary.
+++ ABLT will be implemented for the entire OADB Mach table range

Table 7-10. Time-Domain Matrix Trajectory Variations

Parameter	Description	Time-Domain Matrix Options	Additional Comments
Atmosphere profiles	Standard atmosphere profiles used for all mission scenarios	1962 Standard (STD) KSC Cold Reference (COLD) KSC Hot Reference (HOT)	KSC atmospheres available in "ftn80" file
Wind profiles	Wind velocity and azimuth profiles with respect to altitude. OPS-3 head/tailwinds defined with respect to HAC intercept. OPS-6 head/tailwinds defined with respect to GRTLS pull-out	No wind (NONE) Headwind (HEAD) Tailwind (TAIL)	OPS-3 profiles were uniquely designed using various certification and design profiles. OPS-6 profiles are pre-defined for a specific heading during pullout
L/D uncertainty sets	Predefined sets of uncertainty values applied to longitudinal aerodynamic coefficients (lift, drag, and pitching moment)	Sets 0 (nominal), 21 and 22	Sets correspond to specific atmosphere/wind combinations and C_M values to drive Qbar in the desired direction
DAP	Digital autopilot mode for FCS	Baseline Wrap	OPS-6 and TAL (OPS-3) only use baseline. Baseline/wrap varied for NEOM/AOA.

Various combinations of the parameters identified in tables 7-9 and 7-10 were defined in time-domain matrices created for the GRTLS, NEOM/AOA, and TAL entry flight phases. Unique sets of ICs were designed with state vectors resulting in trajectories that pushed the limits of the IGN&C system or that provided the worst-case conditions expected in flight. Simulation results exhibiting unstable, oscillatory, or otherwise questionable behavior were reviewed for understanding of FCS and IGN&C performance. In several instances, gain studies were performed to verify that the specific simulation case matched expected linear analysis results. IGN&C performance was reviewed for several other cases that had no matching FCAN documentation. To independently verify SDAP results, selected trajectories were also simulated in the A/E SES.

Time-domain results showed that the FCS performed as expected and provided required stability, response, control authority, and accuracy for nearly all trajectories. Cases that lost control or in which

other off-nominal behavior was observed during initial screening and subsequent studies were mostly predicted by the linear analysis results. The behavior of these cases, which were all in AUTO, was primarily a result of applying worst-case aero uncertainties. Only a handful of NEOM and AOA trajectories exhibited off-nominal behavior that was not predicted by linear analysis. The oscillatory behavior observed for these cases was attributed to the interaction of the FCS and guidance as simulated in the IGN&C system, not solely to the FCS. Several other cases were observed that appeared to consist of FCS oscillations or potential DAP-guidance interaction, but were later determined to be expected IGN&C performance for the specific trajectory conditions.

A/E SES Time-Domain Analysis: The role of the SES in the time-domain analysis for FCS certification was twofold. First, SES duplicated select cases from the time-domain matrices to provide an independent set of results that could be compared to SDAP results for validation. Overall, SES simulations showed acceptable comparison to SDAP for both OPS-3 and OPS-6, with most cases showing nearly identical performance. Minor observed differences were attributed to timing and algorithm differences between simulations. Second, MIL analyses performed with the A/E SES forward cockpit were used to help provide rationale for the dispositioning of some FCANs. These FCANs included CSS-specific violations or flight conditions that could not be readily achieved in SDAP. Six OPS-3 and 13 OPS-6 FCANs were taken to the A/E SES for MIL analysis.

7.6.7 Delta Certifications

The generic certification task included two delta certification activities involving angle of attack. The first, in the final iteration of the basic OPS-3 task, was performed because initial high-alpha points between Mach 4 and 9 were above the alpha envelope upper boundary when plotted against Mach rather than Vrel, as was shown in figure 7-24. Results from a delta certification of performance between Mach 4 and 9 for cases above the SODB OPS-3 alpha boundary permitted the upper and lower alpha envelope boundaries to be shifted up by 2 deg to re-center the envelope around the guidance reference alpha profile, as illustrated in figure 7-30.

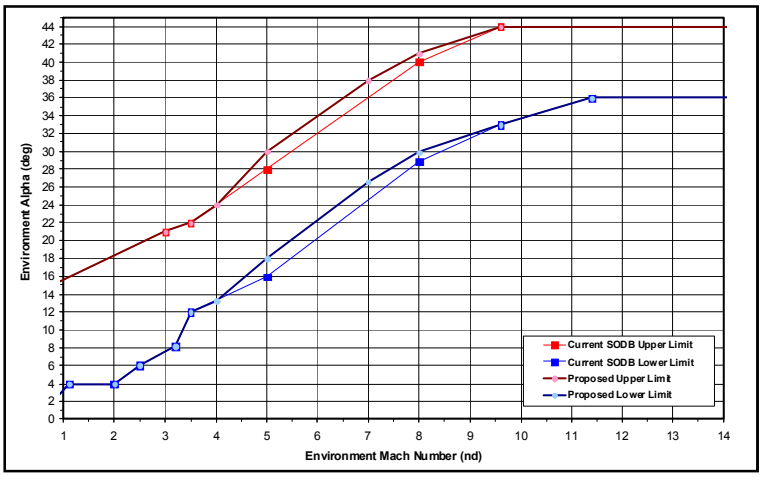

Figure 7-30. Proposed Change in OPS-3 Alpha Envelope Boundaries

The second delta certification occurred late in the program in response to a report from USA FDD that some dispersed trajectories were exceeding the upper alpha boundary for short durations above Mach 10. These exceedances occurred during roll reversals and guidance phase changes in NEOM trajectories, as well as in TAL trajectories during pullout. Rather than expand the proposed envelopes even further or make plans to disposition the failures now expected in this region on a mission-specific basis, the community decided to do a brief study verifying that these time-limited violations were acceptable. SDAP was used to create trajectories that traversed the high alpha region above Mach 10, from which points were selected for linear stability and trim analysis. Figure 7-31 shows relevant trajectory segments and selected flight conditions.

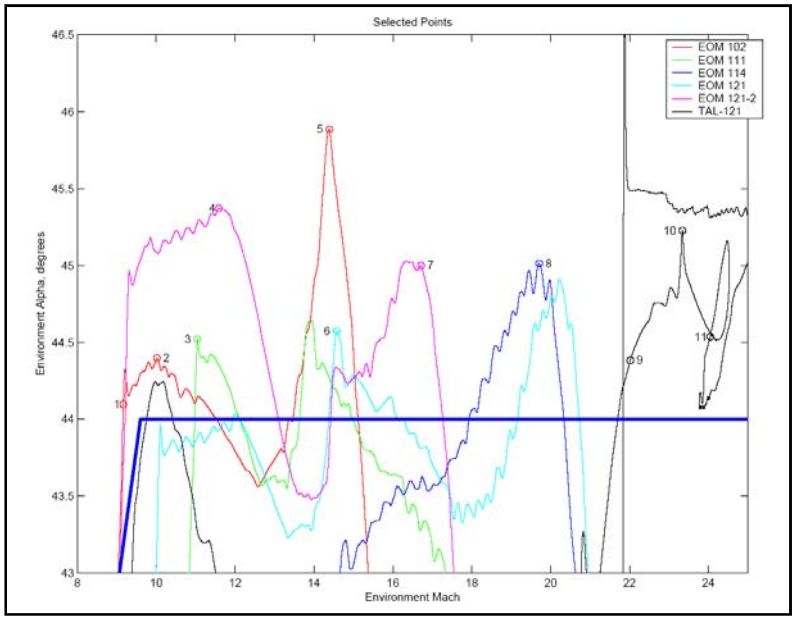

Figure 7-31. Trajectories and Test Points for High Alpha Delta Certification

From the 11 selected flight conditions, 6,408 stability test cases were generated, covering Mach 9.2 to 24, five NEOM and four TAL mass properties sets, wraparound and baseline DAPs, and the usual aero uncertainty sets. There were no stability margin requirement violations, and only 18 cases had margins below Level 2, i.e., DA requirement and DA stability. STRIM results indicated aileron trim saturation for 101 wraparound DAP and 512 baseline DAP cases. However, only 13 baseline DAP cases required more than two yaw jets for trim (2.5 jets maximum). The resulting FCAN was dispositioned with the same methods and rationale as for similar generic certification FCANs. The elevon cove limit of -16.4 deg was exceeded for 42 cases (-17.3 deg extreme), whereas elevon and bodyflap trim positions remained within bluing limits.

7.6.8 GRTLS Aileron Gain Study

The generic certification task included a special study of GRTLS stability sensitivity to the alpha-dependent component of aileron loop gain, XKALP, which was discussed in Section 3.2.7, paragraph "GRTLS GDA Logic Modification." XKALP, a multiplier on GDA that is scheduled as a function of alpha, was initially designed to improve HFGMs at high angles of attack with aft CG. When GRTLS CG locations began moving forward, LFGM requirements led to a change that modified the multiplier depending on the preflight estimate of XCG at ET-SEP. When the expected ET-SEP XCG is forward of 1,090 inches, this multiplier is 1.0 for all values of alpha. For ET-SEP XCG aft of this location, the multiplier ramps from a value of 0.5 for alpha ≥ 45 deg to 1.0 for alpha ≤ 25 deg. The purpose is to counteract the increased aileron effectiveness resulting from high alpha and more down–elevon (positive) deflection for aft XCG locations.

During STS-114 certification, reduced aileron loop HFGMs were encountered for cases with CG locations near to, but forward of, 1,090 inches at high angles of attack, where XKALP is 1.0 for all alpha. Generic certification GRTLS trajectory set 6, with nominal ET-SEP XCG of 1,090, was used to assess the effect of incorrectly estimating the XCG, resulting in use of the forward CG XKALP with aft CG, and vice versa. Test results for cases with XCG = 1,092 and using forward CG XKALP exhibit HFGM values as low as 1.8 dB, compared with 7.8 dB when the correct aft CG schedule is used. Results for cases with XCG = 1,088 using the aft CG XKALP schedule did not show similar degradation in aileron loop LFGM. It has been suggested, therefore, that consideration be given to moving the XCG value for selecting the XKALP I-load forward.

7.6.9 Conclusions

The major conclusion from this study is that the entry FCS is certified to operate acceptably within the constraints outlined in the revised entry GN&C operational limits as defined in Amendment 23 of

NSTS-08934, SODB, Vol. V, paragraph 4.2.2. Acceptable performance outside these constraints has not been verified and is not implied. The FCS design has been verified to be robust, and the Aerojet DAP (both wraparound and baseline) has excellent margins through the majority of the flight envelope. Although the GRTLS DAP shows reduced margins, performance is considered acceptable given the larger aero uncertainties and rapidly changing flight conditions.

7.6.10 Proposed Updates

Figures 7-32 and 7-33 compare the old (SODB) and new OPS-3 Qbar and alpha envelopes. Note that the OPS-3 Qbar envelope is unchanged. Corresponding comparisons for OPS-6 Qbar and alpha envelopes are shown in figures 7-34 and 7-35, respectively. Additional envelope changes and documentation updates are described in References 7-16 and 7-17. The project summary and proposed updates were approved at various boards and panels, culminating at the OCCB on August 17, 2007. The NSTS-07700, Vol. X, Book 1 updates were reviewed outside of board (OSB) by the PRCB, and Amendment 23 of the SODB, Vol. V, containing the revised IGN&C constraints, was released on September 14, 2007.

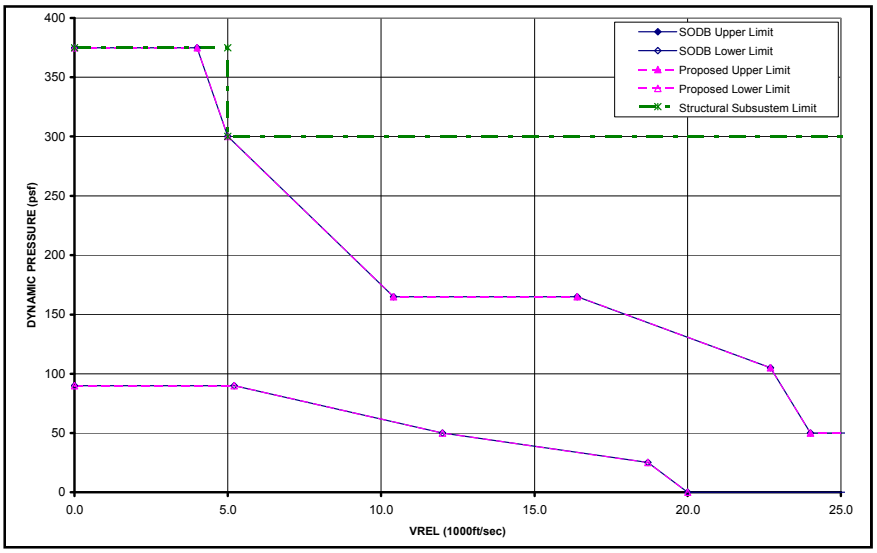

Figure 7-32. OPS-3 Dynamic Pressure Envelopes

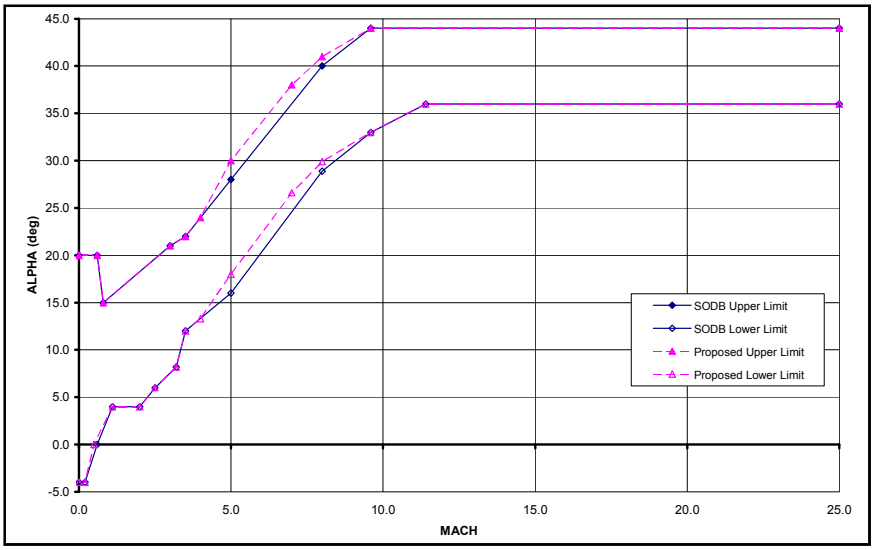

Figure 7-33. OPS-3 Angle-of-Attack Envelopes

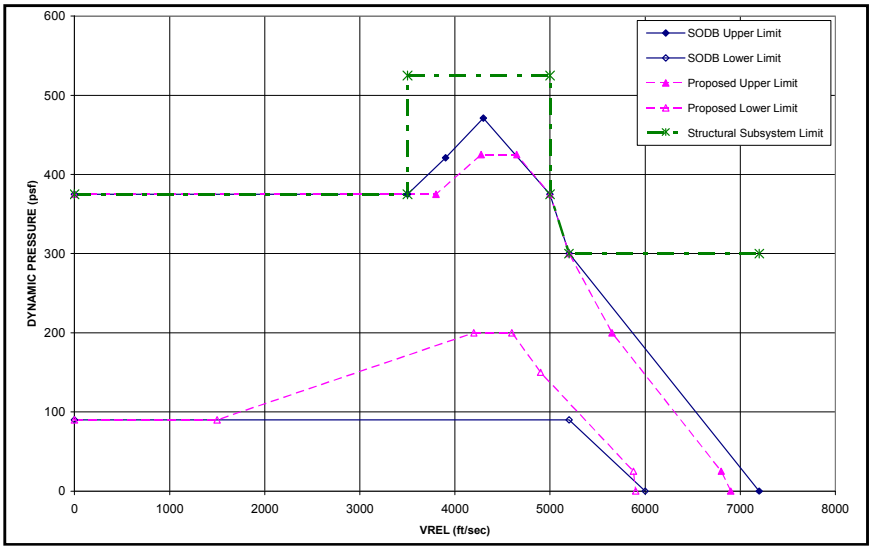

Figure 7-34. OPS-6 Dynamic Pressure Envelopes

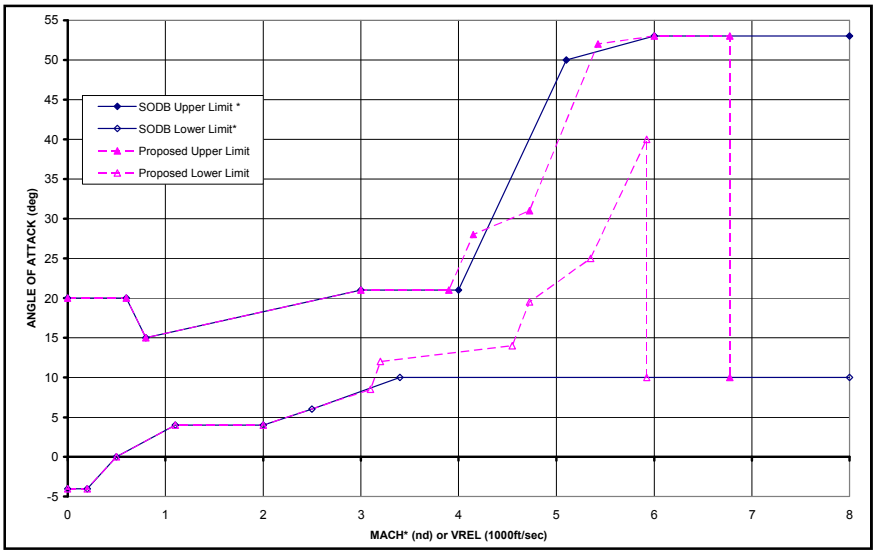

Figure 7-35. OPS-6 Angle-of-Attack Envelopes

8.0 Program Status November 2009

With the landing of STS-128 (*Discovery*) on September 11, 2009, the Space Shuttle entry FCS has successfully controlled the Orbiter through 126 entry-through-landing missions. No serious flight control anomalies or concerns have occurred since STS-1, although numerous DAP changes have been made in response to minor issues as well as to improve various aspects of control capability or to expand operational envelopes. With only six more Space Shuttle missions currently on the Launch Manifest, there are no plans for any additional DAP modifications or major performance evaluations. The generic certification results should cover all of these missions, except for possible updates needed for the month of actual flight. Flexible-body analysis is still required for each mission, however.

The return-to-flight mission-specific and generic recertification tasks have verified that the FCS design is robust and has excellent stability margins for the majority of all flight cases within ISS mission flight envelopes. Although the GRTLS DAP has known regions of reduced stability margins, these are generally due to large aero uncertainties resulting from flight conditions with angle-of-attack or elevon deflection values outside the region covered by entry aero DTO tests. Trajectory simulation evaluations demonstrate acceptable performance in these areas.

The successful accomplishment of recertification efforts is attributable in large part to gains in computing power leading to development of tools that permitted assessment of DAP performance for many more flight conditions and a much greater variety of tests than previously possible. Overall, the return-to-flight efforts of the entry GN&C community have provided many additional benefits to the Space Shuttle Program, including

1) A clear set of entry FCS requirements and understanding of how to use them
2) Corrected, improved, and modernized tools and processes
3) Renewed understanding of expected DAP performance
4) Clarification of regions of flight with low stability margins
5) Complete documentation, including reports with electronic appendices
6) A complete certification database providing support for more accurate, rapid responses to various stability and control issues that may come up on future flights
7) A searchable electronic FCAN database, including detailed documentation on each anomaly to aid in disposition of future issues
8) Improved expertise of the Houston site entry GN&C workforce

Although the processes used for FCS analysis and issue resolution were sufficient for recertification tasks, several areas for improvement that would allow added insight into vehicle performance have been identified, including

1) Step response capability to permit transient evaluation of the flight cases used for stability analysis, similar to early program capabilities
2) NAVDAD error analysis for more flight regimes than considered before certification studies
3) PVAR emulation in time-domain simulations, especially for regions in which LFGMs are deficient.
4) Landing and rollout stability models for two-point and three-point modes of operation, as previously available for 6 DOF stability analyses, response, simulation, and test.
5) Nonlinear FCS LRU (sensor and actuator) uncertainty models for SDAP
6) Integrated guidance and control linear stability model for entry

Three potential improvements to the DAP identified during the analysis are

1) Modifying the XCG value used for selecting the alpha multiplier I-load for the GRTLS aileron gain
2) Extending use of the pitch jets to Qbar = 60 psf
3) Tweaking GRTLS gain schedules to improve balance between HFGM and LFGM during pullout

One minor anomaly that has not been resolved is the phenomenon called entry wobble, which is the occurrence of two to three cycles of low-frequency roll/yaw activity in various intervals between Mach 7 and 2 of nearly every entry utilizing the wraparound DAP. Roll rate generally remains within 2 deg/sec peak-to-peak, with yaw jet pulses occasionally occurring to constrain and damp the activity. Trajectory simulations have not adequately replicated this phenomenon.

9.0 Lessons Learned

Reviews of the entry FCS history and discussions with people involved in its development resulted in several observations on lessons that had been learned during the evolution of the system. Some of the major ones are recorded in the following paragraphs.

Use of Uncertainties: When a new project is started, especially one involving a new system, detailed attention should be given to the role of uncertainties in the design, analysis, and verification process. This subject was addressed by the first question asked by Duane McRuer (Entry GN&C Committee chairman) in the “Williams Committee” review before STS-1. The results of STS-1 demonstrated the correctness of the decision to emphasize the role of uncertainties in the Space Shuttle design and verification process.

All parties involved should agree on the way that various uncertainties are to be combined. The Space Shuttle Program still does not have a consistent method for combining various uncertainties. This was a major topic of discussion during the Design Certification Reviews after STS-51L.

Lesson: The analysis and design process must include uncertainties as a key element.

Early Planning of Flight Test Program: Before the first orbital test flight (STS-1), a group of engineers started the planning and tool development to accomplish the required aerodynamic flight test program. The purpose of this effort was to gather flight test data to validate wind tunnel data and to provide a database to support a reduction in the uncertainties during entry DAP design. It was hoped that these data could be used to quickly remove the limitations on the Orbiter CG envelope.

Lesson: When a flight test program is required to remove limitations, plans and tools should be built in parallel with system development.

Tool Validation/Comparison: With the number of groups involved in this type of project, it is necessary to have a process available to ensure that all the tools being used will produce accurate results. Several times during the process, groups outside the basic community made inputs to upper management about problems they had observed that turned out to be caused by bugs in their simulations. To ensure that the primary flight control tools (e.g., SES, SIMEX, DIGIKON, CSAP, SDAP, SAIL, and FSL) always gave accurate results, two processes were started as part of the Entry 5 DAP design and maintained throughout the process.

The first process was to conduct a site acceptance of each tool by comparing data each time a major database or control system update was incorporated. This was done in three steps: 1) unit tests (e.g., aero slices, actuator step response), 2) system gain and phase margin tests, and 3) trajectory comparisons.

The second process was to obtain data from a second source before a problem was taken to upper management. This ensured that the various groups were in agreement and reduced the probability of a set-up error in generation of the data.

It should be remembered that once a problem has been identified to management, a major effort is required to close out the issue, even if no problem really existed. In some cases, even after the issue is officially closed, management will remember for a long time.

Lesson: The validation of tools is not a one-time action; the process must be continuous over the lifetime of the program. In addition, validation cases should be kept as simple as possible. Making the validation cases complicated will increase the probability of missing coding or modeling mistakes. A good example of this was the set of "common facility tests" defined early in the Space Shuttle Program. The complexity of these tests caused them to be of little use in site acceptance of the various simulation facilities.

Division of Responsibility: When management decides to split responsibility for a system, care should be taken to ensure that good lines of communication are maintained. In the failure of the initial verification effort, proper coordination between the flex and rigid body groups was not maintained; but when these two teams were combined as part of the tiger team, they produced a good design that met the requirements of both areas.

Lesson: Care should be taken to maintain close coordination between groups when responsibility for a single system has been divided.

Dual Use of Switches: When the IUS-related software changes were incorporated for STS-6, it was decided to use the same software switch to select flight control bending filters and flight control elevator schedules. This was easy to do in the software and it made the original change smaller, but it resulted in problems with the definition of mission rules and with I-load selection because the criteria for bending filter selection (payload structural characteristics) and elevator schedules (vehicle XCG) may be unrelated. This dual use was not a problem for single-payload flights, but was a real problem for multiple-payload flights such as STS-13.

Lesson: Software switches should not be used to sequence multiple functions when the selection is based on different or independent criteria.

Data Reduction Capability: Several times during the development of facilities to support the Space Shuttle Program, problems have been encountered in the collection, processing, and/or presentation of data resulting from tests. Review of results of the first test-readiness review for FSL revealed that a significant percentage of the constraints to test were related to data reduction.

Currently, in SMS, only a very limited amount of data is recorded on each run: this has resulted in problems in working with reported anomalies. A good example of this problem occurred during the initial

SMS runs with the STS-41D software. This was the first flight in which the I-load that specified the time between PTI pulses was set to zero. The initial SMS runs resulted in a loss of control that no one could understand or resolve. Almost no data were available for review from these runs; thus they were initially written off as an SMS problem. After several months had passed, a problem with the implementation of the PTI code was found by IBM.

Lesson: When a new test or training facility is being developed, the definition of the data handling system should be given the same priority as any other segment of the design.

Use of Proprietary Equipment: When a decision is made to use off-the-shelf hardware, care should be taken to make sure that NASA and contractor personnel have access to the data required to conduct a complete analysis of the effects of failures in this element on the integrated system. Failure to do so has been a problem in upgrading the landing and rollout systems. The limited amount of documentation available to the flight control community for analysis and modeling of the antiskid box and the nose gear actuator caused problems.

Lesson: While it is desirable from a cost and schedule point of view to use existing equipment, care should be taken to obtain access to the necessary system documentation.

Test Setup: During the hot fire tests, entry DST, and IUS DST, unexpected sustained oscillations were observed by the test team of flight crew and test engineers. Extensive effort was required to understand and explain the causes of these oscillations. In anticipation of this problem, according to plan, the EDST was immediately followed by open-loop structural tests. Physical measurements were obtained to correlate against model and database assumptions. The IUS DST instability, somewhat similar to the EDST anomaly, was caused by test configuration integration and setup.

Lesson: When planning FCS tests such as the entry DST or the IUS DST, LRU installation, avionics integration (LRU unit, end-to-end, closed-loop, GN&C), and interfacility site-acceptance, strong emphasis should be placed on prediction of test results before execution of the test. Pass-fail criteria as well as back-off contingency rules and procedures should be defined, and all necessary test instrumentation and data processing resources should be available.

Analysis Techniques: Two approaches were taken to the design and verification of the entry and landing DAP. The first was classical linear analysis in the frequency domain, and the second was nonlinear time-domain analysis. The linear analysis was used to identify problem areas that would require time-domain analysis. The two approaches should be used as independent cross-checks to validate analysis results.

Lesson: Both linear (frequency-domain) and nonlinear (time-domain) analyses are required for large hybrid systems such as entry control systems. Neither approach should be used as the only analysis technique.

Capturing of Design Logic: As the original system designers have retired, the maintenance of strong corporate knowledge of assumptions and constraints used in the design of the various Space Shuttle systems has become a major problem.

Lesson: Early in the design process, resources and priority must be given to the development of an archiving system to document the rationale for design decisions and to provide ready access to the baseline program by new personnel.

Uncertainties in Crew Procedures: On several occasions, the flight crew was not able to accomplish a manual task as smoothly in flight as they did in the simulations. This resulted in surprises such as the large rates seen during the STS-31 manual bodyflap pulse.

Lesson: When the crew is asked to manually accomplish a task, uncertainties in crew techniques should be evaluated just like other sources of uncertainties in the analysis process.

System Data Provision: Because of limitations in program resources and systems, the Orbiter has limited on-board data recording and downlist capability. This limitation has caused problems in the troubleshooting of both test and flight anomalies. More than once, a test has been repeated to provide additional data for anomaly resolution.

Lesson: The best possible on-board data recording capability should be provided. A small up-front cost may pay large dividends over the life of a program.

Initialization at Mode Changes: Because of the lack of a position sensor on the nosewheel, the initial command had to be open-loop. The choice was made to initialize to zero, which would limit the maximum step change at initialization. When a position sensor was added, the initialization logic was not changed. Another issue has been the running discussion on the initialization of the beta washout filter at the start of MM 602. The current logic (output = 0) was selected based on intact abort analysis; however, with the new emphasis on contingency aborts, the logic may need to be changed to output = input.

Lesson: Care should be taken to minimize the transients at mode boundaries each time a system or requirements change is made.

Manual Requirements: Late system modifications to provide additional command and control capabilities have been costly to the Space Shuttle Program. These include new and updated displays, landing aids, and control system modifications.

Lesson: A program requiring manual command and control should identify these requirements early in the program. This will reduce costly changes later.

10.0 Summary

The development, verification, and flight testing of the DAP was an evolutionary process with contributions from many organizations. The extensive preflight verification program emphasized the need to handle a wide range of variations in aerodynamic, structural, and environmental conditions. After STS-1, numerous changes were made to solve the problems identified in flight, expand the capability of the system to handle heavyweight payloads, improve the system by taking advantage of the results of the flight test program, and add margin in the landing and rollout regime.

Finally, the system, although still undergoing changes to accommodate new program requirements, has performed very well during Orbiter flights and should serve as a good example for future flight control system development programs.

References*

**Note: Documents listed below are internal to the originating organizations, and not generally available to the public.*

3-1 "Shuttle FCS Flex Engineering Analysis Standard Operating Procedures (SOP)," Rockwell International Internal Letter No. JEM-94-027, January 28, 1994

3-2 "Interaction of the STS Ascent/Entry FCS with Dominant Structure and Payload Modes," McDonnell Douglas Technical Services Co. – Houston Astronautics Division, Transmittal Memo 1,1A-TM-EH63B03-17, April 12, 1983

6-1 "Descent 248Klb Heavy Weight Orbiter Verification Final Report," Honeywell Technical Coordination Letter TCL No. SS&V 93-10, March 30, 1993

6-2 "Heavyweight Orbiter Entry Flight Control System Verification Final Report," Rockwell International Internal Letter No. 292-600-JO-93-044, March 31, 1993

6-3 "The Design of the Wraparound Digital Autopilot," Richard S. Jones (NASA/JSC-DM32) and Nicole O. Lamotte (USA-USH-423F), April 1997

6-4 "Forward Xcg Expansion Stability Certification," Honeywell Technical Coordination Letter TCL No. SS&V 98-01, January 16, 1998

6-5 "Orbiter Forward C.G. Expansion," Boeing North American presentation to CCB, October 17, 1997, K. Cason et al.

6-6 "Orbiter Forward C.G. Expansion," NASA/JSC Navigation, Control and Aeronautics Division presentation to PRCB, January 23, 1998, M. Hammerschmidt

6-7 Rockwell International, SD72-SH-0105, Vol. 1, Book 2, Part 1B, "Requirements/Definition Document Flight Control Part 1 Configuration, Performance and Functional Requirements," December 5, 1980, Rev. B, SDM-OFT Baseline

6-8 "Wraparound Digital Autopilot RCS Redline Proposal," Lockheed-Martin presentation by B. Bihari, October 2, 1997

6-9 "Wraparound Digital Autopilot RCS Redline Status," Lockheed-Martin presentation by B. Bihari, February 20, 1998

6-10 "Wraparound Digital Autopilot RCS Redline Recommendation," Lockheed-Martin presentation by B. Bihari, June 19, 1998

7-1 Boeing Report "Integrated Entry Environment Team Final Report in support of the *Columbia* Accident Investigation," May 27, 2003

7-2 "Request for Expansion of GRTLS Dynamic Pressure Envelope," RSOC Descent Flight Design presentation to Entry GN&C Meeting by Philip T. Wilson, January 16, 1996

7-3 "GRTLS Performance Envelope Expansion – GRTLS Pullout Region," USA Ascent-Descent Flight Design presentation to Entry GN&C Panel Meeting by Philip T. Wilson, December 17, 2002

7-4 "GRTLS Envelope Expansion Status Report Update – Problem Analysis," Boeing briefing prepared for ERB presentation by Milt Reed, January 28, 2004

7-5 "Status of GN&C Certification Envelope Problem Resolution," FS&SE ERB presentation, February 12, 2004

7-6 “Verification of the SODB Vol. V GN&C Constraints,” Entry GN&C Panel presentation, May 26, 2004

7-7 “Verification of the SODB Vol. V GN&C Constraints,” FS&SE ERB presentation, June 17, 2004

7-8 Boeing Document NS05HOU151A, “Entry Flight Control Systems Requirements,” December 19, 2007

7-9 Boeing IL-OFSDA-GNH-05-009, “Reverification of the Orbiter Entry Flight Control System in Support of STS-114,” To J. P. Mulholland From J. R. Harder, April 14, 2005

7-10 “STS-114 GRTLS Engineering Evaluation Effect of NAVDAD Errors,” Entry FCS DRB presentation October 20, 2004

7-11 Boeing IL-FSSE-OFSDA-05-030, “STS-121/301 FCS Assessment”

7-12 Boeing IL-FSSE-OFSDA-06-047, “STS-115 Entry FCS Assessment” (Dated 7/17/2006)

7-13 Boeing IL-FSSE-OFSDA-06-068, “STS-116 Entry FCS Assessment” (Dated 10/25/2006)

7-14 Boeing IL-FSSE-OFSDA-07-009, “STS-117 Entry FCS Assessment” (Dated 2/05/2007)

7-15 Boeing IL-FSSE-OFSDA-07-021, “STS-118 Entry FCS Assessment” (Dated 5/8/2007)

7-16 SE07HOU091, “Generic Certification of the Orbiter Entry Flight Control System” (Dated 9/28/2007)

7-17 “Entry FCS Generic Certification,” OCCB presentation, August 14, 2007,

7-18 “STS-125 Mission Specific Entry FCS Assessment Results for May or June Launch,” Entry GN&C Panel presentation, March 4, 2009

7-19 “STS-400 Mission Specific TAL and GRTLS FCS Assessment Results for May or June Launch,” Entry GN&C Panel presentation, March 18, 2009

Documents of General Applicability or Interest*

**Note: Citations preceded by an asterisk are internal to the originating organizations, and not generally available to the public.*

*RSS99D0001, “Operational Aerodynamics Data Book”

*STS 83-0007-OI-R, “Flight Software Subsystems Requirements,” Entry-RTLS DAP, FSSR for applicable software OI and rev

*JSC-19350, “Shuttle Flight Software Initialization Load, Vol. II, Mission I-Load Requirements, for Applicable STS Mission”

*Rockwell International, SD73-SH-0097, Vol. 2E “Space Shuttle Flight Control System Data Book, Vol. II – Orbiter”

Entry Flight Control Off-Nominal Design Consideration: G. P. Bayle, AIAA 82-1602

Flight Control Stability and Trim Analysis Techniques: W. L. Pierson and C. Unger, AIAA 82-1604

Space Shuttle Entry/Landing Flight Control Design Description: G. Kafer, AIAA 82-1601

Space Shuttle Orbital Landing Loads Optimization: Viet Nguyen, AIAA 1995-1202

Flexible Body Stabilization for Space Shuttle Aerosurface Control Loops: P. N. Hamilton, AIAA-1982-1532

Nonlinear Analysis of Shuttle Entry RCS Coupling With Bending Modes: J. F. L. Lee and M. F. Barrett, AIAA-1982-1533

APPENDIX A. Space Shuttle Flight History 1981 – 2009

Historical flight data charts for selected parameters plotted against relative velocity are presented in figure A-1. Data for STS-128 are shown in red, and for previous missions in grey. Where applicable, parameter limits are shown in heavy black lines. Figures A-2 and A-3 show values of the Orbiter weight and XCG location at entry interface for all flights through September 2009. RCS propellant data is shown in figure A-4 (usage due to flight DTOs has been factored out). Flights to the right of STS-94 used the wraparound DAP; these RCS data were presented with more detail in figure 6-29 of this document. Gaps in the flight data charts are due to missing download information (STS-51F and STS-61I RCS data) or loss of vehicle (STS-51L and STS-107.) Table A-1 contains historical information for all of the orbital flights through 2009 (including STS-129, although it had not yet flown at the time of writing).

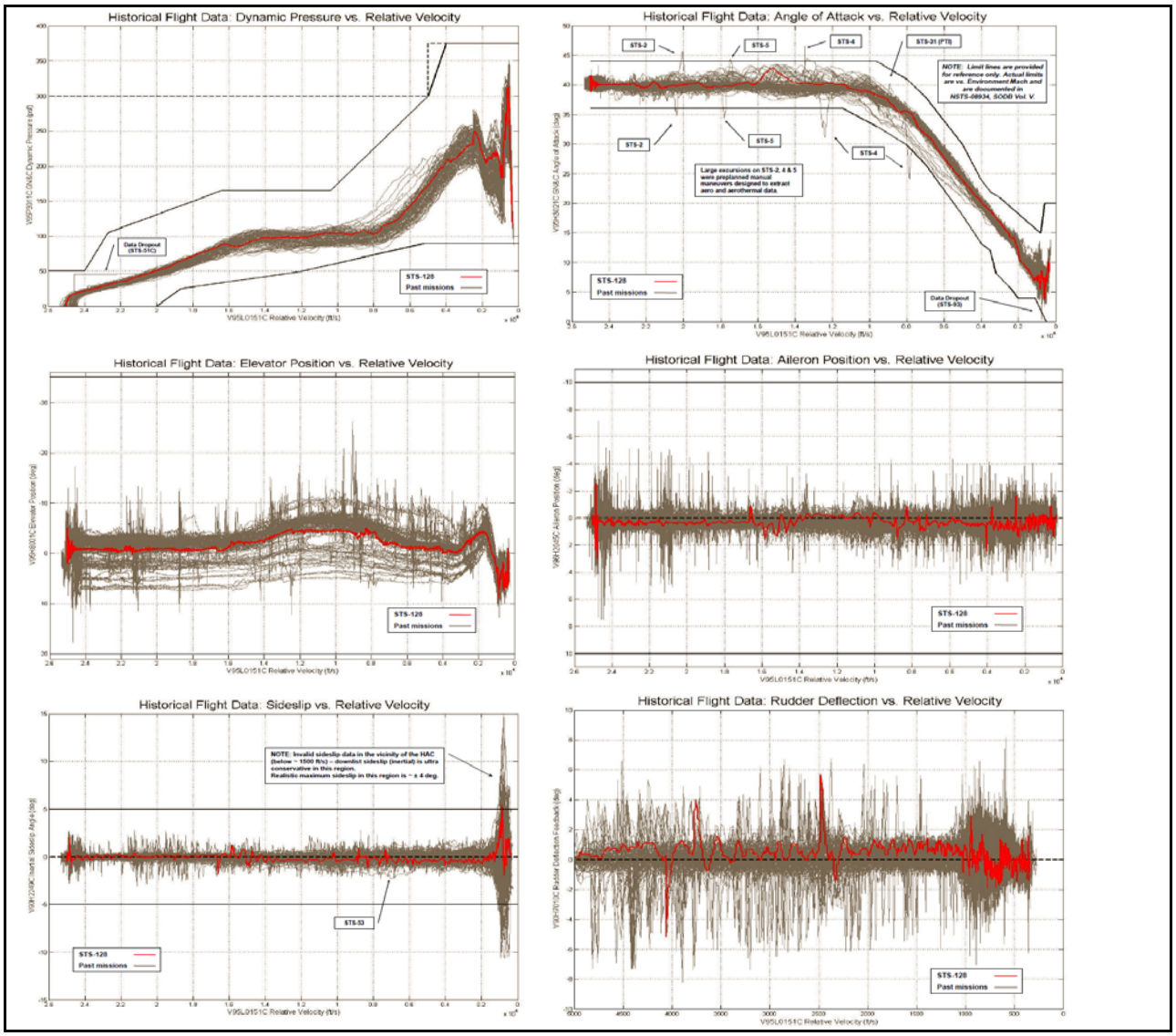

Figure A-1. Historical Flight Data Parameters for STS Missions Through 2009

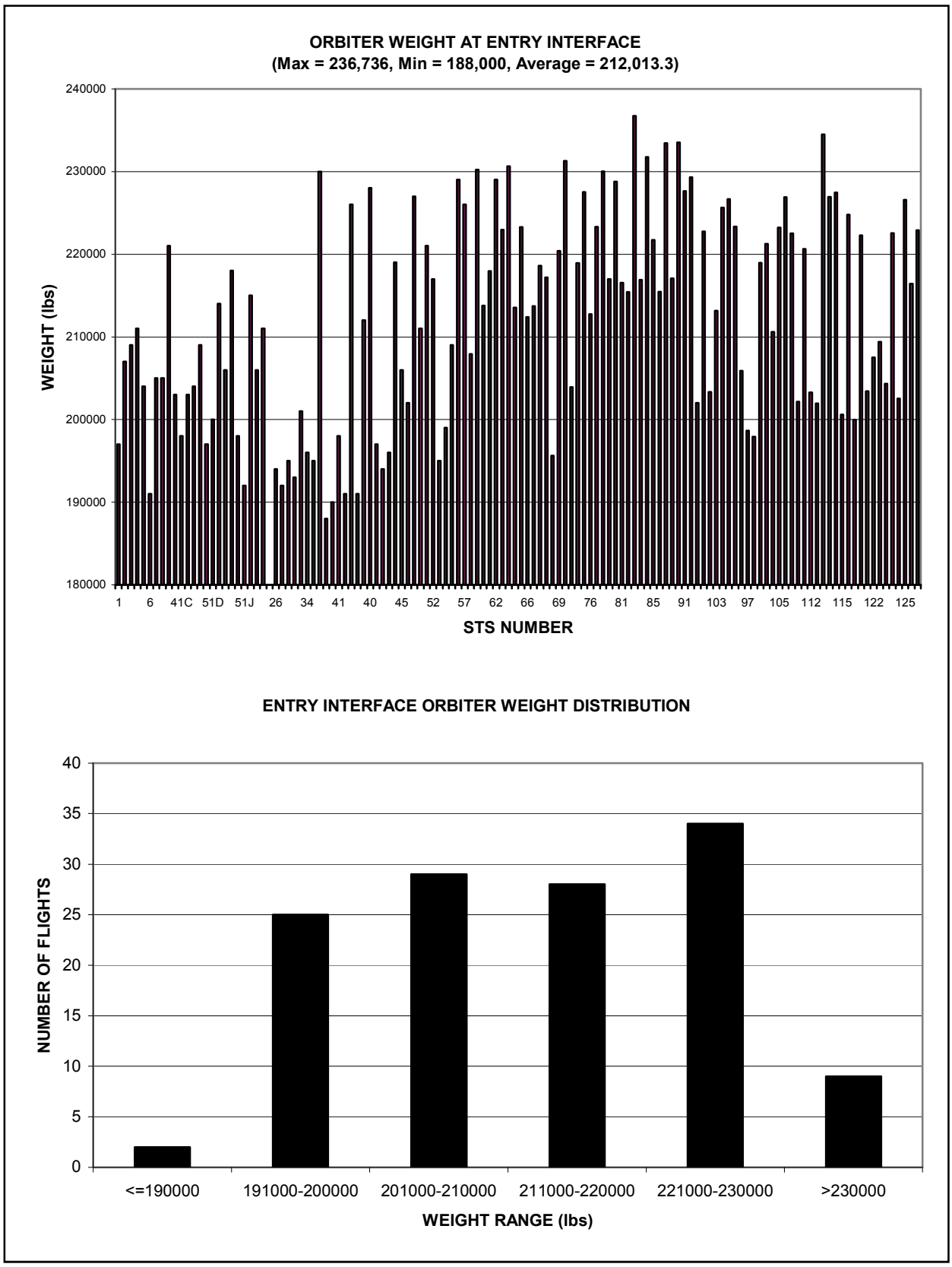

Figure A-2. Orbiter Weight at Entry Interface for STS Missions Through 2009

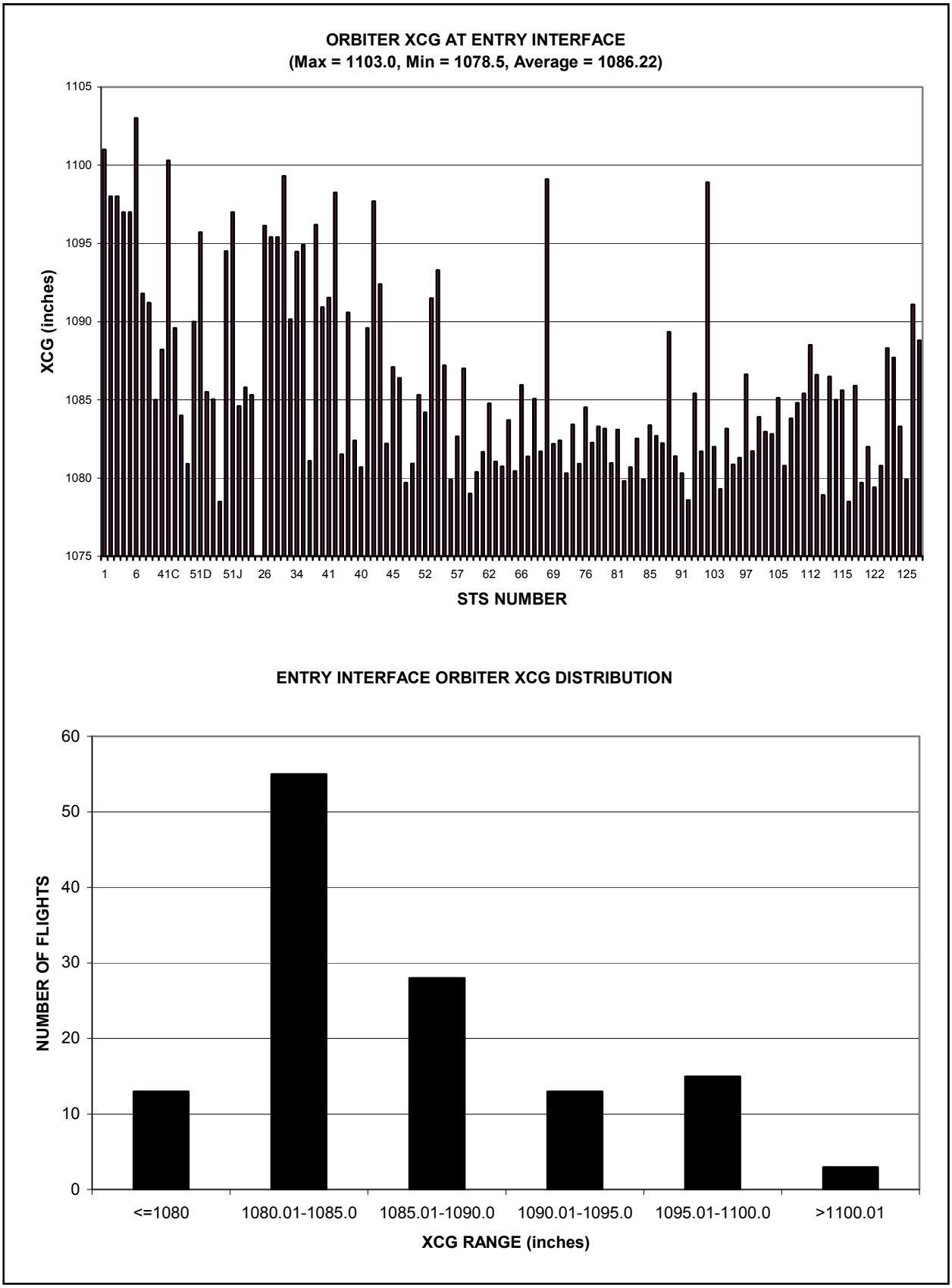

Figure A-3. Orbiter XCG at Entry Interface for STS Missions Through 2009

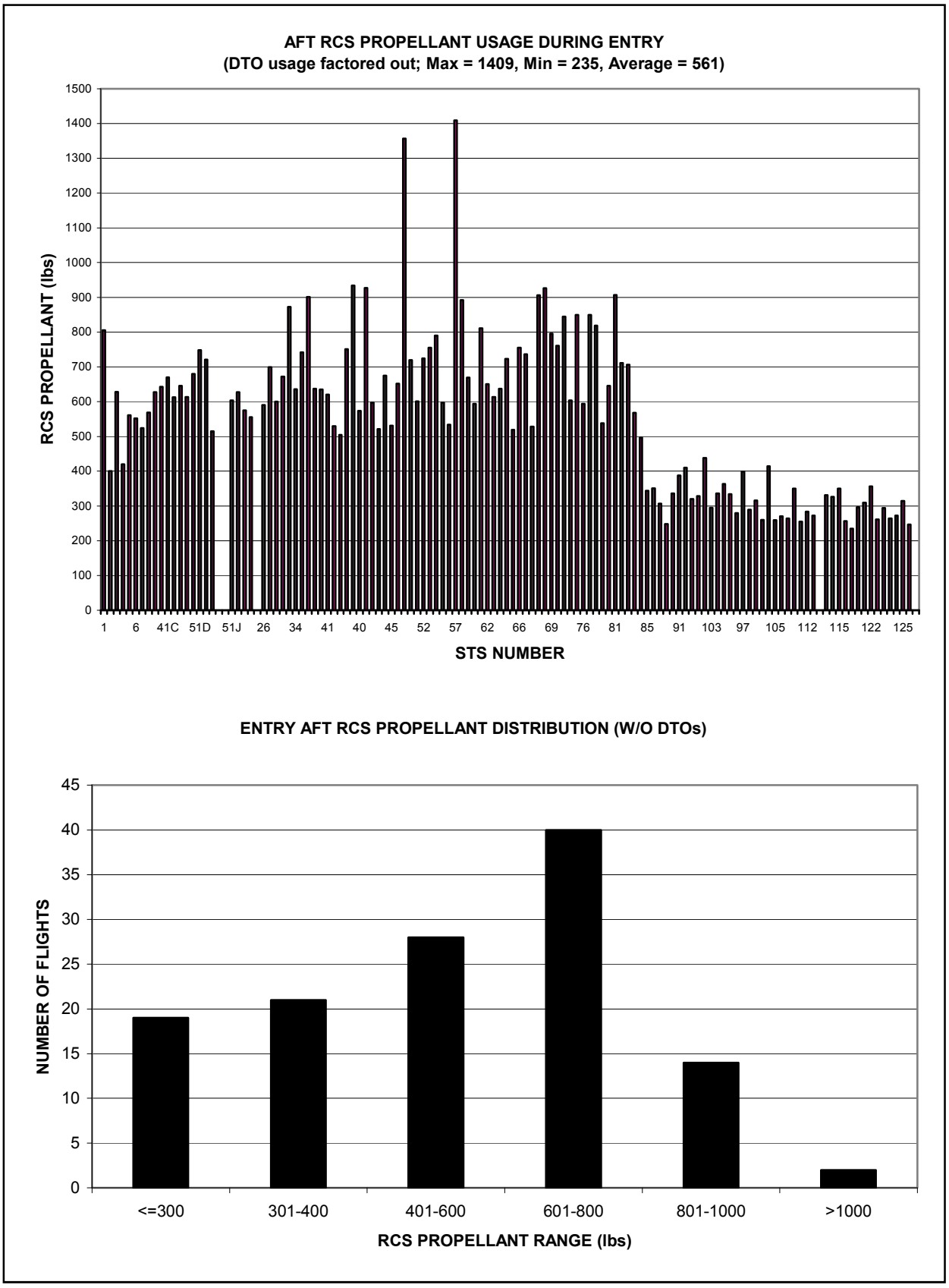

Figure A-4. RCS Propellant Data for STS Missions Through 2009

Table A-1. Space Shuttle Flights 1981-2009

Columbia - OV-102, Challenger - OV-099, Discovery - OV-103, Atlantis - OV-104, Endeavor - OV-105

Order	Launch Date	Mission	Shuttle	Crew	Duration	SW Version	Landing Site	Notes	FCS Notes
1	12-Apr-1981	STS-1	Columbia	2	2d 6h	V16	EDW23	First reusable spacecraft flight; first flight of Columbia	
2	12-Nov-1981	STS-2	Columbia	2	2d 6h	V18	EDW23	Truncated due to fuel cell problem. First test of Canadarm robot arm	
3	22-Mar-1982	STS-3	Columbia	2	8d 0h	V18	NOR17	Shuttle R&D flight, first and only landing at White Sands, New Mexico	FCS remained in AUTO until 120 ft AGS.
4	27-Jun-1982	STS-4	Columbia	2	7d 1h	V18	EDW22	Last shuttle R&D flight, first DoD payload	
5	11-Nov-1982	STS-5	Columbia	4	5d 2h	V19	EDW22	Multiple Comsat launches. First EVA of program canceled due to suit problems	
6	4-Apr-1983	STS-6	Challenger	4	5d 0h	V19	EDW22	TDRS launch; first flight of Challenger; first space shuttle extra-vehicular activity	
7	18-Jun-1983	STS-7	Challenger	5	6d 2h	V19	EDW15	First US woman in space Sally Ride; Multiple Comsat launches; First deployment and retrieval of a satellite SPAS	
8	30-Aug-1983	STS-8	Challenger	5	6d 1h	V19	EDW22	Comsat launch, first flight of an African American in space, Guion Bluford; test of robot arm on heavy payloads with Payload Flight Test Article	First night landing.
9	28-Nov-1983	STS-9	Columbia	6	10d 7h	V20	EDW17	First Spacelab mission	
10	3-Feb-1984	STS-41-B	Challenger	5	7d 23h	V20	KSC15	Comsat launches, first untethered spacewalk by Bruce McCandless II with Manned Maneuvering Unit; first landing at KSC; dry run of equipment for Solar Max rescue	
11	6-Apr-1984	STS-41-C	Challenger	5	6d 23h	V20	EDW17	Solar Max servicing (first satellite rescue by astronauts), LDEF launch	
12	30-Aug-1984	STS-41-D	Discovery	6	6d 0h	OI-4	EDW17	Multiple Comsat launches; first flight of Discovery, test of OAST-1 Solar Array	
13	5-Oct-1984	STS-41-G	Challenger	7	8d 5h	OI-4	KSC33	Earth Radiation Budget Satellite launch; First flight of two women in space Ride and Sullivan; First spacewalk by US woman, Kathryn Sullivan	
14	8-Nov-1984	STS-51-A	Discovery	5	7d 23h	OI-4	KSC15	Multiple Comsat launches, retrieval of two other Comsats Palapa B2 and Westar VI which were subsequently refurbished on Earth and reflown	
15	24-Jan-1985	STS-51-C	Discovery	5	3d 1h	OI-5?	KSC15	First classified Department of Defense (DoD) mission; Magnum satellite launch	

Columbia - OV-102, Challenger - OV-099, Discovery - OV-103, Atlantis - OV-104, Endeavor - OV-105

Order	Launch Date	Mission	Shuttle	Crew	Duration	SW Version	Landing Site	Notes	FCS Notes
16	12-Apr-1985	STS-51-D	Discovery	7	6d 23h	OI-5	KSC33	Multiple Comsat launches, first flight of a sitting politician in space, Jake Garn, first impromptu EVA of program to fix Syncom F3 (Leasat 3)	Failed tire during rollout.
17	29-Apr-1985	STS-51-B	Challenger	7	7d 0h	OI-4	EDW17	Spacelab mission	
18	17-Jun-1985	STS-51-G	Discovery	7	7d 1h	OI-6	EDW23	Multiple Comsat launches	
19	29-Jul-1985	STS-51-F	Challenger	7	7d 22h	OI-5	EDW23	Spacelab mission	
20	27-Aug-1985	STS-51-I	Discovery	5	7d 2h	OI-6	EDW23	Multiple Comsat launches, rescue of Syncom F3 (Leasat-3) by Astronauts	
21	3-Oct-1985	STS-51-J	Atlantis	5	4d 1h	OI-6	EDW23	Second classified DoD mission; DSCS satellite launch; first flight of Atlantis	
22	30-Oct-1985	STS-61-A	Challenger	8	7d 0h	OI-6A	EDW17	Spacelab mission, last successful mission of Challenger	First landing with active NWS.
23	26-Nov-1985	STS-61-B	Atlantis	7	6d 21h	OI-6A	EDW22	Multiple Comsat launches, EASE/ACCESS experiment	
24	12-Jan-1986	STS-61-C	Columbia	7	6d 2h	OI-7	EDW22	Comsat launch, flight of US Congressman Bill Nelson	
25	28-Jan-1986	STS-51-L	Challenger	7	73sec	OI-7		Planned TDRS launch, Loss of vehicle and crew, Teacher in Space Flight	
26	29-Sep-1988	STS-26	Discovery	5	4d 1h	OI-8B	EDW17	TDRS launch; first post Challenger flight	
27	2-Dec-1988	STS-27	Atlantis	5	4d 9h	OI-8B	EDW17	Third classified DoD mission; Lacrosse 1 launch	
28	13-Mar-1989	STS-29	Discovery	5	4d 23h	OI-8B	EDW22	TDRS-D/IUS, IMAX, SHARE I space station radiator experiment.	
29	4-May-1989	STS-30	Atlantis	5	4d 0h	OI-8B	EDW22	Magellan Venus probe launch	
30	8-Aug-1989	STS-28	Columbia	5	5d 1h	OI-8B	EDW17	Fourth classified DoD mission; Satellite Data System launch	
31	18-Oct-1989	STS-34	Atlantis	5	4d 23h	OI-8C	EDW23	Galileo Jupiter probe launch, IMAX	
32	22-Nov-1989	STS-33	Discovery	5	5d 0h	OI-8B	EDW04	Fifth classified DoD mission; Magnum/IUS	
33	9-Jan-1990	STS-32	Columbia	5	10d 21h	OI-8C	EDW22	SYNCOM IV-F5 satellite launch, LDEF retrieval, IMAX	
34	28-Feb-1990	STS-36	Atlantis	5	4d 10h	OI-8C	EDW23	Sixth classified DoD mission; Misty reconnaissance satellite launch	
35	24-Apr-1990	STS-31	Discovery	5	5d 1h	OI-8C	EDW22	Hubble Space Telescope launch	First flight with carbon brakes.
36	6-Oct-1990	STS-41	Discovery	5	4d 2h	OI-8D	EDW22	Ulysses/IUS solar probe launch	
37	15-Nov-1990	STS-38	Atlantis	5	4d 21h	OI-8D	KSC33	Seventh classified DoD mission. Likely SDS2-2 deployed.	
38	2-Dec-1990	STS-35	Columbia	7	8d 23h	OI-8D	EDW22	Use of ASTRO-1 observatory	
39	5-Apr-1991	STS-37	Atlantis	5	5d 23h	OI-8F	EDW33	Compton Gamma Ray Observatory launch	
40	28-Apr-1991	STS-39	Discovery	7	8d 7h	OI-8F	KSC15	First unclassified DoD mission; military science experiments	

Columbia - OV-102, Challenger - OV-099, Discovery - OV-103, Atlantis - OV-104, Endeavor - OV-105

Order	Launch Date	Mission	Shuttle	Crew	Duration	SW Version	Landing Site	Notes	FCS Notes
41	5-Jun-1991	STS-40	Columbia	7	9d 2h	OI-8D	EDW22	Spacelab mission	
42	2-Aug-1991	STS-43	Atlantis	5	8d 21h	OI-20	KSC15	TDRS launch	
43	12-Sep-1991	STS-48	Discovery	5	5d 8h	OI-20	EDW22	Upper Atmosphere Research Satellite launch	
44	24-Nov-1991	STS-44	Atlantis	6	6d 22h	OI-20	EDW05	DSP satellite launch	
45	22-Jan-1992	STS-42	Discovery	7	8d 1h	OI-20	EDW22	Spacelab mission	
46	24-Mar-1992	STS-45	Atlantis	7	8d 22h	OI-20	KSC33	ATLAS-1 science platform	
47	7-May-1992	STS-49	Endeavour	7	8d 21h	OI-21	EDW22	Intelsat VI repair; first flight of Endeavour First 3 person EVA. ASEM space station truss experiment EVA, record four EVAs total for mission.	First flight with drag chute and redundant WOW.
48	25-Jun-1992	STS-50	Columbia	7	13d 19h	OI-21	KSC33	Spacelab mission	
49	31-Jul-1992	STS-46	Atlantis	7	7d 23h	OI-21	KSC33	EURECA (European Retrievable Carrier) and the joint NASA/Italian Space Agency Tethered Satellite System (TSS)	
50	12-Sep-1992	STS-47	Endeavour	7	7d 22h	OI-21	KSC33	Spacelab mission SL-J(Japan).	
51	22-Oct-1992	STS-52	Columbia	6	9d 20h	OI-21	KSC33	LAGEOS II, microgravity experiments	
52	2-Dec-1992	STS-53	Discovery	5	7d 7h	OI-21	EDW22	Partially classified 10th and final DoD mission. Likely deployment of SDS2 satellite.	
53	13-Jan-1993	STS-54	Endeavour	5	5d 23h	OI-21	KSC33	TDRS-F/IUS launch	
54	8-Apr-1993	STS-56	Discovery	5	9d 6h	OI-21	KSC33	ATLAS-2 science platform	
55	26-Apr-1993	STS-55	Columbia	7	9d 23h	OI-21	EDW22	Spacelab mission	
56	21-Jun-1993	STS-57	Endeavour	6	9d 23h	OI-22	KSC33	SPACEHAB, EURECA	
57	12-Sep-1993	STS-51	Discovery	5	9d 20h	OI-22	KSC15	ACTS satellite launched, SPAS-Orfeus with IMAX camera.	
58	18-Oct-1993	STS-58	Columbia	7	14d 0h	OI-22	EDW22	Spacelab mission	
59	2-Dec-1993	STS-61	Endeavour	7	10d 19h	OI-22	KSC33	Hubble Space Telescope servicing	
60	3-Feb-1994	STS-60	Discovery	6	7d 6h	OI-22	KSC15	SPACEHAB, Wake Shield Facility	
61	4-Mar-1994	STS-62	Columbia	5	13d 23h	OI-22	KSC33	Microgravity experiments	
62	9-Apr-1994	STS-59	Endeavour	6	11d 5h	OI-22	KSC33	Shuttle Radar Laboratory-1	First use of "beep trim" derotation.
63	8-Jul-1994	STS-65	Columbia	7	14d 17h	OI-23	KSC33	Spacelab mission	
64	9-Sep-1994	STS-64	Discovery	6	10d 22h	OI-23	EDW04	Multiple science experiments; SPARTAN	
65	30-Sep-1994	STS-68	Endeavour	6	11d 5h	OI-22	EDW22	Space Radar Laboratory-2	
66	3-Nov-1994	STS-66	Atlantis	6	10d 22h	OI-23	EDW22	ATLAS-3 science platform	
67	3-Feb-1995	STS-63	Discovery	6	8d 6h	OI-23	KSC15	Mir rendezvous, Spacehab, IMAX	
68	2-Mar-1995	STS-67	Endeavour	7	16d 15h	OI-23	EDW22	ASTRO-2	
69	27-Jun-1995	STS-71	Atlantis	7 up, 8 dn	9d 19h	OI-24	KSC15	First Shuttle-Mir docking	
70	13-Jul-1995	STS-70	Discovery	5	8d 22h	OI-24	KSC33	TDRS-G/IUS launch	
71	7-Sep-1995	STS-69	Endeavour	5	10d 20h	OI-24	KSC33	Wake Shield Facility, SPARTAN	
72	20-Oct-1995	STS-73	Columbia	7	15d 21h	OI-24	KSC33	Spacelab mission	
73	12-Nov-1995	STS-74	Atlantis	5	8d 4h	OI-24	KSC33	2nd Shuttle-Mir docking. Delivered docking module. IMAX cargo bay camera.	
74	11-Jan-1996	STS-72	Endeavour	6	8d 22h	OI-24	KSC15	Retrieved Japan's Space Flyer Unit, 2 EVAs.	

Columbia - OV-102, Challenger - OV-099, Discovery - OV-103, Atlantis - OV-104, Endeavor - OV-105

Order	Launch Date	Mission	Shuttle	Crew	Duration	SW Version	Landing Site	Notes	FCS Notes
75	22-Feb-1996	STS-75	Columbia	7	15d 17h	OI-24	KSC33	Tethered satellite reflight, lost due to broken tether.	
76	22-Mar-1996	STS-76	Atlantis	6 up, 5 dn	9d 5h	OI-24	EDW22	Shuttle-Mir docking	
77	19-May-1996	STS-77	Endeavour	6	10d 0h	OI-24	KSC33	SPACEHAB; SPARTAN	
78	20-Jun-1996	STS-78	Columbia	7	16d 21h	OI-24	KSC33	Spacelab mission	
79	16-Sep-1996	STS-79	Atlantis	6 (exc.)	10d 3h	OI-25	KSC15	Shuttle-Mir docking	
80	19-Nov-1996	STS-80	Columbia	5	17d 15h	OI-25	KSC33	Wake Shield Facility; ASTRO-SPAS	
81	12-Jan-1997	STS-81	Atlantis	6 (exc.)	10d 4h	OI-25	KSC33	Shuttle-Mir docking	
82	11-Feb-1997	STS-82	Discovery	7	9d 23h	OI-25	KSC15	Hubble Space Telescope servicing	
83	4-Apr-1997	STS-83	Columbia	7	3d 23h	OI-25	KSC33	Truncated due to fuel cell problem	
84	15-May-1997	STS-84	Atlantis	7 (exc.)	9d 5h	OI-25	KSC33	Shuttle-Mir docking	
85	1-Jul-1997	STS-94	Columbia	7	15d 16h	OI-25	KSC33	Spacelab mission	
86	7-Aug-1997	STS-85	Discovery	6	11d 20h	OI-26	KSC33	CRISTA-SPAS	
87	25-Sep-1997	STS-86	Atlantis	7 (exc.)	10d 19h	OI-26	KSC15	Shuttle-Mir docking	
88	19-Nov-1997	STS-87	Columbia	6	15d 16h	OI-26	KSC33	Microgravity experiments, 2 EVAs, SPARTAN	
89	22-Jan-1998	STS-89	Endeavour	7 (exc.)	8d 19h	OI-26	KSC15	Shuttle-Mir docking	
90	17-Apr-1998	STS-90	Columbia	7	15d 21h	OI-26B	KSC33	Spacelab mission	
91	2-Jun-1998	STS-91	Discovery	6 up, 7 dn	9d 19h	OI-26B	KSC15	Last Shuttle-Mir docking	
92	29-Oct-1998	STS-95	Discovery	7	8d 21h	OI-26B	KSC33	SPACEHAB; John Glenn flies again	Lost drag chute door at launch (drag chute not deployed and no issues at landing.)
93	4-Dec-1998	STS-88	Endeavour	6	11d 19h	OI-26B	KSC15	ISS assembly flight 2A: Node 1. First Shuttle ISS assembly flight	
94	27-May-1999	STS-96	Discovery	7	9d 19h	OI-27	KSC15	ISS supply	
95	23-Jul-1999	STS-93	Columbia	5	4d 22h	OI-26B	KSC33	Chandra X-ray Observatory launch	
96	19-Dec-1999	STS-103	Discovery	7	7d 23h	OI-26B	KSC33	Hubble Space Telescope servicing	
97	11-Feb-2000	STS-99	Endeavour	6	11d 5h	OI-27	KSC33	Shuttle Radar Topography Mission	
98	19-May-2000	STS-101	Atlantis	7	9d 21h	OI-27	KSC15	ISS supply	
99	8-Sep-2000	STS-106	Atlantis	7	11d 19h	OI-27	KSC15	ISS supply	
100	11-Oct-2000	STS-92	Discovery	7	12d 21h	OI-27	EDW22	ISS assembly flight 3A: Z1 truss	
101	30-Nov-2000	STS-97	Endeavour	5	10d 19h	OI-27	KSC15	ISS assembly flight 4A: P6 solar arrays, radiators	
102	7-Feb-2001	STS-98	Atlantis	5	12d 21h	OI-28	EDW22	ISS assembly flight 5A: Destiny lab	
103	8-Mar-2001	STS-102	Discovery	7 (exc.)	12d 19h	OI-28	KSC15	ISS supply, crew rotation	
104	19-Apr-2001	STS-100	Endeavour	7	11d 21h	OI-28	EDW22	ISS assembly flight 6A: robotic arm	
105	12-Jul-2001	STS-104	Atlantis	5	12d 18h	OI-28	KSC15	ISS assembly flight 7A: Quest Joint Airlock	
106	10-Aug-2001	STS-105	Discovery	7 (exc.)	11d 21h	OI-28	KSC15	ISS supply, crew rotation	
107	5-Dec-2001	STS-108	Endeavour	7 (exc.)	11d 19h	OI-28	KSC15	ISS supply, crew rotation	
108	1-Mar-2002	STS-109	Columbia	7	10d 22h	OI-28	KSC33	Hubble Space Telescope servicing, last successful mission for Columbia before STS-107	
109	8-Apr-2002	STS-110	Atlantis	7	10d 19h	OI-29	KSC33	ISS assembly flight 8A: S0 truss	

Columbia - OV-102, Challenger - OV-099, Discovery - OV-103, Atlantis - OV-104, Endeavor - OV-105

Order	Launch Date	Mission	Shuttle	Crew	Duration	SW Version	Landing Site	Notes	FCS Notes
110	5-Jun-2002	STS-111	Endeavour	7 (exc.)	13d 20h	OI-29	EDW22	ISS supply, crew rotation, Mobile Base System	
111	7-Oct-2002	STS-112	Atlantis	6	10d 19h	OI-29	KSC33	ISS assembly flight 9A: S1 truss	
112	23-Nov-2002	STS-113	Endeavour	7 (exc.)	13d 18h	OI-29	KSC33	ISS assembly flight 11A: P1 truss, crew rotation, last successful mission before STS-107	
113	16-Jan-2003	STS-107	Columbia	7	15d 22h	OI-29	N/A (KSC33)	SPACEHAB; Loss of vehicle and crew before landing at KSC	
114	26-Jul-2005	STS-114	Discovery	7	13d 21h	OI-30	EDW22	First post Columbia flight. Flight safety evaluation/testing, ISS supply/repair, MPLM Raffaello	
115	4-Jul-2006	STS-121	Discovery	7 up, 6 dn	12d 18h	OI-30	KSC15	ISS Flight ULF1.1: Supply, crew rotation, MPLM Leonardo	
116	9-Sep-2006	STS-115	Atlantis	6	11d 19h	OI-30	KSC33	ISS assembly flight 12A: P3/P4 Truss, Solar Arrays	
117	9-Dec-2006	STS-116	Discovery	7 (exc.)	12d 21h	OI-30	KSC15	ISS assembly flight 12A.1: P5 Truss & Spacehab-SM, crew rotation	
118	8-Jun-2007	STS-117	Atlantis	7 (exc.)	13d 20h	OI-30	EDW22	ISS assembly flight 13A: S3/S4 Truss, Solar Arrays, crew rotation	
119	8-Aug-2007	STS-118	Endeavour	7	12d 18h	OI-30	KSC15	ISS assembly flight 13A.1: S5 Truss & Spacehab-SM & ESP3. First use of SSPTS (Station-to-Shuttle Power Transfer System)	
120	23-Oct-2007	STS-120	Discovery	7 (exc.)	15d 2h	OI-32	KSC33	ISS assembly flight 10A: US Harmony module, crew rotation	
121	7-Feb-2008	STS-122	Atlantis	7 (exc.)	12d 18h	OI-32	KSC15	ISS assembly flight 1E: European Laboratory Columbus, crew rotation	
122	11-Mar-2008	STS-123	Endeavour	7 (exc.)	15d 18h	OI-32	KSC15	ISS assembly flight 1J/A: JEM ELM PS & SPDM, crew rotation	
123	31-May-2008	STS-124	Discovery	7 (exc.)	13d 18h	OI-32	KSC15	ISS assembly flight 1J: JEM - Japanese module Kibo & JEM RMS	
124	14-Nov-2008	STS-126	Endeavour	7 (exc.)	15d 20h	OI-33	EDW04L	ISS assembly flight ULF2: MPLM Leonardo, crew rotation	Landed on shortest and narrowest runway ever.
125	15-Mar-09	STS-119	*Discovery*	7 (exc.)	12d 19h	OI-33	KSC15	ISS assembly flight 15A: S6 Truss, Solar Arrays	
126	11-May-09	STS-125	*Atlantis*	7	12d 21h	OI-33	EDW22	Last Hubble Space Telescope servicing mission (HST SM-04). Final Non-ISS flight.	
127	15-Jul-09	STS-127	*Endeavour*	7 (exc.)	15d 16h	OI-33	KSC15	ISS assembly flight 2J/A: JEM Exposed Facility (EF) & JEM ELM ES.	
128	28-Aug-09	STS-128	*Discovery*	7 (exc.)	13d 21h	OI-33	EDW22	ISS assembly flight 17A: MPLM Leonardo & 6 person ISS crew.	
129	NET 11/16/2009	STS-129	*Atlantis*	6/7 (exc.)	~11d	OI-33		ISS assembly flight ULF3: ExPRESS Logistics Carriers (ELCs) 1 & 2.	Not yet flown

APPENDIX B. Key Individuals

The following is a list of many of the individuals who contributed to the design, development, test, and evaluation of the Space Shuttle Entry FCS. These names reflect a rather hurried recent collective memory dump of several people who have been involved with the program for longer and shorter durations. There are undoubtedly many more names that should be on this list, and apologies are extended for these omissions.

Ken Alder
Jim Bailey
Dave Bateman
Guy Bayle
Dale Bennett
Nick Berlage
Brian Bihari
Thom Brown
Clint Browning
Kyle Cason
Tom Chase
Dick Cleary
Doug Cooke
Wes Dafler
Mr. DeJulia
Ray DeVall
Ed Digon
Dave Dyer
Les Edinger
Joe Engle
Bob Epple
Dr. Steve Everett
Maury Fowler
Gordon Fullerton
Joe Gamble
Don Gavert
Dave Gilbert
Ernie Golan
Ken Hahn
Phil Hamilton
Mark Hammerschmidt
Jim Harder
Hank Hartsfield
Russ Hendrick
Dr. Ken Illif
Dr. Dai Ito
Jack Jansen
Doug Johnson
Gordon Kafer
Paul Kirsten
Jake Klinar
Leo Krupp
Howard Law
John Lee
Chaing Lin
Greg Loe
Ken Mattingly
Robbie McAfoos
Bill McGuire
Larry McWhorter
Glen Minott
Al Moyles
Terry Mulkey
Dan Nelson
Viet Nguyen
John Nishimi
Lee Olsen
Bernie Olson
Tom Payne
Dr Robert. Peterson
Ken Radde
Milt Reed
Bob Reitz
Buddy Schubele
Space Shuttle Astronauts
Ernie Smith
Scott Snyder
Butch Stegall
Howard Stone
Jeff Stone
Alan Strahan
Tru Surber
Tom Tanita
FSL Support Team
SAIL Support Team
John Thuirer
Ron Toles
Gus Tsikalis
Charlie Unger
Brenda Weber
Walt Williams
Dave Wilson
Phil Wilson
Vince Wong
Earl Woosley
John Yeichner
Michael Zyss

APPENDIX C. Approach and Landing Test Flight Phase

(Contributed by Gordon C. Kafer, BATECH)

C.0 Introduction

This addendum complements the entry flight control system (FCS) history by providing a brief walk-through for the atmospheric mission phase, Mach < 3.5, development, after Authority to Proceed (ATP) in 1972, concluding with the Approach and Landing Test (ALT) flights in 1977. There is an extensive collection of archival materials for the development and test of the first integrated spacecraft/winged aircraft, with its quad-redundant avionics architecture. Countless individuals contributed to the success of the system; this material presents one designer's viewpoint.

The objective is to summarize and guide the reader on the following:

- Background before the FCS contract award in 1973
- FCS performance requirements
- Key FCS line replaceable unit (LRU) and digital autopilot (DAP) design and development drivers
- Features of the Horizontal Flight Test (HFT) and ALT control laws
- ALT results
- Some lessons learned

Major activities and history of the program can be found in the references listed under "Suggested Readings" at the end of this appendix. Figure C-1 presents an overview of the Design, Development, Test, and Evaluation (DDT&E) program schedule.

Phase/Milestones		ATP	FC/HFT	ALT	ALT
A	B	C, C'	C	CDR	Jun-Oct
1969	1970	1972	1973	1975	1977
|	|	|	|	|	|
Δ	Δ	Δ	Δ	Δ	Δ > OFT

Legend/Notes: Phase A (Mission Concepts), B (System Requirements), C (Design Definition): ATP (Authority to Proceed), FC/HFT (FCS/Horizontal Flight Test). ALT (Approach and Landing Test), CDR (Critical Design Review), OFT (Orbital Flight Test)

Figure C-1. DDT&E Program Schedule

C.1 History

The Orbiter is an unstable airframe, laterally in the supersonic atmospheric flight regime and longitudinally in the subsonic flight regime. Thus full-time flight control augmentation is required. Flight control design issues/drivers are listed below. Supersonic lateral-directional control was a significant challenge, particularly for an aerosurface-only system, leading to the use of the yaw jets. Flight path control during landing was a major driver for the hardware/software design to yield adequate flying qualities. The close-coupled delta planform, with its large pitch inertia and adverse $Z_{\delta e}$ effect on performance, exacerbated control power, saturation, sensitivity, response time, and pilot-induced oscillation (PIO) problems.

Fundamental drivers in addition to size, weight, power, time, and cost, included

- Flight phase mission(s): broad envelopes for Level 1, 2, and 3 performance
- Static stability (trim/controllability)
- Dynamic stability (rigid and flex body, small and large signal) vs. response
- Aerodynamic and structural mode uncertainties
- Subsystem error/tolerance allocations
- Aerosurface actuators: bandwidth, control power (displacement, rate, hinge-moment), nonlinearities, and accuracy

- Sensors: dynamics, accuracy and nonlinearities, redundancy and location
- Pilot/system response requirements and handling qualities: rotational hand controller (RHC) and physical cues
- General purpose computer (GPC) DAP sampling rates, transport lags, memory, and multiplexer-demultiplexer (MDM) quantization
- Gain scheduling
- Control limiting: command, authority, and rate
- Fail op/fail safe (FO/FS) avionics: failures, moding, downmoding, and reconfiguration
- Robustness to accommodate mission, vehicle and payload changes

Table C-1 presents an overview of the FCS design history as affected by some of these design drivers.

Table C-1. Some FCS Design History Overview

Mach ≤ 3.5 Design Drivers	Preliminary Design, M ≤ 3.5	Revised HFT/ALT Baseline Vehicle 147B Derived
Mission(s), vehicle, program with ascent/orbital/descent trades (manual controls (RHC), FO/FS avionics, the fundamental bandwidth issue)	Powered flight – retractable jet engines or strap-ons for ferry flight, aerosurface control only, manual body flap – full up, down or trail for CG balancing, classical (proven) control technologies – proportional-plus-integral control laws with fixed gains-time/event switched. Landing: go-around, jet-engine swing-wing vs. delta wing configurations, and with an engine-out. Command limiting and stall prevention; minimum backup FCS; redundancy control and DAP checkout control of FCS hardware test operations.	Unpowered* (Shuttle Carrier Aircraft [SCA] for ferry flights), yaw reaction control system (RCS) for supersonic lateral-directional control; measured air-data for guidance, navigation, and control (GN&C) applications. *Since ••=•••-••, for an attitude hold (cruise) autopilot ••=-•• and the pilot flight path control task is made difficult; the HFT DAP attitude hold and indicated air speed (IAS) control functions were eliminated from the ALT baseline control modes. Guidance provides flight path control commands to the FCS
Flight computer	Dedicated (special purpose) 50 Hz for critical paths, 12 bit	GPC Multi-rate: hi-freq 25 Hz, 10 bit
Elevon servo-loop (Hydraulic Research actuator subsystem)* *Moog baselined for OFT	50 rps with 50 rps 1st order aerosurface amplifier (ASA) noise filter, 30 deg/sec elevator and aileron.	20 rps, with 2nd order ASA prefilter yielding an equivalent 10 rps subsystem to satisfy overall performance (stability, response, handling qualities) and resolve small signal quantization effects (e.g., ratchet/rumble – actuator reliability) experienced in Palmdale ground test.

Specifications, requirements, and extensive treatments of response characteristics that provided design engineers with guidelines for flying qualities were available in the Space Shuttle design era, but all dealt with conventionally powered aircraft operating in the subsonic or low-supersonic flight regimes. NASA published a Space Shuttle Flying Qualities Specification to be used as a guideline, which, along with military specifications (MIL Specs) and program experiences, supported GN&C system development.

C.2 FCS Procurement Specification

The FCS procurement specification, MC621-0043, was developed based on applicable MIL Specs, NASA Flying Qualities Requirements (MSC-07151 [1973 internal working paper]), industry experience, simulation, and analysis. The reader is advised to refer to D.W. Gilbert's paper entitled "Space Shuttle Handling Qualities" presented at the NASA JSC Conference, From Challenge to Achievement, June 1983.

The MSC-07151 flying qualities working paper was recommended for those portions of the Orbiter flight for which MIL Spec 8785B has application. Where not addressed in the MSC–07151, class III, Level 1, for powered modes, and class IV, for unpowered modes, should apply. MIL 8785B was to be utilized to ensure that response criteria were consistent with experience from vehicles demonstrating good manual

mode flying qualities. Also, from the August 1973 informal working group meeting, suggested requirements for use in preparation of the FCS procurement specification included

- The need for class IV response and traditional MIL Spec handling qualities during landing for both the pitch and lateral axes with crew comment that "it lands like a dive bomber, it better fly like a dive bomber"
- Incorporation of MIL Spec wording on PIO avoidance
- The class II requirement to yield $\Delta\varphi$ = 30 deg in 1.8 sec for low speed subsonic flight

Note that Table 3.1-1 of the SD72-SH-0105-1 Approach and Landing Test requirements section states, "Ground Effects shall be included in trajectory studies only." Also, HFT/ALT stability and response analysis/simulation was performed only for airborne operation. (Note: This is not to be interpreted as negative. Modeling, database development, tool implementation, and validation tasks were out of scope for analyses of the low-altitude flight phase; stability and response were assessed via trajectory simulations.) Ground proximity and ground vehicle performance were evaluated using time-history trajectory, including man-in-the-loop (MIL), simulations. Touchdown and rollout requirements were to control within gear and tire-load limits, steering control to the runway centerline, and directional control to be stable (via simulation assessment).

C.3 FCS Design Requirements

The following references comprise the collection of specifications and databases for use in the design of the FCS; the next paragraph presents the design problem considerations.

- FC System Specifications:
  - Honeywell FC Subsystem Spec - 1973
  - SSFCS Procurement Spec - MC621-0043, 1973
  - SDM Baseline - SD72-SH-0105, 1976 and revisions, which were based on
    - MSC-07151 - Orbiter Flying Qualities
    - MIL 8785 - Flying Qualities
    - MIL 9490/1797 - USAF Specification
    - MIL 18244 - NAVY Specification
    - Space Shuttle analyses and simulation, system analyses engineering requirements definition, and Sperry Autoland contract work products
- Database assumptions for the preliminary atmospheric FCS design:
  - Orbiter configuration 147B, Aerodynamics Data Book - SD72-SH-0060-1E, 1973
  - Guidance & Control Data Book - SD73-SH-0097A, 1973
  - Digital Flight Control Software Design Requirements, JSC 07759, 1973 [internal document]

Basically, system analysis is the procedure for optimizing an autopilot to the vehicle in which it is to be used. Separate from formal specifications, engineering experience and judgment are required to define an effective and economical product that provides acceptable performance. Methodologies differ; there is no absolute best solution for control mode selection or gain and filter scheduling for stability augmentation and manual/automatic command response. Sensor and input signal definition requires careful consideration for something that can even appear trivial: e.g., $\bar{q}$, Mach vs. $\bar{q}$, or altitude scheduling; TAS vs. EAS vs. IAS speed parameter use; or fixed vs. scheduled feedback time constants and gains to compensate the widely varying airframe dynamics. The tradeoffs and selection of force effectors was, in my view, the single most demanding design task. Indeed, the STS presented a challenging design problem.

C.3.1 FCS Stability Requirements

Table C-2 presents FCS stability requirements as defined in MIL Spec 9490 and as defined in the Orbiter FCS Procurement Specification. It should be noted that the preliminary ALT rigid body design goal was 12-dB gain margins and > 45-deg phase margins.

Table C-2. FCS Stability Requirements Comparison

MIL Spec 9490 (circa 1970) – Minimum Stability Margins*			
Mode Frequency, f_m	**Below $V_{0\ min}$**	**$V_{0\ min}$ to $V_{0\ max}$**	**At V_1**
f < 0.06 Hz	GM = 6 dB (no PM requirement)	GM = 4.5 dB PM = 30°	GM = 3.0 dB PM = 20°
0.06 Hz < f < 1st flex mode	GM = 6 dB (no PM req)	GM = 6.0 dB PM = 45°	GM = 4.5 dB PM = 30°
f > 1st flex mode	GM = 6 dB (no PM req)	GM = 8.0 dB PM = 60°	GM = 6.0 dB PM = 45°
Note: V_0 = operational speed, V_1 = limit speed * As an alternative, the contractor may elect to perform sensitivity analysis and analytically justify margins of up to 50% less than specified values.			
FCS Procurement Spec Minimum Stability Margins			
Frequency f	**Level 1**	**Level 2**	**Design Assessment**
f < 6 Hz Note: Orbiter flex modes are in the ≈ 3.5 – 4.5 Hz range	LFGM = 12 dB HFGM = 6 dB **ALT PM = 45°** OFT PM = 30° Stable large signal	LFGM = 4 dB HFGM = 4dB PM = 20° Stable large signal	GM = 0 dB, PM = 0° or greater as a design goal. Minimum safe operation to a safe landing.
f > 6 Hz	Gain < -6 dB	Gain < -4 dB	All flex modes stable
Long term stability: margins not required, time to double amplitude required			

C.3.2 FCS Response Requirements

MIL Spec (circa 1970)

- Longitudinal time response requirements were expressed in terms of frequency vs. relative damping ratio, and frequency vs. Nz, etc. Roll response was based on time to achieve 30 deg bank angle and time to 63% of the command response with lateral coordination..
- An allowable response delay for Level 1, 2, and 3 flying qualities specified between 0.1 and 0.25 sec.

FCS Procurement Spec (Systems Definition Manual [SDM])

- Time response envelopes were a composite of the MSC-07151 definition, simulation study, and other available criteria including, for example, flight test experience on the F-8 FBW, X-15, C-5A, YF-12/SR-71, X-20, SST and Viggen JA-37 DFCS.
- The preliminary atmospheric flight phase analytic design utilized the C*criteria for longitudinal control.
- Lateral control was conventional with computed coordination versus hi-passed yaw rate.

Flying qualities (handling) from a Cooper-Harper rating (CHR) viewpoint requires attention to the vehicle's stability, maneuver response and controllability, and the pilot's and/or automatic system capabilities.

The fundamental problem for the control system designer is to balance the design to effect acceptable low-, mid-, and high-frequency stability and response performance, and to do so without causing structural resonances and instability. Flight control requirements address small and large signal stability, response to manual and automatic commands, turn coordination, trim, control effectiveness, switching transients, control rate, position and hinge moment limiting, and vehicle motion limiting (p, Nz, Ny, beta, gear/tire loads, etc). System stability affected by nonlinearities (authority, hinge-moment and rate limiting) is of paramount concern.

Figure C-2 illustrates a generalized step response envelope. Table C-3 lists time response parameters as defined in MSC-07151 and in the FCS SDM for ALT.

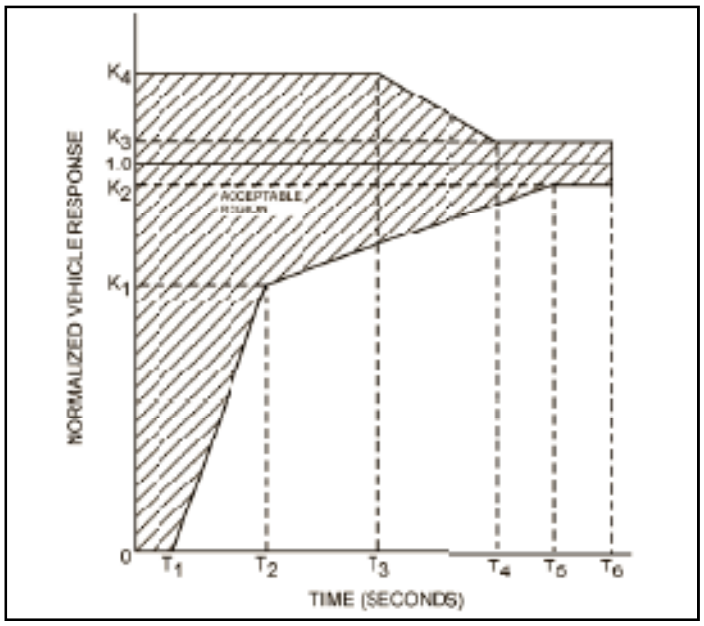

Figure C-2. Generalized Step Response Envelope

Table C-3. Time Response Parameters for ALT

MSC-07151						
	T_1	**$T_{70\%}$**	**$T_{95\%}$**	**$T_{105\%}$**	**T_{SS}**	**Overshoot**
Subsonic	0.2	1.0	2.0	3.0	4.0	25%
Supersonic	0.3	1.5	3.0	4.5	6.0	25%
ALT						
	T_1	**$T_{83\%}$**	**$T_{95\%}$**	**$T_{105\%}$**	**T_{SS}**	**Overshoot**
Pitch Rate	0.2	1.0	5.0	5.0	8.0	30%
	T_1	**$T_{63\%}$**	**$T_{90\%}$**	**$T_{110\%}$**	**T_{SS}**	**Overshoot**
Roll Rate	0.2	1.0	3.0	6.0	8.0	25%

During the FCS detailed design phase, it became apparent that the time response performance requirements would not be satisfied. This was due to DAP forward loop bandwidth considerations (low bandwidth actuators, GPC sampling rates and inherent delay, command shaping and filtering, subsystem nonlinearities, smoothing the 25-Hz commands) that established the balance for overall FCS baseline performance. Following the ALT program, and subsequent hardware and DAP updates for incorporation into the OFT baseline, the SDM was revised to reflect subsonic performance capabilities. For example, T1, which reflects system lags and delays, and thus affects human factors through control sensitivity, was changed to 0.4 sec for OFT.

C.4 FCS Phase C Design Evolution Summary

To describe in detail the evolution of the atmospheric control system would be nearly impossible. The FCS as depicted in figure C-3 has extraordinary design and implementation complexity. OFT baseline documentation is extensive; however, there is no concise case history of detailed design of the OFT precursor, the ALT FCS. Nor does this report, which is intended to present only an overview of the design history, provide all the details. There are numerous books and guides for the design of an air-vehicle control system. Necessarily, each design affects a solution to the new system requirements. Fundamental to any design is the stability and command structure, its control modes, feedbacks, sensed

inputs, and command outputs. The control laws of the Orbiter reflect classical proportional-plus-integral (PI) control system theory and traditional experience and technologies from previous programs.

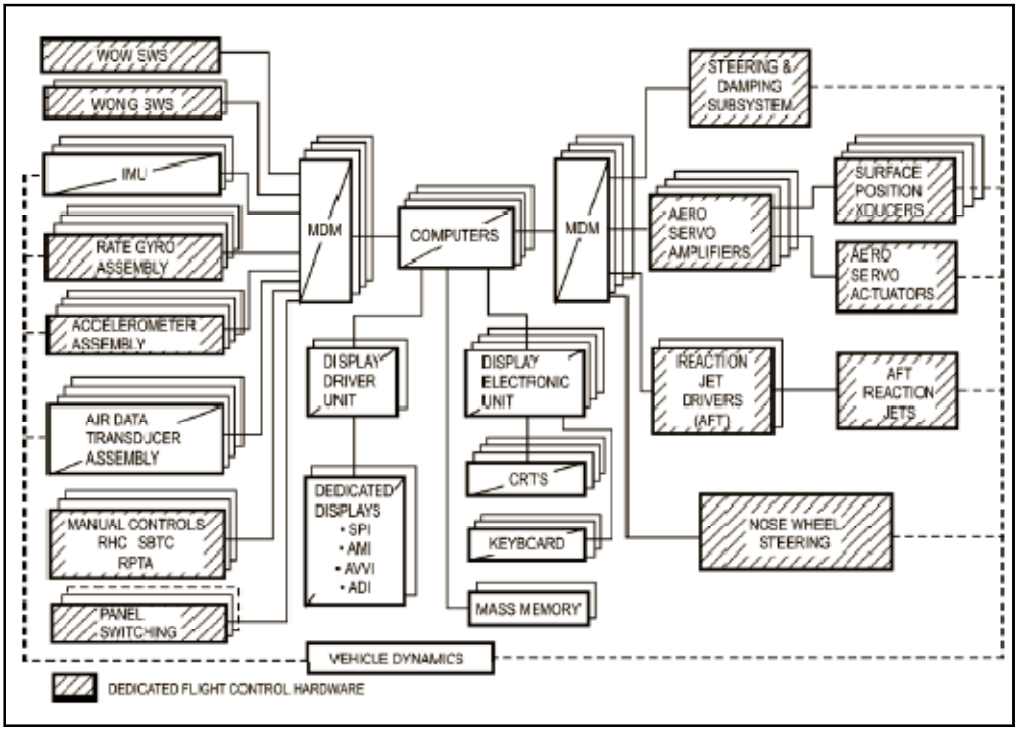

Figure C-3. Entry FCS Hardware Elements

C.4.1 HFT FCS – DAP Overview

Following requirements definition, database tool implementation, and control mode formulation, the design engineer can proceed. The modes for use in the HFT system (powered flight) are listed below. Associated command augmentation system (CAS) block diagrams are provided in figures C-4, C-5, and C-6 to describe the inputs, loop processing functions, and outputs of the pitch, roll, and yaw axes, respectively. Details of the design are not provided graphically or in text because such presentation was considered extraneous for this overview.

- Control modes
  - 3-axis manual direct, DAP software implementation (MD) – elevon, rudder
  - 3-axis stability/command augmentation (CAS)
  - Pitch attitude hold
  - Roll attitude hold
  - Auto TAEM – θ and φ guidance commands
  - Autoland – Nz, IAS, φ, and rollout guidance commands
- Sub-modes
  - MD speedbrake (SB)
  - IAS speedbrake
  - MD bodyflap – 3-position selection

    - Auto bodyflap – 3-position = f(SB, CG)
    - MD nosewheel
    - Auto nosewheel
- Pitch axis C* proportional plus integral (PI) control with:
    - Command signal limiting (N_z, α)
    - Up-elevon (φ)
    - Speedbrake cross-feed
    - Air-data (h < 80,000 ft) M, $\bar{q}$ scheduling
- Lateral axes (PI) control with:
    - Computed turn-coordination vs. classic high-passed yaw rate system
    - No roll auto-trim subsonic

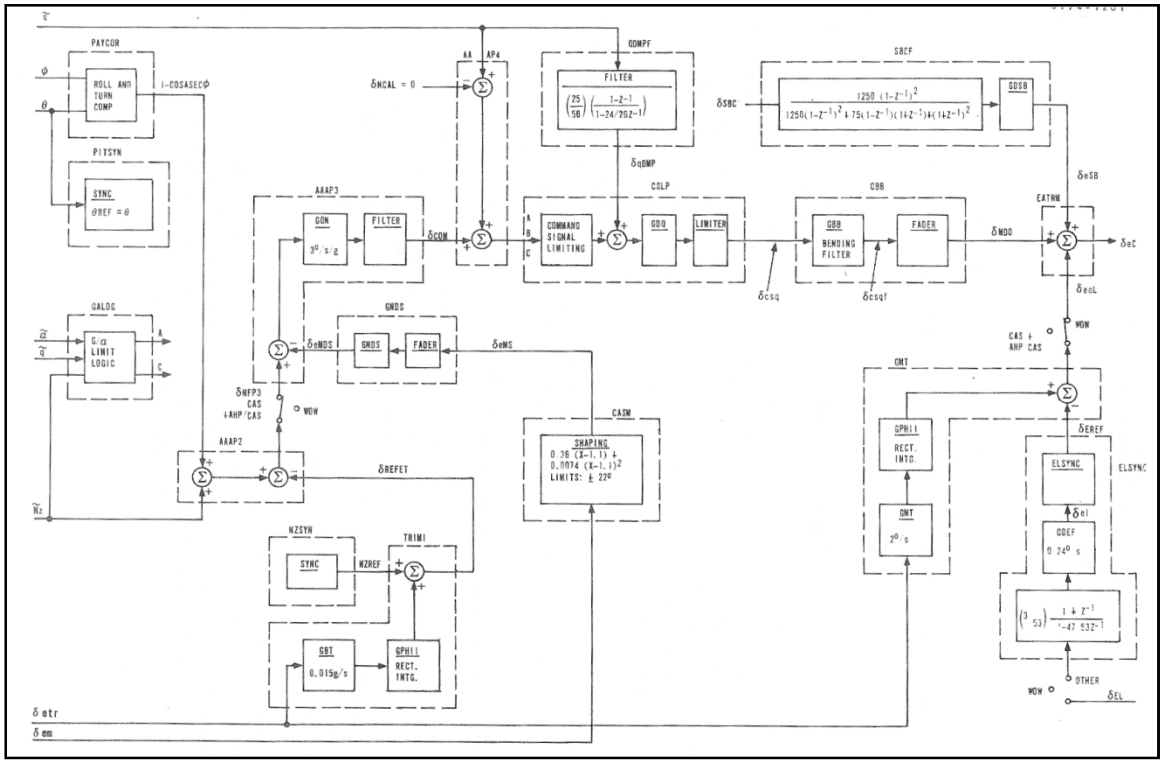

Figure C-4. HFT Pitch Axis CAS Block Diagram

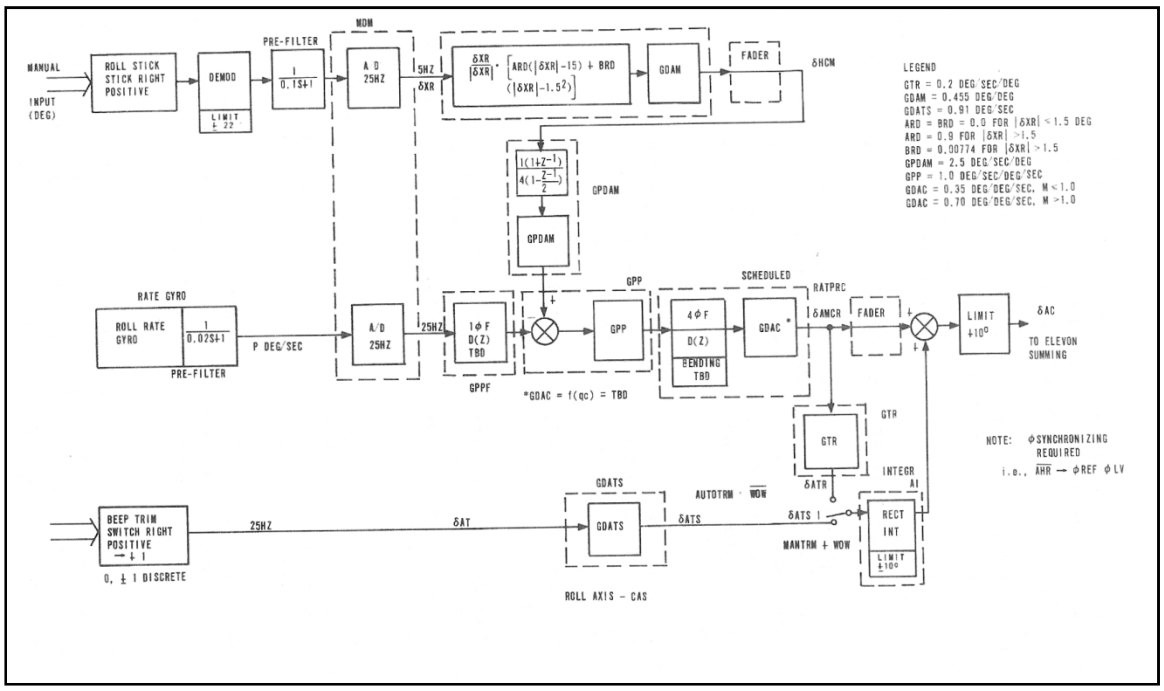

Figure C-5. HFT Roll Axis CAS Block Diagram

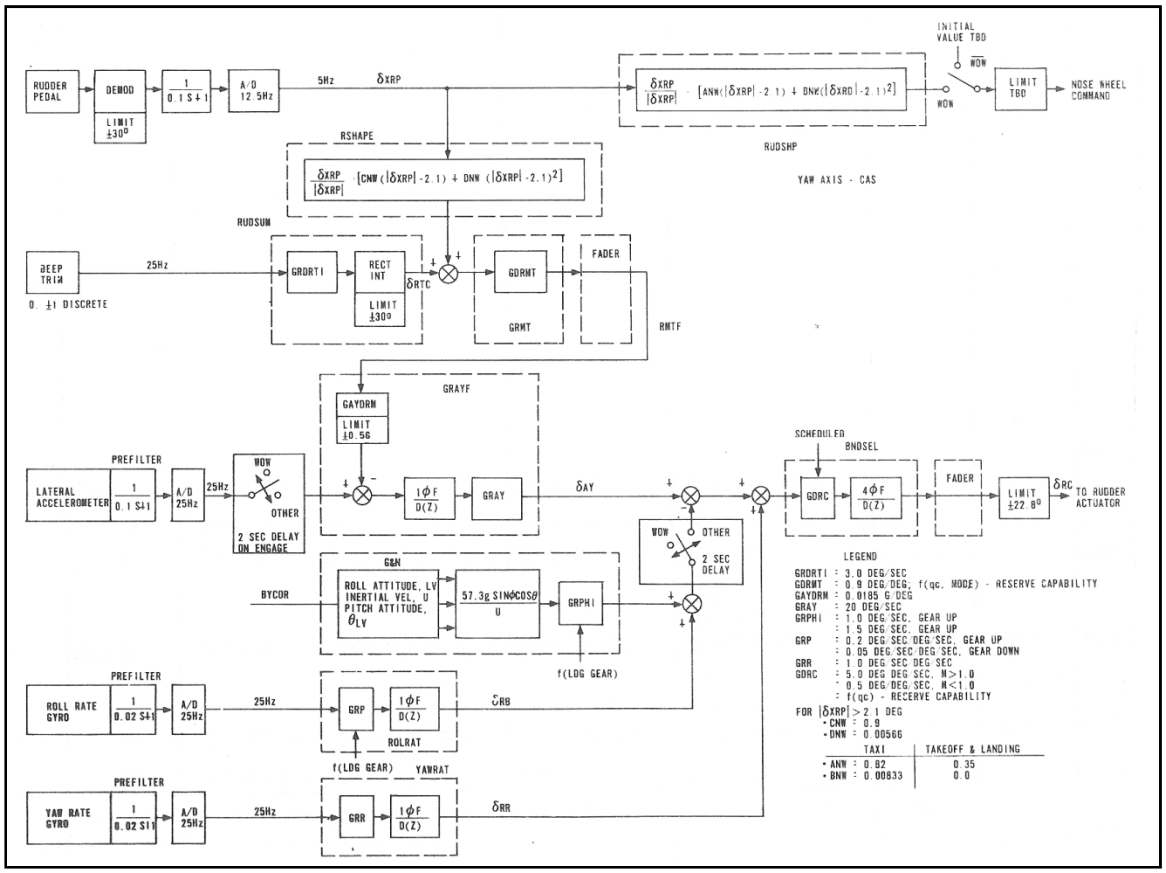

Figure C-6. HFT Yaw Axis CAS Block Diagram

C.4.2 ALT FCS – DAP Overview

- Control modes
  - 3-axis manual direct, DAP software implementation (MD)[1] – elevon, rudder
  - 3-axis stability/command augmentation (CAS), RHC signal processing at 12.5 sps
  - Autoland – Nz, φ guidance commands
- Sub-modes
  - Manual and auto speedbrake (SB)
  - Manual bodyflap – 3-position manual selection
  - Auto bodyflap – 3-position = f(SB, cg)
  - Manual and auto nosewheel
- Pitch axis[2]
  - Pitch rate command, not C*, where C* = Nzp + Cq * q,
  - Proportional plus integral (PI) control:
  - Command signal limiting (Nz, α),
  - Up-elevon (φ)
  - Speedbrake cross-feed compensation
  - Air-data (h< 80,000 ft) M, $\overline{q}$ scheduling
- Lateral axes (PI),
  - Subsonic roll auto trim disabled
  - Computed turn-coordination vs. classic high-passed yaw rate system (this function was added as a crew-selected option to protect against IMU failure)

The pitch axis and lateral axis analytic block diagrams shown in figures C-7 and C-8, respectively, provide an overview of the ALT DAP structure and features. Better readability can be found in the referenced 1976 IEEE Decision and Control paper, which also summarizes the design/analysis approach and techniques. As a footnote, state-of-the-art tools utilized were paper and pencil, slide-rule, Bode template, Wang mechanical calculator, an s-domain Eigenvalue computer application, and time-history study via a hybrid Pace (110v) analog computer interfaced with a Sigma-5 digital computer. The Honeywell THRUST executive program, precursor to SIMEX, controlled the simulation with high frequency effects on the Pace, and the digital FCS implemented in THRUST.

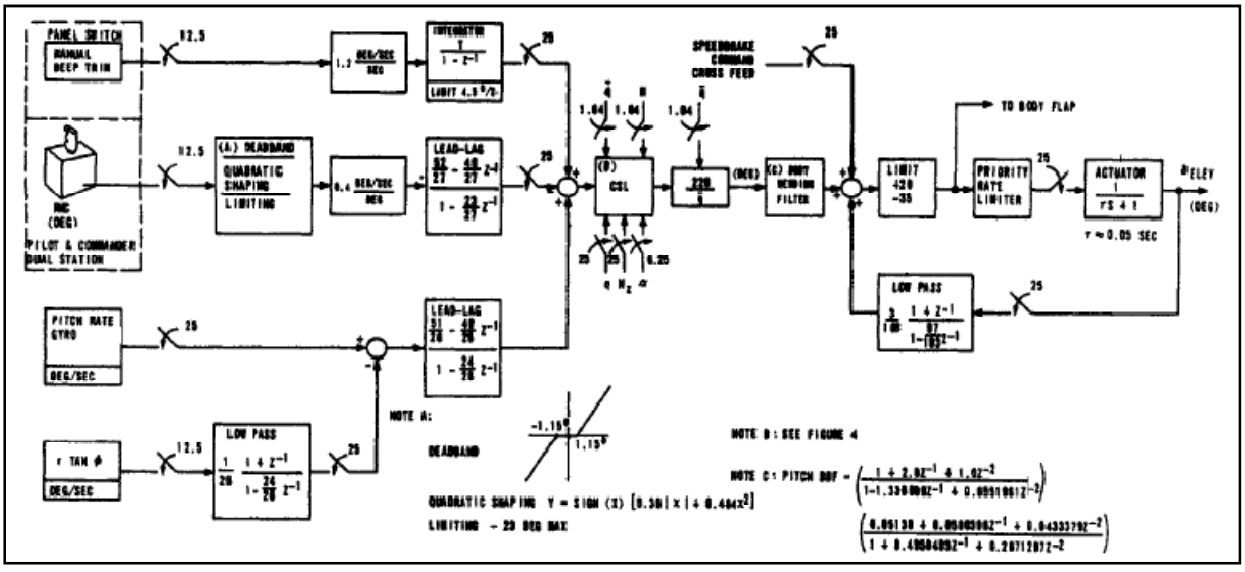

Figure C-7. ALT Pitch Axis Block Diagram

[1] Crew spokesperson, during first active flight FRR, stated MD was flyable, with 70% likelihood of a safe landing from a low-altitude takeover

[2] Extensive MIL simulator studies (TAEM/Approach-Land) were conducted: a "fly-off" on eight (8) control laws decided the baseline

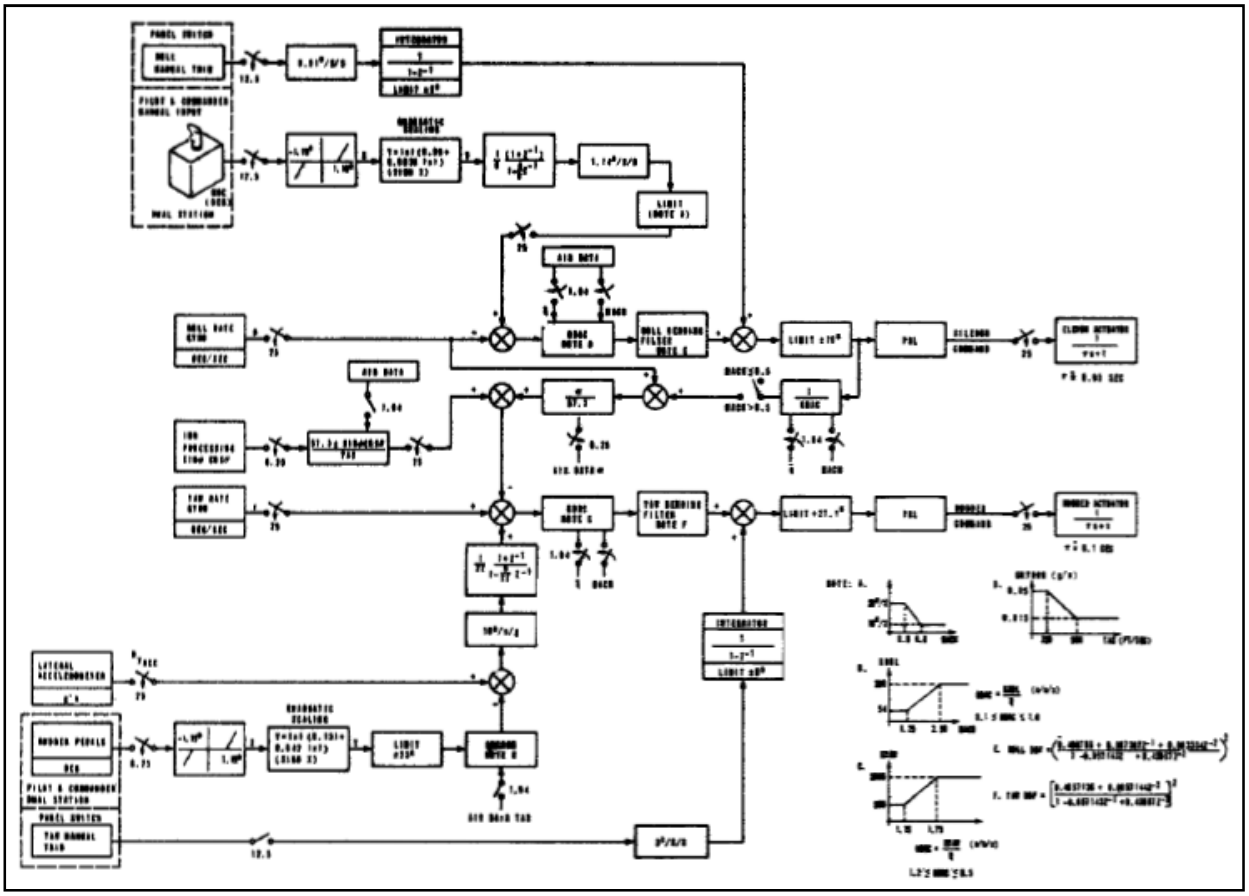

Figure C-8. ALT Lateral Axis Block Diagram

Figure C-9 illustrates the ALT command signal limiter (CSL), and figure C-10 is an overview of the ALT priority rate limiting (PRL) concept. CSL was not implemented in the OFT baseline because of crew disapproval (based on other unprotected scenarios that could lead into dangerous flight conditions) and software build constraints. The ALT PRL employed simple rate command limiting logic based on the assumptions that manual and guidance commands would not cause surface rate saturation and that if limiting occurred, it would only be for short durations.

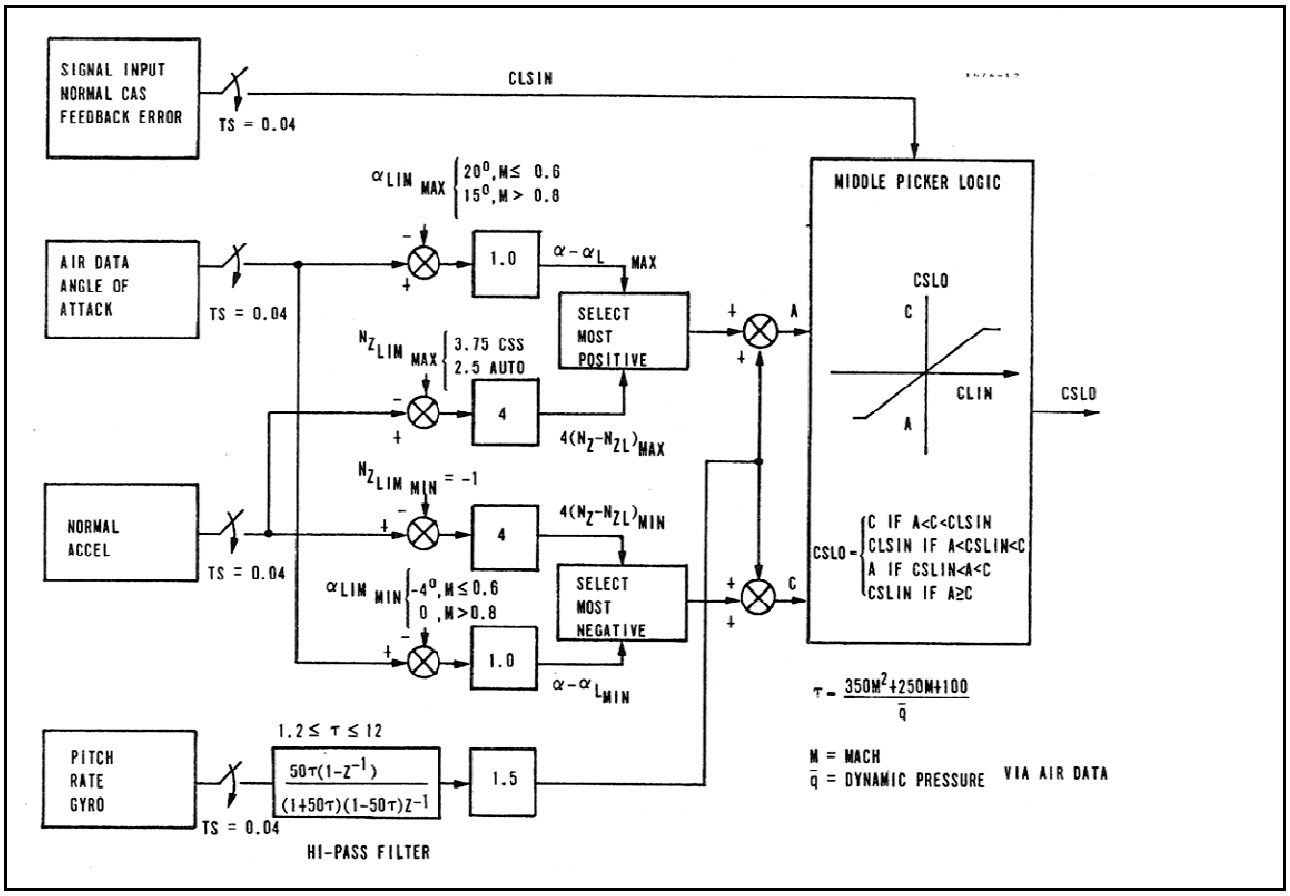

Figure C-9. ALT CSL

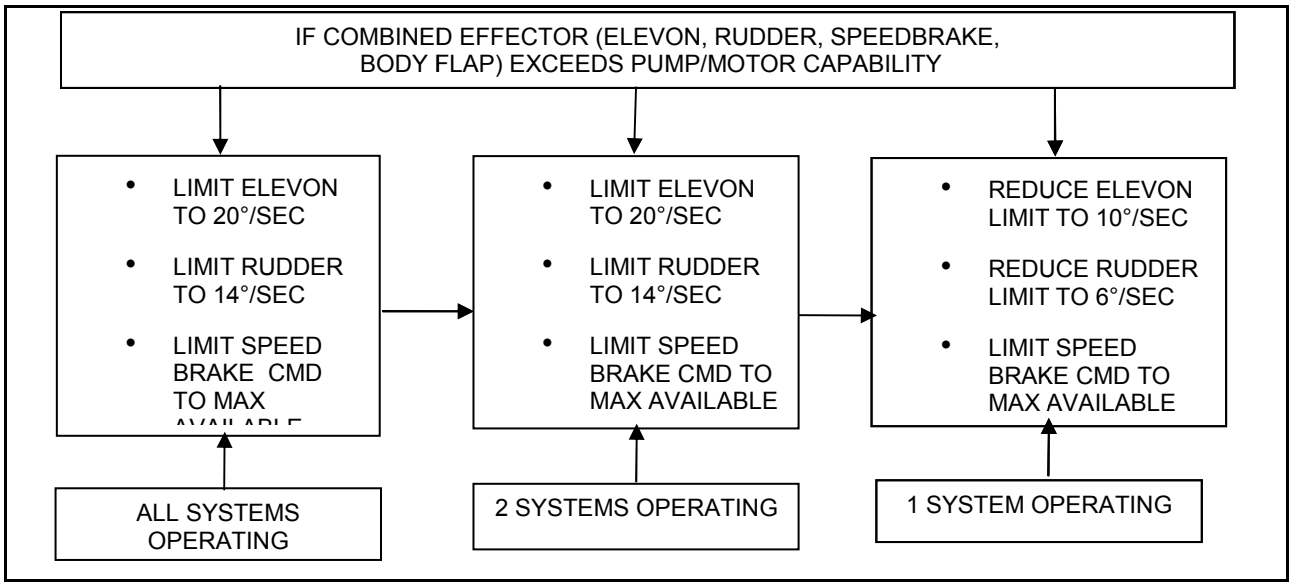

Figure C-10. ALT PRL

C.5 ALT Program Challenges and Answers

Following design, analytic and simulation testing, and correlation with hardware in-the-loop testing, the verified system is ready for flight test. As indicated in figure C-11, significant questions must be addressed to provide quality assurance for flight readiness. Also, model, database, tool/simulation, and equipment differences make correlation of results difficult.

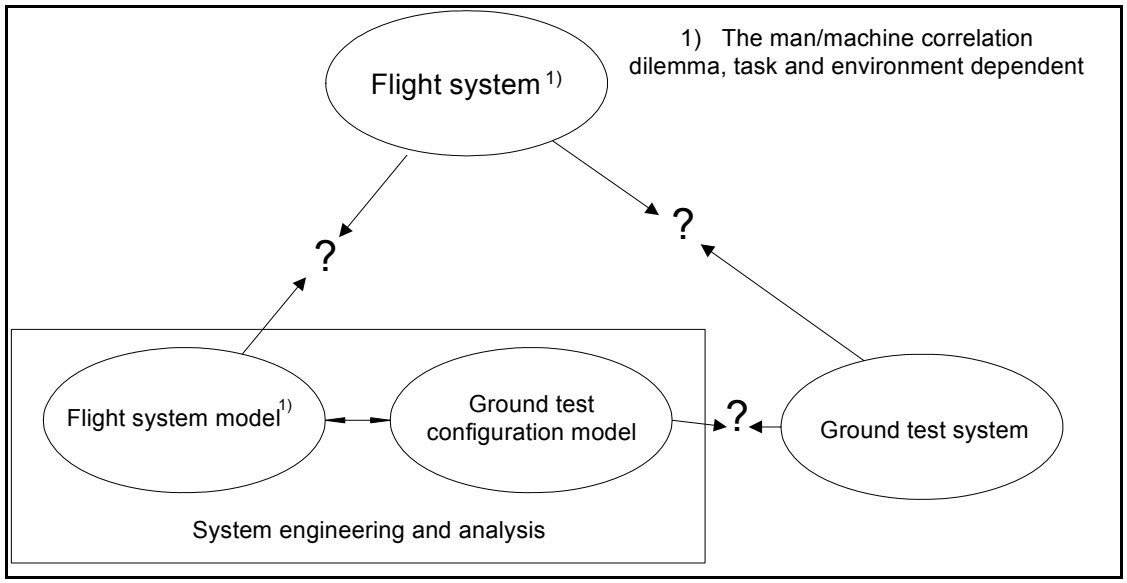

Figure C-11. "The Moment of Truth"

The following list presents many of the challenges encountered during this program, along with some of the answers:

- Modeling, database assumptions, and test plan execution posed challenges for both flex and rigid body; some flex issues are included below.
- Availability/fidelity of ground effects data for the ALT program was lacking for the design and developmental verification test.
    - o OFT and subsequent in-flight measurements led to incremental updates to the aerodynamic database.
    - o Time-varying Influences of landing field and natural environments, vehicle characteristics, and vehicle orientation confirmed expectations of large ground effects uncertainties.
    - o The conservative design assumptions were validated.
- Inadequate ASA/actuator design modeling of DAP quantization effects was revealed during hardware integration tests. Hardware, ASA pre-filter, and software (bending filter) modifications were required.
- Reference frame and database differences to be answered include those relating to structures (X-axis defined positive aft), aero fuselage reference line (FRL) vs. hinge line, etc.; simple uncoupled pilot (step, pulse, double, sinusoidal, i.e., analytic input) model for the complex man, the RHC cockpit cross-axis mounting, etc.
- Flex body models and the database for the early FCS baseline defined different mounting locations for the quad-redundant gyros.
- Natural environment modeling and digital simulation (e.g., of turbulence), as well as the atmosphere model definitions (e.g., 1962 Standard, GRAM95) were a continuing challenge.
- NAV modeling, uncertain aero assumptions, and air-data calibration were significant challenges for FCS flight critical air-data parameters.
- Some OFT examples (i.e., the unprecedented early entry and uncertain AERO/RCS effects of STS-1) yielded results requiring updates to the aero design data and autopilot; surface effectiveness and Cm_o effects that provided real program benefits. (After more than 10 years of GN&C, thermal and aero analyses and simulation, STS-1 was hailed; "incredible flying machine . . . reliable and versatile . . . superb machinery and system," by CDR John Young.)
- Multi-string small signal model evolution to address bit-toggling/redundancy management (RM) selection filter performance (RCS expendable fuel budget) came out of flight test.
- Inter-facility simulation, hardware in-the-loop, ground and air vehicle differences; instrumentation and measurement quality, all required extraordinary attention in the correlation, understanding and resolution of differences.

Table C-4 describes some of the ground test challenges.

Table C-4. Ground Test Challenges

TEST	DESCRIPTION	FCS CHALLENGE
HGVT (horizontal ground vehicle test)	OV-101, FCS inactive, Modal test	Relocate rate gyro, Resonance (not modeled)
¼ scale	Modal test, No FCS	Not modeled payload door friction
Hot fires	FCS active	Quantization/actuator subsystem response leading to ASA and DAP filter redesign; not modeled pitch/yaw coupling; relocate outboard rate gyros
EDST (entry dynamic stability test)—first engineering-sponsored test	OV-102, STS-1 preflight verification	Instability due to model/structure database deficiencies, structure and test configuration effects (on elephant stand stiff vs. planned soft mount)
IUS/DST (dynamic stability test)—engineering-sponsored test	OV-099, version 19 DAP	Finally, predictions correlated with vehicle system results. But there was a procedural error (instability when air bags were not activated)

C.6 ALT Flight Test Overview

ALT, the first step toward STS mission operations, successfully satisfied the objectives to verify the integrated system design, demonstrate subsonic and landing performance capability, and obtain aerodynamic data and independent air-data measurement via the nose boom for use in calibrating the ADS. Engineering flight support was demonstrated and developed for OFT mission use before verification of facilities and processes such as SAIL.

The test program was a multiphase effort: captive flights, captive active flights, flights with crew on-board, and free flights. Table C-5 presents information about the free flights (FF). All flights but the last (FF5/ALT-16) made a lake bed runway. FF5, a concrete runway landing with an objective to demonstrate target landing capability, exhibited a fully developed PIO in both the roll and pitch axes. After a series of studies, DFRC and TIFS flight tests, and Ames simulations, FCS hardware and software modifications were baselined for the upcoming OFT system, as discussed in the main body of this report. (See: www.dfrc.nasa.gov/Gallery/Movie/STS/HTML/EM-0084-02)

Table C-5. ALT Free Flights

Order	Day	Year	Mission	Shuttle	Crew	Duration	Landing Site	Notes
0.1 (1)	12-Aug	1977	ALT-12[6]	*Enterprise*	2	0d 0h 5 m	Edwards	First free flight of Space Shuttle
0.2 (2)	13-Sep	1977	ALT-13	*Enterprise*	2	0d 0h 5 m	Edwards	Second free flight
0.3 (3)	23-Sep	1977	ALT-14	*Enterprise*	2	0d 0h 5 m	Edwards	Third free flight
0.4 (4)	12-Oct	1977	ALT-15	*Enterprise*	2	0d 0h 2 m	Edwards	Fourth free flight; first flight without tailcone (operational configuration)
0.5 (5)	26-Oct	1977	ALT-16	*Enterprise*	2	0d 0h 2 m	Edwards	Final free flight

C.6.1 Pilot-Induced Oscillation (PIO) Discussion

The following PIO discussion includes excerpts from the FCS crew monitor, H. W. Hartsfield, along with this writer's comments. Flying qualities (handling) from a CHR viewpoint require attention to the vehicle's stability, maneuver response, and controllability, and both the pilot's and automatic system's capabilities. System stability is affected by delays and nonlinearities, with force effector authority, hinge-moment, and rate-limiting of paramount concern. Displays also introduce delays to the pilot, adding to the many factors for which the nonlinear, adaptive, time-varying, multiloop, bandwidth-capable pilot must compensate.

Proceeding with the ALT program, studies revealed the FF5 PIO was due to basic man/machine handling qualities, the GPC processing time delay, and nonlinear response caused by elevon rate limiting.

H.W. Hartsfield[1], NASA JSC (code CB), reporting on the orbiter FF5 and OAS, stated, "Despite control sensitivity (*pitch & roll*), pitch response has been crisp and solid. Rate response rapid with good damping, lags not noticed in normal pitch tasks. In landing, pilots control $\dot{h}$; tight, time-constrained control is required. Pilot is located near center of rotation; Orbiter has little 'nose reference' for attitude changes. There is a delay in the perception of $\Delta\dot{h}$ following a control command."

Orbiter control-stick steering (CSS) performance for the nonlinear (avionics & pilot) multiloop system, particularly for large signal gross maneuvers, is indeed sporty. Please see Hartsfield's NASA "Oral History" pages 26-29, and klabs.org/history/history_docs/reports/dfbw_tomayko.pdf, particularly pages 111 ff.

The conclusion was that the landing problem is due to a combination of pilot perception, vehicle configuration, and FCS design, i.e., the total vehicle. *And later, per informal discussion, post STS-4: lateral PIO sensitivity was evident and control during de-rotation required attention.*

Man-Machine Flying Qualities

- FCS has difficulty in the crossover frequency range.
- Landing the balloon-sensitive Orbiter is "sporty": its close-coupled delta planform (adverse lift) response dynamics, the ride qualities (feel and visual cues), the system sensitivity and response dynamics (a function of inertias, weight, CG, and vehicle dependency effects) impose challenging handling qualities to the pilot.
- Nonlinearities, system response lags and delays, and command rate saturation can exacerbate PIO susceptibility.
- From Wright Brothers to date, achieving acceptable man-machine flying/handling qualities has been a challenging problem.

PIO Events and Definitions

- FF 5 and the STS-3 "wheelie" have been defined as PIO events.
- PIO definitions are numerous (10 or more). One is basic: if, with no pilot command and with stability augmentation active, the oscillatory transient is damped, then it was a PIO.
- New designs, with their new requirements and technologies, must deal with this classic problem.

Time Delay Effect on Flying Qualities

Figure C-12 illustrates the results of an F-8 study of the effects of time delay on pilot handling quality ratings. The ALT system exhibited a delay of approximately 250 msec; program experience, MIL Specs, and flight research indicate this effect can lead to a PIO.

[1] Hartsfield worked with the FCS design team throughout the design and development effort.

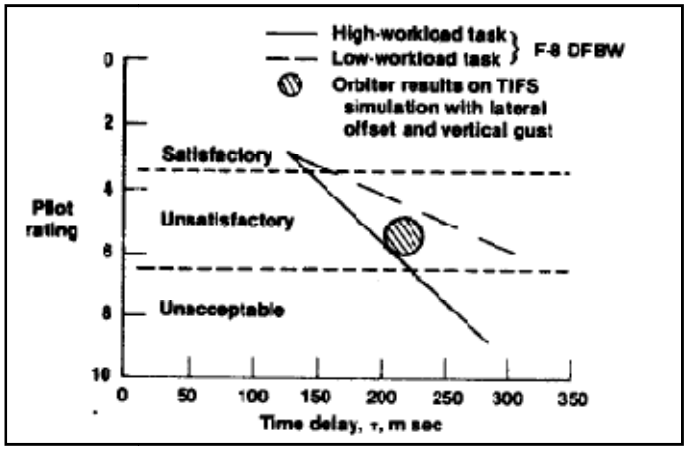

Figure C-12. Results of the F-8 Time Delay Study for the Landing Task

C.6.2 Pilot-Induced Oscillation (PIO) Filter

Figure C-13 illustrates the PIO filter implemented in the OFT FCS to minimize susceptibility to PIO events. A linear filter to notch out the frequencies (2.5-3.0 rad/sec) associated with PIOs from the RHC command was originally considered, but was discarded because its phase lag would add to the lags already inherent in the system that originally caused the PIO susceptibility. Instead, a system was devised to reduce the RHC command gain based on the frequency content of the input.

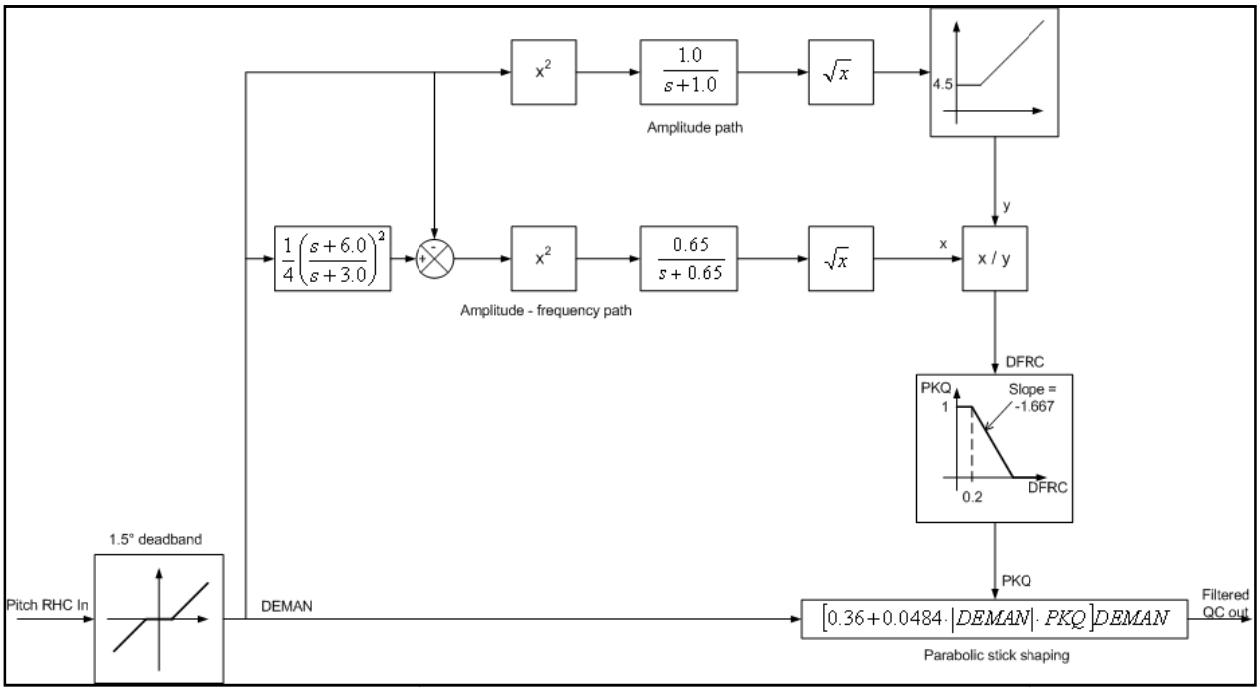

Figure C-13. OFT PIO Filter

The PIO filter has two paths, as labeled on figure C-13. The top one, or “amplitude path,” is designed to produce a signal proportional to the magnitude of the RHC inputs, with little frequency content. The lower one, or “amplitude-frequency path,” effectively differentiates the input (accurate for frequencies of 3 rad/sec and lower) and produces a signal proportional to the product of frequency and amplitude. The division block produces a signal that is proportional to the sensed input frequency, allowing the stick-shaping slope to be reduced when RHC input frequency is near the PIO frequency.

The filter was developed originally with a fixed-base simulation using a general air-to-air tracking task, not the standard Shuttle approach and landing. This technique was good enough to develop and validate a baseline filter structure, but fine-tuning of the gains required full-motion simulations (such as the Calspan

Total In-Flight Simulator and the Ames Research Center's Vertical Motion Simulator) to provide the evaluation pilots with motion cues and appropriate testing tasks. During these tests, the baseline gains were shown to reduce responsiveness by about 50%, which was deemed unacceptable. These changes demonstrate the importance of faithful recreation of the total piloting environment when investigating pilot-aircraft interaction.

A detailed description of the DFRC filter design is contained in the reference: 87928main_H-1119.pdf, and in AIAA-82-4078, "An Adaptive Stick-Gain to Reduce Pilot-Induced Oscillation Tendencies". Yet the Orbiter under stressed man/machine conditions remains PIO-susceptible, particularly for landing tasks requiring combined pitch and lateral maneuvers and for precise main gear touchdown control to satisfy the critical vehicle constraints. (Even the pilot reports from the PIO filter development admit that aggressive control techniques may still cause divergent PIOs in some cases.) Training for the landing tasks, principally via the NASA AMES VMS and in-flight STA testing, ensures that acceptable handling qualities can be expected.

C.6.3 DFRC Landing Study Summary

The DFRC Landing Investigation Report, August 1978, concluded the Orbiter FCS was not satisfactory for operational landings. Also, the software changes made after the ALT flight test did not correct the inherent attitude/flight path control problem caused by aircraft geometry, delta-wing $Z_{\delta e}$, and Nz physical cues at the cockpit. The updates for inclusion in the OFT DAP (i.e., command processing in the fast rate group, pitch axis PIO filter, reduced pitch axis forward loop gain, PRL logic, and increased RHC spring forces) improved handling qualities but were judged to be insufficient.

DFRC continued to study the problem. In early 1983, 14 alternate FCS configurations were evaluated in the RI SES simulation facility. Half of the candidate systems were determined to be satisfactory, but the simulation fidelity was inadequate to provide a rigorous evaluation. Later that year (August 1983) a major FCS landing handling qualities study was conducted at the NASA AMES VMS facility. During this period a new "smart" speedbrake control law and the HUD autoland monitor symbology were also studied.

The FCS handling qualities study provided these conclusions:

- None of the seven revised control laws displayed sufficient improvement over the baseline FCS to warrant change.
- Improvement in handling qualities cannot be achieved through modifications of the baseline DAP software alone.
- Lateral cross-coupling from pitch RHC commands was evident.
- Occasionally lateral oscillations were excited due to dynamics between the pilot's forces and RHC spring forces.

C.7 Lessons Learned/Relearned

- Physical systems place limitations on available bandwidth, which was a major challenge for the design and development of the Orbiter GN&C system. In my view, the aerosurface subsystems (elevon and rudder/speedbrake) and the GPC limitations restricted development of a "robust" control system. One goal in a new design is to build in flexibility to accommodate testing and engineering modifications to support mission operations. Achievement of this goal has been constrained by the GPC architecture, with its limited memory and bandwidth for FCS design.
- Early system engineering/analyses of abort missions, as well as trade studies to establish avionics design, integration, and test requirements, along with subsystem allocations, are essential to minimize DDT&E costs and life-cycle costs. The leader/follower (ENTRY-then-GRTLS) philosophy led to extensive, and continuing, effort.
- Flying qualities criteria have not kept pace with FCS development; some FCS designers are not aware of, or find it difficult to follow and apply, this flight research activity.
- Competent, motivated, dedicated, and dependable engineers, when left alone (OFT tiger team and NWS, for example) with resources, can contribute far better than a large interacting organization.

- Communication is essential. Workers' open, timely, disciplined, and reportable design and integration communications are a significant challenge. The FCS (DRB) and GN&C practice provides an excellent model for this process.
- Specifications, requirements, rules, and regulations are essential; yet there is no substitute for engineering judgment.
- There is a need for customer-approved test demonstration plans that include the test objectives, test measurements, and precision pass-fail criteria for vehicle level and in-flight tests. The plans should provide particular attention to pass-fail criteria for both small and large dynamic response performance, for both uncoupled and coupled pitch and lateral axes dynamics, for linear and nonlinear dynamics, and for pilot handling qualities rating (CHR).
- Software development, documentation, testing, and management worked very well on the Orbiter program.

C.8 Miscellaneous

Accurate, complete, and timely communication of GN&C personnel with MOD is essential to establish flight placards and rules. Flight rules can be found in the NASA.gov, NSTS 12820 Flight Rules archive; Entry and GRTLS checklists in JSC-48019 e.g., (113038main_EntryChecklist_Generic_RevG_1.pdf) and JSC-48005-122 e.g., (202926main_sts122_ascent_checklist.pdf).

Completeness and clarity of communications within the team is essential. As expressed by Brewster Shaw's oral history, "It takes the whole team to make the program go, the people who fly it in space and the people who control it and manage it from the ground. It takes the whole team, and the more we can work together, the better we all perform…..[W]e had a lesson on the landing of STS-9, and the lesson was, 'never let them ***change the software*** in the flight control system without having adequate opportunity to ***train*** with it.'" Indeed, the astronaut oral histories offer significant human factor flying qualities insights.

Critical item list (FEMA/CIL) practice was used in risk assessment and to ensure safety of flight. (Note: the avionics system was not fully implemented as a quad-redundant fail-op/fail safe (FO/FS) system.)

The Orbiter vehicle end item (OVEI) specification required GN&C certification of performance, stability and response. Flight control analyses and time-history response simulation anomalies were documented via the FCAN process. Performance-related trim, RCS and APU expendables, trajectory simulation anomalies, etc., were managed through use of a test requirements document (TRD) process. For reference, a sample of OFT-1 integrated GN&C pass-fail criteria from Rockwell Document SD-78-SH-0145B is shown in table C-6. Operational performance capabilities—i.e., trajectory control (flight envelopes, load and maneuvering limits), landing constraints, and fuel consumption—can be found in the NSTS-08934 (Volume 5) Orbiter Flight Capability Envelopes document. The current preflight assessment pass-fail criteria for entry GN&C are defined in a computer program, PassFail.cpp, which screens entry GN&C SAIL test data for out-of-limit conditions and reports all such conditions for further analysis. The assessment criteria are taken from various Shuttle specifications and other documentation, and were last revised in January 2000. Table C-7 shows a sample page from the current pass/fail criteria spreadsheet.

Flying qualities for a man-rated system will ultimately be measured by the pilot's acceptance of performance for the multitude of tasks required to safely complete the mission. Descent performance requirements, as a function of mission performance Levels 1, 2, and 3 (or Design Assessment) were specified to ensure acceptable manual control (CSS mode) handling qualities. The Cooper-Harper rating scale was used during the design, development, and test (including flight test) phases of the program. Level 1 performance required a CHR rating no greater than 3; Level 2 required a CHR no greater than 6.

It bears mentioning that an extraordinary amount of real-time man-in-the-loop simulator evaluations, dating from 1969 to the present, have led the successful design and development, and provided essential flight-readiness approvals. The primary RI/FSL simulator for ALT and OFT, transitioning to the NASA JSC SAIL, GTS, and SES, along with support from NASA AMES, TIFS, STA, OAS, SMS, Sperry, and DFRC simulators, have amassed runs and CHRs that might rival the quantity of aerodynamic development assessments.

Table C-6. Example of OFT-1 Entry FCS Pass-Fail Criteria

Entry Flight System Tests

Major Mode	Objective	Requirement	Pass/Fail Criteria	Data Requirements			
				Param	Env	Downlist Primary	Downlist BFS
304 H/L*	Verify crew transition to MM 304.	Transition to MM 304 before h = 400,000 ft	When $h \leq 400{,}000$ then MM = 304	ALT MM	H	V90Q8001C	V98X3641X
H/L,	Verify guidance mode pre-entry.	Transition to OPS 304 at ISLECT = 1	When MM = 304, ISLECT = 1	ISLECT MM		V90J1138C V90Q8001C	— V98X3641X
	Verify navigation state errors are within entry interface tolerance at 400K.	Difference between the environment and NAV position and velocity vectors must be within prescribed limits measured LVLH coordinates.	$\Delta V = (\Delta V_X^2 + \Delta V_Y^2 + \Delta V_Z^2)\ 1/2$ = TBD $\Delta P = (\Delta X^2 + \Delta Y^2 + \Delta Z^2)1/2$ = TBD Where $\Delta V_X = V_X(NAV) - V_X(ENV)$ $\Delta V_Y = V_Y(NAV) - V_Y(ENV)$ $\Delta V_Z = V_Z(NAV) - V_Z(ENV)$ $\Delta X = X(NAV) - X(ENV)$ $\Delta Y = Y(NAV) - Y(ENV)$ $\Delta Z = Z(NAV) - Z(ENV)$	V_X V_Y V_Z X Y Z	XDOT YDOT ZDOT XI YI ZI	V95L0190C V95L0191C V95L0192C V95H0185C V95H0186C V95H0187C	V98L0130C V98L0136C V98L0143C V98H0110C V98H0116C V98H0122C
P/L**	Verify no elevon command for $\bar{q}_{NAV} < 0.5$.	If $\bar{q}_{NAV} < 0.5$ psf, ELICMD | < 1.0 ELOCMD | ≥ 1.0 ERICMD | ≥ 1.0 EROCMD | ≥ 1.0	When 0.0 $\leq \bar{q}_{ENV} \leq 0.5$, |ELICMD| ≤ 1.0 |ELOCMD| ≤ 1.0 |ERICMD| ≤ 1.0 |EROCMD| ≤ 1.0	$\bar{q}$ ELICMD ELOCMD ERICMD EROCMD	QBAR	V58K0820C V58K0870C V58K0920C V58K0970C	— V98H3280C — — V98H3284C
H/L	Verify roll jet disengage at $\bar{q}$ = 10.	If $\bar{q}_{NAV} \geq 10.0$, roll jet commands = 0	When $11.5 \leq \bar{q}_{ENV} \leq 20.0$, $U_{XCMD} = 0$	$\bar{q}$ U_{XCMD}	QBAR	V90J1636CB	—
H/L	Verify pitch jet disengage at $\bar{q}$ = 20.	If $\bar{q}_{NAV} > 20$, pitch jet commands = 0	When $23 < \bar{q}_{ENV} \leq 30$, $U_{YCMD} = 0$	$\bar{q}$ U_{YCMD}	QBAR	V90J1636CB	—
H/L	Verify that surface temperature limits are not exceeded.	Vehicle nose, body flap, wing, elevon, and RCC/HRSI interface control points will be checked against both design and soft limits.	Temperatures must be within limits of Table 5.5.1.3.3-6.	T1 T2 T3 T4 T5	(1) (1) (1) (1) (1)		
H/L	Verify orbiter aero-surfaces are initialized properly at MM 304 initialization.	δ_e = 0 deg δ_{SH} = 0 deg $\delta_{BF} = 0.8091(X_{CG}) - 882.78$ where X_{CG} (ft)	$\delta_e = 0 \pm 0.2$ deg $\delta_{SB} \leq 0$ deg δ_{BF} = calculated value ± 0.5 deg	δ_e δ_{SB} δ_{BF} X.c.g.	DELE DSB DBF XCG		

(1)Surface temperatures are calculated in the pass/fail program as shown in Section 5.5.1.3.3.1.

*H/L = Hard limit
**P/L = Performance limit

Table C-7. Sample Page from Revised Entry FCS Pass-Fail Criteria

Entry GN&C Pass/Fail Criteria for SAIL Testcases

PF #	Major Mode	Objective	Pass/Fail Criteria	Data Requirements					Requirement Source
				Var	Env	PASS	BFS	lload	
1	304	Verify no Elevon Cmd for Qbar (nav) < 2.0 psf (Software Check)	If Qbar (nav) <= 2.0, then all four Elevon Cmds must be <= 1.0	Qbar ELIC ELOC ERIC EROC		V95P3011C V58K0820C V58K0870C V58K0920C V58K0970C	V98P3117C ---------- V98H3280C ---------- V98H3284C	V97U09961C	FSW Rqmt (FSSR 7). Elevon Commands are initialized to an I-load at MM 304. The criteria is the I-load plus 1 deg of overshoot.
2	602	Verify Orbiter pitch up to constant Alpha during Alpha Recovery (Software Check)	At MM602 + 25 sec, Alpha must equal 50 deg (+/- 2 deg)	MM Alpha	VIMM0359A	V90Q86001C	V98U2408C	V97U00440C	No Specific Requirement. Criteria derived from starting MM 602 at an Alpha of ~10 deg, pitching up at 2 deg/sec to Alpha = 50 (+/- 2 deg).
3	304 & 602	Verify Roll Jet disengage at Qbar=10 psf (Software Check)	If Qbar >= 10, then UXCMD = 0	Qbar UXCMD		V95P3011C V90J1636C	V98P3117C V98H0524C	V97U0868C	FSW Rqmt (FSSR 7).
4	304 & 602	Verify Pitch Jet disengage at Qbar=40 psf (Software Check)	If Qbar >= 40, then UYCMD = 0	Qbar UYCMD		V95P3011C V90J1638C	V98P3117C V98H0526C	V97U9874C	FSW Rqmt (FSSR 7).
5	304, 305 & 602, 603	Verify Nav State Errors (UVW) are within boundaries (Guidance Hard Limits)	Nav UVW state vector errors must be within boundaries stated in Figure PF-1	These are externally computed variables					
6	301 - 305 & 602, 603	Verify GPS Position State Errors (UVW) are always within FOM limits	GPS Position State Errors (UVW) are always within FOM limits	These are externally computed variables					GPS SRD
7	301 - 305 & 602, 603	Verify GPS FOM is not failed for longer than the limit	Verify GPS FOM is not failed for longer than 2.3 minutes (138 seconds)	G1FOM G2FOM G3FOM		V74U4466B V74U1466B V74U3466B	V98U7319C V98U7239C V98U7352C		GPS SRD
8	304, 305 & 602, 603	Verify Dynamic Pressure Limits are not exceeded (GN&C Envelopes & Structural Limit)	Both Qbar Nav and Env must stay within boundaries stated in Figure PF-2	Qbar Mach	VIMM0287A VIMM0371A	V95P3011C	V98P3117C		SODB Vol 5 (Para 4.2.2, Figure 4.2.2-4).
9	304, 305 & 602, 603	Verify Normal Acceleration levels are not exceeded (Structural Limit)	Nz must be within Limits noted in Figures PF-3	NZ Mass Mach	VIMM0275A VIMM0373A VIMM0371A				SODB Vol 5 (Para 4.2.1.2, Figure 4.2.1.2-1 and 4.2.1.2-2).
10	304, 305 & 602, 603	Verify Lateral Acceleration Limit is not exceeded (Structural Limit)	Ny must be <= 0.5G	NY	VIMM0273A				Unknown Requirement Source.
11	304, 305 & 602, 603	Verify Roll Attitude Limits are not exceeded (Software Check)	Roll must not exceed Limits noted in Figure PF-4 (Entry), PF-5 (GRTLS)	Mach Roll Ang Alt IPHASE CSS	VIMM0371A VIMM0357A VIAM0277A	V90J1117C V72X5240X V72X5243X			FSW Rqmt (FSSR 1).
12	304, 305 & 602, 603	Verify Angle of Attack Limits are not exceeded (Software Limit)	Alpha must remain within Limits stated in Figure PF-6 (Entry), PF-7 (GRTLS)	Mach Alpha	VIMM0371A VIMM0359A				SODB Vol 5 (Para 4.2.2, Figure 4.2.2-1 Entry. Figure 4.2.2-3 GRTLS).

Throughout the program's history, leading to demonstration of compliance with the OVEI specification, overall flying qualities performance CHRs have ranged between 3 and 4[1]. For deficiencies addressed in this document's design history discussion, CHRs greater than 4 were assessed to focus attention on pilot's controllability demands.

C.9 Epilogue

First, a pause to salute the memory of those many no longer with us, all those who could add incredible insights into understanding the design, the lessons learned for this incredible flying machine. Then a few closing remarks.

[1] See, for example, Hartsfield's NASA.gov, Oral history.

NASA's accomplishment in managing this talented, dedicated team is amazing, as are the teams' personal achievements and sacrifices made for STS program success. Communication between the large, diverse industry and research workforce during the heady time after ATP until subcontract awards were released was an extraordinary experience, leading, I think, to the successful teamwork evident yet today. I will not go on and on, but as a proponent of Jake Klinar's "womb-to-tomb" discipline, I'll close with these thoughts.

Two crews and their incredible experimental flying machines were lost on "our watch." Their legacy lives on.

As some might know me as the "storyteller," 'tis time then to hear from the Grook master, Piet Hein, in telling us:

> "Problems worthy of attack prove their worth by hitting back," and
>
> "Our Noblest Achievement: We must expect posterity to view with some asperity the marvels and the wonders we're passing on to it: but it should change its attitude to one of heartfelt gratitude when thinking of the blunders we didn't quite commit."

Wilbur Wright in 1901 said: "inability to balance and steer still confronts students of the flying problem." (And still does—as evidenced by FF5, YF-16A, JAS-39, YF-22. etc!)

Keep up the good work, good luck, continued success, and evermore: a "GO" at throttle-up, a negative return, and "happy landings."

gck '09

C.10 Bibliography and Suggested Readings

1. Dethloff, Henry C., The Space Shuttle's First Flight: STS-1. In *From Engineering Science to Big Science*, NASA/SP-1998-4219, Chapter 12, 1998. http://history.nasa.gov/SP-4219/Chapter12.html
2. Logsdon, John M., ed., *Exploring the Unknown*, *Volume 4: Accessing Space*, NASA SP-4407, 1999. http://history.nasa.gov/SP-4407/vol4/cover.pdf
3. Tomayko, James A., *Computers Take Flight: A History of NASA's Pioneering Digital Fly-by-Wire Project*, NASA SP-2000-4224, 2000. www.nasa.gov/centers/dryden/history/Publications/
4. Hanaway, John F., and Moorehead, Robert W., *Space Shuttle Avionics System*, NASA SP-504, 1989. www.klabs.org/DEI/Processor/shuttle/sp-504/sp-504.htm
5. NATO Research and Technology Organization, "Background Survey of Flight Control Problems," TR-029-002, Chapter 2, Dec. 2000. http://klabs.org/DEI/Processor/shuttle/shuttle_tech_conf/index.htm
6. *Space Shuttle Performance: Lessons Learned*. Proceedings of a conference held at Langley Research Center, March 1983, NASA CP-2283, Part I, 1983.
7. *Space Shuttle Technical Conference* (held at Johnson Space Center, June 1983), NASA CP-2342, 1983. klabs.org/DEI/Processor/shuttle/shuttle_tech_conf/index.htm
8. Kafer, G., Toles, R., and Golan, E., "Digital Control Laws for the Space Shuttle Orbiter," IEEE Decision and Control Conference presentation,1976
9. Brice, T. R. and Sugano, M. J., "The Approach and Landing Test Program of the Space Shuttle Orbiter 101," AIAA paper 78-1446, 1978
10. Smith, J.W.," Analysis of a Longitudinal Pilot-Induced Oscillation Experienced on the Approach and Landing Test of the Space Shuttle," NASA TM-81366, 1981
11. Powers, B.G., "Space Shuttle Pilot-Induced Oscillation," NASA TM-86034, 1984.
12. Smith, J. W. and Edwards, J.W., "Design of a Nonlinear Adaptive Filter for Suppression of Shuttle Pilot-Induced Oscillation Tendencies," NASA TM-81349, 1980.
13. Thompson, Milton O. and Hunley, J. D., *Flight Research: Problems Encountered and What They Should Teach Us*, NASA SP-2000-4522, 2000.
14. Berry, D. T., "Flying Qualities: A Costly Lapse in Flight Control Design." In *Astronautics and Aeronautics*, Volume 20, April 1982.

15. McRuer, D., “Eighty Years of Flight Control: Triumphs and Pitfalls of the Systems Approach,” AIAA paper 81-4166, 1981.
16. Mitchell, D.G., “Identifying a PIO Signature: New Techniques Applied to an Old Problem,” AIAA paper 2006-6495.
17. Tsikalas, G. M., “Space Shuttle Autoland Design,” AIAA paper 82-1604, 1982.
18. Law, Howard G. and McWhorter, Larry, “Shuttle Autoland Status Summary,” AIAA paper 92-1273, 1992.
19. Military Specification MIL-F-8785, Flying Qualities of Piloted Airplanes
20. Military Specification MIL-F-9490, Flight Control Systems: Design, Installation and Test of Piloted Aircraft

APPENDIX D. Simplified DAP Diagrams

The following pages present simplified block diagrams of the Entry DAP pitch and combined roll-yaw axes, based on the OI-25 software release. Each block diagram is followed by pages presenting details of its associated gain schedules, filters, and other relevant information. Body flap, speedbrake, and nosewheel diagrams are also shown; these reflect the actual OI-27 FSSR configurations.

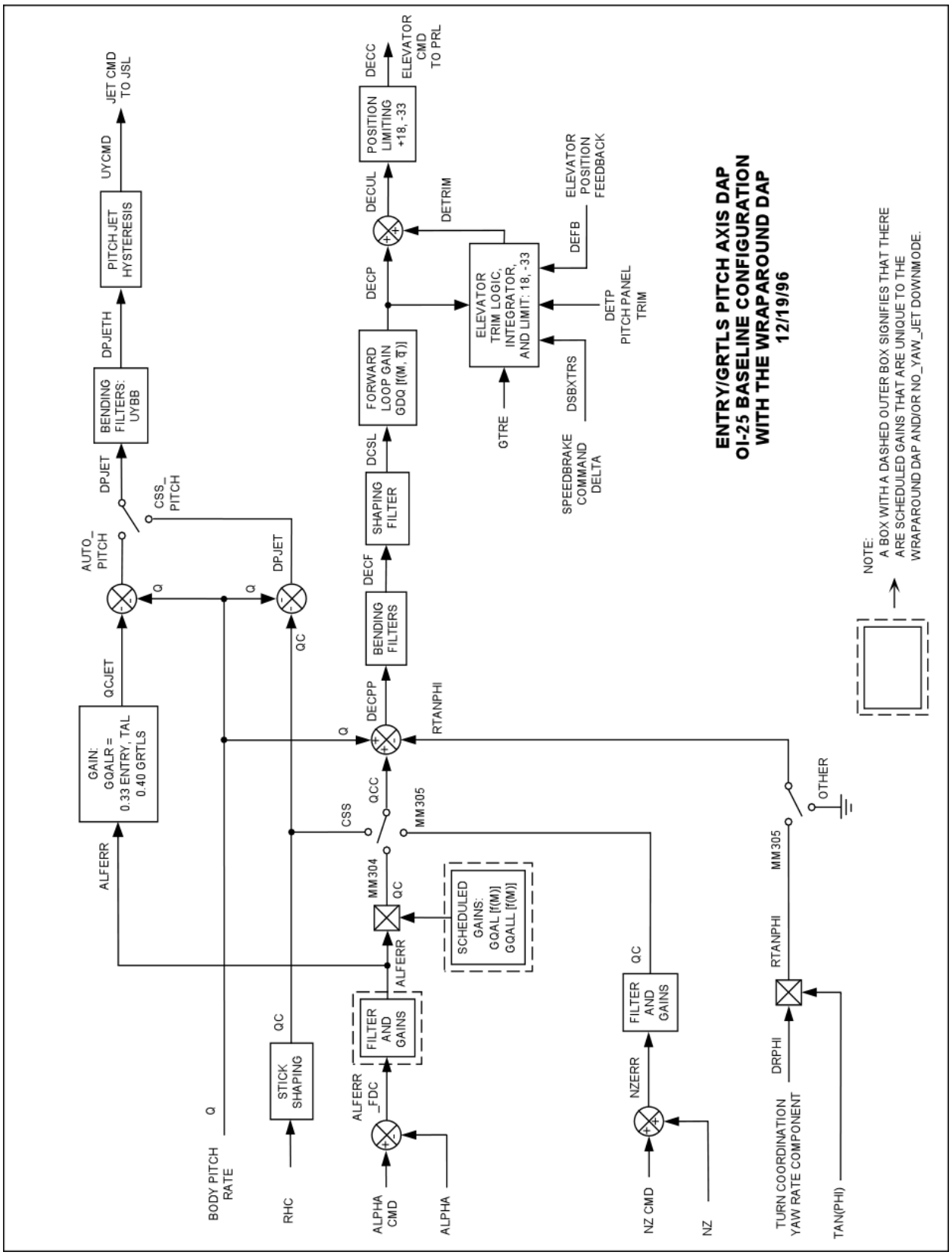

Figure D-1. Pitch Axis DAP Simplified Block Diagram

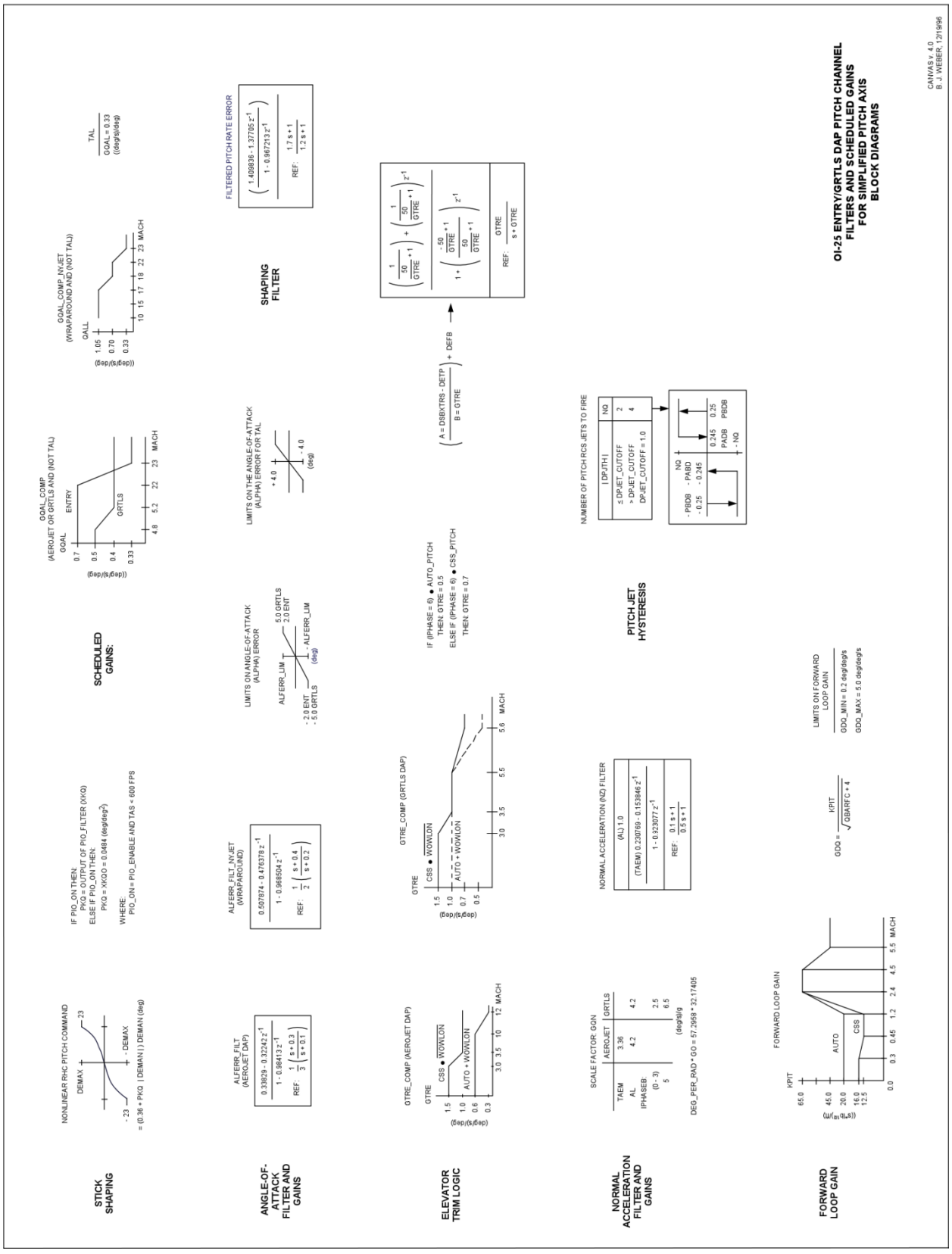

Figure D-2. Pitch Axis Gains and Filters

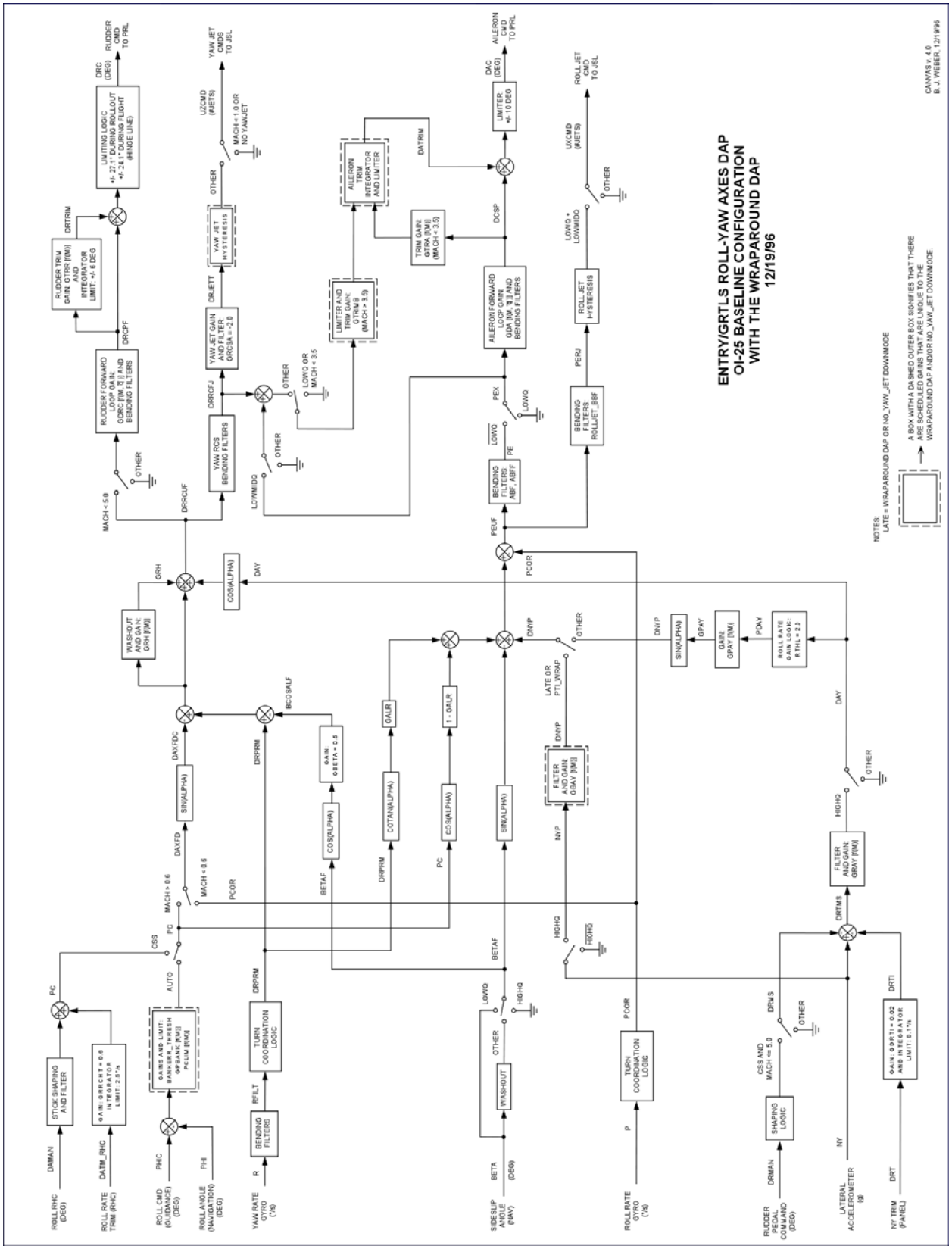

Figure D-3. Roll-Yaw Axis DAP Simplified Block Diagram

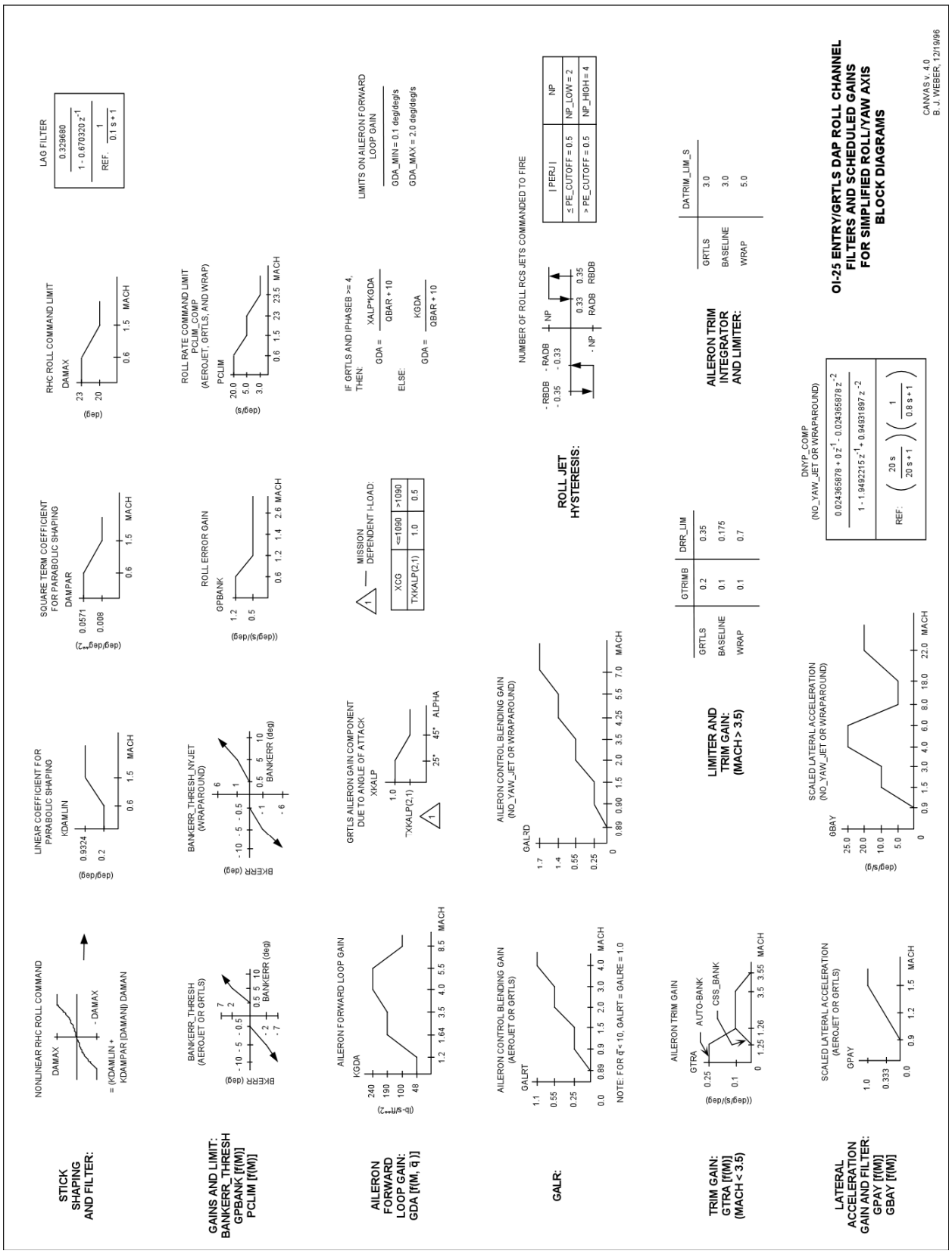

Figure D-4. Roll Axis Gains and Filters

WASHOUT AND GAIN: GRH [f(M)]

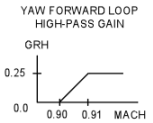

HIGH-PASS FILTER

$$\frac{1.96 - 1.96\,z^{-1}}{1 - 0.923\,z^{-1}}$$

REF: $\frac{2\,s}{s + 2}$

TRIM GAIN: GTRR [f(M)]

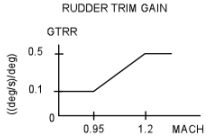

WASHOUT: (BETA FEEDBACK)

HIGH-PASS BETA_FILTER

$$\left(\frac{0.996016 - 0.996016\,z^{-1}}{1 - 0.992032\,z^{-1}}\right)$$

REF: $\frac{20\,s}{1 + 20\,s}$

RUDDER FORWARD LOOP GAIN GDRC [f(M, $\bar{q}$)]

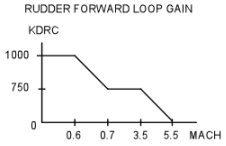

$$GDRC = \frac{KDRC}{QBAR + 10}$$

LIMITS ON RUDDER FORWARD LOOP GAIN

GDRC_MIN = 1.2 deg/(deg/s)

GDRC_MAX = 15.0 deg/(deg/s)

SHAPING LOGIC:

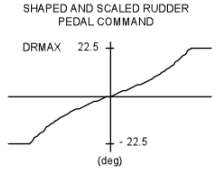

= (0.131 + 0.042 |DRMAN|) DRMAN
WHERE DRMAN IS THE RUDDER PEDAL COMMAND

YAW JET HYSTERESIS: AEROJET AND GRTLS

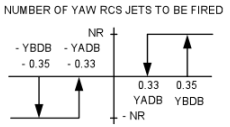

HYST_FLAG	YADB	YBDB
OFF	0.33	0.35
ON	0.33	0.35
$\overline{\text{HIGHQ}}$	| DRJETT |	NR
	≤ 0.5	2
	> 0.5	2
HIGHQ	≤ 0.5	2
	> 0.5	2
	> 1.0	3
	> 1.5	4

YAW JET HYSTERESIS WRAPAROUND:

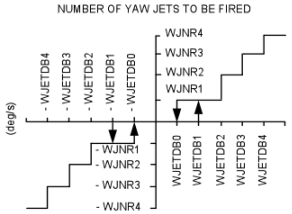

SWITCH LEVEL	NUMBER OF JETS	
	QBAR REGIME	
	NOT HIGHQ	HIGHQ
WJNR1	WJNR1_LOWQ = 2	WJNR1_HIGHQ = 2
WJNR2	WJNR2_LOWQ = 2	WJNR2_HIGHQ = 2
WJNR3	WJNR3_LOWQ = 2	WJNR3_HIGHQ = 3
WJNR4	WJNR4_LOWQ = 2	WJNR4_HIGHQ = 4

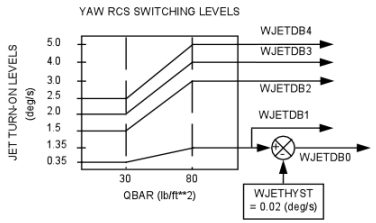

FILTER AND GAIN: GRAY [f(M)]

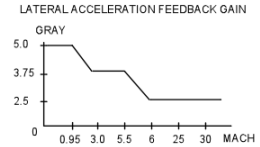

NY_COMP FILTER

$$\frac{0.090910\,(1 + z^{-1})}{1 - 0.81818\,z^{-1}}$$

REF: $\frac{1}{0.2\,s + 1}$

OI-25 ENTRY/GRTLS DAP YAW CHANNEL FILTERS AND SCHEDULED GAINS FOR SIMPLIFIED ROLL/YAW AXIS BLOCK DIAGRAMS

CANVAS v. 4.0
B. J. WEBER, 12/19/96

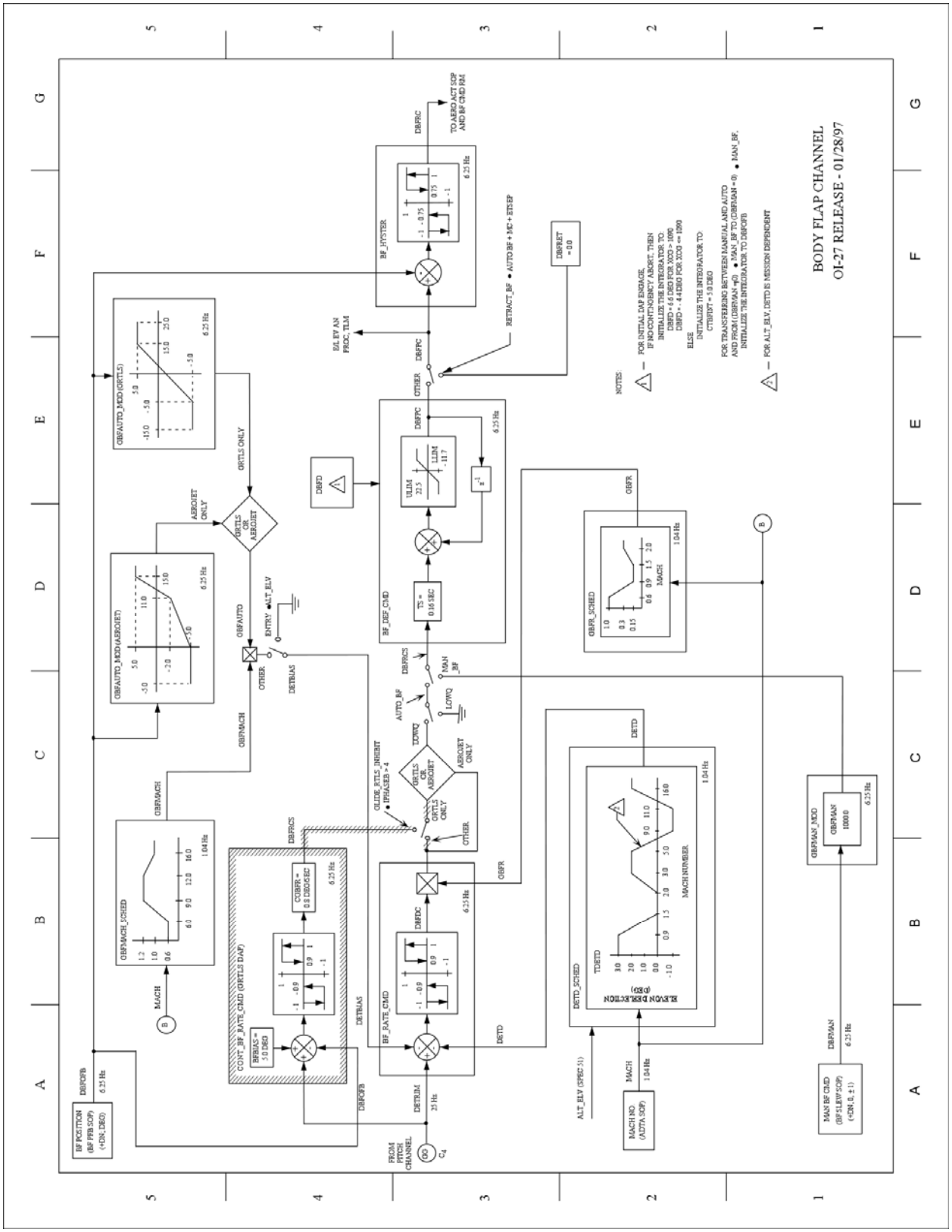

Figure D-6. Body Flap Channel, OI-27 FSSR

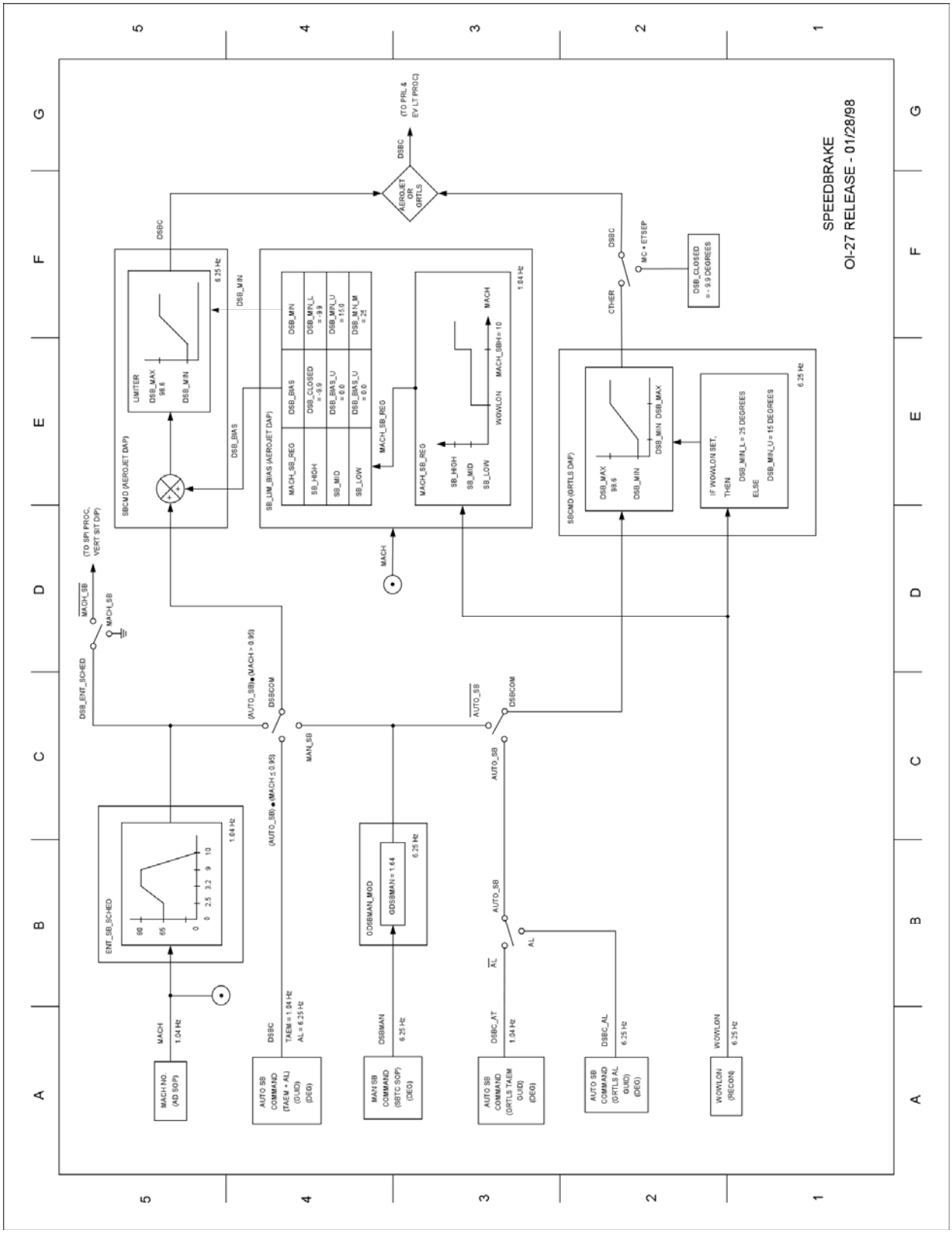

Figure D-7. Speedbrake Channel, OI-27 FSSR

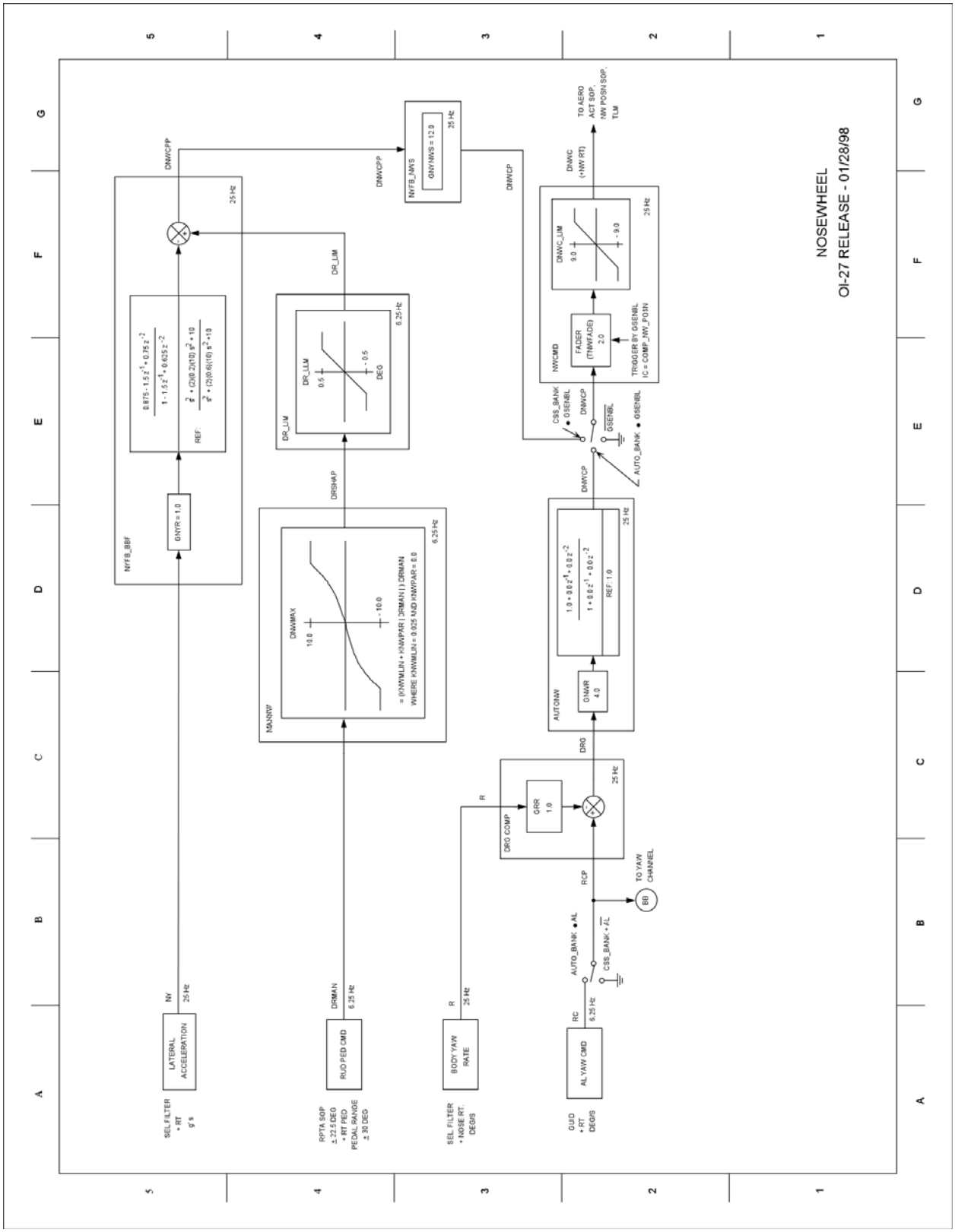

Figure D-8. Nosewheel Channel, OI-27 FSSR